Modelling water quality and ecosystem metabolism in regulated rivers

Devanshi Paresh Pathak

Submitted in accordance with the requirements for the degree of
Doctor of Philosophy

The University of Leeds
School of Geography

July, 2022

DECLARATIONS

The candidate confirms that the work submitted is her own, except where work which has formed part of jointly authored publications has been included. The contribution of the candidate and the other authors to this work has been explicitly indicated below. The candidate confirms that appropriate credit has been given within the thesis where reference has been made to the work of others.

Chapter Two
The work in Chapter Two has appeared in publication as:

Pathak, Devanshi; Hutchins, Michael; Brown, Lee; Loewenthal, Matthew; Scarlett, Peter; Armstrong, Linda; Nicholls, David; Bowes, Mike; Edwards, François. Hourly prediction of phytoplankton biomass and its environmental controls in lowland rivers. *Water Resources Research*, volume 57, page e2020WR028773. Wiley Online Library, 2021. doi: https://doi.org/10.1029/2020WR028773.

Author contributions:
DP conceived the presented work with scientific guidance from MH. DP and MH developed the model. LEB and FE contributed to statistical analysis. DP analysed the data. ML and MB provided management and scientific direction of the contributory monitoring programmes. PS contributed to field data collection. LA and DN contributed to laboratory analysis of the water quality data. DP wrote the manuscript with contributions and review from MH and LEB.

Chapter Three
The work in Chapter Three has appeared in publication as:

Pathak, Devanshi; Hutchins, Michael; Brown, Lee; Loewenthal, Matthew; Scarlett, Peter; Armstrong, Linda; Nicholls, David; Bowes, Mike; Edwards, François; Old, Gareth. High-resolution water-quality and ecosystem-metabolism modelling in lowland rivers. *Limnology and Oceanography*. Wiley Online Library, 2022. doi: https://doi.org/10.1002/lno.12079

Author contributions:
DP conceived the presented work with scientific guidance from MH. DP and MH developed the model. LEB and FE contributed to statistical analysis. DP analysed the data. ML, MB and GO provided management and scientific direction of the contributory monitoring programmes. PS contributed to field data collection. LA and DN contributed to laboratory analysis of the water quality data. DP wrote the manuscript

with contributions and review from MH and LEB.

Chapter Four
DP conceived the presented work with scientific guidance from MH. DP and MH designed the future scenarios. DP performed the scenario analysis using the model developed in Chapter Three and analysed the outputs. DP wrote the chapter with contributions and review from MH, LEB and FE.

Chapter Five
The work in Chapter Five was carried out as a part of a secondment at Norwegian Institute for Water Research (NIVA) and is submitted for publication as:

Pathak, Devanshi and Benoît OL Demars. Metabolism modelling in rivers with unsteady flow conditions and transient storage zones. *Submitted to JGR Biogeosciences*, 2022.

Author contributions:
DP and BOLD derived the model equations. BOLD collected the data. DP and BOLD analysed the data. DP developed the model code, implemented the model and analysed the outputs with scientific guidance from BOLD. DP wrote the manuscript with contributions from BOLD. BOLD, LEB and MH reviewed the manuscript.

ACKNOWLEDGMENTS

I have been fortunate enough to have the support of many people throughout my PhD. Firstly, I would like to thank my supervisor at the UK Centre for Ecology & Hydrology (UKCEH), Mike Hutchins, who guided me at every stage of my PhD. Thanks for always being available whenever I needed your help and guidance, and always motivating and encouraging me to do better.

I would also like to thank my supervisor at the University of Leeds, Lee Brown, for his guidance and support. Thanks for always being extremely helpful whenever I needed a feedback on my work as well as any help related to university procedures. I am thankful to my supervisor, Francóis Edwards, for his support and encouragement, and his help with figuring out the nitty-gritty of the administrative procedures at UKCEH.

My PhD research was funded by the European Union's Horizon 2020 research and innovation programme under the Marie Skłodowska-Curie grant agreement No 765553. I am grateful for the funding and the opportunities it provided me during my research. Many thanks to the UKCEH Thames Initiative (funded by the Natural Environment Research Council, NEC04877), the National River Flow Archive and the Environment Agency for providing me flow and water quality data for modelling. I would like to thank Mike Bowes, Matthew Loewenthal, Gareth Old, Peter Scarlett, Linda Armstrong and David Nicholls for collecting the water quality data and carrying out laboratory analysis for the UKCEH Thames Initiative.

During my PhD, I was fortunate to collaborate with inspiring people. I thank Benoît Demars and Nikolai Friberg at the Norwegian Institute for Water Research for accommodating my remote secondment during the pandemic. Special thanks to Benoît for his guidance, support and encouragement in developing the MUFT model, which continued even after the secondment period was over. I would also like to thank Otra Kraft for providing flow data and boats; Ulrich Pulg and Sebastian Stranzl for providing TDG data and lime addition data; Peter Dörsch for CO_2 GC analyses; Odd Arne Skogan for setting up the Campbell logging station; Knut Olav Oppstad for providing sonar bathymetric data; Benoît Demars, Kirstine Thiemer, Susanne Schneider, Emmanuel Bergan, Astrid Torske, Eirin Aasland for collecting bathymetric and plant data, as well as CO_2 flux with the floating chambers.

I am thankful to be part of the EuroFLOW project. I had an amazing experience collaborating and learning from the people involved in the EuroFLOW project. I am also thankful to Sandie Clemas at the UKCEH and Jacqui Manton at the University of Leeds, who always helped me promptly with both sides of the administrative procedures.

Many thanks to the UKCEH student community, especially my friends Flora, Jordan, Elmer and Dominic for making my PhD experience enjoyable and memorable. Thank you Semeena and Retish for all your support and being there for me. Thanks to Valerie and Luke, who made the pandemic time not only bearable, but also super fun. Thanks Kesha

and Padma, for making my last few months in Oxford so much more fun and memorable. I would also like to thank Anahata, Heli, Kruti and Chitra, who have been my constants for the past 13 years. Special thanks to Anahata for keeping me motivated through phone calls throughout the pandemic.

I am grateful to the support of my family, who has helped me come this far. Thanks to Mummy, Pappa and Dinku for always supporting and motivating me at every step of my life - thanks for always being by my side. Thanks to Mansi, Netu and Athhu for keeping things light and entertaining. Thanks to Acy, George and Vinu for your love and support - I am thankful to our regular video calls that always cheered me up. Lastly, thanks Geet, my partner in everything - this wouldn't have been possible without you.

ABSTRACT

Wide-spread flow regulations have modified rivers globally through changes in multiple environmental stressors that regulate ecosystem processes such as metabolism. Despite ubiquitous river regulation, current metabolism models do not include multiple stressor influences. Additionally, these models were developed for estimation at reach-scale, thus limiting our ability to predict metabolism across expansive river catchments. This thesis aims to expand ecosystem metabolism estimation to regulated rivers, which is achieved by developing two river segment-scale models.

The first model, hourly QUESTOR (Quality Evaluation and Simulation Tool for River-systems), supports metabolism estimation in multi-stressed lowland rivers with flow and water quality regulation. Using a case study of the River Thames in England, I demonstrated the model's application for estimation of metabolism and of its controls such as flow, water temperature, light availability, nutrients and biomass. Comparing this model with statistical modelling provided insights into the multiple stressor controls of metabolism in lowland, regulated rivers. The model also segregates biochemical respiration pathways as well as estimates metabolism at sites without regular monitoring and/or under changing climate-management conditions.

The second model, MUFT (Metabolism estimation in rivers with Unsteady Flow conditions and Transient storage zones), was developed by coupling an unsteady flow routing model and a solute transport model with the two-station metabolism model. I applied the model along a river stretch downstream of a hydropower plant in the River Otra in Norway. The MUFT model presents a parsimonious approach to estimate metabolism for the first time in hydropeaking environments and/or transient storage zones.

Comparing both models, I made recommendations for metabolism modelling in regulated rivers and outlined directions for future research. The modelling approaches presented here unlock new possibilities for broad-scale metabolism estimation across diverse river environments, which in turn will help reduce uncertainties in our global estimates of freshwater carbon fluxes.

CONTENTS

LIST OF FIGURES

LIST OF TABLES

σ	Standard deviation
$1/k_bT$	Transformed water temperature
F_{adv}	Advection delay coefficient
F_r	Fraction of retention
k	Gas exchange coefficient
k_{O2}	Oxygen gas exchange coefficient
k_{PAR}	Half-saturation constant for maximum primary production
k_{rea}	Reaeration coefficient
kz	Gas transfer velocity
n	Number (units)
n_c	Number of well-mixed tanks
O_{sat}	Saturated dissolved oxygen concentration
p	Probability value
P_{GPP}	Rate of gross primary production
P_{GPPmax}	Maximum gross primary production
P_N	Oxygen production during nitrate assimilation by phytoplankton
P_P	Oxygen production during photosynthesis
Q	Discharge
r	Pearson's product moment correlation coefficient
R_A	Autotrophic respiration
R_{ben}	Benthic respiration
R_{ER}	Rate of ecosystem respiration
R_{nitri}	Dissolved oxygen loss from nitrification
R_{wc}	Water column respiration
ADV	Advection
ADZ	Aggregated dead zone
Allscen	All scenarios
Allscen_minus_hr	All scenarios except heterotrophic respiration rate
BOD	Biochemical oxygen demand
BRT	Boosted regression trees

C . . . . . Carbon

Chl-a . . . . . Chlorophyll-a

ClimatePop . . . . . Climate change and population growth scenario

CSTR . . . . . Continuous stirred tank reactor

D . . . . . Dimensional

DIN . . . . . Dissolved inorganic nitrogen

DO . . . . . Dissolved oxygen

DOC . . . . . Dissolved organic carbon

E-flows . . . . . Environmental flows

EA . . . . . Environment agency

ER . . . . . Ecosystem respiration

GA . . . . . Green algae

GLS . . . . . Generalised least squares

GPP . . . . . Gross primary production

HetResp . . . . . Heterotrophic Respiration (scenario)

MCMC . . . . . Markov chain monte carlo

MUFT . . . . . Metabolism estimation in rivers with unsteady flow conditions and transient storage zones

N . . . . . Nitrogen

NEP . . . . . Net ecosystem production

NRFA . . . . . National river flow archive

NSE . . . . . Nash and sutcliffe efficiency

ODE . . . . . Ordinary differential equation

P . . . . . Phosphorus

PAR . . . . . Photosynthetically-active radiation

PBIAS . . . . . Percentage error in mean

$\mathbf{P_{org}}$ . . . . . Organic phosphorus

PON . . . . . Particulate organic nitrogen

QUASAR . . . . . Quality simulation along river systems

QUESTOR . . . . . Quality evaluation and simulation tool for river systems

$\mathbf{R_H}$ . . . . . Heterotrophic respiration

SCD . . . . . Small centric diatoms

SH . . . . . *Stephanodiscus hantzschii*

SRP . . . . . Soluble reactive phosphorus

SS . . . . . Suspended sediment

STW . . . . . Sewage treatment works

TDG . . . . . Total dissolved gas

Temp . . . . . Temperature

TP . . . . . Total phosphorus

UKCEH . . . . . United Kingdom Centre for ecology & hydrology

Urb . . . . . Urbanisation

1

INTRODUCTION

ओ माझी रे, अपना किनारा नदिया की धारा हैं.

O rower, our shore is the river's flow.
- Gulzar

1.1 CONTEXT

Freshwater systems are not only home to an enormous diversity of life (Dudgeon et al., 2006), but also support humankind through a wide range of ecosystem services (Millennium Ecosystem Assessment, 2010). These ecosystem services include provision of resources (food, water, wood) and delivery of cultural, aesthetic and recreational services (Wantzen et al., 2016). Freshwater systems also provide inconspicuous benefits such as regulation of water quality and microclimate, and maintenance of valuable ecosystem processes such as photosynthesis and nutrient cycling that support the overall functioning of the ecosystem (Reynaud and Lanzanova, 2017; Hanna et al., 2018). However, while deriving benefits from these ecosystems, humans – through their ever-expanding anthropogenic activities – have extensively degraded freshwater systems by modifying their physical, chemical and biological properties (Meybeck, 2003).

River ecosystems are influenced by multiple human pressures (Grizzetti et al., 2017). Flow regulation is the leading cause of river modification globally (Grill et al., 2019). Water infrastructure developments such as dams and weirs, and water transfer practices for agriculture, industrial and domestic purposes have degraded river ecosystem health through alterations in natural flow regimes and river connectivity (Poff et al., 1997). Catchment management activities such as urbanisation, industrialisation and land use changes also directly threaten river ecosystem health (Malmqvist and Rundle, 2002), which remain to be further affected by anthropogenic climate change (Vörösmarty et al., 2010). These human pressures regulate multiple environmental stressors (e.g. flow, light availability, nutrient loading, etc.) that interact with each other, and alter river water quality and ecosystem functioning. The environmental stressors operate at different spatial and temporal scale to influence river ecosystem health. Furthermore, the response of river ecosystems to these multiple stressors is often non-linear, which makes it challenging to investigate the causes and mechanisms of human impacts on river ecosystem health (Allan, 2004).

This introduction provides a brief overview of (a) the need to understand river regulation impacts on ecosystem health, (b) the utility of using ecosystem metabolism as a river health indicator and (c) the need to improve existing metabolism modelling approaches. This overview establishes the basis for four new analytical chapters focusing

on modelling water quality and ecosystem metabolism in regulated rivers in the United Kingdom (UK) and Norway.

1.2 River regulation and ecosystem health

River ecosystem health is usually evaluated based on two types of metrics, namely structural indicators and functional indicators. Structural indicators reflect the existing condition of the ecosystem and the river organisms through instantaneous measurements (Von Schiller et al., 2017). Some examples of structural indicators include status of channel morphology, pollutant concentrations, oxygen levels and biomonitoring indices (community structure). Functional indicators reflect system dynamics through repeated measurements that quantify ecosystem processes (Palmer and Febria, 2012) such as nutrient cycling, ecosystem metabolism, organic matter breakdown, pollutant removal rates, etc. (Young et al., 2008).

Flow (discharge) is a key driver of river ecological health because it regulates energy cycling, water quality, physical habitat and biotic interactions in the river (Karr, 1991; Poff et al., 1997). Balancing water availability whilst maintaining ecological health under a growing demand is increasingly becoming a challenge for water managers (Hutchins and Bowes, 2018). Previously, water allocation efforts were biased towards fulfilling anthropogenic demands such as hydropower, irrigation and water supply rather than preserving rivers' health (Viers, 2017). However, in the recent past, the focus of river regulation has expanded to incorporate the ecological needs of rivers along with human demands through the development of the 'environmental flows' (E-flows) concept. E-flows describe *"the quantity, timing, and quality of freshwater flows and levels necessary to sustain aquatic ecosystems which, in turn, support human cultures, economies, sustainable livelihoods, and well-being"* (Arthington et al., 2018). Over time, E-flows approaches have progressed to address a range of ecological, social and economic targets (Poff and Matthews, 2013). Yet, a majority of the E-flows research to address ecological targets so far has been confined to understanding the influence of a single stressor (i.e. flow) on structural indicators of river health. Efforts are required to integrate a more diverse set of environmental stressors and functional indicators in the E-flows research (Acreman et al., 2014), especially under changing climate and water demands.

Functional indicators of river health respond to biotic and abiotic stressors (Palmer and Febria, 2012), capture system dynamics (Bunn and Davies, 2000; Young et al., 2008) and are able to detect even marginal changes in river health impairment or recovery, all of which are challenging to achieve using structural indicators (Palmer et al., 2005). It is also easier to compare river health and its regional controls across different biomes using functional indicators since measurements of functional indicators do not rely on specific species (Young et al., 2006). In addition to representing river health, functional indicators also provide a direct measure of ecosystem services (regulating and supporting services, Millennium Ecosystem Assessment, 2010) that support human needs (Rapport

et al., 1998). Hence, functional indicators need to be included while assessing ecosystem health response to human pressures.

In the context of environmental regulators of river health, the majority of research has focused on managing only flow requirements in rivers since flow is often believed to be the sole variable controlling ecosystem status (Davies et al., 2013). However, changes in flow occur alongside changes in other variables such as temperature, morphology and water quality (Acreman and Dunbar, 2004). Furthermore, in addition to flow regulation, external pressures such as changes in climate, land use and water demand also affect ecosystem processes through modifications in multiple stressors (Mulholland et al., 2001; Acuña et al., 2004). Thus, we need a better understanding of how multiple stressors act in concert with flow to impact ecosystem processes. Instead of limiting the research to understanding flow-ecology linkages, it is equally important to study the response of functional indicators of river health to multiple external stressors to be able to predict river health response to restoration/management actions under a changing environment. The development of conceptual models that integrate the effect of multiple stressors will help diagnose the causes and mechanisms of ecosystem degradation and subsequently help inform management decisions (Bunn et al., 2010).

1.3 ECOSYSTEM METABOLISM

Ecosystem metabolism regulates the incoming and outgoing energy fluxes in river systems through gross primary production (GPP) and ecosystem respiration (ER). GPP is the production of organic matter through conversion of solar energy into organic energy, whereas ER indicates total consumption of organic matter derived from both autochthonous and allochthonous sources. Therefore, ecosystem metabolism provides a direct estimate of the food base and the way energy moves through the river food web (Young et al., 2008), thus representing the life-sustaining capacity of rivers (Fisher and Likens, 1973). Use of ecosystem metabolism as a functional measure of river health is advantageous over other ecosystem processes such as nutrient uptake (Hall and Tank, 2003), denitrification (Bernhardt et al., 2002), microbial respiration (Hill et al., 2002), and organic matter retention and breakdown (Young et al., 2008) because the measurement of ecosystem metabolism is relatively easier and cheaper using automated, water quality sensors.

1.4 METHODS OF METABOLISM ESTIMATION

The history of measuring whole-stream (ecosystem) metabolism can be traced back to the 1950s. Odum (1956) introduced the open-channel method to estimate whole ecosystem metabolism in lotic waters. The subsequent progress has been slow due to a lack of high-resolution data and computational requirements. However, open-channel methods are now becoming increasingly popular to estimate ecosystem metabolism in rivers (Demars

et al., 2015) with the availability of affordable and robust water quality sensors (Rode et al., 2016).

The open-channel methods estimate GPP and ER based on diel variation in dissolved oxygen (DO) in the water column. The rationale behind this method is that DO variation is mainly controlled by biological processes including photosynthesis (GPP) and respiration (ER), and a physical exchange of DO between the water column and the atmosphere (reaeration). GPP and ER in the open-channel methods can be estimated either using an accounting approach (e.g. Izagirre et al., 2008; Demars et al., 2015) or through an inverse approach (e.g. Appling et al., 2018b). The majority of the metabolism models employ the inverse approach of fitting DO curves (Jankowski et al., 2021) using the information of light availability and temperature (Holtgrieve et al., 2010; Hall Jr and Hotchkiss, 2017; Appling et al., 2018b), but in some cases also using information of barometric pressure (Grace et al., 2015) or discharge (Izagirre et al., 2008; Demars et al., 2015; Payn et al., 2017).

Open-channel methods are implemented at a river-reach scale using DO measurements at a single site (e.g. one-station method, Izagirre et al., 2007) or two sites over a reach (e.g. two-station method, Hall Jr and Tank, 2005). To set baseline conditions for river health management, we need to derive expected patterns of metabolism within and across different biomes and river environments. The one-station metabolism models are generally applied at a single site within a river, and estimates from a large number of such sites are amalgamated to assess regional scale mechanisms of metabolism (Appling et al., 2018b; Bernhardt et al., 2022). These one-station metabolism models, although quite robust for homogeneous river reaches without additional influences, are not suitable for sites where river reaches are influenced by water management infrastructures or pollution discharges that could significantly alter river water quantity and quality dynamics. In such cases, two-station models need to be used to estimate metabolism. However, two-station models are only suitable in a limited range of situations, i.e. when certain assumptions regarding the reach length (see Demars et al., 2015) and the positioning of the estimation location with reference to the reservoir (see Reichert et al., 2009) are fulfilled. Furthermore, similar to the one-station methods, two-station methods also do not account for biochemical processes in the estimation of ecosystem metabolism and the estimation is limited to a river-reach scale. To expand metabolism estimation to a broad range of river environments, there is a need to develop river network-scale metabolism models.

In addition to expanding the spatial scale of modelling, it is also important to include the influence of flow variability and biochemical processes in metabolism models since GPP and ER may be sensitive to these processes in regulated rivers (Jankowski et al., 2021). River regulation practices modify metabolism through changes in multiple stressors that influence GPP and ER. For example, reservoir operations regulate GPP through changes in flow, temperature, sediment and nutrient cycling in river stretches downstream of the reservoir (Aristi et al., 2014). ER is shown to strongly respond to sewage discharges (Arroita et al., 2019). Both GPP and ER are altered by disturbances in the flow regime arising from water abstractions or diversions (Arroita et al., 2017). Eutrophication may also influence GPP and ER, either directly or indirectly (Hill et al., 2009). The influence of

multiple stressors on metabolism is usually evaluated using statistical methods (Dodds et al., 2018; Bernhardt et al., 2022). Although statistical approaches derive useful information about sensitivity of metabolism to external stressors, these interpretations are usually limited to the environmental conditions for which the models are built, and carry high uncertainties for predictions in response to change.

Only recently metabolism models have been developed to explicitly include some of the aforementioned stressors such as the inclusion of diel flow variability (Payn et al., 2017) and biomass dynamics (Segatto et al., 2020) in metabolism models. These studies are notable developments in metabolism modelling in multi-stressed river systems. However, we still require network-scale models that integrate metabolic, biochemical and hydrological processes in river system (Bernhardt et al., 2018).

1.5 RESEARCH AIM AND OBJECTIVES

Considering the ubiquitous presence of river management practices, it is important to mechanistically relate multiple environmental stressors to metabolism in modelling approaches (Bernhardt et al., 2018) to elucidate underlying mechanics of metabolic regimes in rivers and consequently, to be able to accurately predict river metabolism outside the range of the available observations. There is also a need to expand metabolism models from reach-scale estimation to larger spatial scale (i.e. river segment/network scale) estimation to derive regional predictors of metabolism as well to include the effect of catchment-scale assemblages of influences (e.g. reservoir operations, water abstractions, pollution loading) on downstream metabolism dynamics.

This thesis overcomes the aforementioned limitations in current practices of metabolism modelling by developing two modelling approaches that are suited for application in rivers influenced by different sets of multiple stressors. Specifically, the model developments are focused on two types of river environments, (1) where flow is regulated from locks and weirs, and water quality is influenced by sewage discharges and land use practices and (2) where flow is regulated by hydropower dams and solute transport is influenced by transient storage zones.

The overall aim of the thesis is to expand metabolism estimation and prediction to regulated rivers influenced by multiple stressors under changing climatic and management conditions. To fulfil this aim, I outline the following research objectives:

1. Develop a high-resolution, process-based model for prediction of water quality and ecosystem metabolism in regulated, lowland rivers

2. Identify multiple stressor controls on ecosystem metabolism in regulated, lowland rivers

3. Predict ecosystem metabolism response under future climatic and management conditions in regulated, lowland rivers

4. Develop a parsimonious process-based model to predict ecosystem metabolism in rivers with unsteady flow conditions and transient storage zones

In this thesis, I present two modelling approaches that facilitate metabolism estimation in regulated rivers influenced by a set of multiple stressors (Figure 1.1). The first model is called the hourly QUESTOR (Quality Evaluation and Simulation Tool for River-systems) model, and is suited for applications in lowland rivers. In Chapters 2 and 3, I show the model development and implementation using a case study of the lower River Thames in England, where flow is extensively regulated through locks and weirs and water quality is severely influenced by nutrient loading from agricultural runoff and sewage treatment works that together cause issues of eutrophication and phytoplankton blooms in the river. Chapter 2 shows the development and application of the hourly QUESTOR model for prediction of phytoplankton biomass and focuses on deriving environmental bounds within which phytoplankton blooms develop in the river. Chapter 3 demonstrates the model application for ecosystem metabolism estimation in lowland rivers using the same case study of the lower River Thames. In Chapter 3, I also evaluate sensitivity of the modelled (using the hourly QUESTOR model) metabolism to multiple environmental stressors using empirical modelling. In Chapter 4, I use the same model setup (of Chapter 3) to predict river metabolism response to future climatic and management conditions in the river.

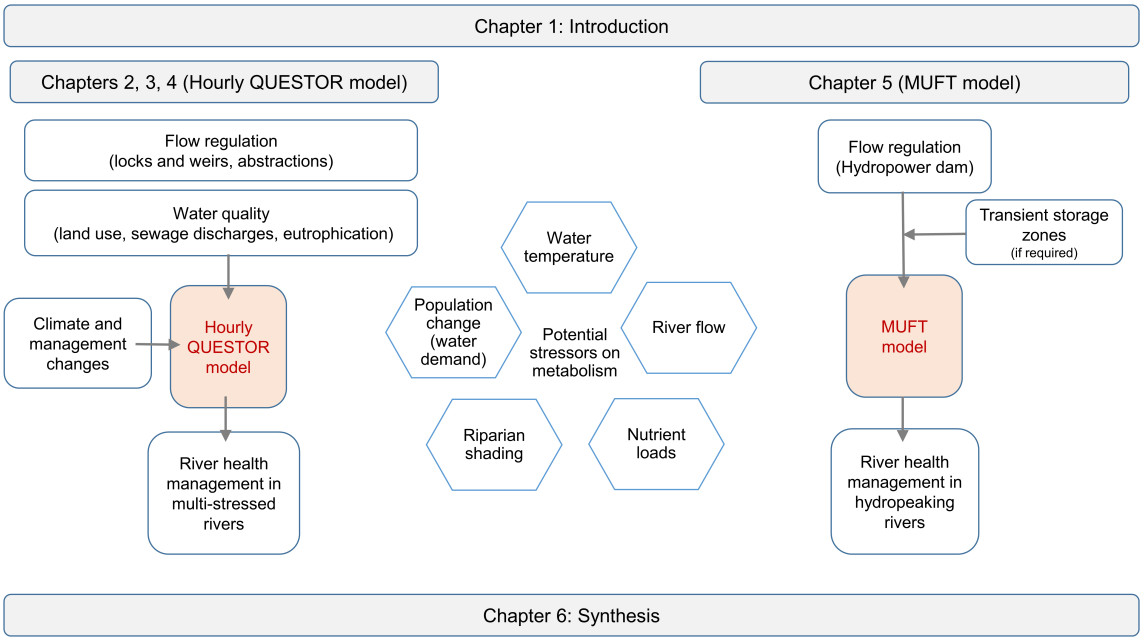

Figure 1.1: Schematic diagram of thesis structure

The second model I developed in this thesis is called the MUFT (Metabolism estimation in rivers with Unsteady Flow conditions and Transient storage zones) model, and is suited for application in hydropeaking rivers. In Chapter 5, I show the model development and application using a case study of the River Otra in Norway, where flow regulation from a hydropower dam causes significant diel fluctuations in flow and excessive plant growth in the river stretch influences dissolved oxygen transport. Chapter 6 provides a synthesis of the work produced in this thesis, where the outputs of this thesis are discussed in the

context of existing literature along with their advantages, limitations and directions for future research.

2

HOURLY PREDICTION OF PHYTOPLANKTON BIOMASS AND ITS ENVIRONMENTAL CONTROLS IN LOWLAND RIVERS

2.1 INTRODUCTION

The biomass and composition of phytoplankton are important indicators of water quality and the biological health of rivers (Villegas and Giner, 1973). Phytoplankton communities are a major source of food for primary consumers through organic carbon production, and act as the primary source of oxygen in many rivers (Köhler, 1995). However, rivers also suffer if there is excessive phytoplankton growth since it may cause oxygen depletion (Hilton et al., 2006), produce harmful toxins (e.g. cyanobacteria), increase water treatment costs (Whitehead and Hornberger, 1984), and interfere with fishing and other recreational activities (Paerl and Huisman, 2009). Hence, it is vital to build an understanding of the controls on phytoplankton, to predict and prevent harmful growth in rivers, especially under the changing climate and environmental conditions (Read et al., 2014).

Phytoplankton growth in rivers is influenced by different environmental controls, and their influence may vary depending upon the river characteristics and local conditions (Reynolds, 2000). River phytoplankton development is often linked to increase in nutrient concentrations (Dodds, 2006; Minaudo et al., 2018). However, a number of studies have also highlighted the role of physical factors such as residence time (Reynolds, 2000), light availability (Domingues et al., 2011) and temperature (Canale and Vogel, 1974) in shaping river phytoplankton populations. These environmental controls generally act in combination to control phytoplankton blooms in rivers such as the combination of flow and light (Hardenbicker et al., 2014), flow, temperature and nutrients (Larroudé et al., 2013), or flow, temperature and light (Balbi, 2000; Bowes et al., 2016).

Several studies have addressed environmental controls of phytoplankton growth in lowland rivers around the world. Lowland rivers are heavily impacted by water abstractions, artificial flow regulation, physical modifications of the channel as well as substantial pollution load discharges from sewage and agricultural runoff (Hutchins et al., 2018). These slow flowing rivers typically have long residence time, which provides sufficient time for water quality to be sensitive to in-stream biogeochemical processes and for phytoplankton to utilise nutrients and grow (Reynolds, 2000). For example, River Thames (UK) exhibited high phytoplankton biomass only at low flows (Lack, 1971). River Meuse (Belgium) showed a combination of physical factors such as flow, temperature and light as important biomass controls (Everbecq et al., 2001). Total phosphorus in the Rideau (Canada) (Basu and Pick, 1997) and grazing in the Moselle (France and Germany) (Descy et al., 2003) have also been found to be important biomass controls. However, most previous studies examined changes in these multiple control relationships at daily to monthly time scales, with higher resolution diel dynamics often being overlooked. Phytoplankton biomass in rivers have shown to respond to rapid

changes in its environmental controls (Bowes et al., 2016). Thus, it is crucial to understand these shorter scale dynamics to predict phytoplankton growth and bloom timings more accurately.

In the River Thames, a regulated lowland river in southern England, substantial efforts have been made to understand phytoplankton response through process-based modelling (e.g. Whitehead and Hornberger, 1984; Whitehead et al., 2015; Lázár et al., 2016). These studies, however, have shown limited predictive ability in modelling large and rapidly developing phytoplankton biomass, suggesting that there is still a need to better understand process interactions (Bowes et al., 2016). For example, there has been uncertainty as to which phytoplankton groups dominate the response. Some studies found green algae to be dominant during peaks in the summer (Lack, 1971; Ruse and Love, 1997) yet subsequent studies have found cool water diatoms to predominate with peaks instead during spring and autumn seasons (Read et al., 2014; Bowes et al., 2016). The daily time-step QUESTOR (Quality Evaluation and Simulation Tool for River-systems) model (Boorman, 2003a) has been developed to simulate phytoplankton (Hutchins et al., 2010) and also been extensively applied in the River Thames (Waylett et al., 2013; Hutchins et al., 2016; Hutchins and Bowes, 2018). However, consistent with other models, QUESTOR applications have also had only limited success in simulating phytoplankton biomass with over-estimation in mid-summer (Hutchins et al., 2016).

Various process-based river models (e.g. Brown and Barnwell, 1987; Everbecq et al., 2001; Reichert et al., 2001) have been applied worldwide to understand phytoplankton dynamics, but these models are rarely tested with high-frequency observations to explore shorter scale dynamics. Phytoplankton modelling applications are generally limited to weekly to daily time-steps. High-resolution modelling has been challenging because of high computational requirements and a lack of high-frequency monitoring data. Even the high-resolution hourly modelling studies done so far (Van Griensven and Bauwens, 2005; Martin et al., 2013; Minaudo et al., 2018; Suarez et al., 2019) do not test the simulations with high-frequency observations of all key variables (temperature, chlorophyll and dissolved oxygen (DO)) and only report model testing against daily (or coarser scale) observations. However, it is now easier to monitor water quality at higher temporal resolutions with the development of low-cost, robust water quality sensors (Rode et al., 2016). Models can utilise high-frequency data sets to understand phytoplankton growth and its environmental controls at finer resolutions, thus ensuring early warnings of blooms in river systems.

The present study was undertaken by modifying an existing water quality model, QUESTOR, to run at shorter time-steps and testing against high-frequency (hourly) water quality measurements (chlorophyll-a (Chl-a), DO and water temperature) at two locations in the River Thames. The model testing was reinforced with testing against daily flow observations and weekly water quality observations at other locations and for other determinands. The overall aim of this study was to test the hypothesis that hourly time-step modelling can improve prediction of phytoplankton biomass and to demonstrate the

utility of the model to study phytoplankton dynamics and its controls in lowland rivers. Specific objectives were to:

(1) develop a model to predict hourly variation and transport of in-stream flow, temperature, nutrients, DO and phytoplankton biomass in the lower Thames,

(2) identify an accurate model structure that represents dominant phytoplankton groups in the lower Thames using a model comparison and sensitivity analysis,

(3) illustrate the extent to which low-frequency water quality observations, used as inputs to the model in the absence of high-frequency observations, can still provide a basis for satisfactory explanation of phytoplankton dynamics in the catchment,

(4) identify favourable environmental conditions for photosynthetic production using the hourly model outputs and evaluate association of phytoplankton biomass with multiple environmental controls using boosted regression trees (BRT) technique.

2.2 METHODS

2.2.1 *Model theory*

QUESTOR is an in-stream, process-based water quality model that allows users to represent rivers as a network of reaches. River reaches are modelled as a set of non-linear reservoirs or well-mixed tanks in series (Figure 2.1). The hourly model is a pseudo 1-D (strictly speaking 0-D) model and assumes fixed channel width with rectangular cross section. The model simulates dynamic solute transport within the river network using ordinary differential equations (ODEs) with a mass-balance approach. The numerical solution of the ODEs is implemented using an explicit fourth-order Runge-Kutta-Merson differential equation solver (DASCRU). This solver operates at variable temporal resolution much finer than hourly reporting of results. The equations characterise major processes affecting model determinands, but include empirical coefficients which need to be calibrated (Boorman, 2003b). The *Stephanodiscus hantzschii* version (SH module, Waylett et al., 2013) of the daily time-step QUESTOR model is modified to account for hourly variations in physicochemical and biological water quality. The key determinands in the model include flow, water temperature, photosynthetically-active radiation (PAR), Chl-a, biochemical oxygen demand (BOD), DO, nitrate (NO_3^-), ammonium (NH_4^+), particulate organic nitrogen (PON), as well as organic and inorganic phosphorus in the water column (Figure 2.2). The equations for the new hourly model version of phytoplankton are explained below and the remaining set of equations for other determinands are provided in Appendix A. The model parameters are listed in Table B.2.

The growth of phytoplankton is estimated using a fixed stoichiometry model where the ratios (by weight) Chl-a:C:N:P are 1:50:10:1 (Hutchins et al., 2010). The new version required modifications in the phytoplankton growth rate parameters as,

$$k^{pho} = C_{phy}.k^{pho}_{ref}.e\left(-\frac{(T-T_{opt})^2}{a^2}\right).f(N).f(L) \tag{2.1}$$

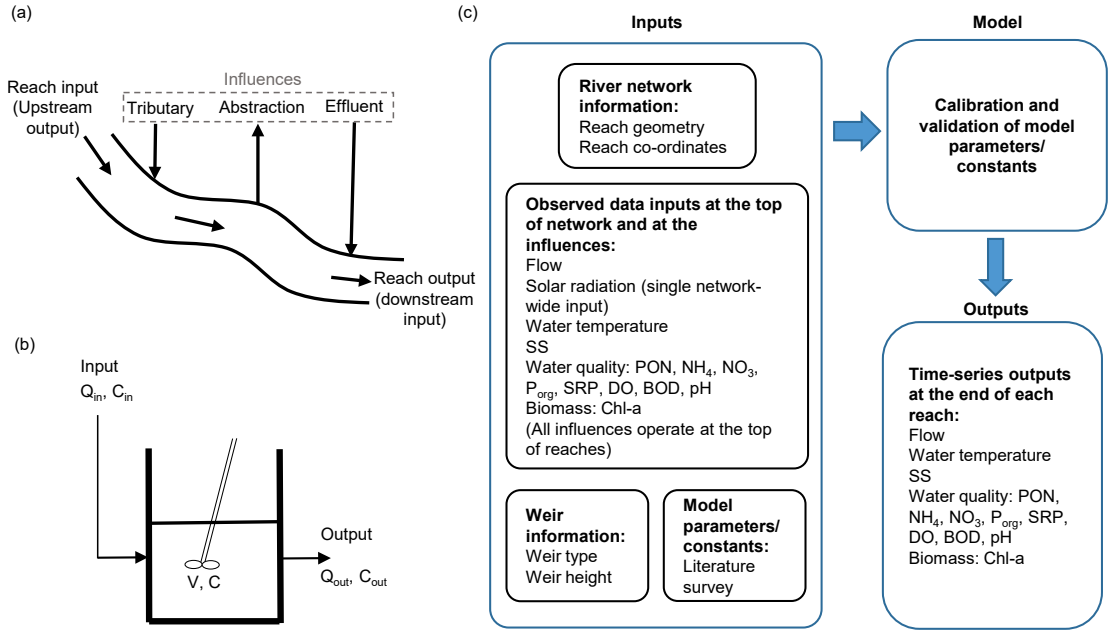

Figure 2.1: Model structure. (a) represents the schematic of a typical reach in the model, (b) represents the conceptualisation of reaches in the model and (c) shows the input and output information in the hourly model. (a) and (b) are modified after Whitehead et al. (1997a). In (b), V represents volume of water in a reach, C represents concentration of water quality determinand, Q_{in} and Q_{out} are input and output flows, C_{in} and C_{out} are input and output concentrations in a reach.

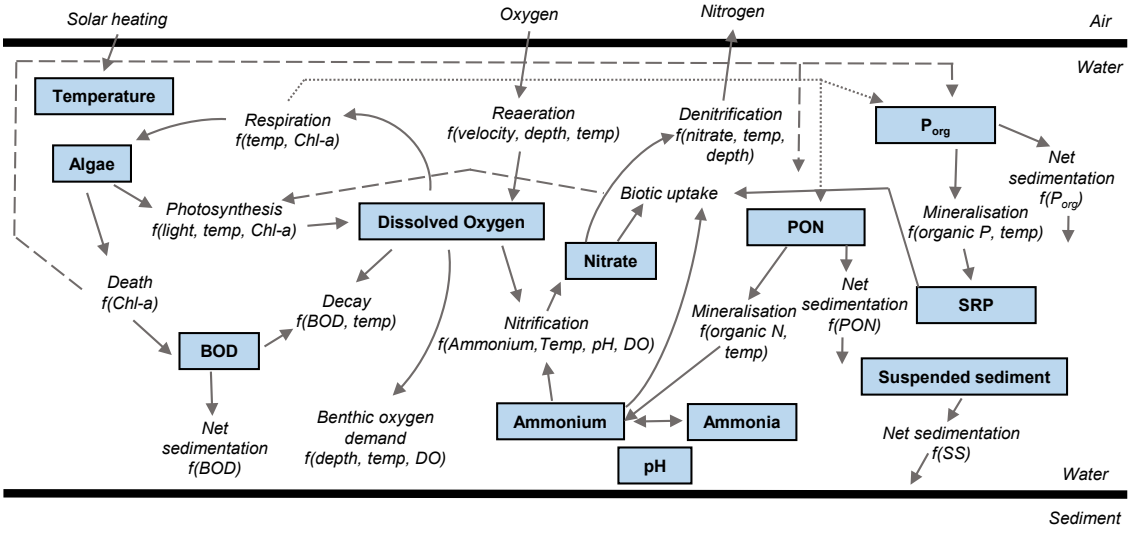

Figure 2.2: In-stream water quality determinands and processes represented in the model (modified after Eatherall et al., 1998).

k^{pho} is the photosynthetic rate (mg L^{-1} h^{-1}), C_{phy} is the concentration of Chl-a (mg L^{-1}), $f(N)$ and $f(L)$ are nutrient and light limitation factors each holding values between 0 and 1, T is water temperature (°C), $T_{opt} = 14$°C and a = 8 °C (Descy et al., 2003) and k_{ref}^{pho} is the maximum phytoplankton growth rate (h^{-1}) at T_{ref}; $T_{ref} = 20$°C.

Temperature limitation factor ($f(T)$) is estimated as,

$$f(T) = e\left(-\frac{(T - T_{opt})^2}{a^2}\right) \tag{2.2}$$

The calculation of nutrient limitation uses Michaelis-Menten kinetics,

$$f(N) = min\left(\frac{N}{N + k_N}, \frac{P}{P + k_P}\right) \tag{2.3}$$

N is nitrate-N plus Ammonium-N (mg L^{-1}), P is inorganic (soluble reactive phosphorus, SRP) plus organic phosphorus (mg L^{-1}), k_N (mg N L^{-1}) and k_P (mg P L^{-1}) are the half-saturation constants for N and P, respectively.

To account for light limitation, attenuation with depth (γ, m^{-1}) is described by the Beer-Lambert Law,

$$\gamma = \gamma_{base} + L_{SS}.C_{SS} + L_{Phy}.C_{phy} \tag{2.4}$$

γ_{base} is the light extinction coefficient in clean water (m^{-1}), C_{SS} is the concentration of suspended sediment (mg L^{-1}), L_{ss} is light attenuation with depth due to suspended sediment (m^{-1} mg^{-1} L) and L_{phy} is light attenuation with depth due to phytoplankton (m^{-1} mg^{-1} L).

Estimation of photolimitation with respect to phytoplankton-specific optimum intensities (Steele, 1962) in the model requires hourly inputs of incoming radiation and a constant value of optimum light intensity,

$$f(L) = \frac{2.718}{\gamma z}.\left[e^{-\frac{R_s L_1 L_2}{L_{opt}} e^{-\gamma z}} - e^{-\frac{R_s L_1 L_2}{L_{opt}}}\right] \tag{2.5}$$

z is the water column depth (m), R_s is the radiation at the surface not reflected (W m^{-2}) (i.e. raw data × L_3), L_1 is the fraction of incoming radiation that is visible light, L_2 is the fraction of visible light used for phytoplankton, L_3 is the fraction of light reaching water surface that is not reflected and L_{opt} is the optimum light intensity for phytoplankton (W m^{-2}).

Respiration calculation requires estimates of respiration fraction and maximum phytoplankton growth rate,

$$k^{res} = C_{phy}.k_{ref}^{res}.k_{ref}^{pho}.\theta^{(T - T_{ref})} \tag{2.6}$$

k^{res} is the phytoplankton respiration rate (mg L^{-1} h^{-1}), k_{ref}^{res} is the reference respiration fraction for phytoplankton (as fraction of k_{ref}^{pho}), θ is the Arrhenius factor for temperature dependencies ($\theta = 1.08$) and T is water temperature (°C); $T_{ref} = 20$°C.

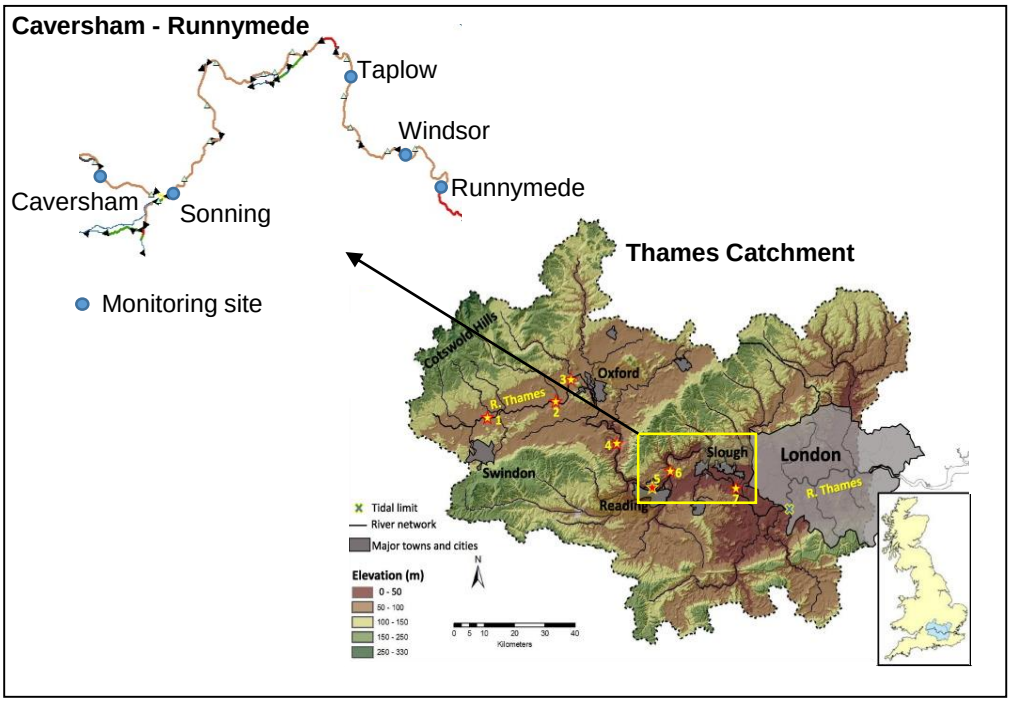

Figure 2.3: River Thames catchment with monitoring locations. Site 5: Caversham; Site 7: Runnymede. (modified after Bowes et al., 2016).

The death of the autotrophs is a combination of grazing and non-predatory mortality. In QUESTOR, death rate is estimated from algal growth limitation due to unsuitable nutrient and light conditions, and the calibration of the death rate constant compensates for the death from grazing,

$$k^{death} = C_{phy}.k_{ref}^{death}.k_{ref}^{pho}.[1 - (f(N).f(L))].\theta^{(T-T_{ref})} \tag{2.7}$$

k^{death} is the phytoplankton death rate (mg L^{-1} h^{-1}) and k_{ref}^{death} is the reference death fraction for phytoplankton (as fraction of k_{ref}^{pho}).

2.2.2 *Study area*

The Thames catchment is situated in southern England with an area of 9948 km² at the tidal limit (Waylett et al., 2013). The catchment has a population of around 15 million people with its uplands characterised by arable and pasture, and the lowland areas covered mainly by urban land uses (Hutchins et al., 2018). Mean annual precipitation and mean daily temperature in the catchment are 700 mm and 11°C, respectively (Crossman et al., 2013). The catchment receives around 40% of its water supply from groundwater sources, which are mainly characterised by Oolitic Limestone and Cretaceous Chalk aquifers (Crossman

et al., 2013). The River Thames is a heavily regulated river with 45 locks and weirs along its course. Catchment rivers that have extensive lock systems or are connected to canals are characterised by higher phytoplankton biomass compared to the unconnected rivers because of longer residence times (Bowes et al., 2012). In general, high phytoplankton biomass is observed in the middle and lower reaches of the catchment and phytoplankton blooms mainly occur during March to July (Bowes et al., 2012). This study focuses on a 62 km long stretch in the catchment from Caversham to Runnymede (Figure 2.3). The river stretch receives inputs from major tributaries such as Kennet, Lodden, and Wye rivers, and sewage treatment works (STW) effluents. In-stream flows are regulated by 14 locks and weirs along the stretch, sometimes resulting in long residence times from reduced flow velocities.

2.2.3 *Data source and model application*

The River Thames is one of the most intensively studied and monitored rivers in the UK (Bowes et al., 2018). The model development here makes use of a combination of weekly to hourly scale existing flow and water quality data of 2 years (2013-2014) (see Table 2.1). Gauged daily flow data were obtained from the NRFA (National River Flow Archive) and were interpolated to hourly time-steps for this application. Nutrient data at multiple sites along the Thames and its major tributaries, sampled at weekly intervals, were obtained from the UK Centre for Ecology & Hydrology's (UKCEH) Thames Initiative research platform (Bowes et al., 2018). Hourly water temperature, DO and Chl-a concentrations at Caversham, Taplow and Windsor sites (Figure 2.3) were generated by the Environment Agency's (EA) National Water Quality Instrumentation Service, using YSI6600 sensors, calibrated every 3 weeks. The quality control procedure for the data collection is provided by Waylett et al. (2013). Chl-a concentration provides a proxy for phytoplankton concentration (Bowes et al., 2012). For chlorophyll observations, aside from the hourly-frequency sensor data, the model uses UKCEH's standard laboratory methanol extraction-based weekly chlorophyll observations at Sonning and Runnymede sites.

Table 2.1: Data source (NRFA, National River Flow Archive; UKCEH, UK Centre for Ecology & Hydrology; EA, Environment Agency)

Variable	Frequency	Data source	Data source reference	Input	Calibration
Flow	Daily	NRFA	http://www.ceh.ac.uk/data/nrfa/	Main channel and tributaries	Main channel
Nitrogen and phosphorus species	Weekly	UKCEH Thames Initiative, EA UK	Bowes et al. (2018), http://environment.data.gov.uk/water-quality/view/landing	Main channel and tributaries	Main channel
Water temperature	Weekly	UKCEH Thames Initiative, EA UK	Bowes et al. (2018), http://environment.data.gov.uk/water-quality/view/landing	Tributaries	Main channel
Water temperature	Hourly	National water quality instrumentation service, EA, UK	https://doi.org/10.5281/zenodo.4288254	Main channel	Main channel
Dissolved oxygen	Hourly	National water quality instrumentation service, EA, UK	https://doi.org/10.5281/zenodo.4288254	Main channel	Main channel
Chlorophyll-a	Hourly	National water quality instrumentation service, EA, UK	https://doi.org/10.5281/zenodo.4288254	Main channel	Main channel
Chlorophyll-a	Weekly	UKCEH Thames Initiative, EA UK	Bowes et al. (2018), http://environment.data.gov.uk/water-quality/view/landing	Tributaries	Main channel

Table 2.1 Continued from previous page

Variable	Frequency	Data source	Data source reference	Input	Calibration
pH	Hourly	National water quality instrumentation service, EA, UK	https://doi.org/10.5281/zenodo.4288254	Main channel	
pH	Weekly	UKCEH Thames Initiative, EA UK	Bowes et al. (2018), http://environment.data.gov.uk/water-quality/view/landing	Tributaries	
Suspended solids	Weekly	UKCEH Thames Initiative, EA UK	Bowes et al. (2018), http://environment.data.gov.uk/water-quality/view/landing	Main channel	
Biochemical oxygen demad (BOD)	Monthly	EA UK	http://environment.data.gov.uk/water-quality/view/landing	Main channel and tributaries	Main channel
Radiation	Hourly	British Atmospheric Data Centre	http://archive.ceda.ac.uk/	Single radiation time-series	
Effluent discharge (water quality)	Monthly, constant hourly	EA UK	http://environment.data.gov.uk/water-quality/view/landing	Main channel	

The model uses single hourly radiation time-series for the whole catchment obtained from the British Atmospheric Data Centre (Mesoscale Improved Data Assimilations of Scatterometer winds Landsat data, MIDAS) for Little Rissington near the River Windrush in Gloucestershire (National Grid Reference 4299 2107). The hourly radiation time-series was modified to account for canopy shading from riparian trees using a fraction of potential solar radiation reaching the river surface as recommended by Waylett et al. (2013). Weir height and type within the river stretch were adapted from the previous model application in the River Thames (Whitehead and Hornberger, 1984). Flow-velocity relationships were derived using a set of three linearised velocity equations that reflect the river hydromorphology and the lock operations in the river (Whitehead and Hornberger, 1984; Waylett et al., 2013).

To establish confidence in the model calibration, testing of phytoplankton response during bloom periods is crucial. Often only one bloom period occurs each year. The hourly model was calibrated using the observed data of the year 2013, which encompassed one large prolonged bloom and one medium-sized bloom, and the model setup was validated using the observed data of the year 2014, which covered two distinct medium-sized blooms. The whole study stretch was divided into 23 reaches (Table B.1), accounting for the influence of tributaries, weir locations, abstractions and sewage treatment works. The hourly model used data at the top of the modelled river stretch (here Caversham) and at the influences as inputs (Figure 2.1, Figure 2.3). Model calibration was carried out using observations at four sites (Sonning, Taplow, Windsor, Runnymede) in the stretch. The calibration was performed using a sequential procedure determinand by determinand, by modifying process-rate parameters, working downstream from site to site. The order of this one by one parameter calibration and the list of sources and sinks of the variables affected by each processes are explained in detail elsewhere (Waylett et al., 2013). The model performance is judged using a combination of Nash and Sutcliffe Efficiency (NSE) and percentage error in mean (PBIAS) statistics (Appendix A).

2.2.4 *Sensitivity analysis*

Previous studies have reported dominance of diatom populations in spring and autumn seasons and green algal groups in summer periods (Lack, 1971; Ruse and Love, 1997; Read et al., 2014). The difference in the timings of dominance can be attributed to their different temperature requirements for growth. Green algae have a higher optimum growth temperature that results in their abundance in summer due to higher temperatures compared to spring/autumn. I tested the hourly model with three algal group representations, namely, *Stephanodiscus hantzschii* (SH), Green algae (GA) (including chlorophytes and cryptophytes) and small centric diatoms (SCD) (up to 15 µm diameter), differentiated based on their temperature preferences. The three models, SH, GA and SCD, use optimum temperatures of 14°C, 24.5°C and 21°C and a values of 8°C, 14°C and 12°C, respectively (in Eq. 2.1) that have been optimised for another lowland river (Descy et al., 2003). All three models were calibrated for growth, death

and respiration rate parameters and were compared with observations to derive the best model that represents phytoplankton populations in the River Thames. I also investigated the temperature constraints on Thames phytoplankton by assessing the goodness of fit of model outputs under a range of assumptions of optimum temperature for growth ranging from 10°C to 26°C with an increment of 2°C.

To evaluate the model sensitivity to change in the temporal resolution of the input data, I tested the hourly model setup with low-frequency water quality inputs. The model has a requirement of hourly time-step input data, which may not be easier to fulfil at times and require recourse to extensive interpolation of sparse data values. Data regarding radiation and hydrology are often available from routine monitoring, but high-frequency water quality information is still difficult to gather. The model setup here uses daily flow data, and hourly water temperature, dissolved oxygen, and chlorophyll data as inputs at Caversham. I filtered weekly data points (Monday, 11 am) from these high-frequency data sets, and interpolated the weekly spot samples' time-series to hourly time-steps to use as inputs in the hourly model. This way I assessed model's applicability both to generate past conditions pre-2000 in the Thames before high-frequency monitoring was established and in other catchments where only low-frequency flow and water quality monitoring is practiced.

2.2.5 *Statistical analysis*

The associations between chlorophyll and multiple environmental variables were evaluated using the BRT machine learning technique. BRT can handle continuous, collinear variables, support non-linear variables with missing data and help identify interactions between explanatory variables (Elith et al., 2008). Recently, it has been widely used to link biological water quality with multiple environmental variables simulated from process-based models (Feld et al., 2016; Rankinen et al., 2019). Here, the simulated/calculated environmental variables (flow, water temperature, nitrate, SRP, PAR) from the hourly model were linked with continuous chlorophyll observations during 2013-2014 at Windsor. R packages `gbm` (Ridgeway, 2007) and `dismo` (Hijmans et al., 2017) were used to run BRT analysis. I also used pair-wise boxplots at the Windsor site to identify favourable environmental conditions within which phytoplankton blooms develop. Hourly model outputs of controlling variables were divided in 10 equal quantile groups, and were plotted against chlorophyll simulations to derive environmental bounds of phytoplankton growth.

2.3 RESULTS

Model results are presented in four main parts: (1) the hourly model performance in simulating environmental controls and phytoplankton biomass, (2) temperature preferences of the dominant phytoplankton species in the model, (3) model testing with

lower temporal resolution of input data, and (4) identification of environmental controls and their influence on phytoplankton biomass. The model performance is evaluated according to the guidelines provided by Moriasi et al. (2007).

2.3.1 *Model calibration and validation*

2.3.1.1 *Flow and water temperature prediction*

The Thames catchment is characterised by high winter flows that decrease in early spring and remain very low during summer and autumn. The hourly model successfully captures this seasonality in flow at Windsor (Figure 2.4). The overall flow simulation indicates an under-estimation of flow volume at Windsor with a percentage mean error (PBIAS) of -9.88 and -11.58 for the calibration and validation periods, respectively (Table 2.2). In spite of the under-estimation, the model satisfactorily simulates flow variation at Windsor with very good NSE values of 0.96 and 0.95 for calibration and validation periods, respectively.

Water temperature in the model is controlled mainly by heat gain or loss from radiation, canopy shading, and the temperature of flow volumes entering the main channel. The average hourly temperature variation shows a clear cycle throughout the year, with daily minimum temperature observed in the early morning hours (6:00-8:00) and daily maximum temperature observed in the late afternoon (16:00-17:00). The temperature simulations were compared with hourly observations at Taplow and Windsor (Figure 2.4), and with weekly observations at Sonning and Runnymede sites (Table 2.2). This comparison shows that the temperature model agrees strongly with the observations throughout the study stretch, with NSE $\geq$ 0.98 and mean errors within $\pm$4% at all calibration sites (Table 2.2).

2.3.1.2 *Water chemistry and DO prediction*

The phosphorus model successfully captures the seasonal trend and magnitude of SRP concentrations with NSE $>$ 0.7 at Sonning and Runnymede (Figure 2.5). Mean error for SRP modelling is around 16% at Runnymede, whereas Sonning shows lower errors (3-6%). The nitrogen model shows relatively poorer fits for nitrate with NSE values ranging from -0.07 to 0.46. As opposed to the SRP model, the nitrate model performs better at Runnymede (NSE = 0.31, 0.46) compared to Sonning (NSE = 0.21, -0.07) for calibration and validation periods. Sonning shows an overall under-estimation (up to 6%), and Runnymede shows an overall over-estimation (up to 2%) of nitrate concentrations.

DO concentrations in the catchment begin increasing in spring, but drops to minimum levels in mid-summer. DO shows high diel variability that coincides with increased photosynthesis and respiration during phytoplankton blooms, both successfully captured by the model (Figure 2.4). The magnitude of DO concentrations, during the bloom period, is over-estimated. During the rest of the year, DO concentrations are generally under-estimated. The calibration run shows satisfactory DO fits with NSE $>$ 0.45 at all calibration sites (Table 2.2). The validation run also shows satisfactory fits at Taplow and

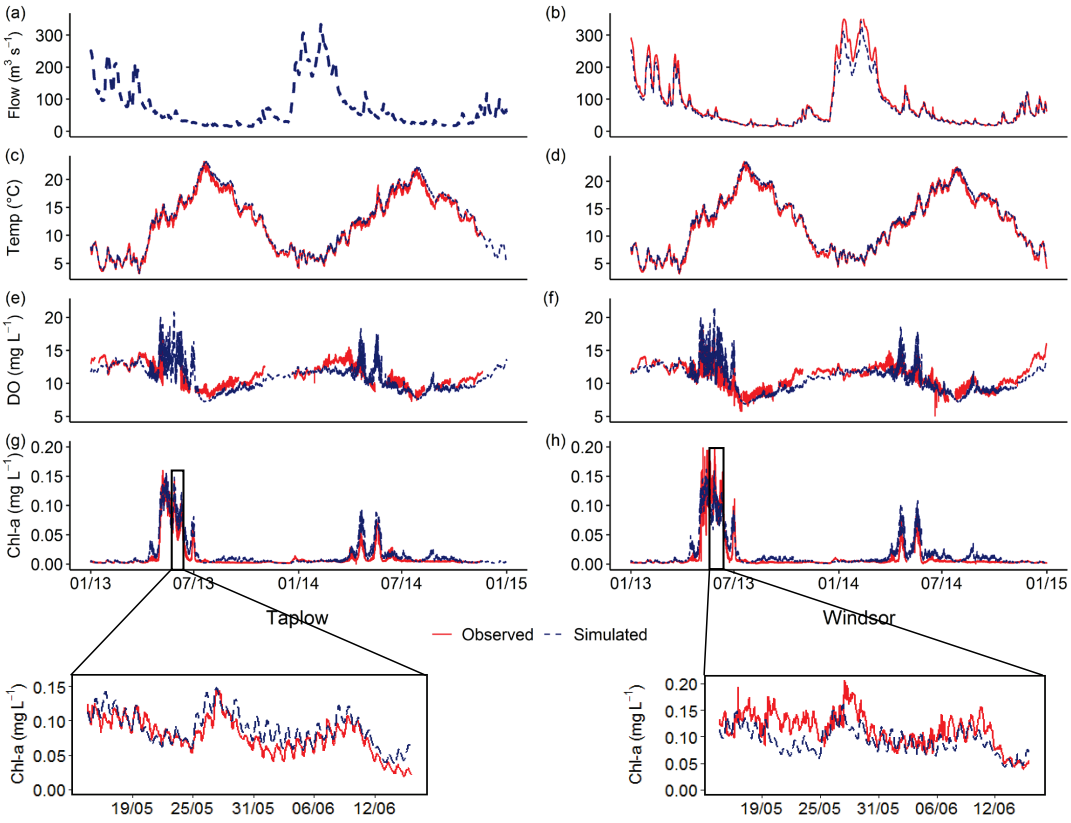

Figure 2.4: Modelled and observed hourly flow, water temperature (Temp), dissolved oxygen (DO), and chlorophyll concentrations (Chl-a) at Taplow and Windsor for calibration and validation runs. Note that observed flow data were not available at Taplow.

Table 2.2: Model performance statistics for calibration (2013) and validation periods (2014). (DO, dissolved oxygen; NSE, Nash and Sutcliffe Efficiency; PBIAS, percentage error in mean; SRP, soluble reactive phosphorus; Chl-a, chlorophyll; Temp, water temperature; Calib, calibration; Valid, validation.)

Period	Determinand	Sonning		Taplow		Windsor		Runnymede	
		NSE (-)	PBIAS (%)	NSE (-)	PBIAS (%)	NSE (-)	PBIAS (%)	NSE (-)	PBIAS (%)
Calib (2013)	Flow					0.96	-9.88		
	Temp	0.99	-2.14	0.98	3.80	0.98	3.52	0.99	1.58
	DO	0.52	12.22	0.49	-4.47	0.46	-0.93		
	Chl-a	0.81	-19.9	0.87	26.16	0.80	12.71	0.73	-34.64
	Nitrate	0.21	-4.17					0.31	1.74
	SRP	0.77	2.92					0.75	16.24
Valid (2014)	Flow					0.95	-11.58		
	Temp	0.98	-3.87	0.98	3.61	0.99	2.35	0.99	-0.9
	DO	0.25	14.99	0.43	-5.11	0.58	-4.29		
	Chl-a	0.78	-20.06	-0.19	60.93	0.20	76.73	0.77	-16.58
	Nitrate	-0.07	-5.97					0.46	1.55
	SRP	0.80	5.47					0.71	16.11

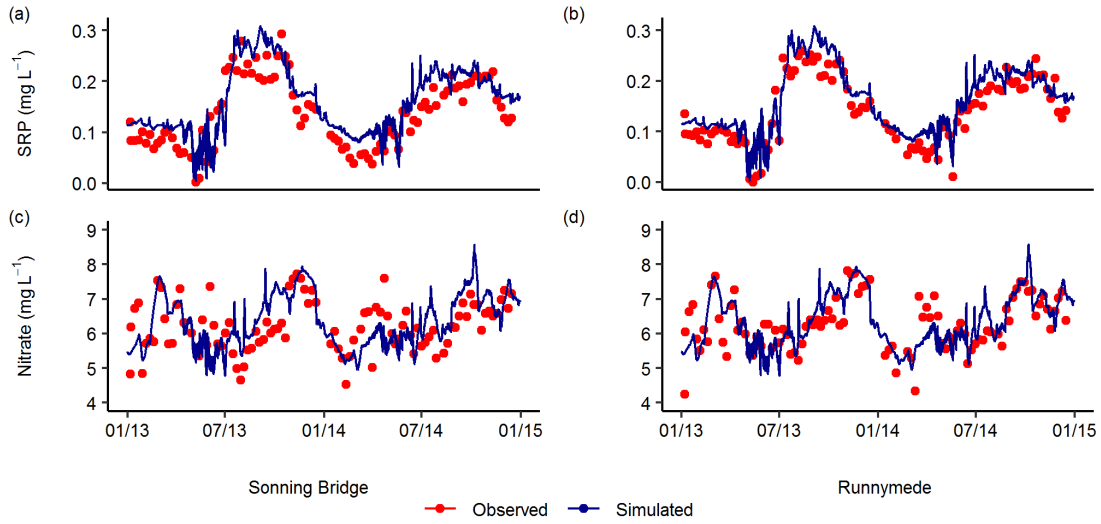

Figure 2.5: Hourly modelled and observed soluble reactive phosphorus (SRP) and nitrate concentrations at Sonning and Runnymede for calibration and validation runs.

Windsor (NSE > 0.43). Model performance at Sonning, however, drops slightly in the validation run (NSE = 0.25). The model satisfactorily captures the seasonal behaviour of DO concentrations at all calibration sites (Figure 2.4, Table 2.2).

2.3.1.3 *Phytoplankton prediction*

Phytoplankton observations during the calibration period (2013) shows much higher levels of peak blooms (up to 0.2 mg L^{-1}) compared to the validation period (2014) with less than half the magnitude (up to 0.1 mg L^{-1}) of the 2013 blooms. Peak levels in the calibration period are under-estimated, but are over-estimated for the validation period (Figure 2.4). The phytoplankton model shows a good performance for the calibration run with NSE > 0.7 at all sites (Table 2.2). Mean errors, however, are relatively high (-35% to 26%) for the calibration run. The calibration run indicates an overall under-estimation at Sonning and Runnymede, and an over-estimation at Taplow and Windsor. For the validation run, the model performs well (NSE > 0.7, PBIAS up to 20%) at Sonning and Runnymede, but with relatively poorer fits at Windsor (NSE = 0.20, PBIAS = 77%) and Taplow (NSE = -0.19, PBIAS = 61%). On average during the growing season, daily minimum and maximum phytoplankton levels are modelled around 6:00 hours and 17:00-18:00 hours, respectively (Figure 2.6a). Modelled diel variability of phytoplankton agrees well with the observations, but the model under-estimates biomass magnitude. The model predicts an increase in the bloom size and diel amplitude from upstream to downstream (Figure 2.6b). Observations also show an increase in the bloom size from Taplow to Windsor, but show reduction in the diel amplitude. Overall, the model identifies the timing of multiple blooms and collapses during the growing season and successfully models phytoplankton dynamics along the river stretch.

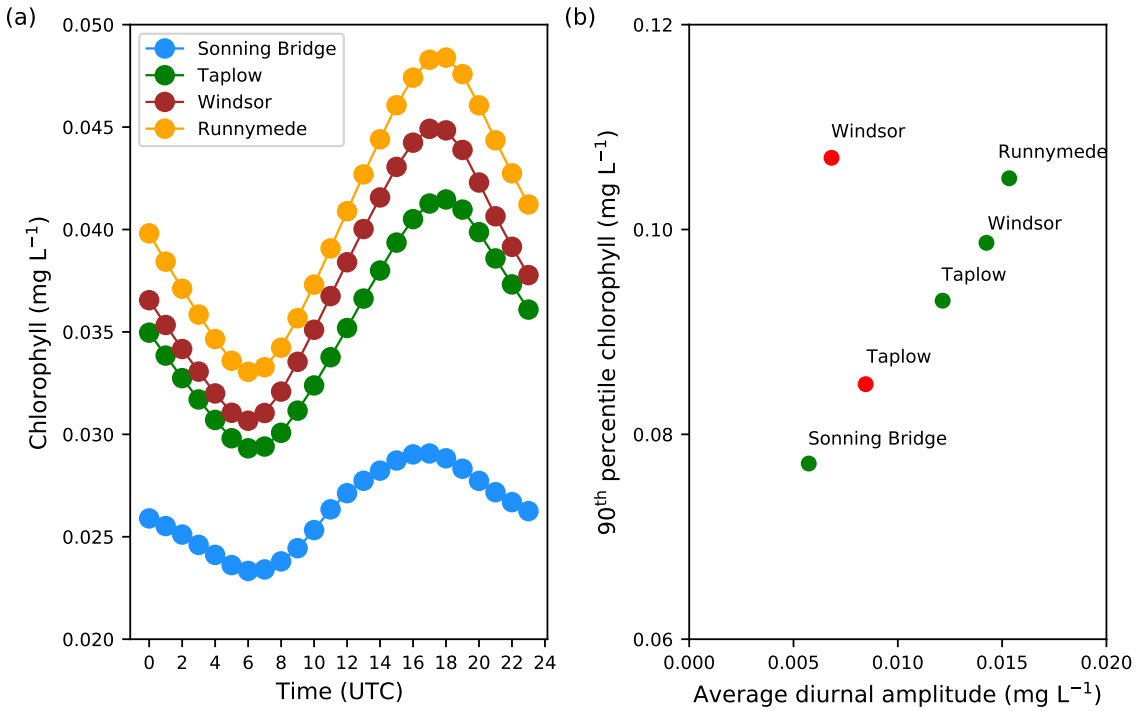

Figure 2.6: Spatial and temporal variation in phytoplankton biomass. (a) represents average diel phytoplankton variation in the model during growing period (April–July) at all calibration sites and (b) shows modelled (green markers) and observed (red markers) spatial variation in 90th percentile chlorophyll concentration with its average diel amplitude during growing period.

2.3.2 *Optimum temperature representation for phytoplankton growth*

All three models, SH, GA and SCD, simulate high biomass during April-September as shown in Figure 2.7a, which is when the differences in model performances can be seen. Although all three models perform well (NSE $>$ 0.6) at Windsor during this period, SH captures the high concentrations most accurately, which is crucial for water quality management. Moreover, GA and SCD models over-estimate biomass from mid-July to mid-September as opposed to the SH model that performs the best to capture low concentrations as well. High optimum growth temperatures in GA (24.5°C, a = 14°C) and SCD (21°C, a = 12°C) models prompt the algal growth after July with increasing water temperature (Figure 2.7a). Growth rate in the SH model, on the other hand, starts decreasing after an optimum temperature of 14°C (a = 8°C), which agrees well with the observations. Sensitivity analysis with the SH model shows better performance (Figure 2.7c) at low optimum temperatures (10–16°C) to simulate phytoplankton blooms during May-June (Figure 2.7b). At higher temperatures ($>$ 16°C), there is an over-estimation of biomass after July. Lower temperatures ($<$ 12°C), on the other hand, under-estimate the blooms at the start of July. The best model fit (NSE = 0.77) is obtained for T14 scenario at an optimum temperature of 14°C (Figure 2.7c).

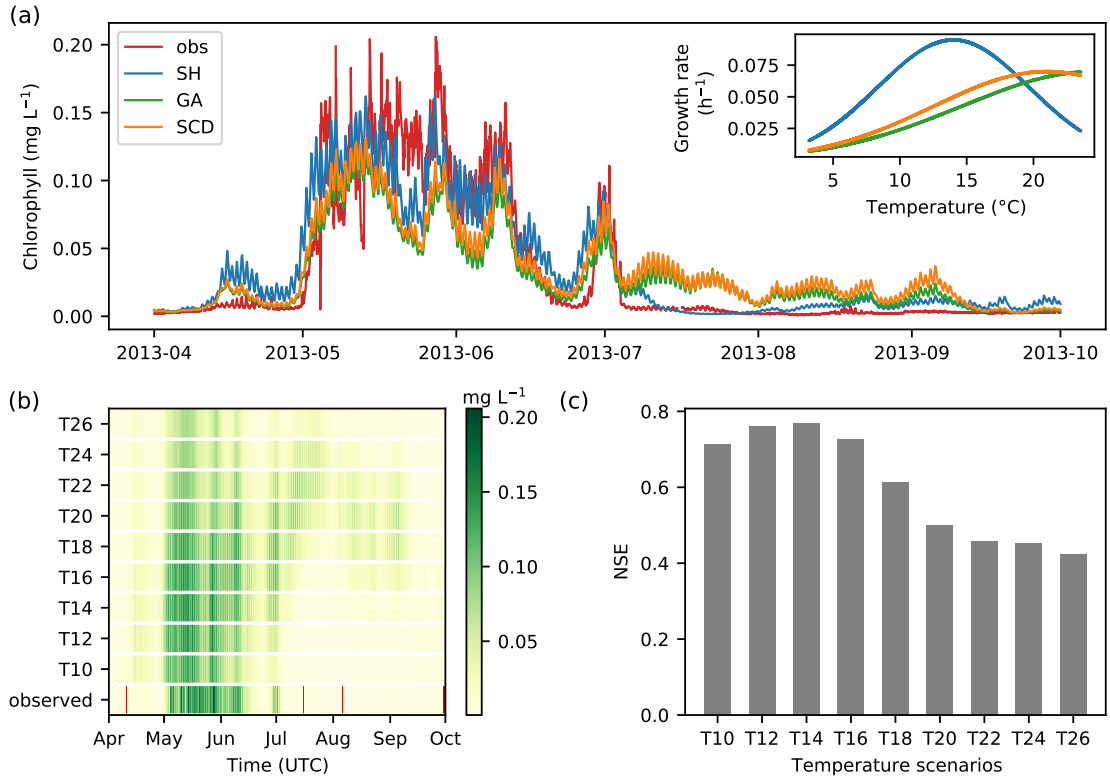

Figure 2.7: Temperature preferences of phytoplankton populations. (a) shows a comparison of modelled and observed chlorophyll concentrations for the April–September, 2013 period for SH, GA, and SCD models at Windsor. (b) represents a comparison of model performance for a range of optimum temperatures from 10°C to 26°C with an increment of 2°C at Windsor. T10 to T26 represent different optimum temperature scenarios for phytoplankton growth. Red lines represent missing data periods. (c) shows goodness of fit statistics (NSE) for all temperature scenarios from T10 to T26 at Windsor. GA, Green algae; SCD, small centric diatoms; SH, *Stephanodiscus hantzschii*.

2.3.3 *Model sensitivity*

The distribution of the simulated chlorophyll concentrations in the weekly input run does not change significantly from that of the hourly input run (Figure 2.8). Model performance declines only marginally with weekly inputs (Table 2.3) and the model captures the phytoplankton blooms. However, the weekly input run still shows a bigger lag in simulating the timings of the development and collapse of blooms compared to the hourly input run (Figure 2.8). The weekly input run also simulates higher phytoplankton growth during September and October months, than the hourly input run, when no blooms are seen in the observed data. In spite of this, the NSE statistics for the weekly input run remain above 0.6 at all sites for the calibration period (Table 2.3). Even for the validation period, the weekly input run shows NSE $>$ 0.7 at Sonning and Runnymede. Statistically, model performance at Taplow and Windsor is poor in both the runs for the validation period, although timings of blooms are represented well.

Importantly the weekly input run still uses hourly radiation time-series; both runs use single radiation time-series for the entire river stretch. The model is also tested with low-

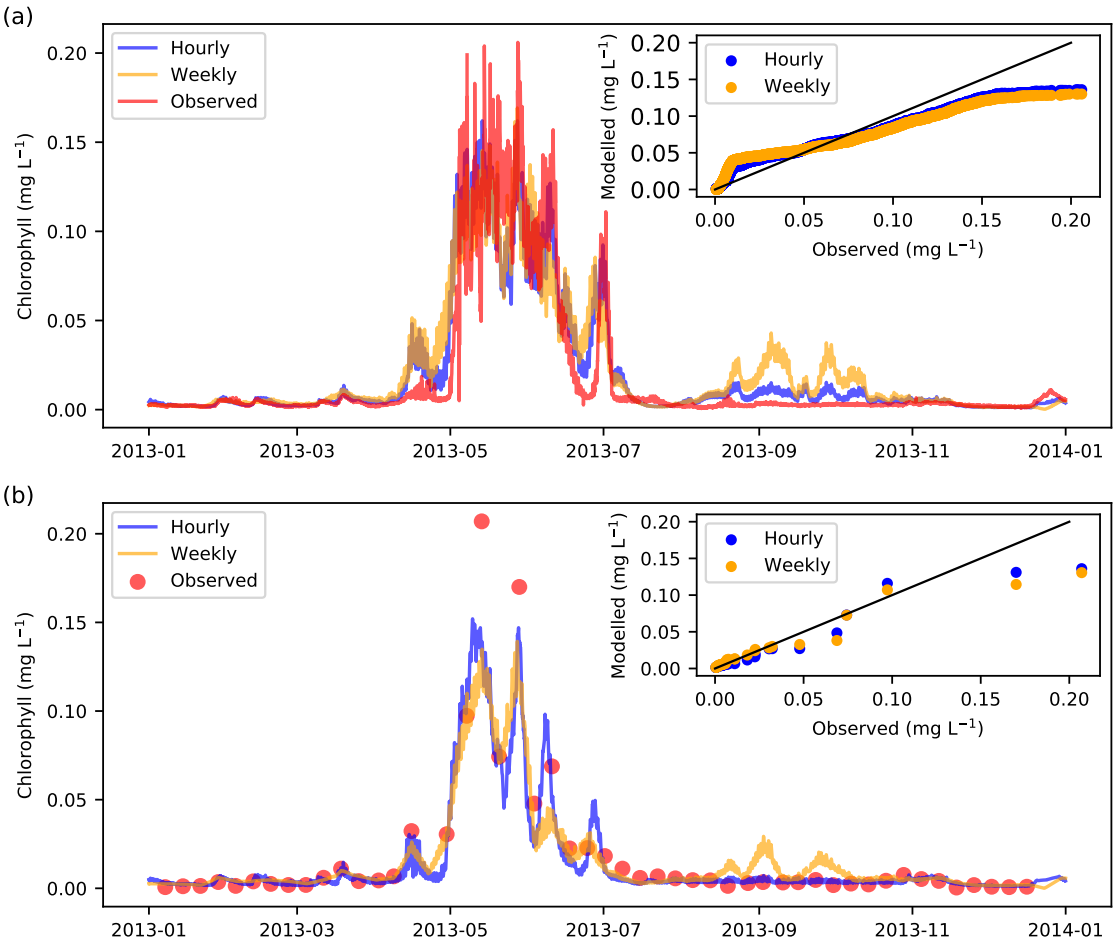

Figure 2.8: Comparison of modelled and observed chlorophyll concentrations for hourly and weekly input runs at Windsor (a) and Sonning (b). Inset figures represent quantile-quantile plots of model performances at Sonning and Windsor.

Table 2.3: Comparison of phytoplankton model performance for hourly and weekly input runs for calibration and validation periods. (NSE, Nash and Sutcliffe Efficiency; PBIAS, percentage error in mean; Calib, calibration; Valid, validation.)

Period	Model	Sonning		Taplow		Windsor		Runnymede	
		NSE (-)	PBIAS (%)	NSE (-)	PBIAS (%)	NSE (-)	PBIAS (%)	NSE (-)	PBIAS (%)
Calib (2013)	Hourly	0.81	-19.9	0.87	26.16	0.8	12.71	0.73	-34.64
	Weekly	0.83	-12.78	0.76	38.32	0.73	23.46	0.64	-29.63
Valid (2014)	Hourly	0.78	-20.06	-0.19	60.93	0.20	76.73	0.77	-16.58
	Weekly	0.83	-5.85	-0.82	90.62	-0.19	104.81	0.70	-3.72

Table 2.4: Seasonal average of limiting factors of phytoplankton growth at Windsor site as calculated in the hourly model

Season	Light	Nitrogen	Phosphorus	Temperature
Spring	0.258	0.984	0.903	0.786
Summer	0.308	0.984	0.946	0.639
Autumn	0.130	0.986	0.954	0.850
Winter	0.097	0.984	0.924	0.431

frequency radiation inputs, but it led to a significant and much larger drop in the model performance with NSE values changing from 0.87 (Taplow), 0.8 (Windsor), and 0.73 (Runnymede) to -2.57 (Taplow), -1.51 (Windsor), and 0.24 (Runnymede) with weekly radiation inputs. Even the daily scale radiation inputs affected the model performance heavily with NSE values of -2.46 (Taplow), -1.60 (Windsor), and 0.10 (Runnymede). This explains the key role of radiation inputs in modelling phytoplankton dynamics. Therefore, I conclude that the hourly model can successfully reproduce phytoplankton dynamics with low-frequency flow and water quality input data in the lower Thames, and the only input necessary at high-resolution in the model is radiation.

2.3.4 *Physicochemical controls on phytoplankton growth*

A multiple stressor analysis using BRT technique shows maximum association of SRP (58%) with chlorophyll followed by water temperature (21.6%), flow (11.6%), nitrate (7.8%) and PAR (1.1%) (Figure C.4). The reduction in nutrients (SRP and nitrate) with high chlorophyll levels suggests that nutrient levels during the growing season are influenced by phytoplankton growth rather than the other way around. It is not always clear which the dependent variable is since nutrients and chlorophyll relationships are intertwined, and hence, SRP and nitrate were removed from the list of predictors. The BRT model excluding the nutrient predictors highlights flow (55%) as the most influencing control followed by water temperature (38%) and PAR (7%). PAR does not represent a strong relationship with biomass variation in the BRT model (Figure 2.9c). Phytoplankton biomass increases with increase in flow and temperature until a certain limit of these controls is reached, and then shows a reversal of response with continued increase in the controls (Figure 2.9a-b). These relationships are also supported by pair-wise boxplots (Figure 2.9d-e), which I used to identify the environmental bounds of flow and temperature within which phytoplankton blooms develop. High phytoplankton populations > 0.03 mg L^{-1} develop with increase in temperature (11-18°C), but are not sustained at higher temperatures. Similarly, blooms only develop at low to mid flows between 30-63 m^3 s^{-1} at Windsor. This suggests that there is an optimum window of these controls where phytoplankton can bloom, and that outside this window, growth is not as strong.

Seasonal variation in growth-limiting controls of phytoplankton was assessed using the hourly model outputs. Table 2.4 represents how light, temperature and nutrient limitations

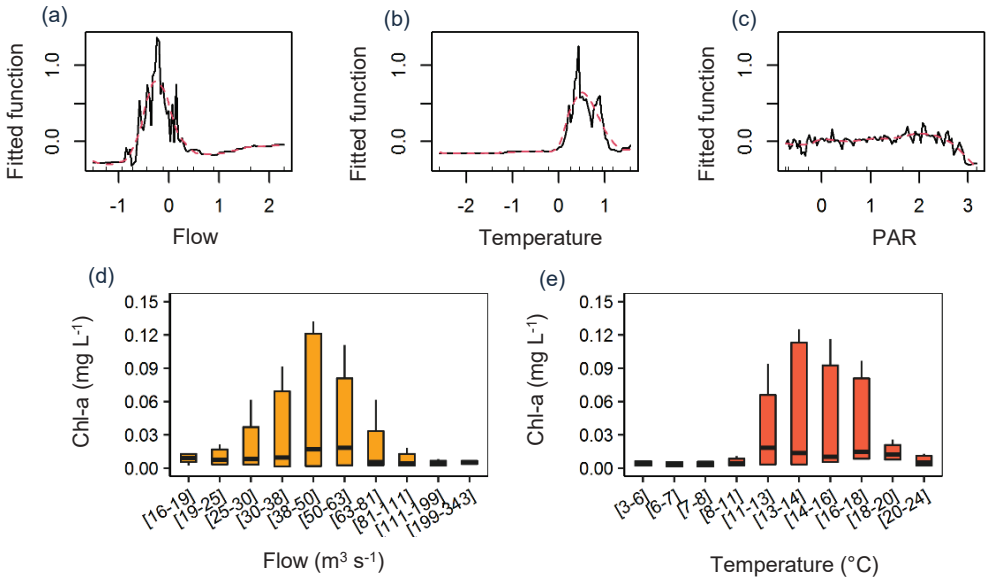

Figure 2.9: Multiple environmental controls on phytoplankton growth. (a–c) represents partial dependence plots for the modelled flow, water temperature and PAR with normalised fitted values of observed chlorophyll concentrations at Windsor in the BRT model. (d–e) represents boxplots of modelled hourly flow and water temperature against modelled hourly chlorophyll concentrations at Windsor. The hinges represent 10^{th} and 90^{th} percentile, and the line within the box represents median chlorophyll concentration. BRT, boosted regression trees; PAR, photosynthetically active radiation.

co-vary seasonally in the model. Note that higher values in Table 2.4 indicate fewer limitations on phytoplankton growth. The hourly model shows light and temperature as key controls that limit phytoplankton growth throughout the year. Seasonal light factor varies from 0.1 to 0.31, and temperature factor varies from 0.43 to 0.85. Nitrogen does not limit phytoplankton growth with its limiting coefficient always being > 0.98. Average seasonal phosphorus coefficient is also higher than 0.9 in all seasons, and remain > 0.8 during the entire monitoring period (except for a few days in May, 2013). Chemical controls do not show limitations on phytoplankton growth, but physical controls show a significant influence.

2.4 DISCUSSION

The hourly model presented here successfully simulates phytoplankton biomass along with other key determinands including flow, water temperature, nutrients and DO along the lower Thames. High-frequency observations within the catchment are utilised as model inputs as well as to support calibration of in-stream process-rate parameters that influence river water quality. Moreover, a model with low-frequency flow and water

quality inputs is also able to characterise phytoplankton dynamics in the catchment, but still requires high-resolution light information. The model representation with dominant species as *Stephanodiscus hantzschii* best explains the phytoplankton variability in the catchment, which is also applicable for many lowland rivers worldwide. The lower River Thames shows significant association of chlorophyll concentrations with residence time, water temperature and light intensity. In the following sections, I discuss the model results from the lower Thames application and review the model's applicability as a phytoplankton prediction and management tool for lowland rivers.

2.4.1 *Hourly model performance*

2.4.1.1 *Modelling environmental controls*

The hourly model successfully simulates the physicochemical and biological water quality variation across the 62 km length of the River Thames. Flow simulations in the model make use of the data of tributary inputs, abstraction volumes and sewage releases, giving very good fits (NSE > 0.9) for flows. Minor differences between the simulations and observations might be due to several reasons. Differences in the flow volume estimation (PBIAS = -9.88, -11.58) could arise because QUESTOR does not include a hydrological component to account for rainfall-runoff processes. Flow simulations highly rely on the calibration of flow routing parameters and a correct representation of water inputs and outputs in the river. The flow routing parameters, adapted from previous studies in the River Thames (Whitehead and Hornberger, 1984; Waylett et al., 2013), are well calibrated for this river. Errors might be attributable to additional influences not currently represented in the model, but these cannot be identified with the available information. Groundwater discharge into the floodplain/river might be important, but the over-estimation of low flows suggests it is less likely. Additionally, sewer overflows from STWs in urban areas close to the river are not specifically represented, which if included, could boost simulated high flows. Nevertheless, the overall model performance for flow is very good, and the model is able to capture the seasonal variability and flow magnitude.

For nutrients, the model performs better in simulating SRP (NSE > 0.7) compared to nitrate (NSE < 0.5). Despite the good NSE fits for SRP concentrations, there is a slight overestimation (Figure C.2). Due to this, phosphorus mineralisation process was switched-off for the entire stretch (Table B.3) as there was already a sufficient pool of inorganic phosphorus simulated from upstream transport, tributary and sewage works inputs. For nitrate simulations, the model simulates a rapid increase in nitrification rate downstream, with the process rate becoming more than twice the upstream rate after merging of a heavily nutrient-enriched tributary, the River Wye (Bowes et al., 2012). The over-estimation of the extreme low ($< 5^{th}$ percentile) and high ($> 99^{th}$ percentile) nitrate concentrations (Figure C.2) might be because the nitrogen sources from incoming tributaries are not well characterised. Currently, the model uses low-resolution time-series of tributary nutrient inputs, and the nitrate fits may improve with higher resolution data inputs.

Diel variability in DO concentrations increases with biomass during growing season because of the increase in autotrophic production and respiration. However, during this period, the magnitude of DO is over-estimated in spite of the good simulation of phytoplankton blooms. This may happen if one or more of the other processes influencing DO variation such as reaeration, benthic oxygen demand, BOD decay, etc. are not accurately represented in the model. However, measurements of these processes are often scarce or absent in rivers and it is difficult to pin-point the processes influencing DO fits in the lower Thames due to lack of data availability. Nevertheless, the model does not show large errors in DO estimates and represents only a minor under-estimation at Taplow (PBIAS = -4.47, -5.11) and Windsor (PBIAS = -0.93, -4.29) during both years. The overall seasonality of DO concentrations is also satisfactorily (NSE > 0.45) captured by the hourly model.

2.4.1.2 *Modelling phytoplankton biomass*

To reproduce phytoplankton dynamics, the model uses high-frequency sensor measurements, which also support the calibration of phytoplankton growth, death and respiration rate constants. Phytoplankton process-rates in rivers around the world have been observed within ranges of 0.06-3 d^{-1} (growth) and 0.06-0.17 d^{-1} (death) (Bowie et al., 1985; Everbecq et al., 2001; Reichert et al., 2001), whereas for the River Thames, studies have reported 0.2-1.35 d^{-1} for growth rate and 0.05-0.23 d^{-1} for death rate (Waylett et al., 2013; Whitehead et al., 2015; Hutchins et al., 2016). The maximum growth rate calibrated for the lower Thames is higher (2.28 d^{-1}), and the death and respiration fractions are 0.1 (Table B.3). The death constant in the model accounts for grazing and non-predatory mortality. Although phytoplankton mortality is a complex process and grazing rates in the river may vary spatially and temporally, the lack of grazing abundance data requires the model to be simple in its representation of mortality to avoid an over-parameterised model. The growth, respiration and death constants mainly control the timing and magnitude of phytoplankton blooms, which the model is able to capture broadly.

High photosynthetic production and respiration is observed during April-July, when the environmental conditions accommodate high phytoplankton growth. The model simulates a clear diel cycle during the growing season, when autotrophic production is maximum. The model successfully captures the timing and magnitude of major peaks at all calibration sites. Previous phytoplankton modelling studies at daily to annual scale in the River Thames have reported NSE values of -5.350 to 0.228 (Waylett et al., 2013), 0.34 to 0.75 (Whitehead et al., 2015) and mean error values up to $\pm$30% (Hutchins et al., 2016; Hutchins and Bowes, 2018). A recent study (Hutchins et al., 2020) with daily time-step QUESTOR model in the Thames for 2013-2014 reported NSE statistics for chlorophyll between -0.17 to 0.22 in the lower Thames reaches. This study simulates hourly phytoplankton variation for the same period, and reports NSE > 0.73 at all calibration sites and mean errors ranging from -35% to 26%. Better performance of the hourly model, compared to the previous modelling studies in the Thames, confirms the hypothesis

that high-resolution modelling can improve the predictions of timing and magnitude of phytoplankton blooms.

Model sensitivity testing with different algal groups derives SH model as the best representing model of phytoplankton growth in the lower Thames. Although the assumptions of green algae and small centric diatoms dominance also provide satisfactory fits, these models do not capture the peak blooms as well as the SH model does and over-estimate low concentrations. Previously, mixed-phytoplankton populations have been reported to best represent phytoplankton biomass in the River Thames using the daily time-step QUESTOR (Waylett et al., 2013), where phytoplankton groups were allowed to thrive regardless of temperature. However, the hourly model, with better agreement with observations, suggests that the phytoplankton in the river do not survive at higher temperatures. Thus, modelling studies at coarser resolution can sometimes result in misleading interpretations about the dominant algal communities and river processes.

The model performs the best with an optimum temperature of 14°C in the lower Thames, which is also observed in other lowland rivers (Descy et al., 2003). *Stephanodiscus hantzschii* is found to be dominant in many lowland, temperate rivers (Everbecq et al., 2001) offering a wider applicability of the hourly model. Observational studies (Lack, 1971; Bowes et al., 2012) including the flow cytometry analysis (Read et al., 2014) in the River Thames showed dominance of diatoms in spring. However, during summer, a lower biomass is observed in the river and smaller pico-chlorophytes dominate the community (Read et al., 2014). Hence, the assumption about the dominant species in the river works well for modelling phytoplankton seasonality. However, it is important to note that the dominance of phytoplankton groups in rivers may change over a year. In reality, different phytoplankton groups compete for resources and their dominance depends on multiple environmental factors that are not just limited to temperature. The current model structure does not incorporate these processes, but future research on model development should focus on including the interplay between different phytoplankton groups.

2.4.1.3 *Model uncertainties*

Process-based water quality models include uncertainties introduced from several sources such as input data quality, conceptual simplifications causing structural uncertainty, and limitations in process understanding of the modeller because of lack of sufficient data (Abbaspour et al., 2015). This is especially a problem in large lowland catchments with inputs from a considerable number of sources. The hourly model in this study is based on the QUESTOR model, which has been widely applied in rivers across Europe. QUESTOR has been tested and subjected to comprehensive sensitivity analysis elsewhere (Deflandre et al., 2006; Hutchins and Hitt, 2019). Moreover, extensive QUESTOR applications in the River Thames provide confidence in calibration of the hourly model parameters and optimised values lie within similar ranges. This study addresses the importance of inputs relative to that of in-stream processes for model predictions by testing the model with low-frequency input data. Through this exercise, I find that the model outputs are not sensitive to the time-scale of flow and water quality inputs, but are highly sensitive to

the radiation inputs. The hourly model requires high-resolution radiation information to estimate phytoplankton growth. Obtaining high-resolution radiation data is feasible either directly or indirectly based on catchment location and sunshine hours, unlike high-resolution river water quality data that are often difficult to obtain. High-frequency inputs should reduce uncertainties in the model, but sparse data from tributaries may still introduce some uncertainties. However, assessment of model uncertainty requires a much more comprehensive analysis, and is out of the scope of this study. The hourly model application in this study is a step forward in high-resolution phytoplankton modelling, and demonstrates an efficient and skilful modelling tool for simulating hourly to annual scale variation in phytoplankton biomass and its controls.

2.4.2 *Environmental controls on phytoplankton biomass*

BRT analysis provides an insight into the nature and importance of associations of phytoplankton with multiple environmental variables, and the box-plots provide information about environmental bounds of these variables that promote harmful algal blooms. River Thames exhibits high nutrient availability throughout the year, and nutrients are consumed by phytoplankton during high growth (Bowes et al., 2016). Instead of nutrient concentrations influencing phytoplankton growth, I find that in fact, the stronger control is the reverse, that of biomass on nutrient availability. Nitrate is present in excess throughout both years due primarily to diffuse input of nitrate-rich groundwaters. The delivery of nutrients to the Thames from diffuse agricultural sources is primarily during winter and autumn high flows. In contrast, phosphorus addition from point sources is constant throughout the year, resulting in high SRP levels during low summer flows (Jarvie et al., 2002). Low flows and elevated SRP levels, in theory, should promote algal growth in the river (Hilton et al., 2006). However, high chlorophyll concentrations coinciding with low SRP levels and low flows (Figure C.4) in this study suggests that (i) the residence time in the river is long enough for phosphorus uptake by phytoplankton biomass for autotrophic production, and (ii) as blooms develop, phosphorus levels start depleting in the river and become limiting.

After excluding the nutrients from the list of controls, the BRT analysis shows highest relative influence of flow (55%) followed by water temperature (38%) and PAR (7%). PAR is sufficiently available throughout the year accounting for the pattern in the relationship between chlorophyll and PAR (Figure 2.9c). This contrasts with findings from the process-based modelling exercise, where high-resolution light information is a crucial predictor to model accurate timing and magnitude of phytoplankton blooms. Light is a complex parameter to consider compared to the other environmental variables as the influence of light on phytoplankton can be a function of past light information in terms of its timing, periodicity and intensity over time (Bowes et al., 2016). Moreover, phytoplankton growth is also influenced by seasonal changes in riparian shading (Hutchins et al., 2010), which are hard to capture in the BRT model using only a simple measurement of PAR. Hourly

Table 2.5: Comparison of environmental bounds (for chlorophyll-a > 0.03 mg L^{-1}) along the river. Thresholds at Caversham were reported by Bowes et al. (2016). (Temp, water temperature)

Variable	Observed		Modelled		
	Caversham	Windsor	Sonning	Windsor	Runnymede
Flow (m^3 s^{-1})	< 30	32-68	28-51	30-63	21-54
Temp (°C)	9-19	10-17	11-18	11-18	11-18

process-based modelling, on the other hand, accounts for these details, albeit with specific assumptions about incoming light information and riparian shading patterns.

Flow and temperature showed an important control on phytoplankton growth. The interactions between flow versus temperature and PAR versus flow also showed significant influences. High PAR promotes phytoplankton growth only at low-mid flows. Moreover, large blooms are observed when temperature and flow interacts within specific ranges. Phytoplankton growth at Caversham has been reported to respond to certain flow and temperature thresholds (Bowes et al., 2016). Downstream of Caversham, lower and upper flow bounds exist for phytoplankton growth (Table 2.5). Majority of high simulated chlorophyll (> 0.03 mg L^{-1}) concentrations only occur when flows are between 21–63 m^3 s^{-1} in contrast to Bowes et al. (2016) who only found high concentrations below 30 m^3 s^{-1} from analysing five years (2009-2013) of high-frequency measurements at Caversham. Flow bounds identified from the observations at Windsor (32-68 m^3 s^{-1}) are in a similar range to the modelled bounds (Table 2.5). Phytoplankton blooms only develop at low flows (< 51-63 m^3 s^{-1} here), when the residence time is long enough for phytoplankton growth. However, the presence of a lower flow bound (> 21-30 m^3 s^{-1} here), below which high concentrations do not occur, also suggests that the phytoplankton biomass cannot remain suspended when the flow becomes too low (< 20 m^3 s^{-1}), and settle in the river (Balbi, 2000).

Due to the SH model assumption of an optimum temperature for growth of 14°C , a consistent temperature range, within which high concentrations are simulated (11-18°C, Table 2.5), is apparent throughout the stretch. Observed data show a temperature range of 10-17°C at Windsor, whereas Bowes et al. (2016) reported a temperature range of 9-19°C at Caversham. The slightly different bounds for temperature are likely indicative of a more complex system than that represented in the model. These differences are likely to reflect largely dominant cool water centric diatoms, but with secondary influences from other groups, such as groups thriving in warmer conditions and attached algae mobilised under turbulent conditions at lower temperatures. Important environmental controls found in this study (flow, light, temperature) are consistent with the findings from other lowland rivers around the world such as the Murray (Bormans and Webster, 1999), the Meuse (Everbecq et al., 2001) and the Severn(Reynolds and Glaister, 1993). Some lowland studies have also highlighted the importance of chemical (nutrients) and biological (grazing) controls, but these are shown to become significant only when physical constraints are reduced (Billen et al., 1994; Reynolds and Descy, 1996; Gosselain et al., 1998).

2.4.3 *Flow regulation and water quality*

Physical factors, such as river residence time and flow variability, play an important role in controlling phytoplankton growth in lowland rivers (Reynolds, 2000). High flows prevent growth by rapid flushing of phytoplankton biomass. The lower Thames reaches are deeper than the upstream reaches with slow-moving water enriched by high floods in the winter and consistent low flows during the rest of the year. Moreover, locks and weirs for navigation throughout the river stretch slow the flow, resulting in increased residence times (Hutchins and Bowes, 2018). Median residence time in the river stretch in this study during 2013-2014 was 40 hours, which varied from 9 to 112 hours at very high (90^{th} percentile) and very low (10^{th} percentile) flows, respectively. One possible solution to avoid high phytoplankton growth in rivers could be via the maintenance of river flow above critical thresholds (Wang et al., 2019), in line with environmental flow concepts (Poff and Zimmerman, 2010). Experimental flow releases have proved to facilitate maintenance of chemical and biological water quality in regulated rivers elsewhere (Lind et al., 2007; Gillespie et al., 2020). As discussed in the previous section, high phytoplankton biomass in the lower Thames is only encountered at low flows below 60 m^3 s^{-1}. Although more evidence is required to use this threshold as a minimum environmental flow in the river, short pulses of high flow release could act as a measure to prevent large algal bloom developments in regulated, lowland rivers like Thames.

2.5 CONCLUSION

An hourly river model is developed for a 62 km stretch in the lower River Thames. By including an hourly mass balance, the model successfully simulates flow, water temperature, DO, nutrients and phytoplankton biomass in the river. The model satisfactorily captures diel variation of phytoplankton dynamics as well as the magnitude and timing of bloom events. The hourly model in this study represents better goodness of fits compared to the previous daily time-step modelling studies in the Thames, and thus, confirms the hypothesis that high temporal-resolution modelling improves phytoplankton growth prediction. The model can predict phytoplankton dynamics from low-resolution water flow and quality with hourly resolution data only needed for solar radiation. This offers a possibility of model application in catchments where high-frequency measurements are not available.

From a range of algal groups tested under sensitivity analysis, a model assuming *Stephanodiscus hantzschii* with optimum growth at 14°C to predominate best represented biomass variation. *Stephanodiscus hantzschii* is also predominant in many lowland rivers worldwide. The model can easily be applied elsewhere and also be adapted in its parameterisation to reflect dominance by different species if needed. Phytoplankton growth in the lower Thames is mainly influenced by hydrological (residence time) and physical controls (water temperature, light intensity), which is typically found in lowland rivers worldwide. I observe that phytoplankton blooms only develop within specific flow

bounds (21-63 m^3 s^{-1}). Identification of flow bounds is useful to prevent major bloom developments and to maintain river water quality. Hence, short-term high-flow release (here, above 60 m^3 s^{-1}), as experimented in other regulated rivers, could form a potential management strategy in critical situations.

This is the first study where a high-resolution hourly model is validated against similarly high-frequency biomass observations. To my knowledge, river modelling studies with all environmental controls at such a temporal and spatial extent have not previously been undertaken. It offers the following powerful possibilities:

(1) feasibility for hourly model application in any river with a single continuous water quality monitoring site in the lower reaches,

(2) reconstruction of past long-term changes in hourly water quality dynamics before continuous monitoring with sensors was widely available,

(3) application to provide early warnings of phytoplankton blooms as well as to evaluate management strategies using scenario analysis,

(4) hourly-scale DO curves and biomass information can be further interpreted to evaluate ecosystem metabolism and to identify low night-time oxygen levels that may threaten ecological health,

(5) the costs for high-frequency monitoring over multiple sites within the river network can be reduced if a reliable modelling tool such as the one described in this study is available.

3

HIGH-RESOLUTION WATER-QUALITY AND ECOSYSTEM-METABOLISM MODELLING IN LOWLAND RIVERS

3.1 INTRODUCTION

Assessments of river ecosystem health have traditionally relied on structural indicators such as channel morphology, water quality or the composition of biological communities (Von Schiller et al., 2017). However, with the advances in high-resolution monitoring techniques (Rode et al., 2016), sensor networks and linked modelling tools are gaining traction for prediction of functional indicators such as ecosystem metabolism. Conventional methods of metabolism modelling, based on Odum (1956)'s open-channel approach, estimate metabolism rates at a river-reach level using continuous dissolved oxygen (DO) measurements at a single site (e.g. one-station method, Izagirre et al., 2007) or two sites over a reach (e.g. two-station method, Hall Jr and Tank, 2005; Halbedel and Büttner, 2014). These models do not account for the influence of upstream changes on the downstream DO advection and transformations within the river network. Moreover, these models do not specifically account for changes in river hydrology and biogeochemistry (exceptions include Payn et al., 2017; Segatto et al., 2020), which could have a critical impact on DO dynamics in the river. Therefore, such models may provide biased interpretations of metabolism estimates (Payn et al., 2017) if the metabolic regime is sensitive to changes in these environmental stressors at the time-step of calculation.

Ecosystem metabolism characterises carbon fixation and mineralisation through gross primary production (GPP) and ecosystem respiration (ER). GPP and ER are sensitive to multiple stressors, which act independently or in combination with other stressors (Heathwaite, 2010; Von Schiller et al., 2017) often presenting a complex interplay of controls. ER is regulated by water temperature (Demars et al., 2011; Perkins et al., 2012) and organic matter supply (Young et al., 2008). Often, light (Mulholland et al., 2001) and in some cases, nutrient availability (Guasch et al., 1995) control GPP. Flow is also an important regulator of GPP. Flooding disrupts GPP seasonality through scouring of benthic producers and organic matter (Uehlinger, 2006) as well as by reducing light availability in sediment-mobilized turbid waters (Aspray et al., 2017). Slow-flowing rivers with clear waters are typically autotrophic due to high light availability and stable flow regimes (Acuña et al., 2011) whilst faster-flowing rivers are typically heterotrophic. Measuring these spatial and temporal dynamics can be difficult, since the spatial resolution of sensor networks is largely limited by logistics of multi-site set up, maintenance and data collection/validation.

GPP and ER estimates from conventional DO mass-balance models are usually empirically related to different environmental stressors to evaluate their sensitivity to these stressors (Izagirre et al., 2008; Beaulieu et al., 2013; Aspray et al., 2017). However, it is also

important to associate these stressors mechanistically to GPP and ER to better understand the underlying controls of metabolic regimes in rivers as well as to predict changes in river metabolism outside the range of the available observations. Whereas several mechanistic water quality models (e.g. Enhanced stream water quality model, Brown and Barnwell (1987); River water quality model, Reichert et al. (2001)) include biochemical processes that affect DO transformations in the water column, they are generally only tested at daily to weekly time-steps. The coarse testing limits their use for metabolism estimation, which is susceptible to sub-daily changes in hydrology and biochemical water quality (Roberts et al., 2007; Izagirre et al., 2008). Therefore, here I combine DO and metabolism modelling using an existing, hourly scale, mechanistic water quality model, the hourly Quality Evaluation and Simulation Tool for River-systems (QUESTOR) model (Chapter 2, Pathak et al., 2021). I implement this approach in a lowland river, the River Thames, in southern England.

QUESTOR is a process-based, in-stream water quality model, which simulates hourly scale variation and transport of river flows, water temperature, DO, nutrients, and phytoplankton biomass in a river network. The model has been previously tested to predict diel variation in physicochemical water quality and phytoplankton biomass in the lower River Thames (Chapter 2, Pathak et al., 2021). I advance this work to estimate metabolism rates from the DO mass-balance module. The hourly QUESTOR model simulates diel changes in the environmental stressors (e.g. light, temperature, flow, nutrients) and their resulting impact on ecosystem productivity and respiration. The model, however, has a relatively more complex structure with many model parameters, thus carrying a risk of attached uncertainties and parameter equifinality during the calibration. Nonetheless, I reduce parameter uncertainties during the calibration process by making use of the abundant literature on water quality modelling that exists for the River Thames catchment (Whitehead and Hornberger, 1984; Waylett et al., 2013; Whitehead et al., 2015; Hutchins et al., 2018)

Whilst process-based models realistically represent the sensitivities of the system to key drivers (Hrachowitz et al., 2014) and capture the short term dynamics (Jankowski et al., 2021), empirical models have long-standing pedigree in providing insight into ecosystems' response to multiple stressors (Izagirre et al., 2008; Beaulieu et al., 2013). Specifically, with the development of machine learning techniques, empirical models can utilise data to learn and increasingly improve model performance (Elith et al., 2008; Feld et al., 2016). Therefore, in addition to the process-based model, I also use an empirical approach to assess the sensitivity of modelled metabolism rates to multiple stressors. A comparison of both models is made to test if the empirical approach can provide accurate predictions and substitute process-based modelling for rapid assessments of river ecosystem health.

The main aims of the study are:

(1) To develop a process-based approach for coupled modelling of in-stream hydrology, biochemical water quality and ecosystem metabolism in lowland rivers.

(2) To analyse spatio-temporal variation in the metabolic regime within the modelled river network (Thames, England).

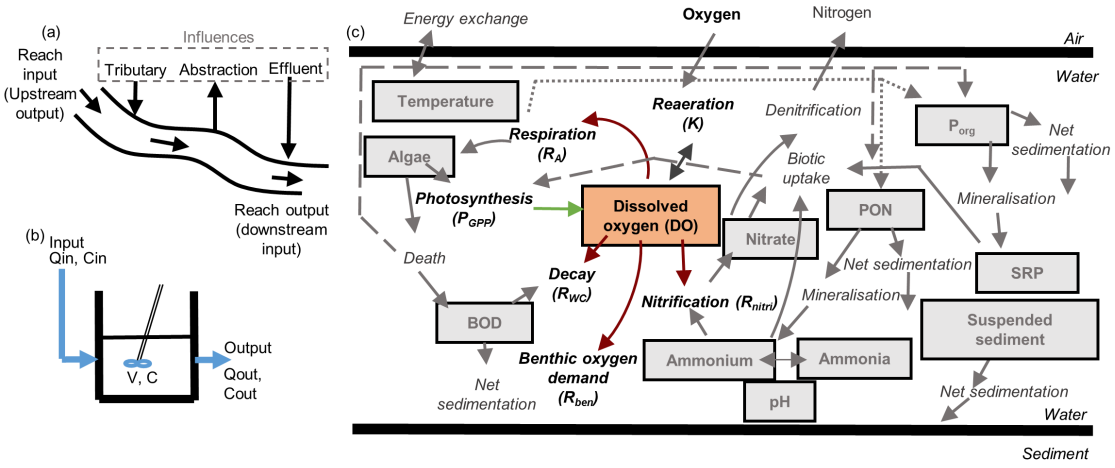

Figure 3.1: Model structure and processes (modified after Pathak et al., 2021). (a) represents the schematic of a typical reach, (b) shows the conceptualization of reaches (C, solute concentration; Q, flow; V, volume), and (c) describes the water quality determinands and processes in the model. BOD, biochemical oxygen demand; PON, particulate organic nitrogen; P_{org}, organic phosphorus; SRP, inorganic phosphorus; SS, suspended sediment.

(3) To perform a sensitivity analysis of GPP and ER to physicochemical determinands using random forest machine learning technique and generalised least squares (GLS) regression modelling.

3.2 METHODS

3.2.1 *Modelling approach*

I use the process-based, hourly QUESTOR model tested in the lower Thames in Chapter 2 (Pathak et al., 2021). A detailed set of equations for all the key variables is provided in Chapter 2 and Appendix A. Here, I summarise the flow and DO modules of the hourly model, and describe the equations for ecosystem metabolism estimation.

3.2.1.1 *Flow routing module*

A simple mass-balance of incoming and outgoing flows is used. The incoming flow in the reach is the balance of the upstream flows plus point-source discharges minus abstractions. Flow inputs from the tributaries at the main channel confluence are scaled upwards based on the location (often some distance upstream) of the gauging station and the contributing catchment area (Hutchins et al., 2020). Therefore, this indirectly includes groundwater contribution at the tributary confluences with the main Thames.

Groundwater contribution to and from the main Thames is assumed to be in balance. Outflow of water from a reach is calculated as,

$$\frac{dQ_{out}}{dt} = \frac{Q_{in} - Q_{out}}{\tau(1-c)} \tag{3.1}$$

where Q_{in} is the total flow into the reach (m^3 s^{-1}), Q_{out} is the flow out of the reach (m^3 s^{-1}), t is the time-step (h), τ is the residence time (h) derived by $l/bQ_{out}{}^c$, l is the length of the reach (m), b and c are reach-specific constants. Constants b and c are calibrated from flow-velocity relationships ($v = bQ_{out}{}^c$), which characterise the hydromorphology and lock operations in the river (Whitehead and Hornberger, 1984; Waylett et al., 2013). The flow routing model facilitates modelling of river residence time, which allows inclusion of the influence of hydrological variation on DO dynamics as discussed in the next section.

3.2.1.2 *Dissolved oxygen module*

The processes controlling DO concentrations within a reach include (a) DO advection, (b) production of oxygen from GPP, (c) loss of oxygen from ER, and (d) oxygen change from reaeration

$$\frac{dC_{DO,o}}{dt} = \frac{1}{\tau}(C_{DO,i} - C_{DO,o} + W) + P_{GPP} - R_{ER} + F \tag{3.2}$$

where $C_{DO,i}$ is the input DO concentration (mg L^{-1}), $C_{DO,o}$ is the output DO concentration (mg L^{-1}), W is the aeration at weirs (mg O_2 L^{-1}), P_{GPP} is the gross primary production (mg O_2 L^{-1} h^{-1}), R_{ER} is the ecosystem respiration (mg O_2 L^{-1} h^{-1}) and F is the aeration at the air-water surface (mg O_2 L^{-1} h^{-1}).

3.2.1.3 *Ecosystem Metabolism*

Oxygen production

Rate of oxygen production (P_{GPP}, mg O_2 L^{-1} h^{-1}) in the river (Eq. 3.3) is given by,

$$P_{GPP} = P_P + P_N \tag{3.3}$$

where P_P is the photosynthetic production (mg O_2 L^{-1} h^{-1}) and P_N is the oxygen produced during nitrate assimilation by phytoplankton (mg O_2 L^{-1} h^{-1}). Although the hourly model supports modelling of macrophytes and benthic algae, this study only includes modelling of phytoplankton biomass, since it is the dominant driver of metabolism in the study stretch (Whitehead and Hornberger, 1984; Lázár et al., 2012). The hourly model not only includes the influence of phytoplankton biomass on DO variation, but also accounts for the influence of light, temperature and nutrient availability on photosynthesis. These details are explained in the description of the phytoplankton model in Chapter 2. Here, I only summarise the equations directly relevant to the DO model.

P_P is a function of photosynthetic rate and phytoplankton concentration in the water column,

$$P_P = k^{pho}(\frac{32}{12}\Delta) \tag{3.4}$$

k^{pho} is the gross photosynthetic rate of autotrophs representing increase in Chl-a during photosynthesis (mg L^{-1} h^{-1}) and Δ is the ratio of carbon to Chl-a in autotrophs (50, Bowie et al., 1985). The ratio of 32/12 represents the mass of oxygen produced in photosynthesis or consumed in respiration per unit mass of carbon fixed.

P_N is estimated as,

$$P_N = k^{pho}(1 - n_{pref})\alpha \tag{3.5}$$

n_{pref} is the autotroph preference for ammonia and α is the ratio of nitrogen to Chl-a in autotrophs (10, Bowie et al., 1985).

$$n_{pref} = \frac{k_{pref}C_{NH4,o}}{k_{pref}C_{NH4,o} + (1 - k_{pref})C_{NO3,o}} \tag{3.6}$$

$C_{NH4,o}$ is the NH_4^+ concentration (mg L^{-1}), $C_{NO3,o}$ is the NO_3^- concentration (mg L^{-1}) and k_{pref} is the preference factor for ammonia over nitrate (Table B.2).

Oxygen depletion

Rate of oxygen depletion (R_{ER}, mg O_2 L^{-1} h^{-1}) in the river includes four pathways

$$R_{ER} = R_A + R_{nitri} + R_{ben} + R_{wc} \tag{3.7}$$

R_A is the autotrophic respiration (mg O_2 L^{-1} h^{-1}), R_{nitri} is the assimilation of oxygen in the process of nitrification of ammonium to nitrate (mg O_2 L^{-1} h^{-1}), R_{ben} is the sediment oxygen demand (benthic respiration) (mg O_2 L^{-1} h^{-1}) and R_{wc} is the BOD in the water column (mg O_2 L^{-1} h^{-1}). R_A is a function of phytoplankton respiration rate (k_{res}, mg O_2 L^{-1} h^{-1}) and temperature. k_{res} is modelled in the phytoplankton model as described in Chapter 2.

$$R_A = k^{res}(\frac{32}{12}\Delta) \tag{3.8}$$

R_{nitri} involves conversion of ammonium to nitrate and requires oxygen for this conversion,

$$R_{nitri} = 4.57k_{nit}C_{NH4,o}\left(\frac{C_{DO,o}}{C_{DO,o} + S_{nitri}}\right) \tag{3.9}$$

k_{nit} is the nitrification rate (h^{-1}) and S_{nitri} is the DO half-saturation concentration for nitrification (mg L^{-1}). The coefficient, 4.57 is derived from the stoichiometry of the reactions and represents the oxygen required to convert ammonia to nitrate.

R_{ben} represents the transfer of oxygen between the overlying water and the sediments (Cox, 2003b). The benthic respiration rate (k_{ben}, h^{-1}) is simulated as a function of stream depth and temperature, where the stream depth and water column oxygen concentration represents the availability of oxygen to the bed.

$$R_{ben} = k_{ben} C_{DO,o} \tag{3.10}$$

$$k_{ben} = \frac{k_{ben20}}{z} \theta^{T - T_{ref}} \tag{3.11}$$

k_{ben20} is a unitless coefficient provided by the user during the calibration, z is the mean water depth of the reach (m), T is the water temperature (°C), T_{ref} is the reference temperature (20°C) and θ is a temperature correction factor (1.08).

R_{wc} represents carbonaceous deoxygenation where oxygen in the water column is consumed by heterotrophic bacteria.

$$R_{wc} = k_{bod} C_{BOD,o} \left(\frac{C_{DO,o}}{C_{DO,o} + S_{bod}} \right) \tag{3.12}$$

k_{bod} is the rate of loss of DO as BOD decays (h^{-1}) and S_{bod} is the half-saturation concentration for the use of DO to satisfy BOD (mg L^{-1}). Note that sedimentation and phytoplankton death also influence BOD as described in Appendix A.

Process rate coefficients for nitrification and BOD in the model are temperature-dependent,

$$k_T = k_{Tref} \theta^{(T - T_{ref})} \tag{3.13}$$

k_T is the process rate at T °C (h^{-1}) and k_{Tref} is the process rate (h^{-1}) at a reference temperature (20°C).

Reaeration

Reaeration estimation (K) in the model accounts for reaeration at the water surface and at weirs. Reaeration at the water surface represents the rate of change in DO concentration (F, mg O_2 L^{-1} h^{-1}) in the water column via the exchange at the air-water interface. F is represented by a transfer coefficient (k_{rea}, h^{-1}, see Appendix A) and a DO deficit term, which is the difference between the saturated DO concentration (O_{sat}, mg L^{-1}) and the actual DO concentration ($C_{DO,o}$, mg L^{-1}) in the water column,

$$F = k_{rea}(O_{sat} - C_{DO,o}) \tag{3.14}$$

Weirs in the river create a head loss, which can aerate or deaerate water depending upon the upstream DO concentrations, creating an instantaneous change in the DO

concentrations. Hence, it is important to consider weirs, especially in a heavily regulated river like the Thames. The aeration effect of weirs (W, mg L^{-1}) is calculated as,

$$W = O_{sat} - \left[\frac{O_{sat} - C_{DO,o}}{R_{ODR}} \right] \tag{3.15}$$

R_{ODR} is the oxygen deficit ratio (Appendix A).

3.2.2 *Empirical analysis*

I performed site-wise (Sonning and Runnymede) GLS regression to examine the sensitivity of GPP and ER to observations of multiple physicochemical determinands. The observations of physicochemical determinands were available on a weekly basis and comprised flow, PAR, water temperature, dissolved inorganic nitrogen (DIN), SRP, dissolved organic carbon (DOC) and suspended sediment (SS) concentration. Temperature observations were transformed to $1/(k_b T)$ as per the Metabolic Theory of Ecology, where T is the temperature in Kelvin and k_b is the Boltzmann constant (8.62 $\times 10^{-5}$ eV K^{-1}). GLS was used to account for the residual autocorrelation using the `nlme` package (Pinheiro et al., 2007). Selection of relevant predictors for GLS models was carried out following Feld et al. (2016). All predictors were log-transformed followed by variable centering (mean = 0) and standardisation (standard deviation = 1) to obtain standardised effect sizes. Collinearity between the predictors was resolved based on a variance inflation factor. A step-wise removal of collinear variables (with a threshold of variance inflation factor > 3, Zuur et al., 2010) was performed with the `usdm` R package (Naimi, 2015). In spite of the collinearity issue, I kept flow in the list of predictors because of its biological relevance.

I performed an exploratory analysis using the random forest (Breiman, 2001) machine learning technique (`randomForestSRC` package, Ishwaran and Kogalur, 2017) to derive the hierarchy of the most influential stressors and interactions that explain GPP and ER dynamics. Random forest analysis aggregates predictions made by multiple decision trees that are trained on bootstrapped data subsets and tested against the remaining observations (Feld et al., 2016). Important stressors and interactions derived from variance inflation factor and random forest analyses were included in the GLS models for the sensitivity analysis. I also added seasonality effect in the GLS models using sine and cosine functions to the week of the year (j), as $sin(2\pi j/52)$ and $cos(2\pi j/52)$ (Watson et al., 2001). Based on Akaike (1973) information criterion, I tested three types of GLS models by including (1) only seasonality predictors, (2) only environmental predictors, and (3) seasonality plus environmental predictors. The best predictors and autocorrelation structure were selected by comparing Akaike information criterion values of all participant models. I selected the final model using a multi-model inference procedure (Grueber et al., 2011). This process includes supplying a global model with the best predictors and autocorrelation structure, and running all possible combinations of models using the

dredge() function in the `MuMIn` package (Barton, 2016). The best approximating model with the highest Akaike weight was chosen as the final model.

I also used river water fluorescence observations (collected at weekly resolution from January to July in 2013 and less frequently at other times during 2013-2014 at Sonning and Runnymede sites: for details see Old et al., 2019) to explore whether ER prediction could be improved by adding water fluorescence information in the GLS models. Fluorescence signals contain information about organic matter composition. Specifically, tryptophan-like fluorescence represents degradable organic matter from farm wastes and sewage discharges and hence, can be related to river BOD (here, R_{wc}) (Hudson et al., 2008). Therefore, my goal was to check if the modelled R_{wc} could be explained in terms of tryptophan-like fluorescence.

3.3 RESULTS

3.3.1 *Model performance*

The model satisfactorily reproduced flow, physicochemical water quality and biomass variation along the river stretch (Table 2.2, Figure 2.4,2.5) (details in Chapter 2, Pathak et al., 2021). High diel fluctuations in DO coincided with high phytoplankton blooms and low flows (Figure 2.4). DO levels were slightly over-estimated in spring and under-estimated during the rest of year. Seasonality and timings of high diel fluctuations were well-captured by the model with Nash and Sutcliffe Efficiency > 0.47 and percentage error in mean up to 11% (Table B.4). Sonning showed overall over-estimation (up to 14%) of DO concentrations as opposed to Taplow and Windsor, which showed slightly under-estimated (up to 8%) DO concentrations (Table B.4). Overall, the model satisfactorily captured the seasonality of DO concentrations along the river stretch.

3.3.2 *Spatio-temporal variation in ecosystem metabolism*

GPP followed phytoplankton seasonality showing maximum productivity during the biomass growing season and low productivity during the rest of the year (Figure 3.2). Peak GPP was higher in 2013 (up to 21 mg O_2 L^{-1} d^{-1}) compared to 2014 ($>$ 10 mg O_2 L^{-1} d^{-1}) due to relative inter-annual magnitudes of phytoplankton blooms (Figure 2.4). Increase in nutrient concentrations did not result in increase in GPP. In contrast, primary production during the growing season reduced nutrient concentrations through uptake (Figure C.10). During the growing season, ER was dominated by autotrophic respiration and more or less mirrored the GPP trend, although with a lesser magnitude ($<$ 10 mg O_2 L^{-1} d^{-1}). In comparison to Runnymede (downstream end), Sonning (upstream site) was characterised by higher nitrification loss throughout the year and higher R_A during the growing season, resulting in generally higher ER upstream.

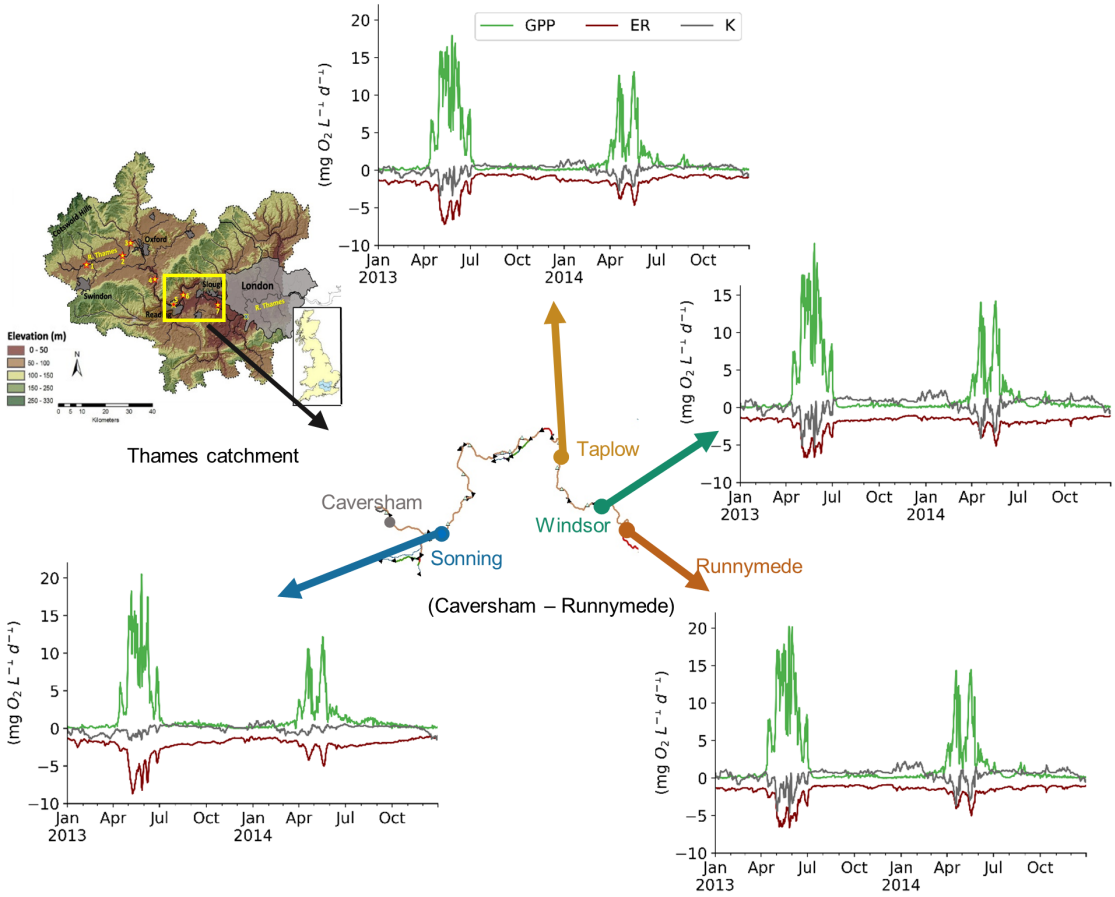

Figure 3.2: River Thames catchment and time-series of modelled gross primary production (GPP), ecosystem respiration (ER), and reaeration (K) aggregated at daily scale at Sonning, Taplow, Windsor, and Runnymede sites during 2013–2014. The catchment map at the top left corner is adapted from Bowes et al. (2016)

Values of k_{rea} varied from 0.2-1.1 d^{-1} to 0.3-2.6 d^{-1} at the upstream (Sonning) and downstream (Runnymede) site, respectively. Higher k_{rea} values at the downstream site were due to shallower depths (mean depth = 1.7 m) and faster velocities (mean velocity = 0.73 m s^{-1}) compared to the upstream site, which showed mean depth and velocity of 2.3 m and 0.49 m s^{-1} as calculated in the model. Total estimated reaeration ranged from -1.6 to +1.1 g O_2 L^{-1} d^{-1} and -4.6 to +2.2 g O_2 L^{-1} d^{-1} at Sonning and Runnymede, respectively. Runnymede showed higher reaeration during the biomass growing season when DO saturation went up to 130-150% (Figure C.5). On average over a day during the growing season, O_{sat} at Sonning and Runnymede varied by 14% and 18%, respectively. During the two years modelling period, DO at Sonning was super-saturated for around 40% of the time (more frequently than at Runnymede, 20%), as reflected by the negative reaeration at Sonning during most of the modelling period (Figure 3.2).

The lower River Thames, particularly in the downstream reaches, was dominantly autotrophic during April-June with GPP/ER > 1 and mainly heterotrophic (GPP/ER <

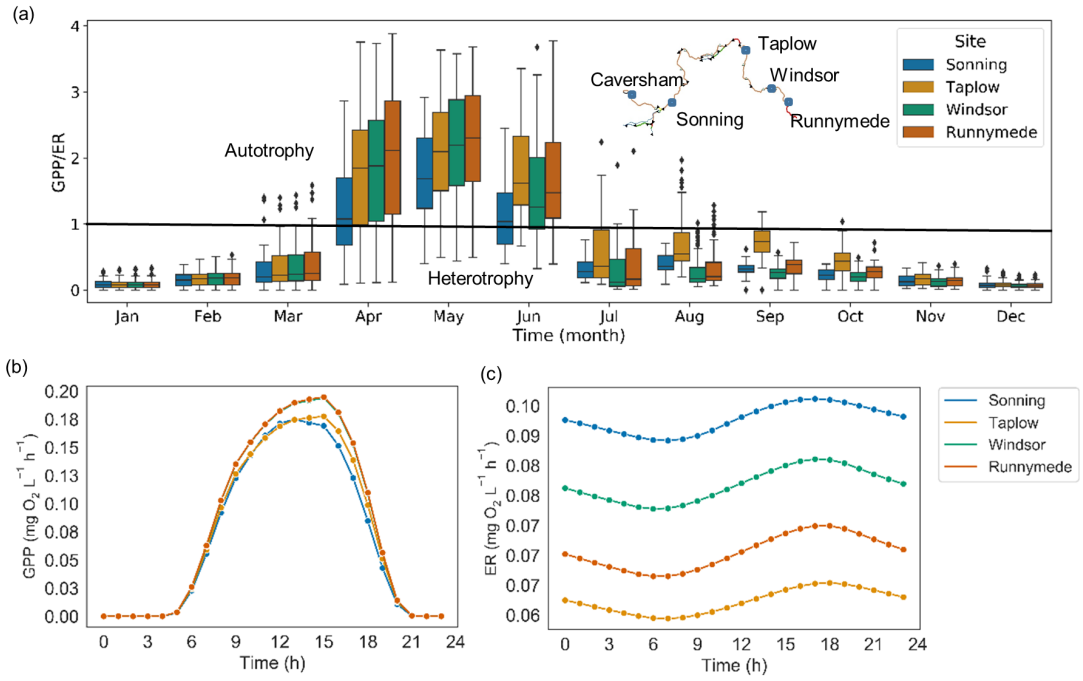

Figure 3.3: Box plot of monthly variation in GPP/ER ratio (a) and time-series of average hourly variation in GPP (b) and ER (c) at all calibration sites during 2013–2014. ER, ecosystem respiration; GPP, gross primary production.

1) during the rest of the year (Figure 3.3). GPP increased up to four times as high as ER during April-June due to large algal blooms. Annual net ecosystem productivity (= GPP – ER) estimates were -192 mg O_2 L^{-1} $year^{-1}$ and 87 mg O_2 L^{-1} $year^{-1}$, and annual GPP/ER ratios were 0.8 and 1.1 at Sonning and Runnymede, respectively. Mid-reaches showed both overall autotrophy at Taplow (net ecosystem productivity = 102 mg O_2 L^{-1} $year^{-1}$, GPP/ER = 1.2) and heterotrophy (net ecosystem productivity = -14 mg O_2 L^{-1} $year^{-1}$, GPP/ER = 1) at Windsor. Excluding the upstream reaches, annual GPP/ER ratio along the channel was close to 1 in the lower Thames.

Downstream reaches showed a lag of up to 4 h for GPP to peak from the upstream site, Sonning. Hourly GPP increased downstream, but ER variation showed no such trend. Average annual hourly ER increased in response to temperature increase during the day and subsided during the night with temperature decrease, showing a hysteresis effect (Figure C.6). Average annual hourly GPP also showed a hysteresis effect with PAR (Figure C.6). Mean daily GPP and ER at upstream (Sonning) and downstream (Runnymede) sites during the two-year period varied from 1.7±3.2 to 2.0±3.8 mg O_2 L^{-1} d^{-1}, and 2.2±1.2 to 1.5±1.2 mg O_2 L^{-1} d^{-1}, respectively.

Relative contribution of autotrophic primary production and respiration was maximum during April-June (Figure 3.4). The rest of the year was characterised by low oxygen production and R_A throughout the river stretch. These months, however, showed another oxygen source through diffusion from air at all sites except Sonning, where diffusion was mainly into the atmosphere (DO sink). During autumn and winter at Windsor and

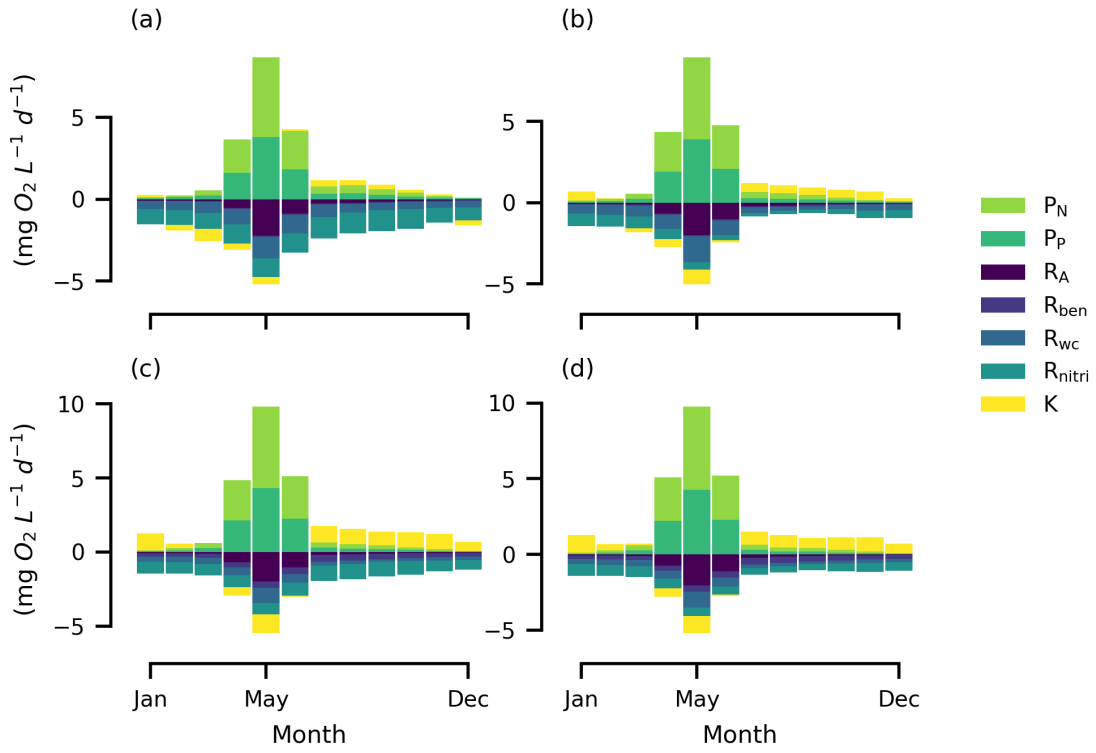

Figure 3.4: Average monthly metabolic source and sink pathways at calibration sites (a) Sonning, (b) Taplow, (c) Windsor, and (d) Runnymede during 2013–2014. K, reaeration; P_N, oxygen produced during nitrate assimilation by phytoplankton; P_P, autotrophic production; R_A, autotrophic respiration; R_{ben}, benthic oxygen demand; R_{wc}, DO loss due to BOD decay; R_{nitri}, DO loss from nitrification.

Runnymede, oxygen addition from reaeration exceeded oxygen production from GPP. R_{wc} and R_{nitri} at Sonning (total 79% of ER) and Taplow (total 70% of ER) mainly governed ER. At Windsor and Runnymede, ER also included significant contribution from benthic communities (17-19%) in addition to the aforementioned processes (60%).

3.3.3 *Sensitivity of river metabolism to multiple stressors*

The variables retained in the best approximating GLS models of GPP included PAR, $1/k_bT$, SRP, flow and seasonality components. For ER, the best approximating GLS models included SRP, flow, SS and seasonality components. Inclusion of seasonality components (sine/cosine terms) improved GLS model performance in all cases. For GPP at Sonning for example, a model with seasonality plus physicochemical predictors (Akaike information criterion = 75.58) performed better than the model with either only seasonality predictors (Akaike information criterion = 136.77) or only physicochemical predictors (Akaike information criterion = 82.61). Final GLS models at both sites showed a good agreement between observed and fitted values with $r > 0.8$ (Table 3.1). However, high values were under-estimated by these models, especially for ER (Figure 3.5). Under-estimation of ER, when investigated using a comparison of R_{wc} and tryptophan-like fluorescence component (Figure C.12), revealed a positive relationship at Sonning ($r = 0.45, p < 0.05$). Runnymede,

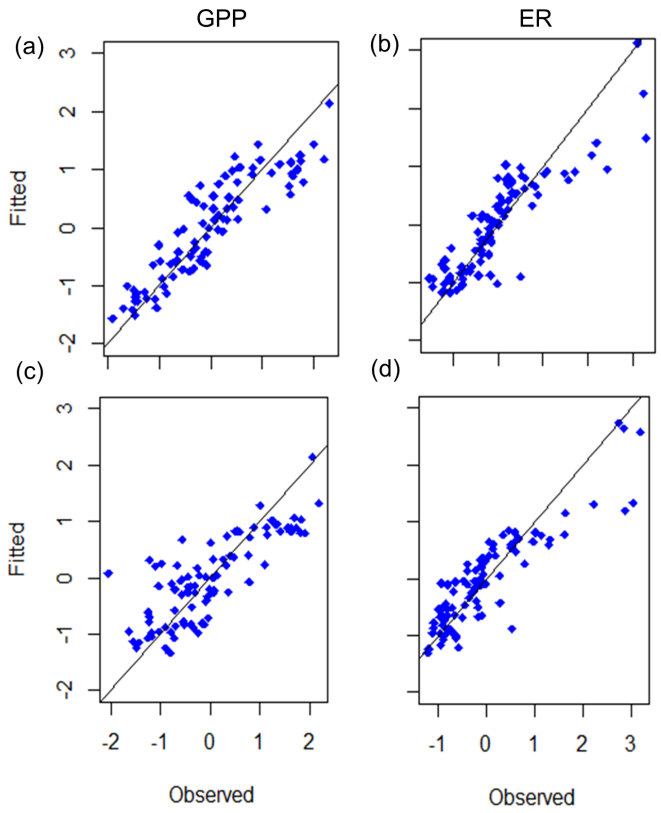

Figure 3.5: Fitted vs. observed values of standardised gross primary production (GPP) and ecosystem respiration (ER) in generalised least squares models at Sonning (a, b) and Runnymede (c, d) sites. The black line in the plots is the y = x line.

however, did not show a significant relationship between R_{wc} and the tryptophan-like fluorescence component.

Significant interaction effects between $1/k_bT$ × SRP and PAR × $1/k_bT$ were found at Sonning for GPP variation (Table 3.1). The interaction between $1/k_bT$ and SRP at Sonning (Figure 3.6a) is an opposing interaction i.e. the effect of one variable is reversed above a certain limit of another variable. Another significant interaction between PAR and $1/k_bT$ is observed to be antagonistic i.e. one variable attenuates the effect of the other variable (Figure 3.6b). Similar to Sonning, Runnymede also showed an opposing interaction between $1/k_bT$ and SRP (Figure 3.6c). The final GLS models of ER did not include any interaction effects.

3.4 DISCUSSION

3.4.1 *Estimating metabolism with process-based modelling*

The model presented here has several advantages over conventional open-channel methods. The hourly model supports network-scale prediction of metabolism rates unlike open-channel methods that are generally applied at a river-reach scale. Network-scale modelling allows us to translate the influence of what is happening upstream

Table 3.1: Summaries for best approximating generalised least squares models for gross primary production (GPP) and ecosystem respiration (ER) with autoregressive structure of order 1 including standardised effect size (SES), standard error of the estimate (SE), t-test value of the coefficient and its associated p value and the Pearson's product moment correlation coefficient (r) for the model fits.

Variable	SES	SE	t value	p	r
GPP-Sonning					
(intercept)	0.132	0.118	1.124	0.264	0.89
PAR	0.369	0.052	7.088	0.000	
$1/k_bT$	-0.223	0.140	-1.599	0.114	
SRP	-0.048	0.074	-0.647	0.520	
Flow	0.370	0.107	3.445	0.001	
sine component	-0.063	0.173	-0.363	0.718	
cosine component	-0.540	0.159	-3.395	0.001	
$1/k_bT \times$ SRP	0.273	0.093	2.950	0.004	
PAR $\times$ $1/k_bT$	0.071	0.044	1.615	0.110	
GPP-Runnymede					
(intercept)	0.078	0.171	0.453	0.651	0.81
PAR	0.416	0.058	7.175	0.000	
$1/k_bT$	0.136	0.180	0.752	0.454	
SRP	-0.102	0.085	-1.195	0.235	
Flow	0.497	0.126	3.950	0.000	
sine component	-0.304	0.230	-1.321	0.190	
cosine component	-0.667	0.209	-3.194	0.002	
$1/k_bT \times$ SRP	0.259	0.107	2.428	0.017	
ER-Sonning					
(intercept)	-0.005	0.109	-0.047	0.963	0.87
cosine component	-0.640	0.130	-4.932	0.000	
sine component	0.067	0.172	0.389	0.698	
SRP	-0.385	0.069	-5.540	0.000	
SS	0.147	0.068	2.163	0.033	
Flow	-0.255	0.163	-1.570	0.120	
ER-Runnymede					
(intercept)	-0.003	0.107	-0.032	0.975	0.88
SRP	-0.544	0.060	-9.023	0.000	
SS	0.127	0.067	1.902	0.061	
Flow	0.312	0.152	2.052	0.043	
sine component	-0.176	0.160	-1.104	0.273	
cosine component	-0.612	0.120	-5.092	0.000	

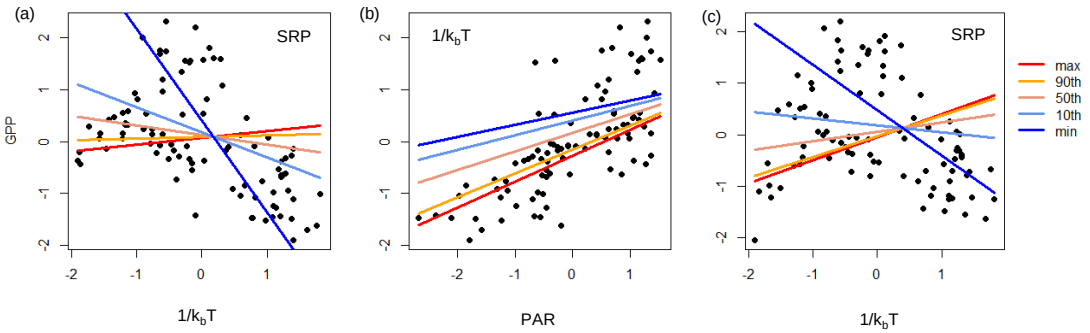

Figure 3.6: Pairwise interactions in generalised least squares models for gross primary production (GPP) at (a) Sonning ($1/k_bT$, SRP), (b) Sonning (PAR, $1/k_bT$), and (c) Runnymede ($1/k_bT$, SRP). Lines represent fitted response to one variable while keeping the second variable values fixed at minimum, maximum, 10^{th}, 50^{th}, and 90^{th} percentiles. $1/k_bT$, transformed water temperature; PAR, photosynthetically active radiation; SRP, inorganic phosphorus.

in the river (e.g. flow management, sewage discharges, etc.) to the downstream DO dynamics. The model presented here is also particularly advantageous over open-channel methods when DO observations are not continuously available. In such scenarios, the estimation of metabolism rates outside of the available data periods relies on further assumptions (see Bernhardt et al., 2018). The hourly model overcomes this challenge as it simulates DO using observations of environmental variables and their process-linkages with DO dynamics, thus eliminating the dependence of metabolism estimation strictly on continuous DO measurements. The model can derive the relative contribution of autotrophic and heterotrophic respiration (here $R_A/P_{GPP} = 0.32$ and 0.35 for Sonning and Runnymede, respectively). Estimates of R_A/P_{GPP} are useful to estimate the autotrophic base of food webs (Hall Jr and Beaulieu, 2013) and to calculate carbon spiralling in rivers (Newbold et al., 1982). Furthermore, the model can be adapted to study the impact of land use changes by translating diffuse nutrient fluxes into tributary inputs. The model is also useful to predict changes in metabolic regime of rivers under different climate and management scenarios (Hutchins et al., 2018).

In spite of the satisfactory reproduction of river water quality dynamics, process-based models invariably include some uncertainties linked to input data quality, process simplifications in the model structure and/or from process knowledge gaps (Hrachowitz et al., 2014). For example, the model in this study assumes that *Stephanodiscus hantzschii* diatoms dominate phytoplankton biomass in the lower Thames throughout the year as found by Read et al. (2014). In reality, multiple algal groups may thrive together and result in within-year compositional change. However, testing of the model using parameters reflecting different phytoplankton groups has reinforced the assumption of diatom dominance (Pathak et al., 2021).

The model also takes a simple approach to calculate reaeration flux. The model uses a previously developed empirical equation (Owens, 1964) to calculate the reaeration

coefficient. Out of several equations reported in the literature, it is recommended (Young et al., 2004; Aristegi et al., 2009) to use the Owens (1964) equation for rivers with low velocities such as the River Thames. Additionally, by comparing the commonly used empirical equations (O'Connor and Dobbins, 1958; Churchill et al., 1962; Owens, 1964) in water quality models (Chapra, 2008), I found that the choice of equation did not affect metabolism rates largely because the reaeration coefficients were relatively low (average k_{rea} = 0.5-1.3 d^{-1}) in the River Thames (Figure C.8). These approaches may be unreliable to use with open-channel methods as (a) it is possible to get a good model fit to the observations because of equifinality in the model and (b) the errors in reaeration estimates will directly translate to GPP and ER estimates (Holtgrieve et al., 2010). However, GPP and ER in the model are simulated from biomass variation and underlying biochemical processes. Moreover, I found that metabolism rates were insensitive to the reaeration values derived for the flow regime of the River Thames (Figure C.8), thus reducing the uncertainties related to reaeration fluxes.

Using the process-based model, I made a detailed quantification of metabolism fluxes, and although the application presented here is data intensive, it can be implemented with lower resolution inputs as shown in Chapter 2 (Pathak et al., 2021). The model application here uses hourly scale inputs of light, water temperature, DO and Chl-a, and daily scale input of flow. However, model sensitivity analysis in Chapter 2 suggests that the model outputs are not sensitive to the time-scale of water quality inputs, but are highly sensitive to that of radiation inputs. If the model is driven by weekly DO, temperature and Chl-a observations, instead of hourly as presented, there is little loss of performance at the downstream sites (e.g. at Windsor, NSE values for DO and Chl-a change from 0.59 to 0.57 and from 0.80 to 0.73, respectively). The outcome from the model sensitivity analysis is reassuring for model applications elsewhere since water quality determinands are irregularly monitored at high-resolution in rivers. Unlike water quality, flow is often routinely (e.g. daily) monitored in rivers, and high-resolution (e.g. hourly) radiation information is easier to obtain either directly or indirectly based on catchment location and sunshine hours (Pathak et al., 2021).

It is still difficult to gather process-rate information in rivers, which is also the case in the lower Thames. For this study, BOD information was only available at a monthly scale and data on benthic oxygen demand were absent. Despite scarce data, the estimates of GPP and ER rates in this study agree well with the findings of Hutchins et al. (2020), who used the Delta method (Chapra and Di Toro, 1991) to estimate metabolism rates in the lower Thames. For prediction of the specific metabolic pathways, we can have more confidence at a larger temporal scale due to the lack of high-resolution process-rate information. Though these limitations may introduce uncertainties during model calibration, other extensive applications of the QUESTOR model in the River Thames (Waylett et al., 2013; Hutchins et al., 2018, 2020) provide confidence in the parameter calibration in this study as the calibrated values (Chapter 2, Pathak et al., 2021) lie within similar ranges.

3.4.2 *Multiple stressor controls on metabolism dynamics*

Faster decline of GPP than ER (Figure 3.3) indicates a decrease in primary productivity compared to biological activity and a shift in river energetics from autotrophic to heterotrophic. The shift in river energetics implies reliance of the metabolic regime on stored algae from summer and/or allochthonous carbon sources during autumn and winter. I find that PAR, water temperature, SRP and flow variation mainly control the GPP dynamics in the lower Thames (Table 3.1). Nitrate concentrations in the river are present in excess throughout the year and do not limit primary production (Chapter 2). Phosphorus concentrations, on the other hand, decrease with high biomass growth and become limiting in summer (Pathak et al., 2021). Light availability, as commonly observed (Bott et al., 1985; Mulholland et al., 2001), increases the GPP with increase in photosynthetic production. High GPP occurred at mid-temperatures (Figure 3.6), which is similar to the findings of Bowes et al. (2016) and Pathak et al. (2021), who reported optimum temperature ranges (~11-18°C) for high phytoplankton growth in the lower River Thames. An opposing interaction between $1/k_bT$ and SRP (Figure 3.6) shows that GPP increases with water temperature, but only at low SRP levels. SRP depletion with increased GPP (Figure C.10) indicates biomass uptake (Bowes et al., 2016). Hence, I believe that the opposing interaction between $1/k_bT$ and SRP is more of a causal effect that occurs during the growing season when phytoplankton utilises SRP and peaks with increase in temperature.

The GLS model derived a positive slope to represent the overall response of GPP to flow variation. However, a closer look at the partial dependence plot of the GPP-flow relationship (Figure C.10) showed that GPP increased only up to a certain flow threshold and began decreasing with further increase in flow (Pathak et al., 2021). Maximum GPP occurred during mid-spring to mid-summer due to the presence of large phytoplankton blooms during periods of low flows (Bowes et al., 2016; Pathak et al., 2021). The rest of the year represented extremely low GPP due to low phytoplankton biomass (Figure 2.4, Figure 3.2). Such a seasonal variation in GPP is commonly observed in temperate rivers, where GPP peaks during periods of high light availability and low flows (Roberts et al., 2007) and significantly reduces during high flows that flush away primary producers (Wang et al., 2019).

High ER occurred during mid-spring to mid-summer in response to high GPP, reflecting high autotrophic respiration of phytoplankton biomass (Figure 3.2). A strong coupling between GPP and ER is common in rivers as a major part of the organic matter produced during photosynthesis is immediately respired by autotrophs and their closely associated heterotrophs (Hall Jr and Beaulieu, 2013). During the biomass growing season, Sonning represented higher overall ER compared to Runnymede because of added contributions from nitrification and BOD decay processes. Lower velocity at Sonning may have promoted higher respiration from organisms suspended in the water column with more residence time to utilise the DO in the reach. Through empirical modelling, I derived SRP, flow and SS to be the most important controls of ER in the river (Table 3.1). Addition of nutrients

in the river did not result in increased biomass growth. On the contrary, I observed high biomass growth coinciding with low SRP levels, suggesting algal uptake. Higher biomass should have resulted in increased decomposer activity (Pascoal et al., 2003) and high resource availability for feeders (Niyogi et al., 2003), causing higher microbial respiration in addition to the high R_A and both contributing to increase in ER. Thus, the co-occurrence of high ER (from algal growth) and SRP depletion may have put SRP in the list of important predictors for ER variation.

On the other hand, high ER in response to high suspended sediments probably indicates organic matter delivery attached to sediments (Roberts et al., 2007; Aspray et al., 2017). Runnymede showed high ER in response to increase in flow, which can again be related to flushing of upstream biomass and organic matter supply along with sediment delivery. However, Sonning showed a negative correlation between flow and ER. Similar to the relationship between flow and GPP, the partial dependence plot (Figure C.11) of ER in response to flow at Sonning showed high ER at mid-flows that decreased at very high flows, as opposed to Runnymede that showed constant ER after a certain flow threshold was reached. GPP at Runnymede still decreased after a certain flow threshold was reached. The relationship between flow-ER at Runnymede indicates that in-spite of the biomass flushing, there is still an allochthonous organic matter supply that supports high respiration.

3.4.3 *Comparing modelling approaches*

In spite of the overall good model performance ($r > 0.8$), peak metabolism rates were under-estimated in the GLS models. Some information about rapidly changing dynamics could have been lost in the empirical modelling as this approach uses weekly time-scale information about the environmental stressors to predict GPP and ER. The under-estimation of GPP can be attributed to the under-estimation of Chl-a concentrations in the process-based model (Table 2.2). ER under-estimation suggests that some important metabolism controls might be missing in the empirical analysis. For example, only a limited number of physicochemical controls were directly included. Land use pressures can also be important as these can contribute large amounts of nutrients and fine particles in the river, and influence primary producers and heterotrophs (Reis Oliveira et al., 2019). However, I have accounted for these influences through proxy variables such as suspended sediment and nutrient concentrations. Although I included flow as a control variable, specific matrices of hydrology (e.g. low-flow events and duration) may improve the model performance. Grazers may also influence ER through phytoplankton predation (Welker and Walz, 1998) and oxygen consumption through respiration (Garnier et al., 1999) with strong seasonal patterns (Schöl et al., 2002). Hence, further research on these controls will be useful to improve model predictions and explain the role of seasonality components in the GLS models. The process-based model, on the other hand, includes the influences of these controls directly (e.g. simulation of hydrology, nutrients and sediment concentrations) or indirectly (e.g. grazing through calibration of death constant).

Additionally, information about organic matter composition may help explain ER under-estimation and improve model performance. R_{wc} at Sonning increased with the tryptophan-like fluorescence component (Figure C.12), which is expected because it represents the presence of organic matter that can be easily degraded by microbes, resulting in high R_{wc}. Runnymede, on the other hand, did not show a significant relationship, probably because of the limited ability of the process-based model to accurately represent BOD fluxes. As discussed earlier, there is a paucity of BOD data, making it difficult to estimate the BOD decay rate parameter precisely in the model. The process-based model cannot incorporate any additional site-specific sources/sinks of BOD (e.g. internal BOD sources from higher trophic levels). Additionally, the poorer fits and the under-estimation of Chl-a concentrations at Runnymede (Table 2.2) suggest that R_{wc} from phytoplankton death is not represented accurately at this site, which may have resulted in a weak relationship between R_{wc} and organic matter availability. Nevertheless, a strong relationship at Sonning still suggests that empirical model performance at the upstream end can be improved with detailed information about organic matter composition as it can be directly linked to BOD (Hudson et al., 2008). Use of water fluorescence indicators (such as full spectra fluorescence excitation–emission matrix or sensors designed to identify tryptophan at specific wavelengths) as an alternative in the absence of BOD information in the river is an important area of future research as it can potentially improve ER prediction in both process-based and empirical approaches.

Although the empirical approach under-estimates the peak values, it is mostly able to mimic the process-based predictions. Combining a physics-based approach with empirical analysis provides powerful possibilities. For example, the empirical models derived in this study can be used for rapid river health assessments across large areas when setting up a complex, process-based model is not feasible. Empirical approaches also provide information about important environmental stressors and their interactions for GPP and ER variation. These established relationships between metabolism rates and environmental stressors can be useful to infer the degradation or recovery of river health following management actions (Jankowski et al., 2021), although the variable importance and effect sizes of environmental stressors should be considered (Feld et al., 2016). A process-based approach, on the other hand, presents a readily available tool to study river ecosystem functioning in response to changing multiple environmental stressors (Heathwaite, 2010). The process-based model in this study can be improved further to create a management tool by linking it with multiple stressor effects such as flow, temperature, nutrients and sediment modifications derived from the empirical approach. Overall, the comparison of empirical and process-based approach provides useful insights into modelling limitations and directions for future work.

3.5 SUMMARY

An approach to estimate ecosystem metabolism rates (GPP, ER) in lowland rivers with a network-scale, process-based water quality model overcomes the current challenges

in metabolism modelling by accounting for oxygen advection under varying flows and oxygen transformations due to biogeochemical processes. Only a few river modelling studies (Payn et al., 2017; Segatto et al., 2020) have attempted to overcome these challenges, but at a much smaller spatial scale (e.g. reach level). The model can easily be extended to an entire catchment if more observations in the catchment are available (Hutchins et al., 2020). The approach presented here uses a previously tested high-resolution river model for water quality prediction in the lower Thames (Pathak et al., 2021). Instead of continuous DO measurements, the process-based approach relies on biomass variation, and the physics of the underlying hydrological- and biochemical-process dynamics to estimate GPP and ER. Therefore, the model has a potential to predict metabolism rates (1) for periods when gaps in continuous DO observations are present, (2) at sites within the modelled river network where continuous monitoring is not carried out and (3) under future environmental and anthropogenic changes. The model presented here is a step forward in high-resolution modelling of long-term, network-scale predictions of river ecosystem functioning, which in turn, can support ecosystem health assessments using functional indicators (Von Schiller et al., 2017).

4

PREDICTING ECOSYSTEM METABOLISM UNDER FUTURE CLIMATE AND CATCHMENT MANAGEMENT CHANGES IN LOWLAND RIVERS

4.1 INTRODUCTION

Lowland river systems around the world are stressed by a combination of pressures such as changing climate, increasing water demand due to population growth and land use intensification, which has resulted in degradation of river ecosystem health (Schinegger et al., 2012). Traditionally, studies on river health assessments have focused on evaluating river ecosystem response to a single stressor such as the effect of changes in flow from dam operations or the effect of nutrient pollution from land use practices. However, with the traditionally dominant stressors being regulated and with other stressors emerging, river ecosystems respond in complex ways to the combination of multiple stressors (Birk et al., 2020). Understanding how these stressors interact to influence river ecosystem health is vital to inform river management and restoration strategies (Lemm et al., 2021). However, the interactions between these stressors are often non-linear making it difficult to predict their net effects on river ecosystem health (Jackson et al., 2016).

Studies of river health assessments increasingly include functional metrics in addition to structural metrics of aquatic ecosystem health (e.g. Feio et al., 2010; Estevez et al., 2017), emphasising the importance of combining both types of metrics for holistic river health assessments. Although structural indicators (e.g. water quality status, channel morphology, biomonitoring indices) provide insight into ecosystem status at the time of measurement, they fail to capture system dynamics (Palmer and Febria, 2012). For example, dissolved oxygen (DO; structural indicator) is widely used to assess river ecosystem health, which is usually established through minimum DO thresholds. Although changes in external controls are reflected in DO concentrations, it is difficult to disentangle their relative influence. On the other hand, a functional indicator such as ecosystem metabolism segregates the influence of physical and biological controls and directly reflects river ecosystem response to change (Jankowski et al., 2021).

Ecosystem metabolism is characterised by gross primary production (GPP) and ecosystem respiration (ER), both of which contribute to carbon cycling and energy flow through food webs in rivers (Demars et al., 2015). GPP and ER are sensitive to multiple environmental stressors, which may influence these metabolism rates either independently or in concert with other stressors (Von Schiller et al., 2017; Pathak et al., 2022). The key environmental controls of metabolism include light, water temperature, hydrology, organic matter dynamics and nutrients (Jankowski et al., 2021). Furthermore, anthropogenic pressures such as flow regulation (e.g. Aristi et al., 2014), sewage discharge (e.g. Arroita et al., 2019) and land management (e.g. Fuß et al., 2017) also influence

metabolism through changes in environmental controls. Several studies have observed ecosystem metabolism to show early indication of ecosystem degradation or recovery in response to stressors (e.g. Young et al., 2008; Arroita et al., 2019). Therefore, studying metabolism response to changes in stressors is important for understanding how river ecosystem health will respond to future changes in climate and catchment management practices, and ultimately for guiding restoration and future management efforts.

Evaluation of metabolism response to a variety of stressors uncovers underlying controls of metabolism (e.g. Beaulieu et al., 2013; Bernhardt et al., 2022). Traditionally, such ecological assessments have relied on statistical methods, where metabolism is estimated using long-term, continuous dissolved oxygen time-series and related to multiple stressors empirically. While statistical tools provide useful insights into sensitivity of metabolism to multiple stressors, extrapolation of the outcomes outside the period of available observations can lead to errors. This can be overcome by mechanistically linking metabolism rates to multiple environmental stressors (e.g. Segatto et al., 2020; Pathak et al., 2022). In addition to understanding the underlying controls of metabolic regimes in rivers, mechanistic modelling of metabolism and its environmental controls is particularly advantageous to predict metabolism response to combined changes in multiple environmental and anthropogenic pressures.

In this study, a mechanistic water quality model, hourly Quality Evaluation and Simulation Tool for River-systems (QUESTOR) (Chapter 3, Pathak et al., 2021), was used to predict ecosystem metabolism response to future climate and management changes in the lower River Thames. Major lowland rivers, such as the Thames, are subjected to a wide range of pressures including flow regulation, water abstractions, channel modifications and pollution discharges from sewage and agricultural runoff (Hutchins et al., 2018) that influence river health. The hourly QUESTOR model can account for these variety of pressures by including their influence on changing environmental controls such as flow, light, water temperature, nutrients, biomass and dissolved oxygen variation in the river. Chapter 3 (Pathak et al., 2022) demonstrated the application of the hourly QUESTOR model in the lowland River Thames for the prediction of ecosystem metabolism along with its environmental controls. Here, the model is used to evaluate ecosystem metabolism response to changes in future climate and catchment management scenarios. Based on the most widespread stressors that are known to affect rivers worldwide (Birk et al., 2020), 11 scenarios are selected in this study that test the influence of either a single stressor or multiple stressors on river ecosystem metabolism.

4.2 METHODS

4.2.1 *Model application and performance*

The hourly QUESTOR model was used to predict water quality (Pathak et al., 2021) and ecosystem metabolism (Pathak et al., 2022) in the lower Thames during 2013-2014. The model was implemented along a 62 km stretch between Caversham and Runnymede.

The entire river stretch was divided into 23 reaches based on the locations of gauging stations, sewage treatment works and tributary confluences (see Table B.1 for river network description). The outputs of the lower Thames model (Pathak et al., 2021, 2022) for years 2013-2014 were used to characterise the baseline water quality status. The model was then used to study river response under future climate and management scenarios. In this study, the results and discussion are focused on the outputs at the Runnymede site of the modelled river network, as it integrates the river response of the entire study stretch.

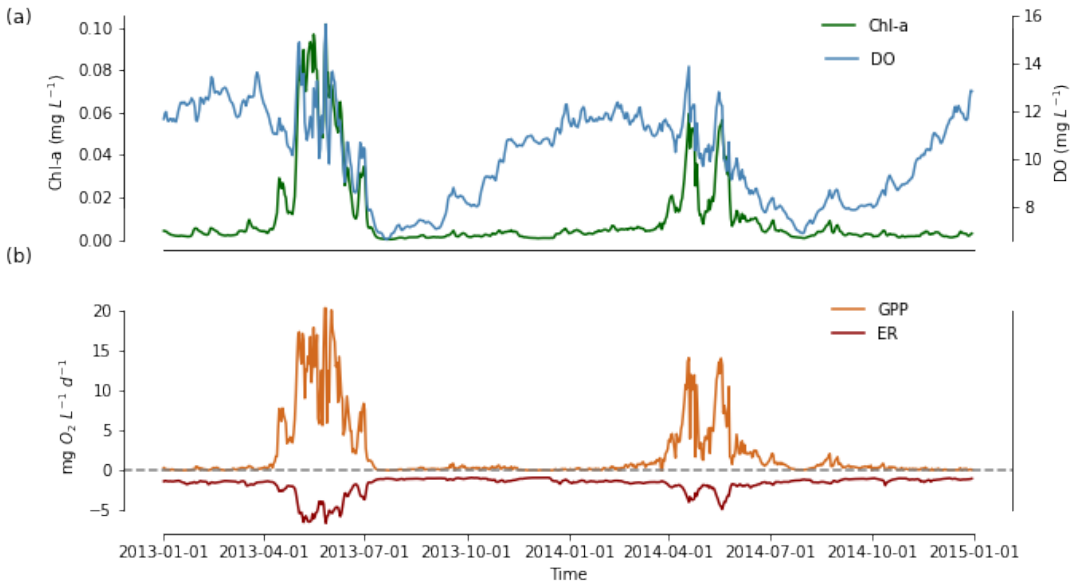

Figure 4.1: Time-series of (a) chlorophyll-a (Chl-a), dissolved oxygen (DO) concentrations, and (b) gross primary production (GPP), ecosystem respiration (ER) at Runnymede in the Baseline scenario

During the baseline period, the lower River Thames ecosystem was influenced by massive phytoplankton blooms from mid-spring to mid-summer (Figure 4.1a) when light, flow and water temperature conditions were favourable. GPP showed a distinct seasonal variation as is commonly observed in temperate rivers (Roberts et al., 2007). High GPP occurred during periods of high light availability, favourable water temperatures (11-18°C) and low flows (21-63 m^3 s^{-1}), and considerably decreased during high flows that flushed away primary producers (Pathak et al., 2021). Due to algal uptake, high GPP coincided with low nutrient concentrations. ER showed a strong coupling with GPP since a major portion of organic matter produced during photosynthesis was immediately respired. ER also increased in response to increase in flow and suspended sediment concentration (Pathak et al., 2022), which probably resulted from flushing of upstream biomass with flow and organic matter delivery attached to sediments. Out of all oxygen sink pathways, R_{nitri} contributed the maximum (34%) to ER followed by R_A (24%), R_{wc} (23%) and R_{ben} (19%). Overall, the river was primarily autotrophic (GPP > ER) during April-June and shifted to heterotrophy (GPP < ER) during the rest of the months. Average annual GPP/ER was found to be close to 1 throughout the lower River Thames.

4.2.2 *Implementation of scenarios*

The goal of the study is to predict river ecosystem response under probable future conditions (~ year 2050). The future scenarios were based primarily on the changes in five variables including flow, water temperature, urbanisation intensity, shading amount, total phosphorus concentrations and heterotrophic respiration rate (Table 4.1), which are known to influence ecosystem metabolism in rivers (Bernhardt et al., 2018; Birk et al., 2020). For example, in lowland rivers regulated by locks and weirs, increased residence time can promote interactions between biomass and nutrients that may increase metabolism (Mulholland et al., 2001). Similarly, metabolism responds to interactions between multiple stressors such as light and temperature (Huryn et al., 2014) or nutrient availability and water abstractions (Pardo et al., 2022), where the combined effect of the stressors on metabolism can be additive, synergistic, antagonistic or opposing in nature.

Future flows hydrology predictions (Prudhomme et al., 2012; Prudhomme et al., 2013) were used to derive percentage changes in river flows in the lower Thames. Specifically, predictions from their Climate and Land-use Scenario Simulation in Catchments (CLASSIC) model run (Crooks and Naden, 2007) at Thames at Kingston site were selected since it was the closest suitable site in the Future flows model runs, integrating hydrological characteristics in the lower Thames catchment. Future Flows Hydrology contains an 11-member ensemble of transient climate projections for Great Britain based on HadRM3-PPE-UK (Hadley Centre Regional Climate Model), which was run under the SRES A1B 'medium emissions scenario' (Special Report on Emissions Scenarios - a balance across all sources) (Murphy et al., 2009). Average values of 11 model runs were used to derive percentage change values corresponding to 5^{th}, 25^{th}, 50^{th}, 75^{th} and 95^{th} percentile flows. A cubic interpolation (interp1d function from `Scipy` package v1.5.0, Virtanen et al., 2020) was used to derive percentage changes in flows for the entire flow duration curve (Figure 4.2). The resulting percentage changes in flows were applied to all input flow duration curves, i.e. at Caversham (model start point) site and at the tributaries within the modelled river network.

For the temperature (Temp) scenario, a constant +2°C change was applied to the water temperature inputs at Caversham and incoming tributaries, based on the UK Climate Projections 2009 (United Kingdom climate projections, UKCP09) scenario (Hutchins and Hitt, 2019).

The urbanisation (Urb) scenario accounts for changes in water abstraction and effluent release practices in the lower Thames. Based on the estimate of future population increase in England (16%, ONS, 2015), a change factor of ×1.16 was used to characterise future water usage and effluent release in the catchment (Hutchins and Hitt, 2019).

The heterotrophic respiration (Hetresp) scenario was included to account for the effect of short-term events such as storms/flooding on river respiration. Such events are predicted to increase in future in terms of frequency and intensity (Sayers et al., 2015), and have a potential to leave long-lasting impacts on river ecosystems. For example, Hutchins et al. (2020) found 70% increase in heterotrophic respiration rates (includes R_{ben} and

R_{wc}) during 2013-2014 after a summer storm in 2012 in the River Thames. They found that high flows elevated organic carbon delivery in the river, which escalated microbial decomposition of the organic matter and consequently, heterotrophic respiration rates.

To present a realistic future it was assumed that management actions will be directed towards restoration of river ecosystem health, which in turn, will help alleviate the negative impacts from worsening climate. To account for future management practices (Management scenario), two scenarios were included, namely (1) riparian zone management to increase vegetation cover (Shade scenario) and (2) reduction in total phosphorus (TP) loading in the river to reduce nutrient pollution (TP scenario). The Shade scenario reflects changes in riparian management strategies that will contribute to increase in bankside vegetation and riparian shading. The effect of changes in riparian shading was included through changes in incident radiation reaching the water surface, i.e. level of fractional light penetration under full leaf canopies as recommended by Waylett et al. (2013). Here, it was assumed that the canopy shading amount will double compared to the baseline condition (fractional light penetration level of 0.40 from 0.70, Hutchins et al., 2018). The TP scenario represents changes in phosphorus loading in the river from point and diffuse sources. A change factor of ×0.6 (Hutchins and Hitt, 2019) was applied to incoming TP concentrations (e.g. effluents and tributaries), reflecting overall reduction in the future TP load in the river.

A total of 11 scenarios were implemented in addition to the Baseline scenario as described in Table 4.1 that included either a single stressor or a combination of multiple stressors. For interpretations, the scenarios were divided in mainly three groups, (1) Management, (2) ClimatePop and (3) Allscen. The Management scenario combined Shade and TP scenarios to represent future water quality management practices. The ClimatePop scenario reflects future changes in environmental variables and includes Flow, Temp, Urbanisation and Hetresp scenarios. Finally, the Allscen scenario combines all variables to predict the overall river response to future changes. The next section describes the river ecosystem response to the scenarios mentioned here. The model outputs are reported in terms of a decrease or increase in monthly median values of response variables unless explicitly mentioned otherwise.

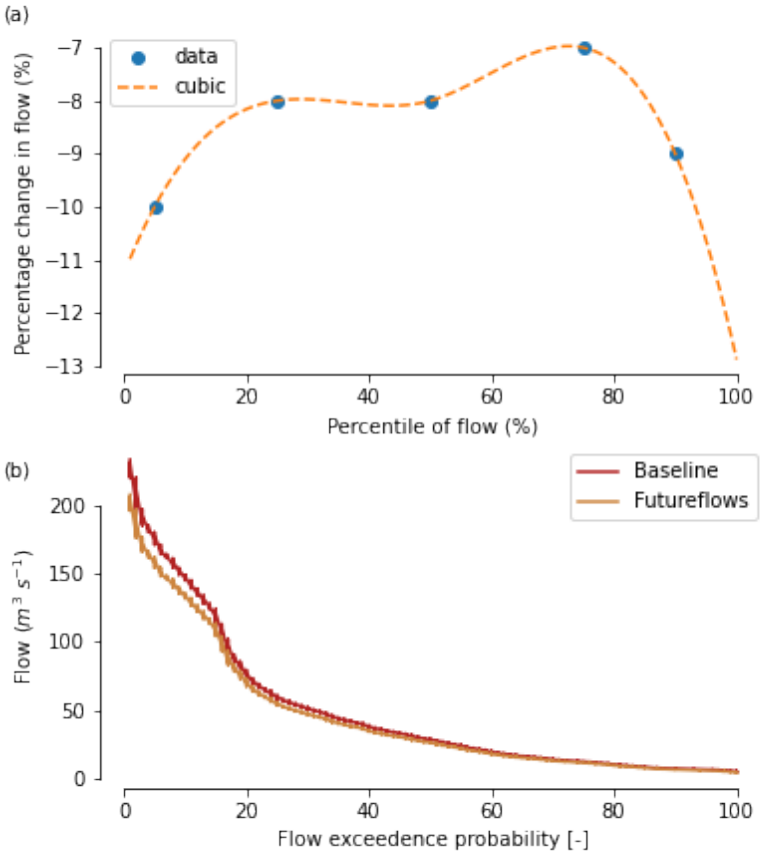

Figure 4.2: (a) Percentage changes in flows in the Future flows model run in the lower Thames and (b) flow duration curve at Caversham

Table 4.1: Details of the scenarios applied in the lower Thames. The column 'References' provides some examples of studies that highlight the importance of specific variable on ecosystem metabolism.

Scenario	Variable	Change	References
Baseline	Present day condition (2013-2014)	-	
Flow	Flow	Future predictions from Future flows hydrology (Prudhomme et al., 2013)	Val et al. (2016), Acuña et al. (2005), Bowes et al. (2016)
Temp	Temperature	+2 °C (Hutchins and Hitt, 2019)	Demars et al. (2011), Demars et al. (2016), Song et al. (2018)
Urb	Urbanisation	×1.16 (ONS, 2015)	Calizza et al. (2012), Pardo et al. (2022)
Shade	Riparian shading	0.40 (Hutchins et al., 2018)	Bernhardt et al. (2022), Hutchins et al. (2010)
TP	Total phosphorus	×0.6 (Hutchins and Hitt, 2019)	Bowes et al. (2012), Jankowski et al. (2021)
Hetresp	Heterotrophic respiration rate	70% increase (Hutchins et al., 2020)	Cook et al. (2015), Leggieri et al. (2013)
Climate	Flow, Temperature		
ClimatePop	Flow, Temperature, Urbanisation, Heterotrophic respiration		
Management	Riparian shading, Total phosphorus		
Allscen	Flow, Temperature, Urbanisation, Riparian shading, Total phosphorus, Heterotrophic respiration rate		
Allscen_minus_hr (incl. all variables in Allscen except heterotrophic respiration rate)	Flow, Temperature, Urbanisation, Riparian shading, Total phosphorus		

4.3.1 *Impact of future climate and population growth on ecosystem metabolism*

Future Flows projections in the river suggest overall reduction (on average 8%) in flows throughout the year (Figure 4.2). Low flows in the lower River Thames are projected to reduce further (up to 13%) with changing climate and population growth, which puts the river at an increased risk of prolonged low flow periods (July-October) in future. Metabolism rates, however, are not drastically altered with predicted reduction in the future flows either due to climate change or population growth. Urbanisation lowers GPP during July-September and increases ER throughout the year (Figure 4.3), albeit these changes are $< 10\%$. Similarly, flow reduction from climate change does not have a significant influence on GPP and ER, except during low flow months when reduction in GPP is apparent and median GPP decreases up to 25%. Overall, metabolism is predicted to strongly respond during low flow periods in response to the changes in future hydrology and urbanisation.

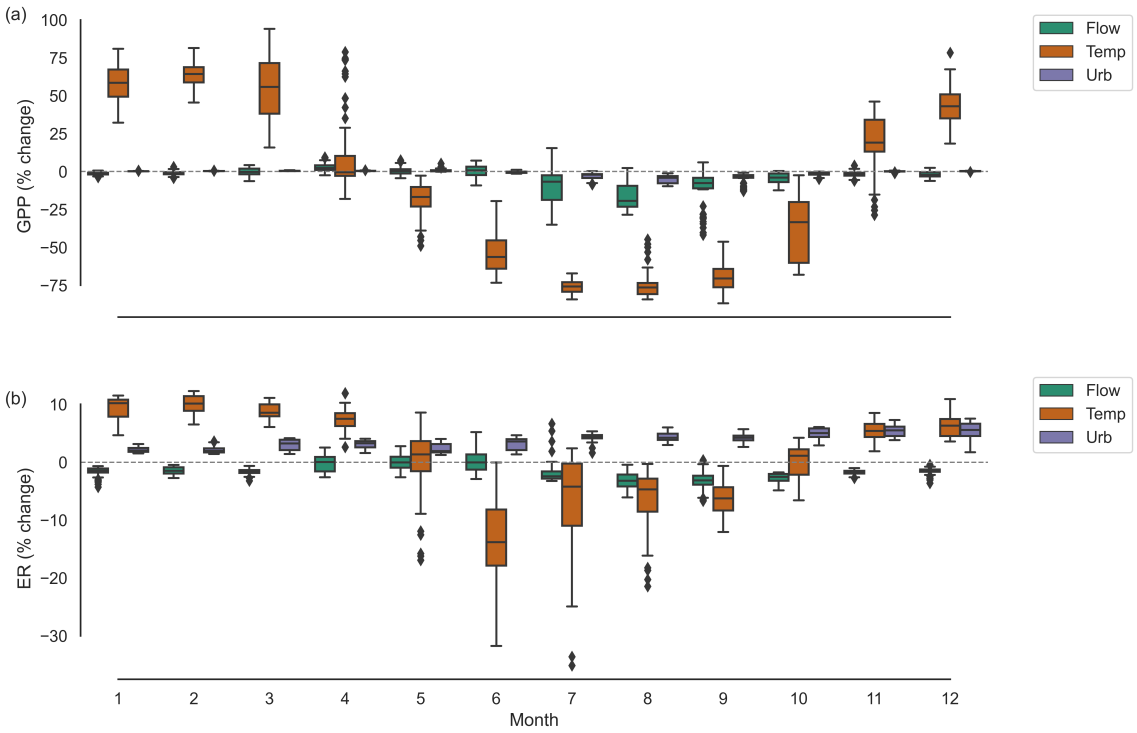

Figure 4.3: Monthly percentage change in daily (a) gross primary production (GPP) and (b) ecosystem respiration (ER) in response to Flow, Temp and Urb scenarios

In contrast to flow, future changes in water temperature show a significant impact on both GPP and ER throughout the year. The model predicts 20-75% reduction in median GPP with temperature increase during May-October (Figure 4.3a), when river water is warmer compared to the other months (Figure C.14). The co-occurrence of temperature increase with low flow conditions during May-October results in unfavourable environment for diatom growth as (1) high temperatures ($> 18°C$) do not favour phytoplankton growth and (2) extremely low flows (< 20 m^3 s^{-1}) result in

settlement of biomass (Chapter 2). In contrast, during the colder months (i.e. November-April), river flows are higher and temperature increase supports phytoplankton growth, resulting in 10-70% increase in monthly median GPP in the Temp scenario. Despite the high percentage increase, GPP still remains < 5 mg O_2 L^{-1} d^{-1} due to extremely low GPP in the Baseline scenario during November-April.

Similar to GPP, ER also increases during November-April in the Temp scenario for about 10% (Figure 4.3b). During June-September, the model predicts around 5-15% reduction in median ER, which is mainly governed by R_A response to future warming since R_A decreases (40-60% reduction) with temperature increase due to biomass depletion during these months (Figure C.17). On the contrary, heterotrophic respiration (R_H) is predicted to increase with temperature increase in all months except June. R_{wc} (10-15%) and R_{nitri} (< 5%) fluxes decrease with temperature increase during June-October because of biomass (Figure C.15) and ammonium depletion, respectively. R_{ben}, on the contrary, increase (5-13%) with temperature increase throughout the year. The % increase in R_{ben} is lower (~5%) in June compared to the other months, which suggests that R_H response to temperature is governed by R_{ben}. The combined effect of flow and temperature scenarios on ecosystem metabolism is found to be antagonistic, where the overall effect of both scenarios is less than the sum of their individual effects. It should be noted that the future projections of flow and temperature change are opposite in nature.

4.3.2 *Impact of management practices on ecosystem metabolism*

Phytoplankton growth in the lower Thames is highly sensitive to light intensity. Increase in riparian shading will suppress harmful phytoplankton blooms (up to 30%) and consequently median primary production (up to 54%) during late spring and early summer (Figure 4.4). Phytoplankton blooms during mid-spring are not influenced by shading as leaf-cover period begins from May and lasts till November. The model predicts 25-65% reduction in median GPP during the leaf-cover period with maximum reduction in September-October months (> 60%) (Figure 4.4a) when reduction in Chl-a is also the highest (Figure C.15). DO in the river does not show a strong response to changes in the tree shading amount, and shows only 5-13% reduction in median values during May-June. Similarly, ER shows significant reduction (> 10%) only during May-June. R_A responds in a similar way to GPP with up to 60% reduction in median values (Figure C.17) during leaf-cover period due to Chl-a depletion (Figure C.15). In the Baseline scenario, high R_{wc} levels coincide with phytoplankton bloom period (Figure C.18), possibly because respiration and decomposition (from bloom crashing) during April-June contribute to high BOD decay in the river. The Shading scenario causes a decrease in R_{wc} during the leaf-cover period when Chl-a also decreases. R_{ben} shows only slight reduction due to increased canopy cover with highest reduction during May-June (Figure C.19), which is probably the cause of DO depletion during May-June (Figure C.16).

The response of water quality and metabolism rates to reduction in TP loads is similar to their response to the increase in riparian cover, although the degree of change is much

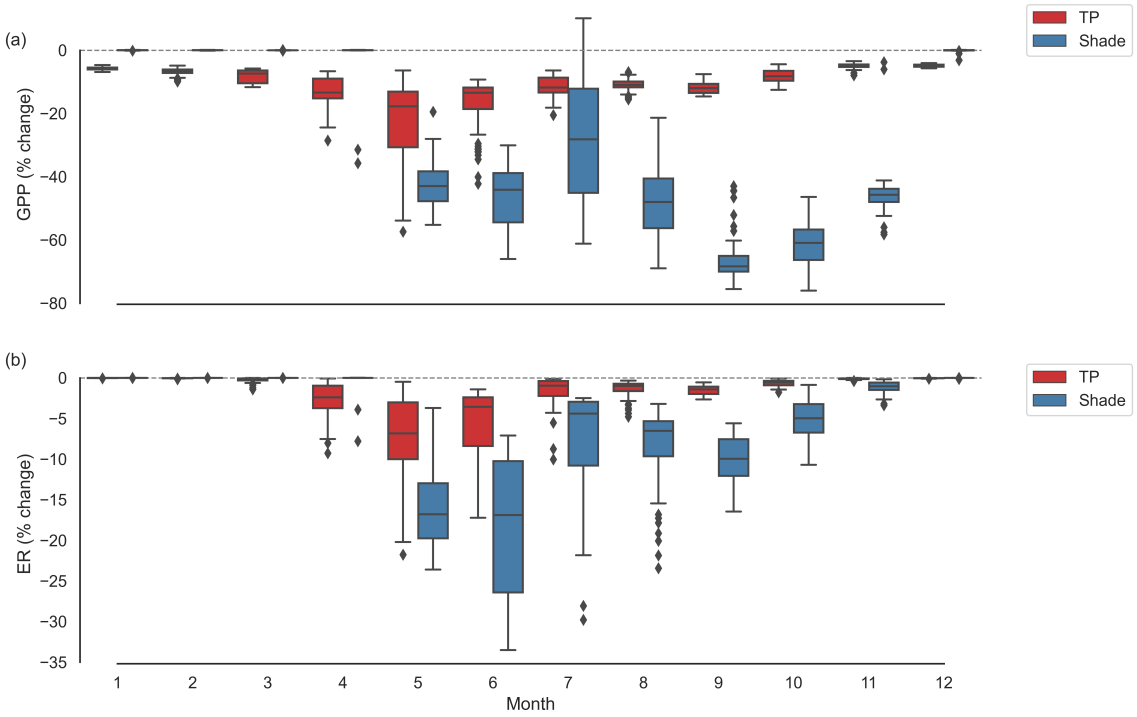

Figure 4.4: Monthly percentage change in daily (a) gross primary production (GPP) and (b) ecosystem respiration (ER) in response to Shade and TP scenarios

smaller. For example, peak Chl-a concentrations during phytoplankton bloom period show 18-19% decrease with TP reduction as opposed to 25-30% decrease for increase in the riparian cover. GPP and ER decrease during April-October in the TP scenario (Figure 4.4) as biomass depletes due to limited nutrient availability. The decrease in the median GPP ($< 20\%$) and ER ($< 10\%$) is still small compared to the Shading scenario that decreases median GPP and ER up to 60% and 20%, respectively. Similar to the climate scenarios, the combined effect of the management scenarios is antagonistic as the combined effect of the TP and Shading scenarios cause lower reduction in metabolism rates than the sum of these individual scenarios.

4.3.3 *Environmental versus management impacts*

A comparison between ClimatePop and Management scenarios is made to differentiate the influence of future environmental changes from management actions. Contrary to expectations, future changes in the environment (Flow, Temp, Urb, Hetresp) improve river water quality in terms of biomass growth, with up to 40% reduction in the bloom size (maximum monthly Chl-a) during the growing season. Management actions show a reduction in maximum monthly Chl-a throughout the year. During the growing season, both scenarios reduce the bloom size to a similar degree – which is when the river health is at risk from harmful phytoplankton growth. In spite of the reduction in bloom size, peak monthly Chl-a concentrations during the growing season still remain at high concentrations (> 0.03 mg L^{-1}). Environmental changes result in oxygen depletion throughout the year. During the phytoplankton growing season, minimum

DO concentration decreases up to 28% from the present conditions. Minimum DO concentration in the river is predicted to fall to harmfully low levels (below 6 mg L^{-1}) during several months (May, July-September). Management actions do not significantly alter DO concentrations in the river. ClimatePop scenario shows that GPP increases (> 40%, monthly median) during late-autumn and winter (Figure C.13) when the river environment is colder and wetter, and reduces during the rest of the period (9-93%, monthly median) due to an unfavourable combination of extremely low flows and high temperatures for phytoplankton growth (Chapter 2, Pathak et al., 2021). ER increases throughout the year in response to the ClimatePop scenario (12-39%, monthly median), except during May-June (Figure C.13) when the response of ER is governed by autotrophic respiration. As opposed to the ClimatePop scenario, the Management scenario causes overall reduction in both, GPP (up to 72%, monthly median) and ER (up to 23%, monthly median), mainly due to the effect of riparian shading on phytoplankton growth.

4.3.4 *Metabolic fingerprint of the lower River Thames*

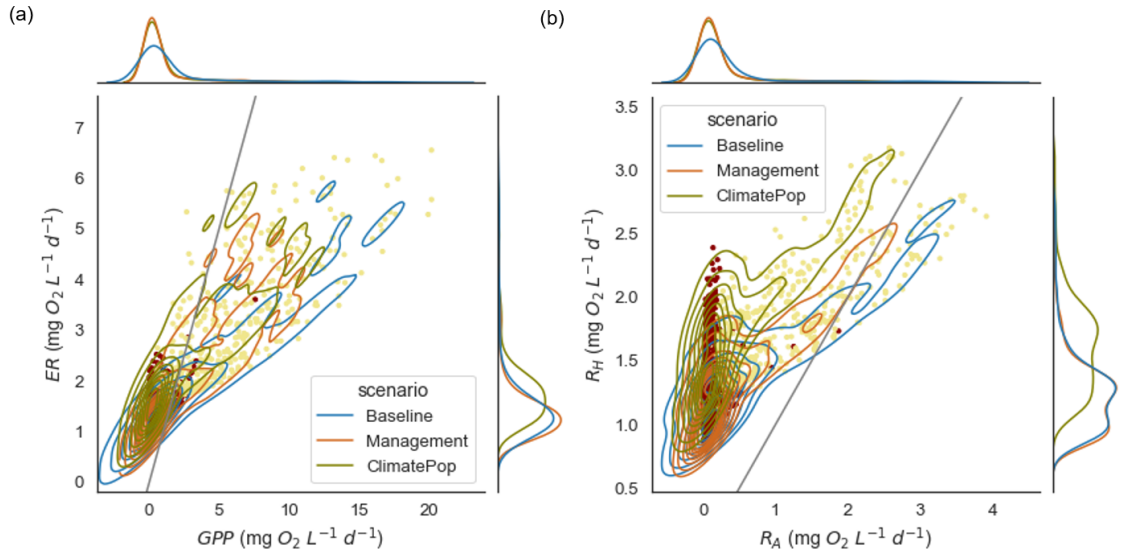

Figure 4.5: Metabolic fingerprint for Baseline, ClimatePop and Management scenarios. Data points in yellow represent values during the biomass growing season and the points in maroon represent values during the rest of the year. The plots in the upper and right panels represent probability density curves for gross primary production (GPP) and ecosystem respiration (ER), respectively. R_A, autotrophic respiration; R_H, heterotrophic respiration.

To further investigate river ecosystem response to future environmental changes (ClimatePop scenario) and management actions (Management scenario), metabolic fingerprints are used as diagnostic tools. The majority of data points in the Baseline fingerprint lie above the 1:1 line, which indicates river heterotrophy during most of the year (Figure 4.5). However, during the phytoplankton growing season (April-June), the river shifts to autotrophy with peak metabolism rates lying below the 1:1 line. Future environmental and management changes compress the metabolic fingerprint from the

Baseline scenario, by increasing and decreasing the low and high values of metabolism rates, respectively. Boundaries of peak metabolism rates are slightly more compressed by the management actions compared to the climate changes. Both future scenarios show a shift in the fingerprint, with future scenario fingerprints moving closer to the 1:1 line compared to the Baseline. These shifts occur because GPP and ER are projected to decrease and increase respectively under climate-management changes, which will lower the GPP/ER ratios from > 1.

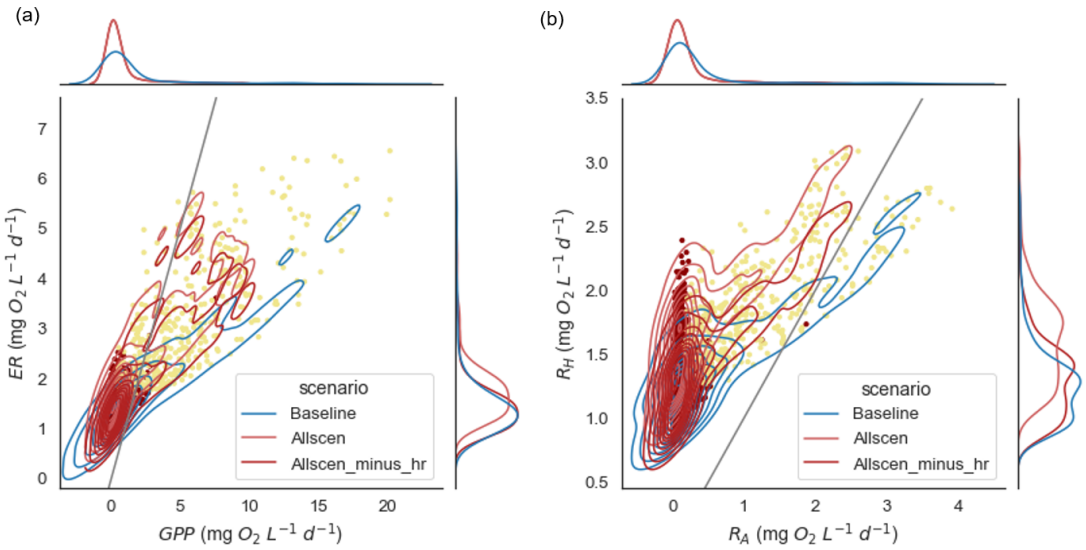

Figure 4.6: Metabolic fingerprint for Baseline, Allscen and Allscen_minus_hr scenarios. Data points in yellow represent values during the biomass growing season and the points in maroon represent values during the rest of the year. The plots in the upper and right panels represent probability density curves for gross primary production (GPP) and ecosystem respiration (ER), respectively. R_A, autotrophic respiration; R_H, heterotrophic respiration.

The distribution of metabolism rates does not change from the Baseline to the Management scenario. Although the ClimatePop scenario does not show a change in the GPP distribution, respiration values in this scenario are clustered at an increased ER rate compared to the Baseline scenario (Figure 4.5a). High ER is mainly attributed to the increase in R_{wc} and R_{ben} rates that may result from short-term flooding/storm events. This effect can be observed in Figure 4.5b with an overall increase in R_H from the Baseline to the ClimatePop scenario. Reduction in peak R_A in Figure 4.5b can be attributed to biomass depletion during the growing season. R_H contribution in the Baseline scenario is generally higher than R_A, with some exceptions during the phytoplankton bloom period when algal respiration is high. However, environmental and management changes alter this behaviour with fewer (Management) or no (ClimatePop) instances where R_A/R_H is > 1. Such a change in respiration dynamics persists even without the consideration of increased R_{wc} and R_{ben} rates from short-term events (Allscen_minus_hr scenario; Figure 4.6b).

4.4 DISCUSSION

4.4.1 *Future response of ecosystem metabolism in the lower Thames*

The climate scenario included here projects a warmer and drier river compared to the present conditions. The model predicts that, in general, future climate will increase metabolism rates during winter and spring seasons, but reduce metabolism rates during summer and autumn seasons. Regulated rivers with stable flows and high light availability generally exhibit high annual productivity and respiration compared to the rivers influenced by hydrologic disturbances (Bernhardt et al., 2022). The lower Thames also shows high metabolism rates during stable, low flow conditions (Figure 4.1). The influence of future flow forecasts and urbanisation on the river productivity is also only relevant during July-September months when the baseline river conditions represent stable, low flows (Figure C.14). During the rest of the year, metabolism does not exhibit a significant change in response to these environmental changes. However, it should be noted that the predictions in the Future flows hydrology are made assuming medium emission scenarios (Prudhomme et al., 2013), and the change in hydrology does not vary more than 13% for the entire range of river flows. Notable changes in the river hydrograph due to extreme climate events and/or flow regulation are still likely to alter the metabolic regime of the river considering flow is an important regulator of metabolism in the river (Chapter 3, Pathak et al., 2022). Flooding events (Uehlinger, 2000; Cook et al., 2015; Hutchins et al., 2020) or artificial water releases (environmental watering) during low flow periods (Wallace and Furst, 2016) may significantly modify ecosystem metabolism. Here, the model indirectly accounts for the influence of such short-term, high flow events (Hetresp scenario), and predicts that events escalating the input of organic matter to rivers may boost heterotrophic respiration up to 30% more than the present conditions in the river.

In this study, it is assumed that management practices will be put into action to mitigate the future climate influence on river ecosystem and to maintain healthy ecosystem functioning. Therefore, TP management scenario assumes that future TP loading in the river will be lower compared to the baseline conditions. The relationship of phosphorus with phytoplankton blooms has been previously documented in the Thames catchment (Bowes et al., 2012), with phosphorus enriched rivers showing larger phytoplankton blooms. Decreased discharge from sewage treatment works generally reduces downstream metabolism due to decreased nutrient and organic matter availability (Gücker et al., 2006; Arroita et al., 2019). In the lower Thames, I observe a decrease in metabolism rates, but the reduction is mainly observed during April-October months when lower levels of nutrients limit phytoplankton growth. The insignificant response of biomass and metabolism during the rest of the months could occur because nutrient concentrations during this period are still high despite TP reduction, thus not limiting phytoplankton growth. The river may also exhibit high metabolism in spite of reduced nutrient concentrations because of legacy

nutrient stores or because of a decoupled (or nonlinear) response of biomass growth to changes in nutrient concentrations in the river (Jarvie et al., 2013).

In contrast to the TP scenario, the Shading scenario shows drastic changes in the ecosystem response with around 40% and 10% more reduction in median GPP and ER, respectively than the TP scenario. In the baseline condition, the lower Thames shows high GPP and ER peaks from April to June when river flows are low and stable, and temperature conditions are suitable for phytoplankton growth. However, phytoplankton biomass reduces significantly when light availability reduces due to increased riparian shading during May-November (Figure 4.4). Light is the primary limiting factor for GPP in many rivers (Mulholland et al., 2001). Despite the sparse tree coverage and the wide river channel, shading has been shown to have significant influence on water quality in the River Thames (Bachiller-Jareno et al., 2019). To account for the influence of riparian shading in the Thames, the model uses a constant estimate of fractional light penetration (during leaf-cover period) that was derived by Waylett et al. (2013) and validated by Bachiller-Jareno et al. (2019). However, it should be noted that spatial and temporal heterogeneity in shading is common due to changes in local canopy characteristics (e.g. canopy structure, coverage and tree height), landscape characteristics (e.g. channel orientation and width), sun position (over a day and over a year) and seasonality in riparian vegetation structure (Li et al., 2012; Savoy et al., 2021). Overall, the model outputs suggest that management efforts to increase the tree cover are more efficient than TP reduction to reduce the magnitude of harmful phytoplankton blooms in the river. Increasing riparian cover is also more cost-effective compared to TP reduction from sewage discharge and land use practices (Hutchins et al., 2010).

I also used metabolic fingerprints to assess river metabolism response to the multiple stressor scenarios considered in this study. Bernhardt et al. (2018) proposed metabolism fingerprints as diagnostic tools for comparing annual patterns of metabolism across rivers or across years for the same river - although only a few subsequent studies have reported river metabolism fingerprints (e.g. Arroita et al., 2019; Blaszczak et al., 2019). Metabolic fingerprints provide interpretations of both peak and median metabolic rates as well as variance in GPP/ER ratio. The annual GPP/ER ratio at Runnymede is > 1 in the Baseline scenario (Pathak et al., 2022). However, with changes in future environmental and management conditions, the instances where GPP/ER > 1 are lowered because future scenarios significantly reduce the high peaks of biomass during the growing season. Metabolic fingerprints are also useful to evaluate the response of river ecosystem to future scenarios (or stressors). Bernhardt et al. (2018) hypothesised that hydrological disturbances and sediment loading in rivers will compress the fingerprint, whereas higher light, nutrient and carbon availability will expand the fingerprint. The outputs in this study agree with this hypothesis. I find that the ClimatePop scenario (flow reduction, temperature increase, urbanisation) compresses the Baseline metabolic fingerprint (Figure 4.5). The Management scenario assumes reduced light and TP availability, which again compresses the metabolic fingerprint as expected (Arroita et al., 2019). Flooding events should compress the fingerprint according to the aforementioned

hypothesis. However, as this study only considers the effect of flooding on R_H, metabolic fingerprint expands in response to the Hetresp scenario due to an increase in ER from higher organic matter availability. The combined effect of environmental and management scenarios is to compress the metabolic fingerprint from the Baseline scenario. Although the boundaries of metabolism change in future conditions, the centroids (dominant metabolic rates) of metabolism fingerprints do not vary significantly in future conditions (exception include Hetresp scenario). By comparing metabolic fingerprints from several river systems, we will be able to determine how different types of river ecosystems will respond to river management activities under a changing environment.

4.4.2 *Stressors in lowland rivers*

The scenarios presented in this study are limited in their representation of probable future changes in terms of the direction and intensity of change. For example, the Flow scenario considered in this study assumes a small decrease (up to 13%) in river flows. However, accelerated climate change may cause drastic variations in river hydrology with higher frequency of extreme events such as flooding and droughts. Extreme changes in hydrology may alter patterns of organic matter availability (Acuña and Tockner, 2010; Cook et al., 2015) through its control on biomass growth and allochthonous delivery. Although the model indirectly accounts for the influence of flooding events on respiration through Hetresp scenario, it employs a crude assumption of constant 70% increase in respiration rate throughout the year based on the findings of Hutchins et al. (2020). Heterotrophic respiration may present intra-annual variability with a strong variation in the degree of change as it depends on multiple factors that influence riverine organic matter dynamics such as climatic conditions (e.g. Val et al., 2016; Von Schiller et al., 2019), flow regulation and variation (e.g. Marcarelli et al., 2010), effluent discharges (e.g. Izagirre et al., 2008) and biomass degradation (e.g. Zhang et al., 2017).

Nutrient dynamics in rivers are also influenced by hydrology in addition to urbanisation and land use practices. The QUESTOR model accounts for this coupled relationship between hydrology and catchment management practices for modelling nutrient dynamics in the river. These relationships are important to include in modelling since primary production and nutrient cycling processes in rivers are often closely associated (Roberts and Mulholland, 2007). For scenario analysis, this study assumes improvements in phosphorus management practices in the river, but riverine phosphorus concentrations may still increase if effluent dilution capacity is reduced in response to persistent low flows (Bussi et al., 2017). High nutrient availability in the river may boost metabolism rates (Dodds, 2007) through changes in oxygen source (P_P, P_N) and sink (R_{nitri}) pathways. Land use changes such as agricultural intensification may lead to increased nitrogen concentrations in the river, although a more likely future encompasses a reduction in agricultural land due to a decrease in agriculture profitability (Bussi et al., 2017; Fezzi et al., 2017). Nitrogen management scenario is not included here since nitrogen concentrations do not limit phytoplankton growth in the river. However, nitrogen may play a bigger role

in influencing primary production with reduction in future nitrogen concentrations (e.g. Dortch and Whitledge, 1992; Mackay et al., 2020).

Light and temperature are often found to be key controls of river metabolism (Roberts et al., 2007). This study also found an influence of changes in light and water temperature on river metabolism though application of Shading and Temp scenarios, respectively. The model predicts improvements in water quality and a reduction in GPP with increased shading during biomass growing season that is similar to what is found elsewhere (Burrell et al., 2014; Nebgen and Herrman, 2019). Warming increases and decreases both GPP and R_A in cold and warm months, respectively (e.g. Zoboli et al., 2018). R_H is predicted to increase in response to warming throughout the year, which is also in line with previous findings (Demars et al., 2011; Song et al., 2018). The model also accounts for the influence of light availability on water temperature dynamics, which may ultimately influence river metabolic regime (Huryn et al., 2014; Nebgen and Herrman, 2019). Overall, the model predicts an expected response of metabolism to changes in light and temperature scenarios. However, the model assumption of cool water diatoms as the dominant biomass producers throughout the year (Pathak et al., 2021) may not hold true in these scenarios since changes in light and temperature may create favourable growing conditions for other phytoplankton communities (Descy et al., 2003), which may modify the river metabolic regime.

Other important pressures of river metabolism that are not explicitly included in this study, but may influence future river metabolism are changes in land use practices (Bernot et al., 2010), grazing rates and their seasonality (Schöl et al., 2002), eutrophication (Genzoli and Hall Jr, 2016), and channel hydraulics (Mulholland et al., 2001). Despite the limitations in the scenarios considered in this study, the model is able to derive insights into the response of river metabolism to future environmental and catchment management changes in the lower River Thames. Process-based models such as QUESTOR are powerful tools to determine ecosystem response to individual as well as multiple environmental stressors. Such scenario analysis exercises are useful to guide future river restoration measures.

5

METABOLISM MODELLING IN RIVERS WITH UNSTEADY FLOW CONDITIONS AND TRANSIENT STORAGE ZONES

5.1 INTRODUCTION

Biotic CO_2 emissions from rivers can be estimated through the metabolic balance of rivers, thus contributing to our understanding of the global carbon cycle (Raymond et al., 2013; Hotchkiss et al., 2015; Demars et al., 2016). Whole-stream metabolism characterises carbon fixation and mineralisation through gross primary production (GPP) and ecosystem respiration (ER) in streams and rivers. GPP and ER are integral measures of riverine biological processes (Bernhardt et al., 2018) and can serve as important indicators of whole-river health (Young et al., 2008; Von Schiller et al., 2017; Ferreira et al., 2020).

Ecologists have developed robust models for whole-stream metabolism estimation based on diel oxygen changes in open channels (Odum, 1956; Demars et al., 2015; Holtgrieve et al., 2016) including book-keeping methods with Monte-Carlo simulation (Demars, 2019) or inverse models with Bayesian procedure (Holtgrieve et al., 2010; Hall et al., 2016; Appling et al., 2018a). However, these models were developed for reach-scale estimation and for a limited range of river environments (Appling et al., 2018b). For example, the open-channel metabolism models do not account for the influence of sub-daily flow variation and transient storage zones on dissolved oxygen variation at river-network scale despite these features being prevalent in many rivers influenced by flow regulation (Zimmerman et al., 2010) and with vegetated stretches (Kurz et al., 2017), respectively. Civil engineers have also produced water quality models for oxygen prediction to address river sanitation issues (Streeter and Phelps, 1925; Beck and Young, 1975). These models are applicable to entire river networks (Cox, 2003a,b), whereas this is just emerging in the ecological literature (Segatto et al., 2020, 2021; Pathak et al., 2022). Therefore, we can integrate implementations from both these fields to build parsimonious models applicable to a wider range of river environments than those currently studied through open-channel metabolism models.

Quantification of transient storage in metabolism models may be crucial as these zones are potential hotspots of metabolism in rivers due to longer residence times (Fellows et al., 2001; Mulholland et al., 2001; Argerich et al., 2011). These zones are characterised by stagnant pockets of water due to presence of biofilms, dense patches of aquatic plants, hyporheos or eddies of deep pools (Bencala and Walters, 1983; Ensign and Doyle, 2005; Bottacin-Busolin et al., 2009). Several models have been developed to simulate the impact of transient storage on solute transport in rivers such as the Transient Storage Model (Bencala and Walters, 1983; Runkel, 1998; Manson et al., 2001) and the Aggregated Dead Zone (ADZ) model (Beer and Young, 1983; Wallis et al., 1989). The proportion of transient storage and the exchange rate of water molecules between the main channel and the storage

zone may change with flow (Manson et al., 2010; Wallis and Manson, 2018), but current models were designed to work under steady flows.

The assumption of steady flow conditions in metabolism models may not hold true in regulated rivers. Wide-spread flow regulation for reservoir operations in rivers around the world has altered the frequency and magnitude of sub-daily flow variation and consequently impacted healthy ecosystem functioning (Poff and Zimmerman, 2010). The timings and magnitude of flow releases determine trends in metabolism. Reduction in flow variability can elevate downstream metabolism (Aristi et al., 2014), whereas abrupt high flow releases can reduce tailwater metabolism (Uehlinger et al., 2003). The studies analysing flow regulation impacts on ecosystem metabolism have mainly looked at coarser temporal scale using Odum (1956)'s two-station method at a river-reach scale, where homogeneous hydraulic conditions are assumed over a period of day, i.e. impact of average daily flow on average daily metabolism (e.g. Uehlinger et al., 2003; Aristi et al., 2014; Chowanski et al., 2020). However, metabolism models need to account for sub-daily flow variability, especially considering recent trends in the rapidly changing energy markets (e.g. switch to renewable energy) that may enhance the sub-daily variability in flow (hydropeaking) in tailwaters (Ashraf et al., 2018). To address these limitations, a river network model for stream metabolism requires the run of a flow routing model ahead of implementing the two-station method (Whitehead et al., 1997b; Cimorelli et al., 2016; Payn et al., 2017). The prospect of simply adding water transient storage using advection-dispersion equations (Chapra and Runkel, 1999; Demars et al., 2015) to these more complicated models is daunting because many additional parameters would need to be estimated or well constrained to apply the models at river-network scale under varying flow conditions, as exemplified with nutrient cycling (Ye et al., 2012).

This study overcomes these limitations through development of a parsimonious model for Metabolism estimation in rivers with Unsteady Flow conditions and Transient storage zones (MUFT) that can be extended to a river-network scale. To demonstrate the model's development and implementation, I used a case study of the River Otra in southern Norway. The MUFT model was implemented along an 11 km river stretch downstream of a hydropower plant, where dam operations cause significant diel fluctuations in flow. To include the influence of diel flow variation in the MUFT model, I coupled a simple unsteady flow routing model adapted from the QUASAR (QUAlity Simulation Along River systems) model (Whitehead et al., 1997b) with a two-station stream metabolism model (Odum, 1956). The study stretch also demonstrates delayed oxygen transport compared to water velocity, which could be attributed either to the transient storage created from excessive plant growth in the river reach or to the dual flow regulation by dams at the upstream and downstream ends of the study stretch. To account for these probable mechanisms of oxygen transport, I tested two model formulations, (1) ADZ model that accounts for transient storage zones (Wallis et al., 1989) and (2) ADV (advection) model that accounts for dual flow regulation impact on oxygen transport (Beck and Young, 1975). In the MUFT model, these formulations (ADV or ADZ) are coupled with the unsteady flow routing and the two-station stream metabolism models. Previously, studies have proposed

modifications in the QUASAR flow routing model to simulate unsteady flows (Sincock and Lees, 2002) as well as proposed coupling of ADZ and original QUASAR (steady flow) models to simulate non-conservative solutes (Lees et al., 1998). The MUFT model combines these efforts by coupling the unsteady QUASAR model and the ADZ model to simulate non-conservative solutes.

I show metabolism estimation using both inverse and accounting (book-keeping) approaches in the MUFT model. While the accounting method is not predictive, it allows an independent estimation of the light parameters for GPP that are used to better constrain the inverse model and avoid issues of equifinality. The modelling approaches presented in this study not only provide theoretical benefits for studying the impact of transient storage zones and unsteady flows on metabolism dynamics, but also promote practical applications for the management of tailwater river ecosystems.

5.2 THEORY

I first selected a flow routing model to simulate discharge downstream of a hydropower plant, with upstream flow boundary conditions (from e.g. gauging station, rainfall-runoff simulations) as model input. I present the flow model equations in this section, but any flow routing model of user's preference can be used. Further, I present associated metabolic models of dissolved oxygen (DO) concentrations under unsteady flow conditions with increasing complexity. In the next section, I show how to apply these models to a case study.

5.2.1 *Flow routing model*

To simulate unsteady flows in the MUFT approach, I adapted the flow routing model proposed by Sincock and Lees (2002), who based their approach on the QUASAR model (Whitehead et al., 1997b) originally designed for slowly time-varying flows (quasi steady-state). Because of the steady flow assumption, the original QUASAR model assumes the flow and solute travel times to be equal. However, under unsteady flow conditions, the travel time of flood wave can be expressed in terms of kinematic wave velocity (celerity), which is higher than the mean flow velocity (Sincock et al., 2003) and consequently, solute velocity. The ratio m of the average celerity (c, m s^{-1}) to the average flow velocity (u, m s^{-1}) is expressed following Sincock et al. (2003),

$$m = \frac{c}{u} = \frac{dQ/dA}{Q/A} \tag{5.1}$$

where Q is discharge (m^3 s^{-1}), A is the cross section area of flow and m may be approximated as 5/3 (Chapra, 2008).

The celerity (c, m s^{-1}) of the flood wave for a reach of length L (m) is,

$$c = \frac{L}{T_{flow}} \tag{5.2}$$

where T_{flow} represents the travel time of the flood wave (s).

It is assumed that T_{flow} may be partitioned into dispersion (T_{fladz}) and advection (τ_{fl}) terms using a fraction of retention F_r,

$$T_{fladz} = F_r \times T_{flow} \tag{5.3}$$

$$\tau_{fl} = (1 - F_r) \times T_{flow} \tag{5.4}$$

The flow routing model includes a simple mass-balance of incoming and outgoing flows and assumes fixed channel width with rectangular cross-section. Lateral groundwater inflows and discharge from small tributaries were assumed to be negligible within reaches. In a river network, the flow of major tributaries may be inserted at the upstream edge of a reach. River reaches may be represented as a series of non-linear reservoirs. The flow model simulates water transport through a series of n non-linear reservoirs followed by a time lag parameter (τ_{fl}, s) that lags the routed hydrograph without attenuation (Figure 5.1a). The changes in flow are represented as,

$$\frac{dQ_t}{dt} = \frac{Q_{i,t-\tau_{fl}} - Q_t}{F_r T_{flow}} \tag{5.5}$$

where Q is the flow leaving the reach at time t, Q_i is the flow coming into the reach at time t. Eq. 5.5 accounts for the travel time (T_{flow}) derived from celerity (Eq. 5.2) as opposed to the travel time derived from mean flow velocity as is commonly done in original QUASAR model applications.

5.2.2 *Metabolic model in a well-mixed reach under unsteady flow conditions*

I developed the metabolic model of DO dynamics (Eq. 5.6) by combining two approaches, (1) the conservative solute transport model proposed by Whitehead et al. (1997b) to simulate DO transport with unsteady flows and (2) the stream metabolism two-station method proposed by Odum (1956) to simulate in-stream DO sources and sinks from metabolism and air-water gas exchange processes. The detailed proof of both models were given in the original publications. Note that Eq. 5.6 does not account for water transient storage.

$$\frac{dC_t}{dt} = \frac{Q_{i,t}}{(Q_t \times T_u)}(C_{i,t} - C_t) + \frac{1}{z_t}(P_{GPP,t} - R_{ER,t}) + k(C_{s,t} - C_t) \tag{5.6}$$

where C_i is the incoming DO in the reach (mg O_2 L^{-1} equivalent to g O_2 m^{-3}), C is the DO leaving the reach (mg O_2 L^{-1}), P_{GPP} is the gross primary production (g O_2 m^{-2} min^{-1}), R_{ER}

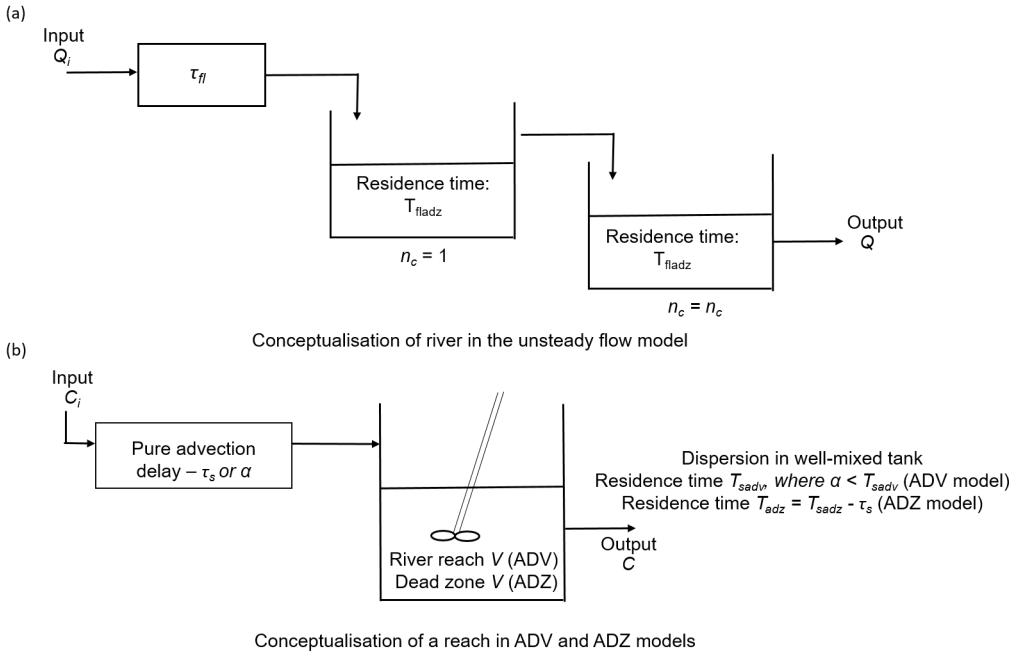

Figure 5.1: Conceptualisation of river reaches in the (a) unsteady flow model adapted from Sincock and Lees (2002) and (b) ADZ model adapted from Lees et al. (2000) for conservative solute C

is the ecosystem respiration (g O_2 m^{-2} min^{-1}), k is the gas exchange coefficient (min^{-1}) and C_s is the expected oxygen solubility (mg O_2 L^{-1}). T_u (min) represents the mean flow travel time, which is equal to the solute travel time for a well-mixed reach.

5.2.3 *Metabolic model with pure advection and a well-mixed reach under unsteady flows (ADV model)*

In long reaches where solute transport is dominated by advective transport as opposed to dispersion, it may be necessary to explicitly take into account pure advection as follows (Beck and Young, 1975):

$$\frac{dC_t}{dt} = \frac{Q_{i,t-\alpha}}{(Q_t \times T_{sadv})}(C_{i,t-\alpha} - C_t) + \frac{1}{z_t}(P_{GPP,t} - R_{ER,t}) + k(C_{s,t} - C_t) \tag{5.7}$$

$$\alpha = F_{adv} \times T_{sadv} \tag{5.8}$$

where F_{adv} is the advection delay coefficient. The addition of pure advection α (see Table 5.1) in the first term of the equation allows to have the two DO concentration curves in phase without modifying their shape (simple time translation), with $\alpha \leq T_{sadv}$ (Beck and Young, 1975). Note that T_{sadv} is equivalent to T_u for the ADV model.

5.2.4 *Metabolic model with pure advection and transient storage (dispersion) under unsteady flows (ADZ model)*

The influence of transient storage in the metabolic model is included using the ADZ concept (Beer and Young, 1983; Wallis et al., 1989) as proposed by Sincock and Lees (2002), who coupled the unsteady QUASAR flow model with the ADZ model for a conservative solute. ADZ model was selected for its simplicity and its conceptual similarity to the unsteady QUASAR flow model (Figure 5.1). The original QUASAR model assumes the river reach to be a perfectly mixed system. ADZ model conceptualises the river reach as an imperfectly mixed system, where solute is subjected to pure advection followed by dispersion in a lumped active mixing zone (Beer and Young, 1983; Wallis et al., 1989; Lees et al., 2000). The metabolic model becomes:

$$\frac{dC_t}{dt} = \frac{Q_{i,t-\tau_s}}{(Q_t \times T_{adz})}(C_{i,t-\tau_s} - C_t) + \frac{1}{z_t}(P_{GPP,t} - R_{ER,t}) + k(C_{s,t} - C_t) \tag{5.9}$$

The ADZ model partition the overall solute travel time T_{sadz} into dead-zone residence time T_{adz} and advection lag τ_s, equivalent to partitioning total reach volume into the volume of water transient storage and main channel.

$$T_{adz} = T_{sadz} - \tau_s \tag{5.10}$$

For reaches affected by transient storage, the effective solute transport velocity (u_s) is lower than the mean flow velocity (u) due to solute retention in the storage zone. The relationship between these velocities can be described using a solute-lag coefficient β (Lees and Camacho, 2000) as,

$$u_s = \frac{u}{1+\beta} \tag{5.11}$$

Considering Eq. 5.1, Eq. 5.2 and Eq. 5.11, travel time and advection lag for a solute in the ADZ model can be described in terms of flow parameters (Sincock, 2002),

$$T_{sadz} = m(1+\beta)T_{flow} \tag{5.12}$$

$$\tau_s = m(1+\beta)\tau_{fl} \tag{5.13}$$

5.2.5 *Modified two-station model for the accounting method*

Eq. 5.9 can be simplified to derive net ecosystem production ($P_{NEP} = P_{GPP} - R_{ER}$) using Euler finite-difference approach, which gives the two-station accounting approach under varying discharge,

$$P_{NEP,t} = \left(\frac{C_{t+\Delta t} - C_t}{\Delta t} - \frac{Q_{i,t-\tau_s}}{(Q_t \times T_{adz})}(C_{i,t-\tau_s} - C_t) - k(C_{s,t} - C_t)\right) z_t \tag{5.14}$$

Note that Eq. 5.14 can easily be adjusted for the other metabolic models presented above (Eq. 5.6 and Eq. 5.7). This approach allows to estimate average R_{ER} during the dark hours (photosynthetically-active radiation (PAR) < 1 µmol-photons m^{-2} s^{-1}) and deduce $P_{GPP,t}$ by difference ($P_{NEP,t} - R_{ER,t}$) during the light hours assuming constant R_{ER} throughout the day (see Demars et al., 2015). Daily GPP (P_{GPP}) is simply the sum of $P_{GPP,t}$ throughout a day,

$$P_{GPP} = \frac{\int_{t_0}^{t_{end}} P_{GPP,t}\, dt}{1\, day} \tag{5.15}$$

5.2.6 *Photosynthesis-light relationship*

The accounting method has the advantage, over the inverse modelling approach, of deriving instantaneous and daily GPP without making any assumption on the photosynthesis-light relationship. The most appropriate link function may thus be selected by plotting $P_{GPP,t}$ as a function of PAR_t. The function is substituted to $P_{GPP,t}$ in the metabolic models (Eq. 5.6, Eq. 5.7 or Eq. 5.9). The parameters of the link function may be used as constants or enabled to constrain the priors (through their uncertainties) in the inverse model, thus reducing issues of equifinality. Here, instantaneous gross primary production (P_{GPP}) was modelled as a function of PAR with a Michaelis-Menten type equation to include the light-saturation effect on photosynthesis (Demars et al., 2011),

$$P_{GPP,t} = \frac{P_{GPPmax} \times E_{PAR,t}}{k_{PAR} + E_{PAR,t}} \tag{5.16}$$

where $E_{PAR,t}$ is the photosynthetically-active radiation (µmol-photons m^{-2} s^{-1}) at time t, P_{GPPmax} is the maximum GPP (g O_2 m^{-2} min^{-1}) and k_{PAR} is the PAR at which half the P_{GPPmax} is attained (µmol-photons m^{-2} s^{-1}).

P_{GPPmax} and k_{PAR} in the inverse model were estimated using a least-squares minimisation algorithm. It is implicitly assumed that light conditions are spatially uniform along the modelled channel length and PAR only varies with time.

5.2.7 *Dissolved oxygen saturated concentration*

The expected oxygen solubility (C_s, mg L^{-1}) was estimated from Standing Committee of Analysts (1989) as follows,

$$C_s = \frac{C_{atm}(P - V_P)}{101.325 - V_P} \tag{5.17}$$

where C_{atm} is the oxygen solubility under normal atmospheric pressure (mg L^{-1}), P is the observed atmospheric pressure (kPa) and V_P is the saturation vapour pressure of

water (kPa). C_{atm} and V_P were estimated as a function of water temperature T (range of application 0-50°C, Demars et al., 2015),

$$C_{atm} = -0.00005858T^3 + 0.007195T^2 - 0.39509T + 14.586 \quad (5.18)$$

$$V_P = 0.0000802T^3 - 0.000717T^2 + 0.0717T + 0.539 \quad (5.19)$$

5.3 CASE STUDY

5.3.1 *Study area*

The River Otra flows through forests and alpine uplands in the valley of Setesdal and is the largest river in southern Norway. The river drains a catchment area of 4000 km² and runs for about 240 km until it meets the North Sea at Kristiansand (Wright et al., 2017). The river is extensively used for hydropower production (about 4 TWh per year) through construction of dams and water transfers, with Brokke being the largest hydropower station in the valley (Rørslett, 1988; Wright et al., 2017).

I applied the models within a 10780 m long river section located downstream of the Brokke hydropower plant (Figure 5.2). This section drains about 1900 km² (Wright et al., 2017). The river stretch can be considered an artificial system with its flow and water level controlled by Brokke hydropower plant at the upstream end and Hekni dam at the downstream end. The oscillating demands on energy production can cause flow to vary from ~ 20-80 $m^3 s^{-1}$ within 24 h under low summer flows. The hydropower plant effluent can also release water highly supersaturated in dissolved gases depending on water intakes (streams *versus* reservoirs) independently of discharge (Pulg et al., 2016). No such supersaturation events were observed during the short term study period here (Demars et al., 2021). In addition to the controlled flow, the river reach also shows profuse growth of the aquatic plant *Juncus bulbosus*, which may create significant amount of water transient storage, delaying solute transport time relative to the velocity of water (Ensign and Doyle, 2005; Kurz et al., 2017).

5.3.2 *Sensor deployment and bathymetry*

DO and water temperature were monitored using O_2 and temperature sensors (miniDOT PME) at site 2 (Figure 5.2). A monitoring station was also installed at site 3 to monitor dissolved oxygen and water temperature (Xylem - Andeeraa optode 4831), photosynthetically-active radiation (LICOR Quantum LI190R-L), air temperature and atmospheric pressure (Barometer RM Young 061302V) using a Campbell data logger (CR1000X). Data from the monitoring station were transferred daily through a Campbell Scientific 4G modem CELL215. Data were logged at 5 min time intervals from 4th (10:00 am) to 8th (15:35) August 2019. The sensor at site 2 was installed vertically facing down in

Figure 5.2: Study stretch in the River Otra spanning from Brokke to Hekni. Monitoring locations of river flow (red circle) and dissolved oxygen (black filled circles) are marked on the map.

the main current at mid depth, tied to a post. The sensor at site 3 was inserted into a plastic pipe fixed on Straume bridge, and protruded in the main current. The oxygen sensors were cross calibrated in 100% air saturated water in a bucket before and after deployment and small corrections ($< 3\%$ DO saturation) were applied, as previously reported (Demars, 2019).

Total dissolved gas (TDG) was monitored at site 1, 2, 3 and 4 every 30 min at infrequent intervals during a five year period (2012-2017) with Total Gas Analysers 3.0 (Fisch- und Wassertechnik (Pulg et al., 2016) based on the Weiss-saturometer principle (Weiss, 1970). The saturation is measured as the percent dissolved air in the water relative to expectation from ambient air pressure. The saturometer has an accuracy of $\pm$10 hPa, which is approximately $\pm$1% TDG.

Several thousands georeferenced water depth points were taken throughout the reach with a measuring stick north of Straume and Lowrance sonar in the downstream part to Hekni (Figure D.1), and cross calibrated with discharge. Changes in water depth were determined from absolute pressure difference (see Moe and Demars, 2017) between atmospheric pressure and submersible pressure sensors inserted into a perforated plastic tube at sites 1-4 recording at 30 min time intervals (Onset HOBO data loggers U20L-04, accuracy equivalent to 4 mm for water level).

5.3.3 *Flow-velocity*

Hourly flow data at Brokke (hydropower plant effluent and river) and Hekni sites were obtained for a duration of 8 days (3/8/2019-10/8/2019) from the hydropower company. Flow observations were not available at Rysstad Øy and Straume, where metabolism is estimated. Flood wave travel times at these sites were derived from solute travel time using the travel time relationships proposed by Sincock et al. (2003). I used these travel time relationships to back-calculate solute and flow travel time parameters from velocity estimates (Table 5.1). Velocity estimates in the river reaches were derived using two approaches.

Average velocities for the first section (site 1-2: steep, shallow, fast flowing, cobble bed) were determined using Manning's equation: $v = (1/n)A/{P_m}^{2/3}S_c^{1/2}$, where n is the Manning roughness coefficient (0.04, cobble bed), A is the cross-sectional area of the river channel (m²), P_m is the wetted perimeter of the river channel (m) and S_c is the channel slope (0.0016 m/m). A and P_m were calculated using changes in water depth. This method could not be applied further downstream due to partial control on water level by Hekni dam.

Average velocities for the second section (site 2-3: very wide, gentle slope, sandy bed) and the third section (site 3-4: narrow, water level controlled by Hekni dam) were estimated from section length (L) and mean travel time (T_s) of large peaks in TDG, where $u_s = L/T_s$. I used cross correlation function in R (Venables and Ripley, 2002) to identify average travel time lags (h) between TDG time-series across the sites. Large TDG super-saturation events (threshold > 130% at Brokke) with time lag correlation coefficient > 0.4 were selected for the estimation of velocity. These velocities were plotted against discharge at Hekni (averaged for corresponding event duration) to establish flow-velocity relationship for each reach. TDG travel times ranged between 2-12 hours and 7-13 hours in the second (site 2-3) and third sections (site 3-4), respectively. This method could not

Table 5.1: Velocity and travel time formulations in the ADV and ADZ models for the River Otra back-calculated based on the travel time relationships proposed by Sincock et al. (2003). (CSTR, continuous stirred tank reactor)

	ADV model	ADZ model
Solute velocity	$u_s = bQ^c$	$u_s = bQ^c$
Solute-lag coefficient	$\beta = 0$	$\beta = 1.55$ (see Appendix D)
Mean flow velocity	$u_{adv} = u_s$	$u_{adz} = (1+\beta) \times u_s$
Celerity	$c_{adv} = m \times u_{adv}$	$c_{adz} = m \times u_{adz}$
Water residence time in CSTR	$T_{uadv} = L/u_{adv}$	$T_{uadz} = L/u_{adz}$
Total solute travel time	$T_{sadv} = T_{uadv}$	$T_{sadz} = L/u_s$
Advection delay	$\alpha = F_{adv}T_{sadv}$	$\tau_s = T_{sadz} - T_{uadz}$
Dead zone residence time		$T_{adz} = T_{uadz}$

be applied in the first section as the temporal resolution of the TDG data was too coarse relative to the mean travel time (< 1 h).

I established relationships between flow and TDG velocity as $u_s = bQ^c$ for three discernible sections. Ideally a conservative solute should be used to estimate flow-velocity parameters (b, c). While TDG is not a conservative tracer, the selection of the largest peaks to differentiate from noise and the very low gas exchange rate in these sections gave a similar result to a continuous addition of lime under high flow conditions (about 102 m^3 s^{-1}) monitored with electric conductivity sensors deployed at Straume (site 3) and Hekni (site 4). Power regressions between the velocities of TDG waves and corresponding mean flows at Hekni provided values of constants b and c for the second ($R^2 = 0.78$) and third sections ($R^2 = 0.56$) (Figure D.2, Table D.1). Water travelled fastest in the first section (Brokke-Rysstad Øy) with a mean velocity of 0.73 m s^{-1}, slowest (0.14 m s^{-1}) in the widest section with high plant growth (Rysstad Øy-Straume) and slow-flowing in the narrower and deeper third section (0.27 m s^{-1}) for a 50 m^3 s^{-1} discharge.

5.3.4 *Gas exchange rate*

The gas transfer velocity (kz) of CO_2 was estimated as the flux of CO_2 (F_{CO2}, mmol m^{-2} h^{-1}) determined using floating chambers equipped with infra-red gas analysers (following Bastviken et al., 2015) relative to the CO_2 saturation deficit as follows ($C_s - C$, mmol m^{-3}),

$$kz = \frac{F_{CO2}}{C_s - C} \tag{5.20}$$

More specifically, CO_2 efflux (or influx) were estimated in 33 half-hour runs, from the average of three chambers for each run drifting freely at the water surface and logging at 30 s time intervals. The runs were conducted between March 2020 and August 2020 under varying temperature, discharge and depth. The calculations of CO_2 flux for individual chambers followed Martinsen et al. (2018). Water samples were collected at the beginning and end of each run in 120 mL glass bottles to determine the CO_2 saturation deficit. Water bottles were filled to the rim and capped underwater, then crimped. Mercuric chloride

($HgCl_2$) was immediately added to stop biological processes (100µL of half saturated solution per 120 mL bottle). The samples were kept cool (+4°C) and in the dark until the day of gas analysis. The samples were warmed and weighed at room temperature, a 30 mL helium headspace was created, the samples were weighed again (to determine the volume of water removed from the bottle), and shaken gently horizontally for at least an hour. The headspace was analysed by gas chromatography and concentrations were calculated following Yang et al. (2015). It was checked that the addition of $HgCl_2$ did not affect the determination of CO_2 (Borges et al., 2019; Koschorreck et al., 2021).

The specific flux F_{CO2} was not related to water temperature, discharge, depth or velocity. Thus $kz = 0.022 \pm 0.004$ m h^{-1} was estimated as the slope of the regression line between specific CO_2 flux and CO_2 saturation deficit (Figure D.3). In theory the regression line should go through the origin, but the uncertainties were reasonable given the modest range of dissolved CO_2 saturation (70-267%). Thus knowing average depth ($z = 1.82$ m) during the chamber runs, the gas exchange coefficient was calculated for CO_2 as $k_{CO2} = 0.012 \pm 0.002$ h^{-1}.

Finally, the oxygen gas exchange coefficient k_{O2} was simply calculated from $k_{O2} = k_{CO2}/0.81$ (Demars, 2019), where the constant 0.81 accounts for differences in the rates of CO_2 and O_2 diffusion in water independently of temperature (Davidson, 1957). The estimate of k_{O2} (0.35 ± 0.07 d^{-1}) indicated low gas exchange, comparable to other rivers with similar depth-velocity (< 2 d^{-1}, Palumbo and Brown, 2014). k_{O2} was used as a constant in the metabolism models (k in Eq. 5.6, Eq. 5.7, Eq. 5.9) to simulate reaeration flux.

5.3.5 *Model application and parameter estimation*

I developed the model code in Python (3.6.3). Flow and solute dynamics in the river were described using ordinary differential equations and solved through an accounting method using finite difference approximation and inverse modelling using odeint() function from the `Scipy` package (v1.5.0) in python. The odeint() function solves ordinary differential equations using lsoda solver from the FORTRAN library odepack.

The boundaries of the river network for model implementation were decided based on data availability. The modelling approach presented here requires observations at minimum two sites in the river, one for input and one for parameter calibration. Although the model implementation in this study is limited to one reach, the model can be extended for multi-reach application. The flow routing model was first implemented at 5 min time-steps for the river stretch between Brokke and Hekni since flow hydrographs were available at these two sites. Similarly, the solute model was implemented at 5 min time-steps for the river stretch between Rysstad Øy and Straume since oxygen observations were available at these sites.

Model parameters in the inverse model were estimated using a two-step calibration process (similar to Sincock and Lees, 2002), where flow parameters were first optimised with respect to the observed flow, prior to the optimisation of solute transport relationships and metabolic parameters. Flow parameters can be optimised between the gauging sites on

reach-by-reach basis in downstream direction. Flow time-series at Brokke and Hekni were used to first optimise F_r parameter. Flow at Rysstad Øy and Straume were then modelled using the optimised value of F_r.

Solute travel times in the River Otra were derived as described in section 5.3.3. Next, metabolic parameters (P_{GPPmax}, k_{PAR}, R_{ER}) were optimised in the process of fitting oxygen time-series. Model parameters were optimised using a least-squares minimisation approach with the Nelder-Mead algorithm (Gao and Han, 2012) from the `lmfit` package (v1.0.1) in Python. Lower and upper bounds were provided from prior knowledge to constrain the inverse model parameters and avoid parameter equifinality. Initial values of P_{GPP}, k_{PAR} and R_{ER} were provided from the outputs of the two-station accounting method. F_{adv} was optimised in the modified two-station model (ADV formulation, accounting method) by minimising the residual sum of squares of GPP-PAR link function (Eq. 5.16), and was used as a constant in the inverse ADV model. Metabolism parameters were assumed to be constant over a period of 24 h for a given reach.

I sampled Bayesian posterior distribution of solute model parameters using the Markov Chain Monte Carlo (MCMC) algorithm using the `emcee` package (v3.0.2) in python. This method calculated the log-posterior probability ($ln\, p(\theta_{true}|D)$) of the model parameters (θ) given the data (D),

$$\ln p(\theta_{true}|D) \propto \ln p(\theta_{true}) - \frac{1}{2}\sum_n [\frac{(g_n(\theta_{true}) - D_n)^2}{{S_n}^2} + \ln(2\pi {S_n}^2)] \tag{5.21}$$

where $ln\, p(\theta_{true})$ is the log-prior. The second term on the right represents log-likelihood, $ln\, p(D|\theta_{true})$, where g_n is the generative model, D_n is the data and S_n is the measurement uncertainty. Note that I did not use the MCMC algorithm for parameter optimisation. Instead, I first optimised the model parameters using the Nelder-Mead algorithm and later used the MCMC algorithm to sample from the posterior distribution of these optimised values to obtain parameter uncertainties and covariance.

5.4 RESULTS

Performances of flow routing and metabolism models were evaluated separately. River flows were simulated ahead of the metabolism estimation and outputs from the flow routing model were fed as inputs in the metabolism model. An initial visual inspection of flow and DO curves showed that water travelled faster than DO within the study reach (Figure D.4). Such a time lag could result either from the dual water regulation at Brokke and Hekni or from the excessive vegetation in the river reach between Rysstad Øy and Straume. Therefore, to account for this time lag, I included both potential causes in the model formulations i.e., pure advection (ADV, Eq. 5.7) and also including transient storage (ADZ, Eq. 5.9) for metabolism estimation. In this section, I present the results of the flow routing and metabolism model applications. Furthermore, I provide posterior probability distribution of optimised model parameters in the inverse metabolism model.

5.4.1 *Influence of hydropower plant on DO dynamics along the reach*

The O_2 turnover in the second section (site 2-3) was only 14%, calculated as $O_{2,\text{turnover}} = 1 - 1/exp(kL/u)$ (rearranged oxygen footprint equation, Demars et al., 2015), where L = reach length (4660 m), u = average water velocity (8.03 m min^{-1}) and k = reaeration coefficient (0.00025 min^{-1}). The output suggests that 86% of the oxygen variability at Straume (site 3) can be attributed to the variability of oxygen at Rysstad Øy (site 2). It is known that the hydropower plant affects greatly total dissolved gas variation at Rysstad Øy (Pulg et al., 2016). Hence, the conventional one-station model (Odum, 1956; Appling et al., 2018a) or averaged two-station model (Demars et al., 2011; Demars, 2019) would not provide reliable metabolism estimates in the study section. It also highlights the difficulty of the task of disentangling metabolism from background noise, notably the hydropower plant effluent at Brokke representing 87% of median flow, i.e. most of the O_2 mass flux.

5.4.2 *Flow routing model*

The flow routing model was able to capture the timing and magnitude of flow peaks and troughs (Figure 5.3). The model estimated average 61% retention for flow in the river stretch (F_r = 0.61). Minor discrepancies between modelled and observed flows were expected because the model does not account for the effect of flow regulation at the downstream (Hekni) end that causes rapid rises and falls in water level at Hekni. Nevertheless, the flow routing model satisfactorily reproduced flow variation at Hekni with goodness-of-fit (R^2) of 0.87 (Figure 5.3b).

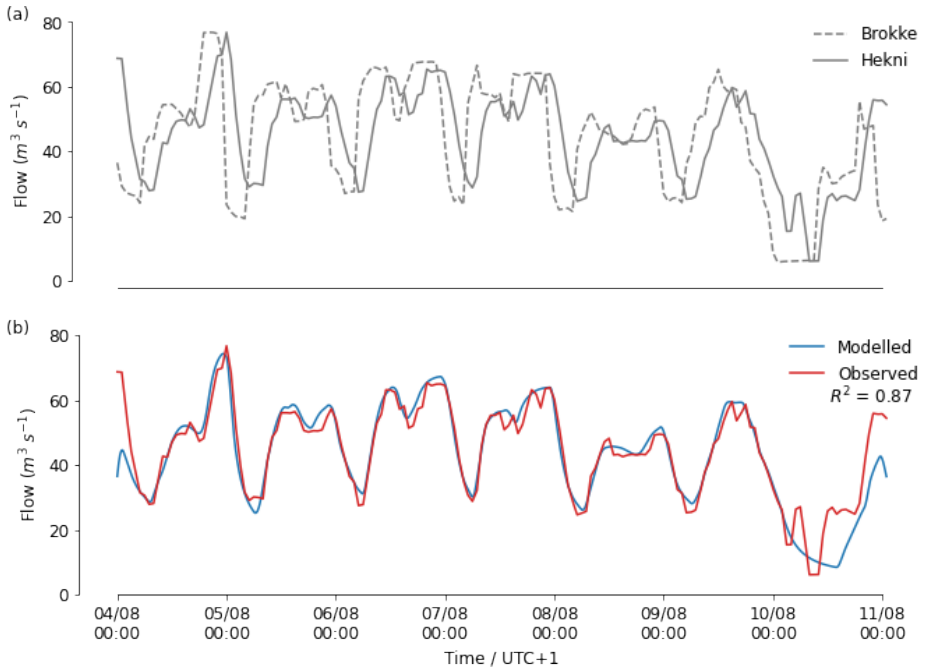

Figure 5.3: Comparison of flow observations at Brokke and Hekni sites (a) and modelled and observed flows at Hekni site (b) at 5 min time-steps

5.4.3 *Modified two-station model (accounting method)*

Modified two-station model formulation with only pure advection (ADV) performed better than the formulation with pure advection plus transient storage (ADZ) (Figure 5.4). The two-station ADZ model simulated sudden drops in NEP at Straume around mid-day, suggesting a sudden decrease in GPP around mid-day since ER was assumed to be constant. Variation in PAR did not explain the mid-day drops in GPP (Figure 5.4c). While an afternoon lull in GPP has often been reported, the estimated mid-day drops in NEP were not driven by biological production, but indicated a systematic error in the metabolism estimates resulting from errors in the simulation of DO mass flux. The mass flux of DO in the river largely followed flow variation. The upstream site (Rysstad Øy) showed concurrent decline in flow and DO in the afternoon owing to changing water demand for power plant operations (Figure D.4). The downstream site (Straume) did not show a concurrent decline in DO and flow, but showed shoulders in the DO time-series earlier in the day (around mid-day). These shoulders result from delayed transport of DO from Rysstad Øy to Straume (Figure D.4) since oxygen variation at Straume is highly influenced by oxygen variation at Rysstad Øy (explained in section 5.4.1). Although the two-station ADZ model accounts for these delayed transport mechanisms through transient storage influence, the model was unable to model NEP variation accurately. The ADV model, on the other hand, was able to resolve the issue of mid-day drops in GPP to a larger extent.

Both models showed a positive relationship between photosynthesis and light, with saturation of photosynthesis under high light intensity (Figure 5.4). The ADV model (R^2 = 0.56, Figure 5.4a) represented a slightly better regression fit than the ADZ model (R^2 = 0.44, Figure 5.4b) for GPP-PAR link function (Eq. 5.16). The estimates of half-saturation light intensity in both models (Figure 5.4) were in line with what is commonly observed in freshwater systems (k_{PAR} = 100-500 µ mol quanta m^{-2} s^{-1}, Demars et al., 2011). The estimates of P_{GPPmax} and k_{PAR} fitted in the GPP-PAR link function (Figure 5.4) served as priors in the inverse model when simulating GPP as a function of PAR.

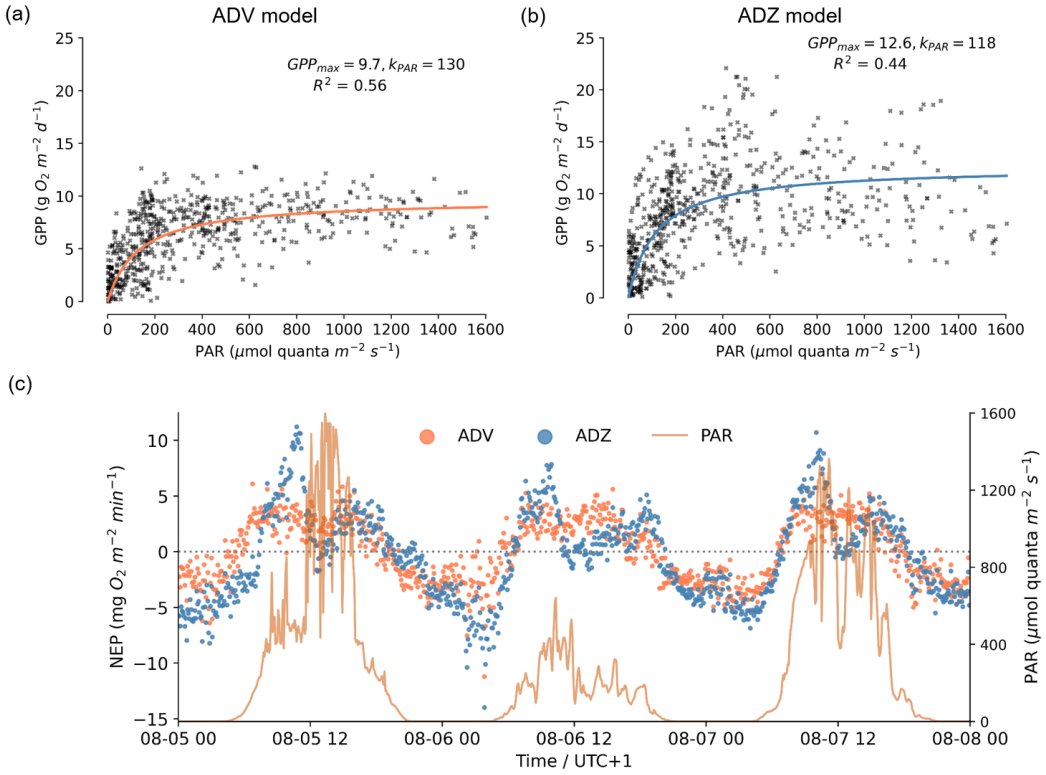

Figure 5.4: Non-linear regression between gross primary production (GPP) and photosynthetically-active radiation (PAR) in the modified two-station (a) ADV and (b) ADZ models at Straume. (c) shows the variation in net ecosystem production (NEP) and PAR in the modified two-station models at Straume. Negative values of GPP are not shown in panels (a) and (b).

5.4.4 *Inverse metabolism model*

Both ADV and ADZ formulations captured the overall DO variation at Straume (Figure 5.5), but the ADV model performed significantly better than the ADZ model to capture the overall trend and magnitude of oxygen variation. The ADZ model showed a small time lag between the observed and modelled DO concentrations, which indicates inaccuracies in the simulation of DO mass flux with flow. Note that the flow-velocity relationships derived for TDG in the study reach does not cover the entire range of observed flows during the modelling period (e.g. equations derived for velocities at Q > 50 m^3 s^{-1} for reach 2, Figure D.2).

Estimated values of metabolism parameters in the ADV model are generally lower than the estimates of the ADZ model (Table D.2). The ADV model (R^2 = 0.96) derived a better overall goodness-of-fit than the ADZ model (R^2 = 0.83). Therefore, I selected the ADV model to sample Bayesian posterior distribution of metabolism parameters using the MCMC algorithm. P_{GPPmax} and R_{ER} parameters showed a strong positive correlation during the first two days of the modelling period (> 0.86). Other significant correlations were observed between k_{PAR}-P_{GPPmax} (0.95) and k_{PAR}-R_{ER} (-0.63) on the third day. Despite these high correlations, I find that the median values (and maximum likelihood estimates) of all metabolism parameters lie in a close range of the values optimised by the

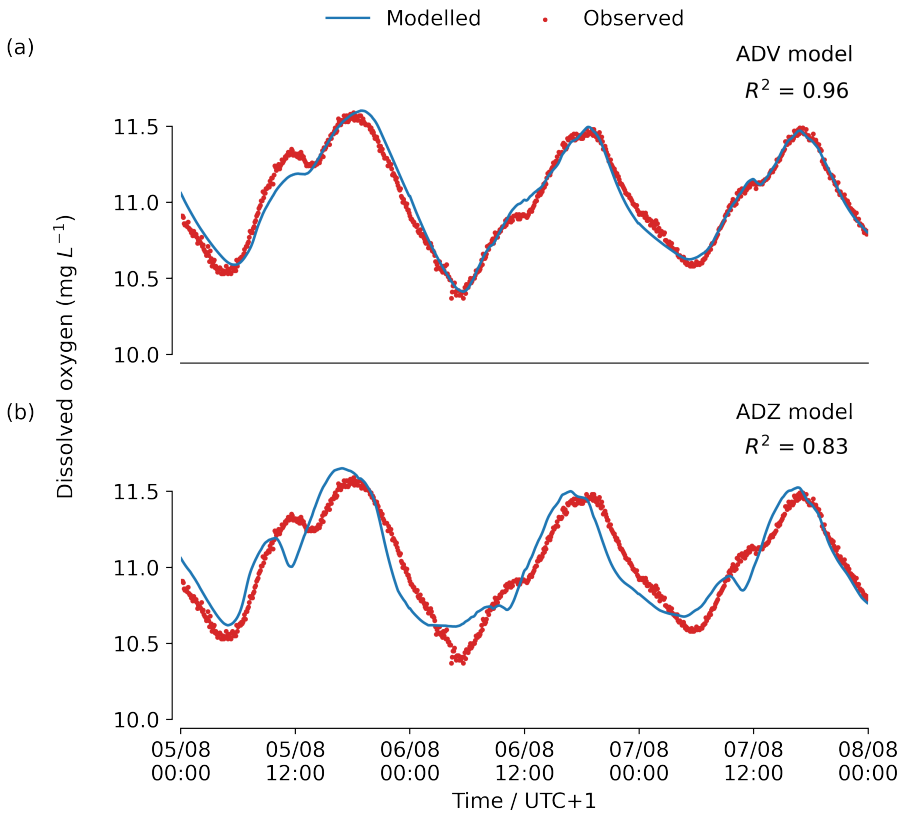

Figure 5.5: Comparison of modelled and observed dissolved oxygen concentrations at 5 min time-steps at Straume in the inverse (a) ADV and (b) ADZ formulations

Table 5.2: Median values of posterior probability distribution of the inverse ADV model parameters with 1-σ uncertainty derived from the MCMC runs and optimised parameter values by the Nelder-Mead least-squares minimisation algorithm (in brackets). Units are g O_2 m^{-2} d^{-1} for P_{GPPmax} and R_{ER}, and µmol quanta m^{-2} s^{-1} for k_{PAR}.

Parameter	Day 1	Day 2	Day 3
P_{GPPmax}	8.64±0.16 (8.64)	12.38±0.12 (12.96)	11.52±0.24 (11.52)
k_{PAR}	144±5 (144)	144±1 (144)	461±32 (461)
R_{ER}	3.46±0.09 (3.46)	4.61±0.05 (4.32)	4.03±0.04 (4.03)

Nelder-Mead minimisation algorithm (within 1-σ uncertainty) (Table 5.2, Figure 5.6). The performance of the MCMC algorithm was judged using the estimate of average acceptance fraction, which was found to be within an acceptable range (0.2-0.5, Foreman-Mackey et al., 2013) in all cases. Figure 5.7 shows the variation in NEP and the relationship between GPP-PAR as estimated in the inverse ADV model.

5.5 DISCUSSION

The MUFT model application here demonstrates how the impact of hydropeaking (i.e. sub-daily flow fluctuations) and transient storage can be included in the estimation of metabolism. The better performance of the ADV model compared to the ADZ model here suggests that despite the initial hypothesis, river vegetation may not produce significant

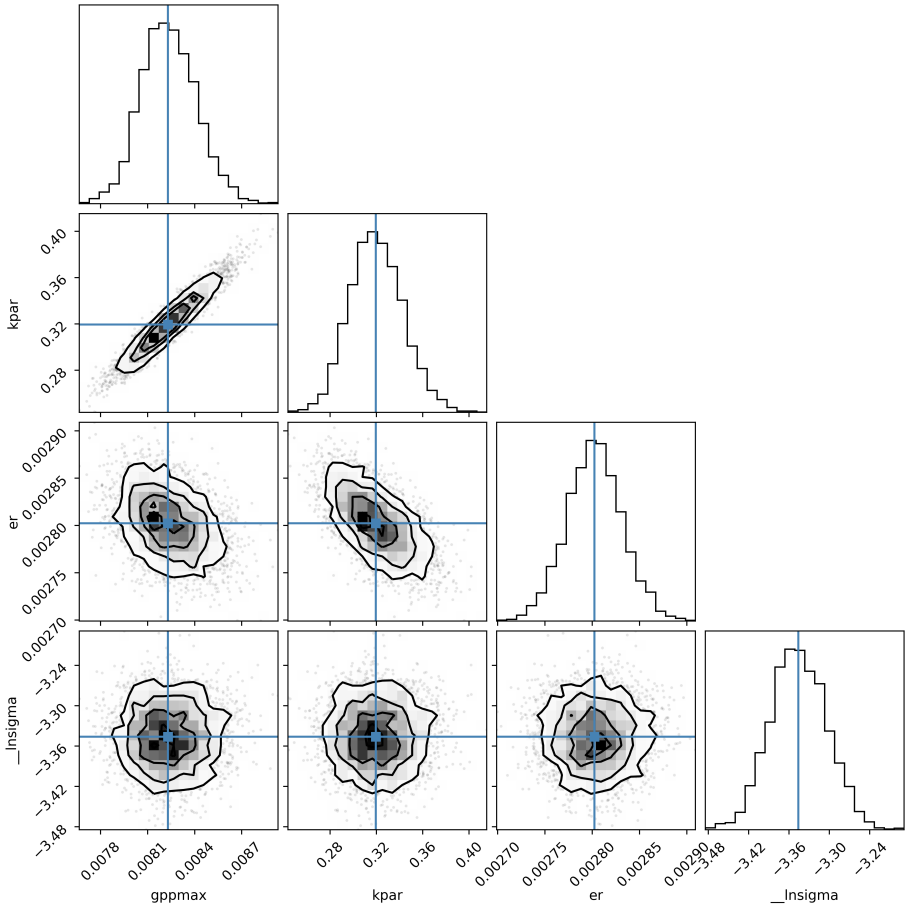

Figure 5.6: Posterior distribution of inverse ADV model parameters gppmax (P_{GPPmax}), kpar (k_{PAR}) and er (R_{ER}) using MCMC algorithm on day 3. Blue lines show the median values of posterior probability distribution of model parameters. _lnsigma parameter is used to estimate the true uncertainty in the data.

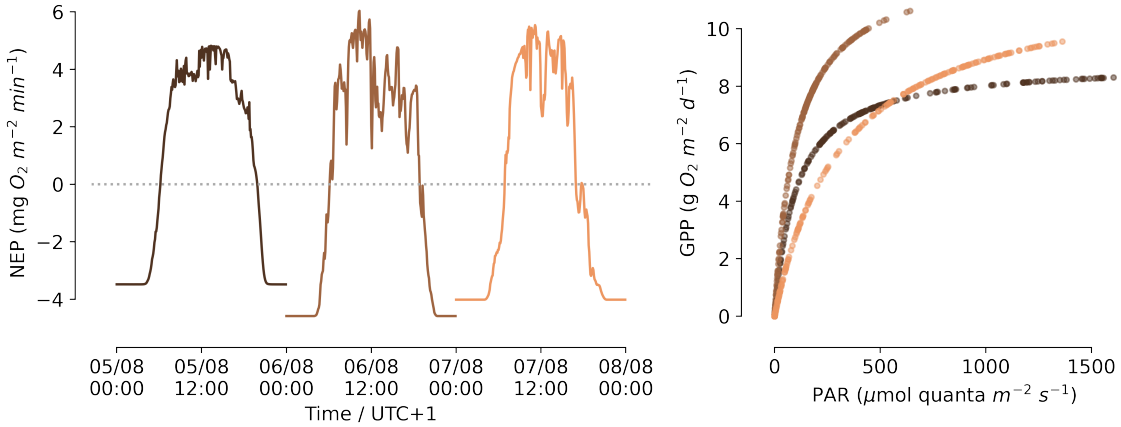

Figure 5.7: Estimated net ecosystem production (NEP) (a) and modelled GPP-PAR relationship (b) at Straume in the inverse ADV model. GPP = gross primary production and PAR = photosynthetically-active radiation.

transient storage (ADZ) and that introduction of pure transportation delay (ADV) in the model may be sufficient to characterise DO dynamics at Straume during the modelling period. However, due to limited data availability, it is difficult to confidently pinpoint the dominant transport mechanism in the river. Since, the aim of this study is to present a

general model application for metabolism estimation, I do not delve in to the specifics of the process-dynamics in the River Otra. In this section, I discuss the differences in the inverse and accounting modelling approaches along with their limitations and the possibilities of future model improvements.

5.5.1 *Comparison of the inverse model with the modified two-station model*

Discrepancies in the outputs of the inverse and modified two-station models mainly arise from the differences in the model structures. For example, the numerical solution of the ODE equation in the modified two-station model uses a simple Euler finite difference scheme as opposed to a more robust lsoda solver from the FORTRAN library odepack (Hindmarsh, 1983) in the inverse model. Moreover, both models characterise GPP in different ways. The accounting approach, although advantageous for not assuming the type of relationship between GPP and PAR, may fail to segregate the influence of flow on DO mass flux from the influence of biological production on DO transformations, when DO mass flux and/or solute-lag coefficient are not characterised accurately. On the other hand, the inverse model is able to segregate these influences up to a certain extent because GPP is modelled as a function of PAR.

Another difference between the two approaches is the parameter calibration process. The two-station method involves an accounting approach where NEP is directly estimated from oxygen observations without any parameter calibration procedure. Daily average ER is then estimated during dark hours, and GPP is calculated as a difference between NEP and daily average ER. The inverse model, on the other hand, optimises model parameters in the process of fitting modelled DO to observed DO time-series using a least-squares minimisation algorithm; hence, providing more confidence in the model estimates. Admittedly, the inverse approach includes more number of model parameters, corresponding to a larger number of degrees of freedom and consequently, the risk of parameter equifinality (Spear and Hornberger, 1980). However, as demonstrated in this study, equifinality may be reduced by constraining the parameter space with prior knowledge of the river system and by minimising the number of unknown parameters by using field measurements to the extent feasible (e.g. Du et al., 2014). Often, random sampling methods such as MCMC algorithms are useful to estimate uncertainty in the optimised model parameters (e.g. Segatto et al., 2021) as represented in this study. Furthermore, sensitivity analysis may also be used to identify the most influential parameters for the simulations (e.g. Vandenberghe et al., 2001).

Although the modified two-station approach is simpler and quicker compared to the inverse model, its application is limited to a much smaller spatial scale, i.e. river-reach scale. Additionally, the two-station accounting approach relies on continuous DO measurements at both sites in the river reach of interest, which is often not possible due to adverse field conditions, drifting of sensors, etc. (Wagner et al., 2006). On the contrary, the inverse model is an apt alternative to estimate long-term trends in metabolism at a river-network scale even when there are gaps present in continuous DO measurements at calibration sites.

Despite the differences laid out here, I showed that the outcomes from the two-station accounting approach are useful to constrain the metabolism parameters in the inverse model. Therefore, both approaches are complementary rather than competitive.

5.5.2 *Modelling limitations and future efforts*

The parsimonious model MUFT relies on certain assumptions. For example, the flow routing model approximates constant flow parameters for the entire reach between Brokke and Hekni because it employs reach-by-reach calibration method between gauging stations. In this study, a constant retention parameter was assumed for the entire river section between Brokke and Hekni. This assumption is not realistic since river hydraulics vary within the stretch (discussed in section 5.3.3). Although I accounted for heterogeneity using reach-wise flow-velocity relationships in the flow routing model, such data may not be easily available in other rivers. It is important to estimate flow parameters precisely because small errors in flow parameters may result in large errors in metabolism estimates when flow dominates the mass flux of oxygen in the river. Multiple non-linear storage tanks ($n_c > 1$) may be more appropriate when the river section is heterogeneous, but increasing n_c value did not significantly improve model performance in this case. Parameter sensitivity analysis (e.g. Sincock et al., 2003) may also be employed prior to MCMC simulations to identify an appropriate model structure and reduce bias in the flow parameters. However, a more detailed investigation of parameter bias is out of the scope of this study.

It is difficult to derive a physical understanding of travel time mechanisms because of the lumped parameter structure of the MUFT model. Characterisation of oxygen travel time from flow based parameters integrates flow and metabolism models and therefore, overcomes this issue to a certain extent. However, it is still difficult to relate travel time parameters to river hydraulic properties and interpret the physical significance of model coefficients because of the crude description of dead zone (ADZ, Wallis et al., 1989) and advective transport (ADV, Beck, 1976) in the model. For example, I found ADZ residence time to be poorly related to metabolism. A lack of strong relationship may partly be attributed to the assumption that TDG velocity $\approx$ solute velocity in the river. This assumption may introduce some bias in NEP estimates. Conservative tracer experiment may help characterise solute travel time parameters (e.g. T_{sadz}, T_{adz}, β) more accurately and consequently, help reduce the bias in metabolism estimates. A poor relationship may also occur from model's inability to account for the diversity of transient storage components that contribute to different metabolic processes (e.g. autotrophic and heterotrophic production) (Haggerty et al., 2009). One way to account for diverse transient storage zones is through resazurin tracer experiments, to segregate metabolically active transient storage from a less-active transient storage (Haggerty et al., 2009; Argerich et al., 2011). However, the possibility of a weak or non-existent relationship between transient storage and ecosystem functioning cannot be neglected (Bernhardt et al., 2002; Webster et al., 2003). Nonetheless, in spite of limited available data and a simplified structure,

both formulations of the model are able to provide fairly accurate predictions of oxygen transport and dispersion in this as well as previous studies (Lees et al., 2000; Santos Santos and Camacho, 2022). The MUFT model thus offers an alternative with a trade-off between accuracy and complexity.

Another simplification in the MUFT model is in the way in-stream processes are modelled. The ADZ formulation, in particular, assumes that metabolic activity occurs in the transient storage zone, and not during oxygen advection. Lees et al. (1998) proposed a mass decay term for non-conservative solutes (e.g. ammonium). However, it is difficult to characterise mass decay of oxygen during advection through a single term, when coupled with stream metabolism approach. On the other hand, the ADV formulation does not have this issue since it assumes that advection process is dominant in the river reach. The model also includes a simple formulation of metabolism fluxes, but a more complex formulation may be included if necessary. I find that a Michaelis-Menten type equation adequately simulates GPP in the River Otra, but the model can be easily modified to include other formulations such as linear (Payn et al., 2017) or hyperbolic tangent function (Jassby and Platt, 1976; Holtgrieve et al., 2010). I assume constant ER over a day to keep the model structure simple, but ER may be varied as a function of water temperature (Holtgrieve et al., 2010; Song et al., 2018) if deemed necessary in the river system. Estimate of gas-exchange coefficient k is crucial since a small bias in k may lead to a large bias in metabolism estimates (Hall Jr and Ulseth, 2020). k may be modelled as a function of river hydraulic properties (Raymond et al., 2012) or may be estimated during model calibration with prior information from empirical relationships or direct measurements (Holtgrieve et al., 2010). Here, k is estimated from floating chamber studies, performed under a limited range of flows. Use of a constant k value during the modelling period was adequate in this case because the study reach represented slow-flowing water with considerably low gas-exchange compared to metabolism, thus limiting biases in metabolism from biases in k.

In the River Otra, I find that both inverse modelling approaches are able to predict oxygen variation in the study reach, although performance of the ADV model is significantly better than the ADZ model. The MUFT modelling approach presents opportunities to estimate metabolism in rivers with unsteady flows and/or transient storage zones. Popular approaches of solute modelling with unsteady flows (e.g. flood routing models based on Saint-Venant equations) or including transient storage zone effects with steady flows (Bencala and Walters, 1983; Runkel, 1998; Manson et al., 2010) use partial differential equations (one-dimensional) to simulate water and solute movement. The MUFT model, on the other hand, takes a simpler approach by characterising river reaches as non-linear storage zones in series (zero-dimensional), and simulates water and solute movement using ordinary differential equations. Due to its parsimonious structure, the model includes fewer calibration parameters. Furthermore, the model offers flexibility in selecting an appropriate formulation (e.g. unsteady flows, solute transport mechanisms) that best represents the river conditions.

5.6 SUMMARY AND CONCLUSION

This study presents a coupled modelling approach (MUFT) to estimate whole-stream metabolism in rivers with unsteady flow conditions and transient storage zones. The MUFT model integrates flow and oxygen modelling based on travel-time relationships proposed by Sincock and Lees (2002), which were originally built on QUASAR (Whitehead et al., 1997b) and ADZ (Wallis et al., 1989; Lees et al., 2000) models. I proposed an additional model formulation for dominant advective transport (ADV) based on the model developed by Beck and Young (1975). The MUFT approach can be applied through inverse modelling or accounting method (two-station method) according to user's preference and data availability. I demonstrated the application of the MUFT model in the River Otra in southern Norway. I found that the accounting method is simpler, but shows high bias in metabolism estimates when oxygen mass flux is not precisely modelled. The inverse modelling approach is more robust as it employs least-squares minimisation algorithm to optimise model parameters. Moreover, the inverse model supports investigation of parameter uncertainties and correlations through Bayesian sampling of posterior distributions.

The MUFT approach presents opportunities to estimate whole-stream metabolism in hydropeaking river environments as well as in rivers influenced by transient storage zones. While the model application here is demonstrated only for a short stretch of the river with limited data, the model can be modified in future to estimate long-term trends in metabolism in larger river networks when sufficient data are available. With increasing feasibility of high-resolution, long-term oxygen monitoring in rivers (Appling et al., 2018a,b; Bernhardt et al., 2022), it is possible to extend the model for network-scale metabolism prediction. Using the knowledge of river hydraulics, the inverse model may also be able to predict metabolism rates at sites within the river network where continuous monitoring is not carried out (e.g. Pathak et al., 2022). In future, the model can be expanded for metabolism prediction under future changes such as warming, extreme weather events and river management practices - a research area that calls for more attention (Bernhardt et al., 2018).

6

SYNTHESIS

6.1 OUTPUTS OF THE THESIS

This thesis has produced two models to estimate ecosystem metabolism. Both model developments target applications in rivers influenced by different types of pressures: (1) flow regulation through locks and weirs with multiple stressors influencing river water quality (e.g. sewage discharges, eutrophication), and (2) flow regulation through hydropower dams with/without excessive plant growth influencing solute transport.

The first model is a high-resolution, process-based water quality model that simulates ecosystem metabolism along with its environmental controls at hourly timescale in lowland rivers. This model was developed by modifying an existing water quality model, Quality Evaluation and Simulation Tool for River-systems (QUESTOR), to run at higher temporal resolution. The hourly QUESTOR model was tested along a 62 km stretch in the lower River Thames for a 2 year period. Chapters 2 and 3 described model development and its application, and demonstrated that the hourly model can successfully predict phytoplankton biomass and ecosystem metabolism in lowland rivers.

Chapter 2 showed that modelling at higher temporal resolution (hourly scale) improves prediction of the timing and magnitude of phytoplankton blooms, which are often a concern for healthy river ecosystem functioning. Therefore, the model can be used to provide early warnings of phytoplankton blooms. The model also facilitates identification of flow and temperature bounds that promote harmful phytoplankton growth ($>$ 0.3 mg L^{-1}), which is useful to devise potential management strategies for maintenance of good river water quality.

Chapter 3 presented a novel approach to estimate ecosystem metabolism in lowland rivers (influenced by multiple stressors) using the hourly QUESTOR model introduced in Chapter 2. The hourly QUESTOR model overcomes the current challenges (see Bernhardt et al., 2018) in metabolism modelling since it accounts for oxygen advection under slowly varying flows and for oxygen transformations due to biochemical processes. The model also allows characterisation of specific biochemical pathways of oxygen sinks, and hence derives a comprehensive understanding of different respiration pathways in the river (e.g. autotrophic and heterotrophic respiration). Furthermore, I derived the most influential stressors and their relationships with metabolism rates using empirical modelling as shown in Chapter 3. A comparison of process-based and empirical approaches was useful for understanding mechanisms of multiple stressor influence on metabolism and for recommending ways to improve process-based modelling using the outputs of the empirical approach.

In Chapter 4, I used the hourly QUESTOR model to evaluate river ecosystem response to future climate and management conditions in the lower Thames. I tested 11 scenarios that

included future changes in either a single or a combination of multiple stressors. Deriving the response of ecosystem metabolism under future climate and management conditions is vital to guide river restoration and future management efforts. In the lower Thames, I found that the climate and management scenarios considered in this thesis will compress the metabolic fingerprint in future.

The second model, Metabolism estimation in rivers with Unsteady Flow conditions and Transient storage zones (MUFT), couples an unsteady flow routing model with the two-station metabolism method. The MUFT model can be applied using an accounting method (book-keeping) and/or inverse modelling approach. The model also allows flexibility in selecting an appropriate model structure to suite hydrological and solute transport characteristics in the river. For example, Chapter 5 described two model formulations that can be selected based on the dominant solute transport mechanism (either advective or dispersive transport) in the river of interest. In Chapter 5, I showed the development and implementation of the MUFT model using a case study of the River Otra in Norway. The model was successfully implemented in an 11 km river section below a hydropower dam, where flow shows significant diel fluctuations from dam operations and oxygen transport is influenced by excessive plant growth. The MUFT model is advantageous over conventional metabolism models because it offers opportunities to estimate metabolism at higher spatial scale in hydropeaking rivers, which was not done before using a simple, parsimonious model.

6.2 Ecosystem metabolism for river health management

6.2.1 *Ecosystem metabolism as a river health indicator*

It is becoming increasingly evident that river health assessments need to move from only focusing on structural metrics (e.g. water chemistry, biomass) to also including functional metrics (e.g. metabolism, nutrient cycling) (Palmer and Febria, 2012). To maintain river health at a 'good ecological status', the European Union Water Framework Directive prescribes biological, hydromorphological and physicochemical criteria. Dissolved oxygen (DO) is an important indicator of river ecological status, but the majority of ecological assessments have relied on discontinuous DO measurements to assess river health. Discontinuous measurements of DO do not provide information about ecosystem processes. Regular monitoring of DO has now become feasible with advances in robust sensor technology (Rode et al., 2016), but it is difficult to segregate the influence of environmental and anthropogenic controls by just looking at the DO data. Ecosystem metabolism (derived from continuous DO time-series), on the other hand, not only reflects the changes in these controls, but also separates the influence of biological and physical controls on DO (Jankowski et al., 2021). Long-term time-series of metabolism have also been shown to provide early warnings of ecosystem degradation and recovery (Bernhardt et al., 2018; Arroita et al., 2019) and hence, metabolism is often advocated as an important indicator of river health (Young et al., 2008).

6.2.2 *Modelling ecosystem metabolism*

6.2.2.1 *One-station models*

Inverse modelling approaches with Bayesian analysis are generally more popular for metabolism estimation due to their robustness (Jankowski et al., 2021). Especially, one-station, inverse approaches are widely employed in current metabolism models (e.g. Grace et al., 2015; Winslow et al., 2016; Appling et al., 2018b). These widely-used one-station metabolism models work on certain assumptions (Demars et al., 2015; Appling et al., 2018b): (1) the river reach is well mixed, (2) metabolism and gas exchange rates are homogeneously distributed within the reach of estimation and (3) sources of oxygen in the reach are limited to photosynthesis, gas exchange with the atmosphere, and water flowing from upstream. Due to these assumptions, one-station methods cannot be used in reaches that have any discontinuities in the upstream river reach such as reaches with inputs from major tributaries or wastewater treatment plants as well as reaches where sub-daily flow variation persists (e.g. hydropeaking rivers). These limitations have confined whole-stream metabolism estimation to river environments that conform to these assumptions. However, with increasing river regulation practices around the world, it is especially important to develop models that support metabolism estimation in rivers that are influenced by multiple pressures such as water abstractions, damming and pollution loading. The selection of a model for metabolism estimation broadly depends on two criteria – river characteristics and data availability. The majority of the metabolism methods use continuous time-series of DO, photosynthetically-active radiation (PAR) and water temperature, and sometimes also make use of discharge, barometric pressure, solute travel time, salinity, etc. When data for the key variables are available at few sites in the river and when the aforementioned assumptions (of one-station method) are fulfilled in the river reach, the existing one-station models are powerful tools for metabolism estimation. These models also allow error propagation in metabolism estimates through prior information of parameters, through estimation of parameter uncertainties as well as through simultaneous quantification of gas exchange and metabolism (Appling et al., 2018b). Furthermore, these models are useful for aggregating estimates from a large number of sites within and across rivers to infer regional patterns and predictors of whole-stream metabolism (Beaulieu et al., 2013; Bernhardt et al., 2022). The challenge, however, becomes evident when the assumptions of one-station method are violated.

Recently, researchers have tried to address this problem by extending current models or through introduction of new modelling approaches, which I will discuss throughout this section when relevant. The models presented in this thesis (hourly QUESTOR and MUFT) mainly address the third aforementioned assumption of the one-station method for the purpose of metabolism estimation in regulated rivers. In the following sections, I will talk about applicability of the models introduced in this thesis for metabolism estimation in specific, regulated river environments (not covered by one-station models) and discuss how they advance upon the existing modelling approaches.

6.2.2.2 *Metabolism modelling under unsteady flows*

The one-station method assumes steady flow conditions in the river reach meaning the reach must not be influenced by water abstractions and water inputs from dams, canals and pollutant discharge points (Appling et al., 2018b) that may potentially result in large diel fluctuations in flow. Diel variations in flow are especially common in river stretches located below hydropower dams, where significant fluctuations in flow occur in the process of managing power demands (Zimmerman et al., 2010). Changes in flow directly influence river ecosystem processes including metabolism (Poff and Zimmerman, 2010). For metabolism estimation in river reaches below dams, two-station models (Hall et al., 2016) are required to account for the processes influencing DO changes over a reach rather than a single point. However, two-station models assume constant DO transport velocities over a reach during the period of analysis (Payn et al., 2017) and the estimation in these models is limited to a single river reach. In cases where flow changes during the period of analysis, the assumption of constant DO transport velocity is violated and hence, metabolism estimation in these cases require a more sophisticated approach such as coupling of a flow routing model with a two-station metabolism model (e.g. Payn et al., 2017). A full dynamic flood wave routing, based on Saint-Venant's equations and commonly used in 1-D hydrological models, is ideal in unsteady flow conditions. The MUFT model uses a simpler flow routing model (Sincock and Lees, 2002) than a dynamic wave routing model (e.g. Payn et al., 2017), and couples it with a two-station metabolism model. The choice of a simpler structure in the MUFT model is beneficial because different modules (e.g. flow routing, transient storage zone, metabolism) of the model are compatible, and because the model offers benefits of reduced complexity (0-D) with less number of model parameters over 1-D hydrological models. Reduced complexity in models is advantageous since it minimises data requirements, model sensitivity and issues of parameter equifinality (Lindenschmidt, 2006).

6.2.2.3 *Metabolism modelling in transient storage zones*

Transient storage (or hyporheic) zones in rivers are created mainly from two mechanisms, (1) from the hydrological interaction between surface water and groundwater compartments (called hyporheic zones) or (2) from water entrapment and exchange between fast-moving water and in-channel dead zones such as pools, eddies and excessive vegetation (Bencala and Walters, 1983; Gooseff et al., 2005; Haggerty et al., 2009). Transient storage zones are characterised with higher residence time compared to free-flowing water. Therefore, these zones are potential hotspots of metabolism and nutrient cycling. For accurate estimation, it is vital to include the influence of transient storage zones in metabolism model applications in rivers where solute transport is influenced by these zones.

Usually, transient storage zone influence is modelled using traditional advection-dispersion equations (Bencala and Walters, 1983; Runkel and Bencala, 1995), where model parameters are estimated from solute tracer experiments. These transient storage models

include 1-D solute transport with sources and sinks representing exchange (Bencala and Walters, 1983; Runkel, 1998; Haggerty and Reeves, 2002). In later advancements with these models, studies proposed a use of resazurin as a 'smart-tracer' to characterise metabolically active transient storage in river systems (Haggerty et al., 2009; Argerich et al., 2011). While these models are advantageous, they were developed for steady flow conditions and are relatively more complex than the other suite of transient storage models developed around the same time such as the Aggregated Dead Zone (ADZ) model (Beer and Young, 1983; Wallis et al., 1989). The ADZ model is a lumped model with a simpler structure and has proved to perform equally well in streams and rivers (Lees et al., 2000). Owing to the similarity in the conceptual basis, the MUFT model adapts the representation of transient storage zones from the ADZ model and couple it with the unsteady flow routing and the two-station metabolism model. The final model, MUFT, was able to successfully simulate oxygen transport and estimate metabolism rates in my case study, River Otra, where it was crucial to include the influence of both, unsteady flows and transient storage zone, in the estimation of whole-stream metabolism. The MUFT model also has an ability to move beyond conventional reach-scale estimation of metabolism to larger spatial scales subject to data availability.

6.2.2.4 *Metabolism modelling in multi-stressed environments*

The processes controlling DO changes in a river reach in the one-station models include DO production from photosynthesis, DO loss from ecosystem respiration and oxygen exchange at the air-water interface (Figure 6.1). Processes such as nitrification, organic matter availability and biomass changes may also influence DO changes in rivers, but the one-station models do not specifically account for these processes. Lowland rivers around the world are influenced by multiple pressures such as flow regulation, water abstractions, channel modifications, eutrophication and pollution discharges from sewage treatment works (Schinegger et al., 2012). Rivers that are influenced by such multiple pressures show complex interactions between metabolism and multiple stressors such as flow, sediment and physicochemical water quality. Thus, it is crucial to account for these multiple stressors in a mechanistic way in models to derive accurate interpretations of ecosystem metabolism.

Similar to the MUFT model, the hourly QUESTOR model also addresses the third aforementioned assumption of the one-station method, but in a different context. The hourly QUESTOR model is suitable for river reaches that are influenced by flow regulation through locks and weirs (slowly varying flow in my case study), water abstractions, eutrophication, and inputs from wastewater treatment plants and tributaries. The model can also be linked to groundwater models/estimates (Hutchins et al., 2018). Previous modelling efforts have accounted for some of the controls mentioned above. For example, models have estimated metabolism as a function of biomass (Segatto et al., 2020), but keeping it as a latent variable. Several water quality models (e.g. Enhanced stream water quality model, Brown and Barnwell (1987); River water quality model, Reichert et al. (2001)) include multiple controls, but these models are tested at coarser resolutions

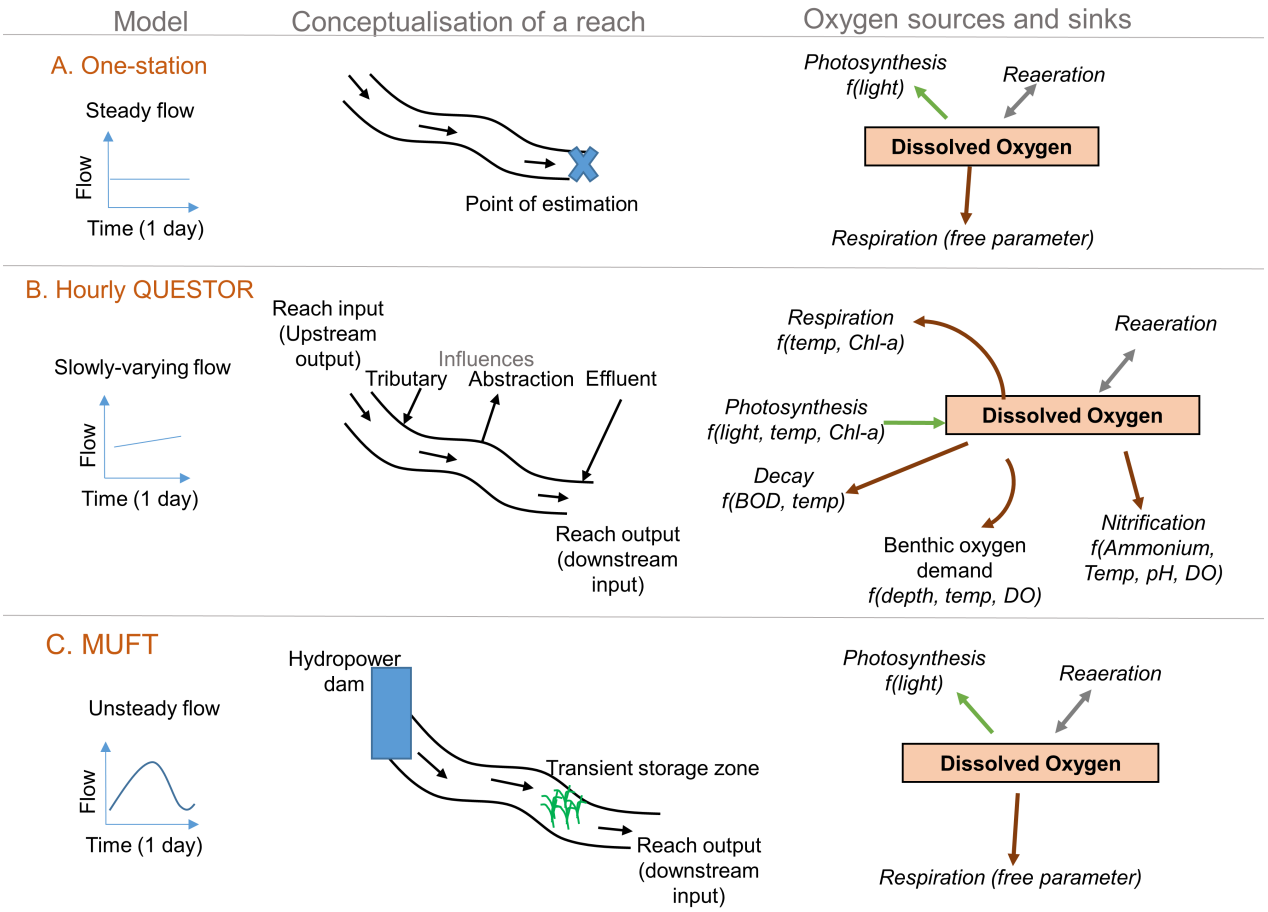

Figure 6.1: Conceptual diagrams of flow regimes, reach structures and oxygen source-sink processes in one-station, hourly QUESTOR and MUFT models. Points of estimation in the hourly QUESTOR (b) and MUFT (c) models are end points of all reaches in the modelled network.

and do not specifically focus on estimating whole-stream metabolism. The hourly QUESTOR model addresses these limitations and also facilitates quantification of specific biochemical pathways of ecosystem respiration, which is crucial to estimate autotrophic base of food webs as well as to to calculate carbon spiraling in rivers (Hall Jr and Beaulieu, 2013). Furthermore, unlike one-station models, the hourly QUESTOR model estimates metabolism based on the physics of the underlying hydrological and biochemical processes, thus removing the dependence on continuous DO time-series that often have data gaps due to adverse field conditions and maintenance issues.

6.2.2.5 *Hourly QUESTOR versus MUFT*

In addition to addressing the aforementioned limitations (third assumption of one-station models) in current modelling approaches, the models presented in this thesis also offer other additional advantages. Both models (hourly QUESTOR and MUFT) have a potential to predict long-term trends in whole-stream metabolism at a river-network scale. The hourly QUESTOR model application demonstrates this advantage in Chapter 3 where the model predicts metabolism at hourly scale for a period of 2 years at multiple sites

along a 62 km river stretch. Although the application of the MUFT approach in Chapter 5 is limited to a short time-period and a single river reach because of data constraints, the model can be extended to a wider river network and implemented to predict long-term metabolism trends when data are available. Because these models simulate river reaches like continuous stirred tank reactors in series, estimation of metabolism is also possible at sites where monitoring of all environmental variables is not carried out, but the information about river reach hydraulics is available. This is a considerable advantage over current metabolism models that focus on estimation at a single river reach and rely on continuous DO time-series for metabolism estimation. The model structures also allow the translation of upstream changes in river flow and quality dynamics (e.g. water abstractions, pollution loading) to downstream sites of interest. Therefore, both models can be used as predictive tools to assess impacts of restoration measures on downstream river reaches. This thesis demonstrates this application in Chapter 4 where metabolism is predicted under future climate and management scenarios using the hourly QUESTOR model.

Although both models presented in this thesis share several common advantages as mentioned above, these models are considerably different in their approach to estimating ecosystem metabolism (Table 6.1). The models are suited to specific types of river systems and the choice of model will depend on the river characteristics and the multiple stressors that modify the river water quantity and quality. The other major difference lies in the representation of processes in both models (Figure 6.1). In terms of simulating in-stream oxygen sources and sinks, the MUFT approach is closer to the widely used two-station models in ecological studies, whereas the hourly QUESTOR model is closer to the widely used water quality models in civil engineering applications. The hourly QUESTOR model estimates metabolism based on the underlying hydrological and biochemical processes and simulates flow, water temperature, PAR, biomass and nutrient concentrations in addition to DO. Therefore, the hourly QUESTOR model is more complex and involves many model parameters compared to the MUFT model. The MUFT approach, on the other hand, is a simpler, parsimonious approach to estimate metabolism with fewer parameters. As the hourly QUESTOR model involves simulation of several water quality determinands, the data requirements for model inputs and calibration are also higher compared to the MUFT approach. Both models also differ in their parameter estimation process. The hourly QUESTOR model involves sequential calibration process, where parameters are calibrated determinand by determinand from upstream to downstream sites. It is possible to use more robust parameter optimisation algorithms with water quality models (e.g. Soil and water assessment tool - SWAT, Abbaspour et al., 2007). However, the hourly QUESTOR model does not include the parameter optimisation feature at the moment. The MUFT model, on the other hand, employs a least-square optimisation algorithm to estimate model parameters. The MUFT application can also provide additional information about parameter covariance and uncertainties using Bayesian methods as shown in Chapter 5. Overall, both models offer useful applications in different types of river environments as demonstrated in this thesis. Parsimonious approaches are generally better and should

be prioritised when possible. However, when rivers are influenced by multiple stressor interactions, it is also crucial to employ models that include these process-interactions to provide accurate interpretations of river metabolism dynamics.

Table 6.1: Details on data requirements, methods and processes used in the hourly QUESTOR and MUFT models. The parameters in the first column are adapted from the summary information table (Table 2) by Jankowski et al. (2021) for several metabolism models. This table shows where the hourly QUESTOR model and the MUFT model stand in comparison to the existing metabolism models (reviewed in Jankowski et al., 2021)

	Hourly QUESTOR model	MUFT model
Environment	Flow regulation through weirs, water abstraction, eutrophication, pollution discharges	Flow regulation through hydropower dams, transient storage zones
Software	Fortran	Python
Time-series input data	Flow, light, water temperature, nutrients, suspended sediment, dissolved oxygen, chlorophyll-a	Flow, light, water temperature, dissolved oxygen, atmospheric pressure
Discrete input data	Reach hydraulics, mean water depth, velocity-discharge relationship, volume of sewage discharges and water abstractions, tributary inputs of water quantity and quality, weir type and height	Reach hydraulics, mean water depth, velocity-discharge relationship
Parameter estimation method	Sequential calibration	Bayesian
Gas exchange coefficient calculation	Empirical equation	Floating chamber experiments
Uncertainty estimates	Fourier amplitude sensitivity test	Posterior distribution
Outputs	GPP, ER, flow, light, water temperature, nutrients, suspended sediment, dissolved oxygen, biomass	GPP, ER, flow, dissolved oxygen

6.2.3 *Environmental controls of ecosystem metabolism*

Similar to terrestrial systems, lotic systems do not show regular trends in productivity and respiration cycles because these systems are controlled by combinations of several external stressors, which themselves may not have a periodicity (Bernhardt et al., 2018, 2022). Rivers may represent disparate controlling mechanisms for metabolic regimes because of their dynamic nature and spatial variability in their physical, chemical and biological characteristics (Dodds et al., 2018). These controlling factors are scale dependent. Alberts et al. (2017) provide a conceptual template of critical drivers of stream metabolism acting at the watershed and local scales (see Figure 1 in Alberts et al., 2017). The regional template can comprise climate, vegetation and topography drivers that regulate watershed and local scale controls on stream metabolism. Land use changes operate at the watershed scale, and control flow and nutrient fluxes entering into rivers. On the other hand, temperature, light and organic matter inputs are mainly determined by riparian land use at the local scale. In addition to the spatial scale, the temporal scale also controls how different stressors (e.g. temperature, light, vegetation, flow) affect gross primary production (GPP) and ecosystem respiration (ER). These controls further vary within and across river biomes and river sizes. In this section, I discuss my findings (Figure 6.2) on the multiple environmental controls of ecosystem metabolism in lowland rivers (particularly the lower River Thames, Chapter 2-4) in context of the existing literature on commonly observed environmental controls of metabolism in river ecosystems. The findings on multiple environmental controls of metabolism in the lower River Thames are derived using a combination of process-based (hourly QUESTOR) and empirical modelling approaches.

Temperature and light are key controls of ecosystem metabolism in rivers (Roberts et al., 2007). Temperature variations are found to influence water quality, biotic conditions and ecosystem functioning processes such as primary production, self-purification and nitrification in rivers (Poole and Berman, 2001; Caissie, 2006). Light availability controls primary production by autotrophs. The light regime is influenced by multiple factors such as turbidity levels, topographic shading and riparian shading (Savoy and Harvey, 2021). Seasonal variation in riparian vegetation may significantly influence light availability in temperate rivers, where maximum light is available in early spring before leaf out and during late autumn after the litterfall (Hill and Dimick, 2002; Roberts et al., 2007). Changes in light availability are found to alter the relationship between temperature and ecosystem metabolism in rivers (Huryn et al., 2014; Nebgen and Herrman, 2019). Some studies have also reported synergistic interaction between light and water temperature to influence river metabolism (Beaulieu et al., 2013). In the lower River Thames, light and temperature significantly influence metabolism dynamics. GPP increases in response to increase in light availability and reaches maximum levels within an optimum temperature range (Bowes et al., 2016; Pathak et al., 2022). ER responds in a similar manner to GPP during biomass growing season when autotrophic respiration governs ER variation. Often, temperature is shown to have a stronger control on ER compared to GPP in rivers (Demars et al., 2011). As a result, studies have predicted increase in ER with future warming, indicating an increase

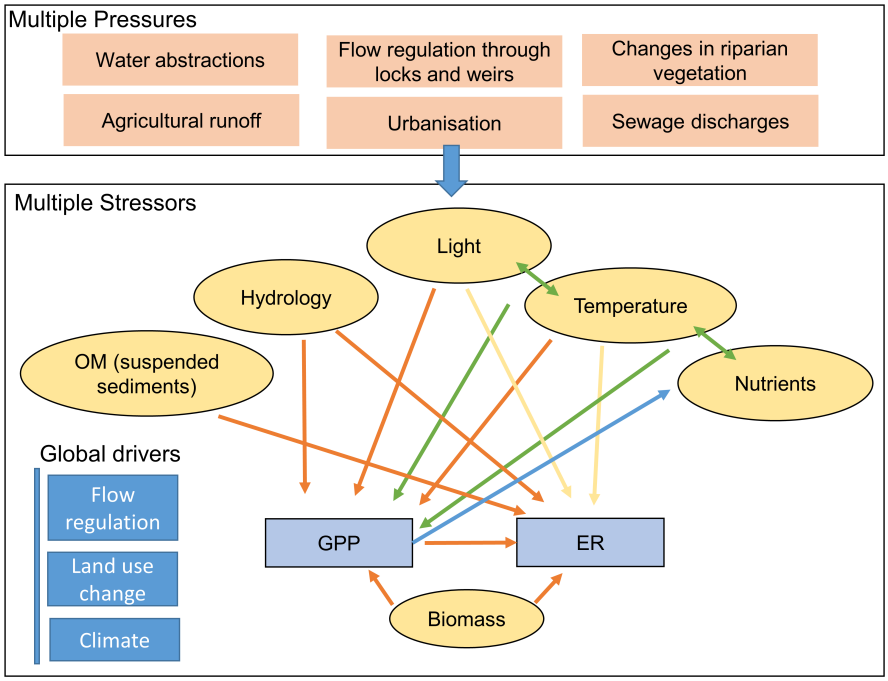

Figure 6.2: Key controls of ecosystem metabolism in the lower River Thames. Orange arrows represent direct effects, yellow arrows represent indirect effects, green arrows represent interaction effects and blue arrows represent reverse effects. All stressors (in yellow, oval boxes) influence each other, but their interrelationships are not shown for brevity. OM, organic matter; GPP, gross primary production; ER, ecosystem respiration.

in atmospheric CO_2 contributions from river systems (Demars et al., 2016). I found a similar pattern of increase in heterotrophic respiration with future warming in the lower River Thames (Chapter 4).

Flow regime also affects ecosystem structure (e.g. microbes, plants, animals) and functioning (e.g. organic matter decomposition, nutrient cycling) that may directly or indirectly influence ecosystem metabolism rates (Von Schiller et al., 2017). The lower River Thames shows a strong coupling between GPP and ER, which is commonly observed in rivers (Hall et al., 2016) as a major part of the organic matter produced during photosynthesis is immediately respired by autotrophs and their closely associated heterotrophs (Hall Jr and Beaulieu, 2013). However, the coupling between GPP and ER may be disturbed by extreme hydrological events. For example, high floods are shown to reduce GPP in rivers due to scouring and export of benthic sediment beds in rivers (Uehlinger and Naegeli, 1998; Uehlinger, 2006) or from increased turbidity (Uehlinger, 2000; Izagirre et al., 2008). Low flows can cause drying of stream bed and hamper the functioning of benthic primary producers (Datry, 2012), although studies have also found improvements in ER due to organic matter accumulation during post-drought recovery (Acuña et al., 2005). The lower Thames shows highest GPP during low flow conditions due to high biomass growth, which significantly subsides during the rest of the year. Such a seasonal variation is often observed in temperate rivers, where GPP peaks during periods of high light availability and low flows (Roberts et al., 2007) and significantly reduces during high flows that flush away primary producers (Wang et al., 2019).

Nutrient loading may also impact metabolism and become significant when light and other disturbances are not limiting (Hill et al., 2009). For example, riparian vegetation removal and flow regulation may render rivers vulnerable to nutrient availability because of reduced light limitation and disturbance frequencies in rivers (e.g. Sabater et al., 2000). Removal of riparian vegetation can also lead to increased nutrient delivery in rivers, which in turn may increase GPP rates (Young et al., 2008; Alberts et al., 2017). There is still limited proof suggesting control of nutrient availability on metabolism in rivers (Hoellein et al., 2013). Few studies have shown increase in GPP and ER from increase in nitrogen and/or phosphorus loading (e.g. Kominoski et al., 2018) or have suggested nutrient concentrations to be secondary drivers of metabolism (Dodds and Cole, 2007; Young et al., 2008). Contrarily, some studies have discovered reverse causality, i.e. metabolism variation to have a strong control on riverine nutrient dynamics (Roberts et al., 2007; Heffernan and Cohen, 2010; Jarvie et al., 2018). The outputs in the lower Thames agree with the latter findings and show a negative relationship between metabolism and nutrient concentrations because of biomass uptake (Chapter 3). Nitrate concentrations in the river are present in excess throughout the year and do not limit primary production. Phosphorus concentrations, on the other hand, decrease with high biomass growth and become limiting in summer.

Organic matter variation also influences river metabolism. ER rates in rivers are strongly controlled by organic matter availability, and hence the capacity of rivers to support or transport organic matter downstream determines the extent of GPP-ER coupling (Bernhardt et al., 2018). Establishing a relationship between metabolism and organic matter availability is challenging. ER is influenced by the composition of organic matter (dissolved and particulate fractions of organic matter), which in turn is regulated by a combination of environmental controls. Particulate organic matter availability in rivers is often linked to seasonality of riparian vegetation (Tank et al., 2010) and hydrological events (Raymond and Saiers, 2010). In low-gradient large rivers, floodplain-channel connectivity is also important to regulate particulate organic matter availability (Minshall et al., 1985). Dissolved organic mater availability in rivers can be linked to riparian soil type (Mulholland et al., 1997), terrestrial leaf litter (Kaplan and Newbold, 1993), in-stream primary production (Kaplan and Bott, 1989) as well as anthropogenic activities (Meng et al., 2013). The bioavailability of organic matter is also crucial in driving respiration, and can be determined by tracing organic matter origins (e.g. fluorescence analysis, Hudson et al., 2007). Due to lack of data, I could not establish a relationship between organic matter availability and metabolism in the lower Thames. However, using limited water fluorescence observations in the river, I observed a positive relationship between water column respiration and tryptophan-like fluorescence (represents degradable organic matter). These findings indicate a potential control of organic matter availability on ER dynamics in the river. Such a relationship has also been observed in a previous modelling study in the River Thames, where heterotrophic respiration was found to increase with dissolved organic carbon delivery from flooding (Hutchins et al., 2020). There is a need

to systematically include the dynamics of particulate and dissolved fractions of organic matter in stream metabolism models (see Segatto et al., 2020).

It is vital to study interactions between key stressors of ecosystem metabolism that I just discussed (light, temperature, flow, nutrients, organic matter) to predict how ecosystem metabolism will be modified by global drivers such as warming, land use changes and flow regulation (Bernhardt et al., 2018). However, sufficient information is not yet available to establish such interactions at regional scales. The effects of multiple stressors are difficult to separate and hence, metabolism response to changes in global drivers is difficult to predict. Modelling tools such as the hourly QUESTOR (Chapter 4) presented in this thesis can help predict and disentangle river ecosystem response to these multiple stressors. In the lower Thames case study, the hourly QUESTOR model predicts that metabolism will generally increase during winter and spring, but reduce during summer and autumn seasons in response to predicted changes in climate (hydrology, temperature). Future hydrology and urbanisation changes will not significantly alter metabolism, although it is important to consider that the predicted future changes in flow are considerably low for the study site (Prudhomme et al., 2013). High flow events still have a potential to boost heterotrophic respiration up to 30% more than the present conditions (Chapter 4). The model predicts that reduction in total phosphorus (TP) loads from sewage treatment works and incoming tributaries will reduce GPP during the biomass growing season. However, management efforts targeting light availability (e.g. riparian shading) are found to be more efficient compared to TP reduction practices. Overall, both climate and management scenarios considered in this thesis predict improvements in river water quality, especially during the biomass growing season when the river health is at risk from harmful phytoplankton growth and oxygen depletion. Chapter 2-4 in this thesis demonstrated hourly QUESTOR model's application in analysing multiple stressor controls of ecosystem metabolism by, (a) modelling metabolism as a function of underlying hydrological and biochemical controls, (b) deriving response variables (GPP, ER) for empirical models to analyse stressor importance and interactions and (c) predicting ecosystem metabolism under future climate and management scenarios for river restoration and management.

6.3 Research limitations and future directions

6.3.1 *Data requirements*

Data requirements for metabolism estimation largely depends on the objective and the type of the model used (Jankowski et al., 2021). Here, I outline the data requirements for metabolism estimation using the two models presented in this thesis (see Table 6.1). For the MUFT model application, continuous time-series of DO, discharge, water temperature and atmospheric pressure at minimum two sites in the river reach are required for model input and calibration. PAR is also crucial and ideally should be measured at the river site. However, it may not always be feasible to measure PAR directly, in which case, it can be modelled using remote sensing information (Holtgrieve et al., 2010; Waylett et al.,

2013) with careful considerations. Mean river depth can be derived as discharge divided by mean velocity and mean stream width. Accurate estimation of mean velocity and solute residence time is important, especially in river reaches with significant transient storage (Lees et al., 2000). Ideally, a conservative tracer such as salt slug (Hall Jr and Hotchkiss, 2017) should be used to derive residence time and velocity estimates, but other approaches (e.g. use of TDG as shown in Chapter 5) may be employed if estimates can be validated with observations. Furthermore, tracer experiments for varying discharge should help derive empirical relationships between discharge and velocity, which is useful for upscaling metabolism estimates (Raymond et al., 2012). Application of the hourly QUESTOR model in multi-stressed rivers (affected by eutrophication and wastewater discharges) requires biomass and nutrient information in addition to the data for the variables mentioned above. Some information about riverine process-rates (benthic oxygen demand, biochemical oxygen demand) is also needed for parameter calibration in the hourly QUESTOR model.

The hourly QUESTOR model has more extensive data requirements compared to the MUFT model. It can be difficult to gather data for all variables at high-resolution since routine monitoring practices generally do not include high-frequency measurements of water quality. To investigate this limitation, I evaluated model's sensitivity (the hourly QUESTOR) to the frequency of input data in Chapter 2. I find that the model outputs are not sensitive to the time-scale of water quality inputs, but are highly sensitive to that of radiation inputs. The outputs of the sensitivity analysis are encouraging for model applications elsewhere since PAR can be modelled in the absence of direct field measurements. Nevertheless, high-resolution data are still crucial to minimise uncertainties in the interpretations of metabolism pathways. There is a need to include water quality variables in regular monitoring practices. Long-term data from regular monitoring will not only help monitor ecosystem metabolism, but will also help investigate the environmental controls of river ecosystem health.

6.3.2 *Modelling limitations*

The modelling approaches presented in this thesis are not exempt from limitations. Both models presented here do not include characterisation of rainfall-runoff mechanisms in their flow routing modules, and hence rely on external estimation when these effects are required to be included (e.g. to derive future hydrology). The simple flow routing module in the hourly QUESTOR model is unable to capture rapid changes in flows and water quality that could occur from river regulation such as dam operations (Cox, 2003b). Therefore, in rivers with rapidly changing flows, the flow routing module of the MUFT model should be used.

Accurate characterisation of gas exchange coefficient remains challenging, especially using open-channel approaches in rivers with low productivity and high gas exchange (Hall Jr and Ulseth, 2020). Several methods exist for estimation of gas exchange coefficient varying from direct measurement (e.g. floating chamber studies, Lorke et al., 2015) to

empirical approaches (e.g. relating gas exchange to river hydraulics, Raymond et al., 2012) to Bayesian methods (e.g. partial pooling, Appling et al., 2018a) and many more (see Hall Jr and Ulseth, 2020). It is crucial to accurately estimate gas exchange in the MUFT model since the estimation of ER and gas exchange coefficient is interlinked. This is not an issue for the hourly QUESTOR model since metabolism rates are not directly dependent on gas exchange estimates, but are estimated based on the underlying physics of the environmental controls (Segatto et al., 2020; Pathak et al., 2022). In any case, characterisation of gas exchange is not a matter of significant concern in this thesis because river reaches in both case studies represent slow flowing water with negligible gas exchange compared to metabolism. However, the selection of gas exchange estimation method is crucial to limit errors in metabolism (Hall Jr and Ulseth, 2020), especially in turbulent rivers where gas exchange is significant (Ulseth et al., 2019).

Uncertainties in process-based models are inevitable and may propagate from a variety of sources such as errors in field measurements, model structure and process understanding due to lack of data (Abbaspour et al., 2015). It is especially a concern with process-based models that have huge data requirements because there is a possibility of having acceptable outputs through multiple pathways (parameter values, inputs, etc.), called parameter equifinality (Beven and Freer, 2001). Although the hourly QUESTOR application in this thesis doesn't include a separate uncertainty estimation, the daily QUESTOR model (basis of hourly model) has been tested and subjected to comprehensive sensitivity analysis elsewhere (Deflandre et al., 2006; Hutchins and Hitt, 2019). This thesis also makes use of the existing literature on water quality modelling in the River Thames (Whitehead and Hornberger, 1984; Whitehead et al., 2015; Hutchins et al., 2018) to minimise parameter uncertainties during the calibration process. Extensive applications of the QUESTOR model in the River Thames provide confidence in calibration of the hourly model parameters since optimised values lie within similar ranges.

In the MUFT model application (Chapter 5), I demonstrated the quantification of parameter uncertainties and covariance using a Bayesian approach. The MUFT model involves optimisation of parameters using a least-square minimisation approach and sampling of Bayesian posterior distribution of model parameters using the Markov Chain Monte Carlo (MCMC) algorithm. Bayesian approaches are becoming more popular in metabolism modelling (e.g. Holtgrieve et al., 2010; Grace et al., 2015; Appling et al., 2018a) since these approaches allow inclusion of errors from multiple sources of data and formal propagation of uncertainties in parameter estimates (Holtgrieve et al., 2016). Although the MUFT model involves a formal quantification of parameter uncertainties, the model application in this thesis is limited to a short time-period for a single river reach. Assessment of the model for multiple reaches using long-term data is needed for further evaluation of parameter covariance and process understanding.

6.3.3 *Future research directions*

For comprehensive comparisons of metabolic regimes within and across river systems as well as to predict metabolism under changing global drivers, long-term, high-frequency data at multiple sites within the catchment are required. However, data are usually collected for shorter time periods and at few sites within the river, mainly due to logistical reasons. Only recently, has it become feasible to monitor high-frequency water quality with the availability of cheap and robust water quality sensors (Rode et al., 2016). The advances in sensor technology has made it possible to collate large-scale, high-frequency water quality observations, many of which are freely available online such as data sets maintained by the National Ecological Observatory Network (NEON) (https://www.neonscience.org/data) and the Global Lakes Ecological Observatory (GLEON) (Hanson et al., 2016). Specifically, data amalgamation initiatives such as STREAMPULSE are especially valuable, where river metabolism data from published studies are gathered and hosted on an open-access platform (www.data.streampulse.org, Appling et al., 2018b). However, these data sets are mainly focused on rivers across the United States and more such compilation efforts are required for European rivers as well.

Future modelling studies should focus on improving the existing knowledge about how ecosystem metabolism will respond to changing environmental conditions and anthropogenic actions. To achieve this, synchronous information of ecosystem metabolism and its environmental controls is required for diverse river environments. For example, a recent study by Bernhardt et al. (2022) compiled metabolism estimates for more than 200 rivers across the United States, and found light and flow regime to control ecosystem metabolism. However, due to the lack of data and modelling techniques, they did not relate metabolism to other environmental variables (temperature, nutrients or biomass) and did not include river environments such as those considered in this thesis. Future broad-scale metabolism assessments require inclusion of diverse environmental controls and river environments. For example, most metabolism work around the world has been focused on small rivers that are not heavily impacted by pollution, and only few studies have focused on large rivers (e.g. Dodds et al., 2013; Hall et al., 2016). Furthermore, studies analysing impacts of dam operations on river biological health have traditionally relied on structural indicators (e.g. fish, algae, invertebrates) instead of functioning indicators such as metabolism. This thesis fills this gap up to a certain extent. Further applications of the models presented in this thesis will elucidate metabolism controls across more diverse river ecosystems than those currently studied. That being said, more methodological and application-based efforts are required to expand metabolism estimation in river conditions that are not included in this thesis such as when the river is ice covered (Mejia et al., 2019) or when the flow is intermittent (Stanley et al., 2004; Acuña et al., 2005).

Human modifications and river management have affected river health around the world by altering hydrological and water quality regimes (Sabater and Tockner, 2009). For example, reservoir operations alter metabolism through changes in flow (Sabater and Tockner, 2009), temperature (Olden and Naiman, 2010), delivery of organic carbon,

sediments, nutrients and biomass (Kunz et al., 2011). Although studies have looked at the impacts of natural events such as droughts (Acuña et al., 2005) and flooding (Uehlinger, 2000) on metabolism, few studies have looked at the impacts of river management actions on metabolism (Levi et al., 2013; Kupilas et al., 2017; Chowanski et al., 2020). Further research is required to understand metabolism response to river management actions to guide future river restoration strategies (Hall Jr, 2016). For example, characterising metabolism at several places across the catchment can help identify high productivity areas that could support endangered species (Kaylor et al., 2019). Effectiveness of river restoration actions can be analysed using long-term estimates of metabolism (e.g. Batt et al., 2013). Long-term data on metabolism can also support segregation of ecological response from anthropogenic actions, and therefore support assessments of ecosystem degradation or recovery using metabolism as an indicator of river health (Roley et al., 2014; Bernhardt et al., 2018; Arroita et al., 2019). Our understanding of controls of metabolism is continuously improving, and we need more assessments of metabolism within and across biomes to provide reference conditions for river management.

Ecosystem metabolism assessment in freshwater systems is an emerging field of research due to its role in understanding freshwater contribution to the global carbon cycle and due to the ease of monitoring and estimating metabolism using DO observations. Recent efforts (Appling et al., 2018b; Bernhardt et al., 2018; Koenig et al., 2019; Bernhardt et al., 2022) have focused on broad-scale estimation of metabolism as well as on deriving regional controls of ecosystem metabolism across different biomes. Such broad-scale assessments are extremely useful to reduce uncertainties in our global estimates of freshwater carbon fluxes. This thesis directly contributes to these efforts by introducing two new modelling approaches, hourly QUESTOR and MUFT, that expand metabolism estimation to river networks influenced by diverse set of environmental stressors, resulting from different types of river regulation. Through model development and implementation in this thesis, I have demonstrated that the hourly QUESTOR and MUFT models unlock new opportunities (a) to estimate whole-stream metabolism, (b) to study multiple environmental controls of metabolism and (c) to forecast river ecosystem health under changing climatic and management conditions in regulated, multi-stressed river systems. Future studies should build on these advances and focus on comparing metabolic regimes across diverse river environments, while using an increasingly improving pool of freshwater data sets and metabolism modelling techniques.

APPENDICES

A

HOURLY QUESTOR MODEL

A.1 MODEL THEORY

The change in water temperature is calculated as follows,

$$\frac{dT}{dt} = \frac{(T_i - T)}{\tau} - \frac{H(H_{flux})}{z} \tag{A.1}$$

where T_i is the mean temperature (°C) from all sources, T is the temperature of water leaving the reach (°C), H is the heat flux coefficient (m^{-1}), $H_{flux} = L_{in}.R_s – L_{out}.R_o$, L_{in} is the incoming radiation factor (m^4 °C W^{-1} h^{-1}), R_s is the incoming solar radiation (W m^{-2}), L_{out} is the outgoing radiation factor (m^4 °C W^{-1} h^{-1}) and z is the mean water depth of reach (m). The largest component for the outgoing radiation is the long wave back radiation, which is given by $R_o = 0.97\sigma T^4$ (in which 0.97 is the emissivity constant of a water surface, σ is the Stefan-Boltzmann constant (5.67051 $\times 10^{-8}$ W m^{-2} k^{-4}) and T is the temperature in °K).

The processes considered in the nitrogen model include transformation of particulate organic nitrogen to ammonium, nitrification and denitrification. The equation characterising the rate of change in particulate organic nitrogen (PON) is,

$$\frac{dC_{PON,o}}{dt} = \frac{(C_{PON,i} - C_{PON,o})}{\tau} - k_{min}.C_{PON,o} + \alpha.k^{res} + \alpha.k^{death} - \frac{v_{sed}.C_{PON,o}}{z} \tag{A.2}$$

where $C_{PON,i}$ is the input PON concentration (mg L^{-1}), $C_{PON,o}$ is the output PON concentration (mg L^{-1}), k_{min} is the mineralisation rate (h^{-1}), k^{res} is the respiration rate of autotrophs (h^{-1}), k^{death} is the death rate of autotrophs (h^{-1}), v_{sed} is the settling velocity (m h^{-1}), C_{phy} is the concentration of chlorophyll-a (Chl-a) (mg L^{-1}) and α is the ratio of nitrogen to Chl-a in autotrophs.

The change in ammonium (NH_4) is represented as,

$$\frac{dC_{NH4,o}}{dt} = \frac{(C_{NH4,i} - C_{NH4,o})}{\tau} - k_{nit}.C_{NH4,o}.\left(\frac{DO}{DO + S_{nit}}\right) + k_{min}.C_{PON,o} - n_{pref}.k^{pho}.\alpha \tag{A.3}$$

where $C_{NH4,i}$ is the input NH^+_4 concentration (mg L^{-1}), $C_{NH4,o}$ is the output NH^+_4 concentration (mg L^{-1}), k_{nit} is the nitrification rate (h^{-1}), S_{nit} is the dissolved oxygen (DO) half-saturation concentration for nitrification (mg L^{-1}), k^{pho} is the photosynthetic rate of autotrophs (h^{-1}) and n_{pref} is the autotroph preference for ammonia.

The change in nitrate is calculated as,

$$\frac{dC_{NO3,o}}{dt} = \frac{(C_{NO3,i} - C_{NO3,o})}{\tau} + k_{nit}.C_{NH4,o}.\left(\frac{DO}{DO + S_{nit}}\right) - k_{den}.C_{NO3,o} - (1 - n_{pref}).k^{pho}.\alpha \quad (A.4)$$

where $C_{NO3,i}$ is the input NO^-_3 concentration (mg L^{-1}), $C_{NO3,o}$ is the output NO^-_3 concentration (mg L^{-1}) and k_{den} is the denitrification rate (h^{-1}).

Process transformations for organic and inorganic phosphorus are included in the model as explained below. The change in organic phosphorus (P_{org}) is calculated as,

$$\frac{dC_{Porg,o}}{dt} = \frac{(C_{Porg,i} - C_{Porg,o})}{\tau} - k_{Pmin}.C_{Porg,o} + k^{res}.\beta + k^{death}.\beta - \frac{v_{sed}.C_{Porg,o}}{z} \quad (A.5)$$

where $C_{Porg,i}$ is the input P_{org} concentration (mg L^{-1}), $C_{Porg,o}$ is the output P_{org} concentration (mg L^{-1}), k_{Pmin} is the phosphorus mineralisation rate coefficient (h^{-1}) and β is the ratio of phosphorus to Chl-a in autotrophs.

The change in inorganic phosphorus (here soluble reactive phosphorus, SRP) is represented as below,

$$\frac{dC_{SRP,o}}{dt} = \frac{(C_{SRP,i} - C_{SRP,o})}{\tau} + k_{Pmin}.C_{Porg,o} - k^{pho}.\beta \quad (A.6)$$

where $C_{SRP,i}$ is the input SRP concentration (mg L^{-1}) and $C_{SRP,o}$ is the output SRP concentration (mg L^{-1}).

The change in suspended sediment (SS) concentration in the model is represented as,

$$\frac{dC_{SS,o}}{dt} = \frac{(C_{SS,i} - C_{SS,o})}{\tau} - v_{sed}.C_{SS,o}.z \quad (A.7)$$

where $C_{SS,i}$ is the input SS concentration (mg L^{-1}) and $C_{SS,o}$ is the output SS concentration (mg L^{-1}).

The change in biochemical oxygen demand (BOD) is calculated as shown below,

$$\frac{dC_{BOD,o}}{dt} = \frac{(C_{BOD,i} - C_{BOD,o})}{\tau} - k_{bod}.C_{BOD,o}.\left(\frac{C_{DO,o}}{C_{DO,o} + S_{bod}}\right) - \frac{v_{sed}.C_{BOD,o}}{z} + \frac{32}{12}.k^{death}.\Delta \quad (A.8)$$

where $C_{BOD,i}$ is the input BOD concentration (mg L^{-1}) (mean from all sources) and $C_{BOD,o}$ is the output BOD concentration (mg L^{-1}).

Several process rate coefficients (e.g., k_{min}, k_{nit}, k_{bod}) in the model are temperature-dependent as below,

$$k_T = k_{T_{ref}}.\theta^{(T-T_{ref})} \tag{A.9}$$

where k_T is the process rate at T °C (h^{-1}), k_{Tref} is the process rate (h^{-1}) at a reference temperature T_{ref} that is 20°C and θ is a temperature correction factor.

Denitrification rate (k_{den}, h^{-1}) is represented as,

$$k_{den} = \frac{k_{den20}}{z}.10^{0.0293T} \tag{A.10}$$

where k_{den20} ($m\ h^{-1}$) is the denitrification parameter provided by the user.

For reaeration at surface in the DO module, saturated DO concentration (O_{sat}) is calculated using the equation attributed by Bowie et al. (1985) to Elmore and Hayes (1960), assuming pressure to be 1 atmosphere and salinity as zero.

$$O_{sat} = 14.652 - 0.41022T + 0.007991T^2 - 0.0000777774T^3 \tag{A.11}$$

Reaeration coefficient (k_{rea}, h^{-1}) is estimated using an empirical relationship between velocity and depth derived by Owens (1964),

$$k_{rea} = \frac{(5.3.v^{0.67}.1.024^{T-20})}{z^{1.85}} \tag{A.12}$$

For reaeration at weirs, oxygen deficit ratio (R_{ODR}) is calculated based on water temperature (T), degree of pollution (A), weir height (H) and type (B) (Gameson, 1957),

$$R_{ODR} = 1.0 + [(0.38ABH).(1.0 - 0.11H).(1.0 + 0.046T)] \tag{A.13}$$

where A is dependent on the percentage oxygen saturation (POS) as shown below,

Table A.1: Degree of pollution (A) for percentage oxygen saturation (POS) in the model

POS (%)	A
≥60	1.8
60-40	1.6
40-10	1.0
<10	0.65

POS is calculated using O_{sat} and the actual DO concentrations in the water column as below,

$$POS = \left(\frac{C_{DO,o}}{O_{sat}}\right).100 \tag{A.14}$$

B varies based on the weir type as shown below,

Table A.2: Values of B in Eq. A.13 for weirs in the model

Weir type	B
Free-fall	1
Sloping	0.4
Step	1.3
Cascade	0.8

A.2 ASSESSMENT OF MODEL PERFORMANCE

Model performance was assessed using a combination of Nash and Sutcliffe Efficiency (NSE) and percentage error in mean (PBIAS) statistics. NSE value represents how well the model explains the variance in the observed time-series data. The value of PBIAS indicates up to what extent the model under (negative) or over-estimates (positive) the observed data trends. NSE and PBIAS statistics are calculated by Eq. A.15 and Eq. A.16, respectively.

$$NSE = 1 - \left[\frac{\sum_{i=1}^{n} (Y_i^{obs} - Y_i^{sim})^2}{\sum_{i=1}^{n} (Y_i^{obs} - Y^{mean})^2} \right] \tag{A.15}$$

$$PBIAS = \left[\frac{\sum_{i=1}^{n} (Y_i^{obs} - Y_i^{sim}).100}{\sum_{i=1}^{n} (Y_i^{obs})} \right] \tag{A.16}$$

Y_i^{obs} is the ith observed value, Y_i^{sim} is the ith simulation value, Y^{mean} is the mean of the observed data and n is the total number of observations.

B

HOURLY QUESTOR MODEL: IMPLEMENTATION AND CALIBRATION

Table B.1: River network description in the hourly model (W = weir, T = tributary, D = sewage treatment works, A = abstraction, Calib = calibration)

Reach Name	Reach Length (km)	Calib Site	Influence Type	Influence Description
Caversham	3.5			Start Point
Kennet			A,T,D,W	River Kennet influences including Kennet at ufton bridge, Clayhill brook, Smallmead ditch, Reading STW, Blake's weir and Kennet-Avon canal
Sonning	3.7	Yes	W	Caversham weir
Shiplake Lock	1.1		W	Sonning weir
Wargrave	3.5		W	Shiplake weir
Marsh Lock, Henley	4.0		T	Lodden River
Remenham	6.9		W	Marsh weir
Hurley Lock	1.2		T	Fawley court Stream, Hamble brook
Temple Lock	2.7		W	Hurley weir
Marlow Lock	1.3		W	Temple weir
Dial Close, Cookham Dean	1.9		W	Marlow weir
Stone House	2.3		D	Hurley STW
Bourne End	1.1		D	Little Marlow STW
Cookham Bridge	5.0		T	Wye River
Boulter's Lock	2.9		W	Cookham weir
Taplow (Bray Lock)	1.7	Yes	W	Boulter's weir
Dorney Reach	3.5		W	Bray weir
Boveney Lock	0.9		A,T,D	Bray pumping station, Cut River, Maidenhead STW
Windsor Racecourse	3.3		W	Boveney weir
Romney Lock	1.3		T,D	Boveney ditch, Slough STW
Windsor (Datchet)	5.0	Yes	W	Romney weir
Sunnymeads	0.7		A	Datchet and Sunnymeads intakes
Old Windsor	2.8		D,W	Windsor STW, Old Windsor weir
Runnymead	1.7	Yes		End Point

Table B.2: Values of global model parameters

Symbol	Definition	Value	Unit
H	Heat flux coefficient	0.005	m^{-1}
T_{ref}	Reference temperature for reactions	20	°C
θ	Temperature correction factor for BOD decay	1.047	-
θ	Temperature correction factor for nitrification	1.085	-
θ	Temperature correction factor for hydrolysis	1.08	-
θ	Temperature correction factor for benthic oxygen demand	1.08	-
θ	Temperature correction factor for phosphorus mineralisation	1.08	-
θ	Temperature correction factor for respiration of phytoplankton	1.08	-
θ	Temperature correction factor for growth of phytoplankton	1.08	-
S_{nitri}	Half saturation concentration for nitrification	1	mg L^{-1}
S_{bod}	Half-saturation concentration for satisfaction of BOD	1	mg L^{-1}
k_{pref}	Preference factor for ammonia over nitrate	0.1	-
k_N	Half saturation constant for N in phytoplankton	0.1	mg L^{-1}
k_P	Half saturation constant for P in phytoplankton	0.01	mg L^{-1}
L_{opt}	Optimum light intensity for phytoplankton	60	W m^2
α	Ratio of nitrogen to Chl-a in autotrophs	10	-
β	Ratio of phosphorus to Chl-a in autotrophs	1	-
Δ	Ratio of carbon to Chl-a in autotrophs	50	-
γ_{base}	Light attenuation in clean water	0.01	m^{-1}
L_{ss}	Light attenuation per mg of SS	0.01	m^{-1} mg^{-1} L
L_{phy}	Light attenuation per mg of phytoplankton	10	m^{-1} mg^{-1}
k_{ref}^{pho}	Growth rate maximum for phytoplankton	0.095	h^{-1}
k_{ref}^{res}	Respiration rate maximum for phytoplankton	0.2	-
k_{ref}^{death}	Death rate maximum for phytoplankton	0.2	-
L_1	Fraction of incoming radiation that is visible light	0.5	-
L_2	Fraction of incoming visible light useful for photosynthesis	0.5	-
L_3	Fraction of light reaching water surface that is not reflected	0.6	-
L_{in}	Incoming radiation factor	1	m^4 °C W^{-1} h^{-1}
L_{out}	Outgoing radiation factor	1	m^4 °C W^{-1} h^{-1}

Table B.3: Calibrated process-rate parameters

Parameter	Value	Unit
Global parameters		
Growth rate maximum for phytoplankton	0.095 (2.28)	h^{-1} (day^{-1})
Respiration rate maximum for phytoplankton	0.2 (0.1 in the phytoplankton model)	-
Death rate maximum for phytoplankton	0.2 (0.1 in the phytoplankton model)	-
Reach-scale parameters		
PON to NH^{+}_{4} rate	0	h^{-1} (day^{-1})
NH^{+}_{4} to NO^{-}_{3} rate	0.05-0.2 (1.2-4.8)	h^{-1} (day^{-1})
Denitrification rate parameter	0	m h^{-1} (m day^{-1})
Benthic oxygen demand rate	0.000833-0.004 (0.02-0.096)	h^{-1} (day^{-1})
BOD decay rate	0.025-0.04 (0.6-0.96)	h^{-1} (day^{-1})
BOD sedimentation rate	0	h^{-1} (day^{-1})
P mineralisation rate	0	h^{-1} (day^{-1})

Table B.4: Dissolved oxygen (DO) model performance statistics (Chapter 3) for calibration (2013) and validation periods (2014).

Period	Determinand	Sonning		Taplow		Windsor	
		NSE (-)	PBIAS (%)	NSE (-)	PBIAS (%)	NSE (-)	PBIAS (%)
Calib (2013)	DO	0.63	11.14	0.47	-8.35	0.59	-6.78
Valid (2014)	DO	0.31	14.35	0.31	-8.13	0.50	-7.91

C

HOURLY QUESTOR MODEL: OUTPUTS

C.1 SUPPORTING FIGURES FOR PHYTOPLANKTON MODELLING IN CHAPTER 2

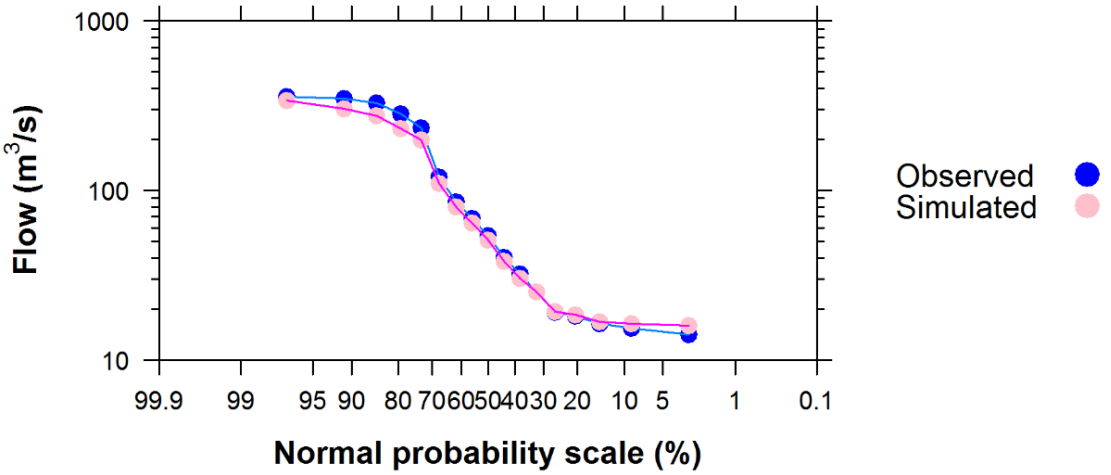

Figure C.1: Modelled (hourly QUESTOR) and observed flow duration curve at the Windsor site in the River Thames

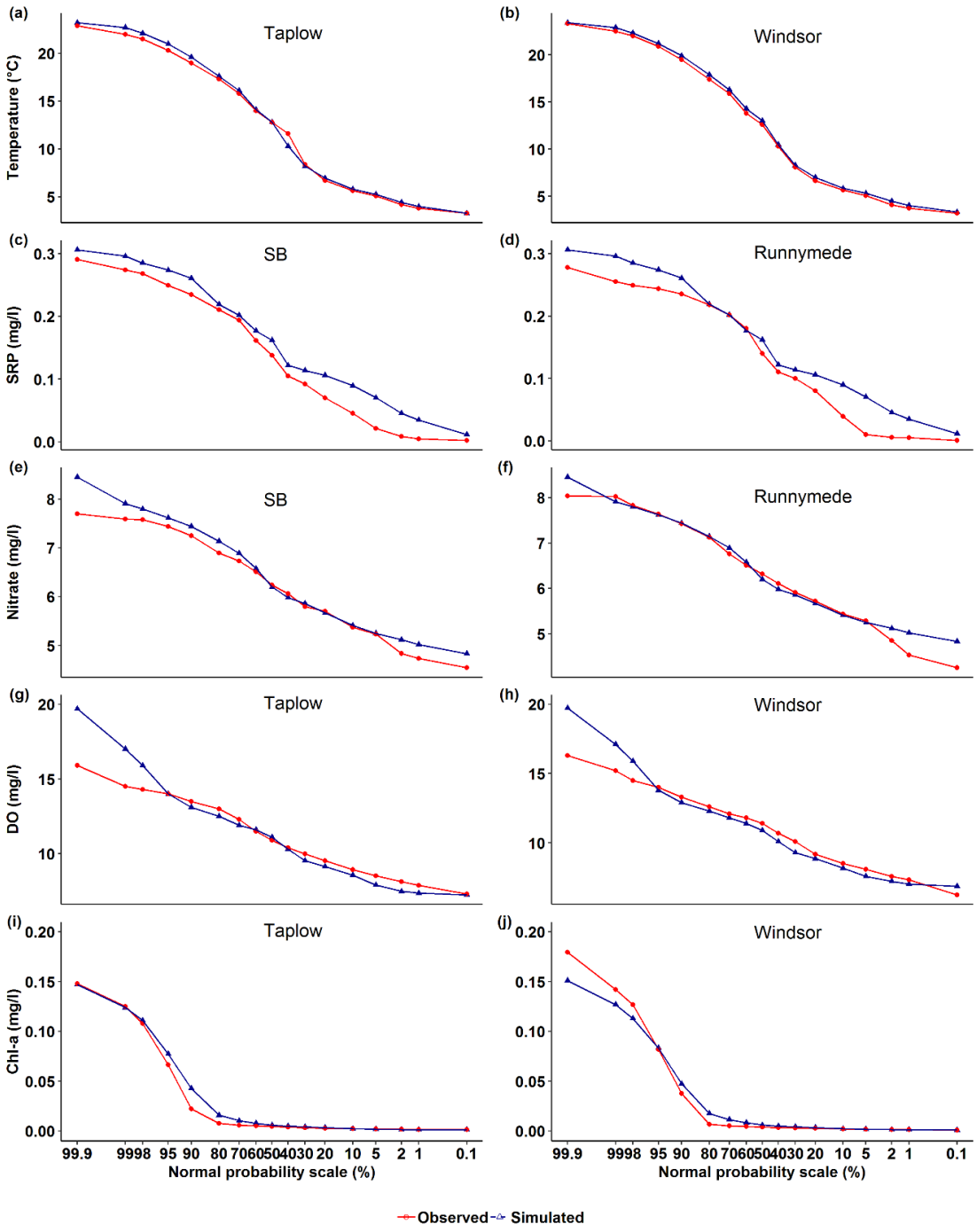

Figure C.2: Modelled (hourly QUESTOR) and observed quantile distribution of water temperature (panels a and b), dissolved oxygen (DO) (panels g and h) and chlorophyll (panels i and j) concentrations at Taplow and Windsor, and of nitrate (panels e and f) and soluble reactive phosphorus (SRP) (panels c and d) at Sonning Bridge (SB) and Runnymede during 2013-2014

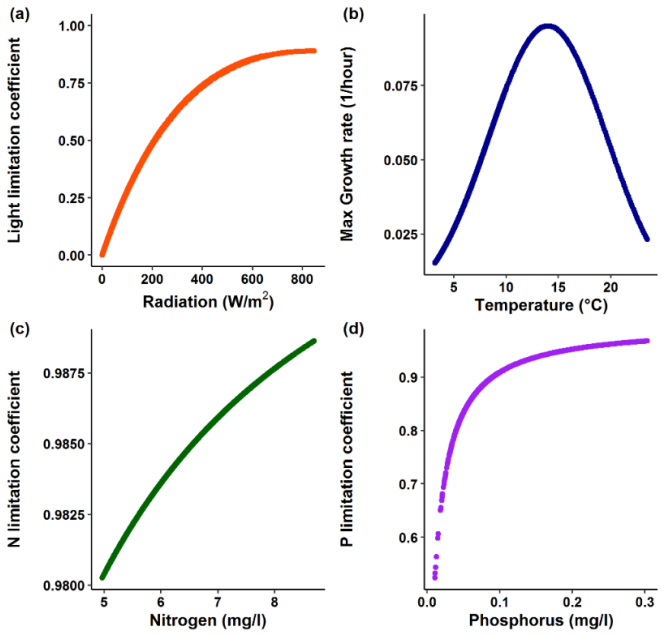

Figure C.3: Representation of phytoplankton growth-limiting factors including light limitation (a), temperature dependence (b), nitrogen (N) limitation (c) and phosphorus (P) limitation (d) in the hourly QUESTOR model (example of Windsor site)

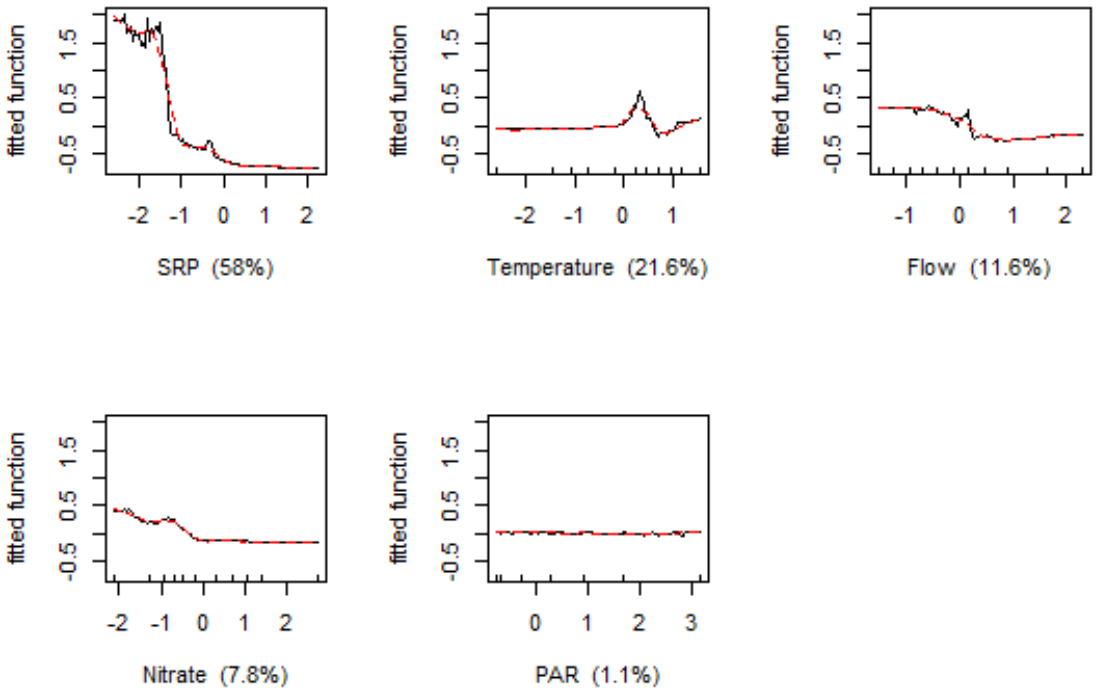

Figure C.4: Partial dependence plots for the modelled soluble reactive phosphorus (SRP), nitrate, flow, temperature and photosynthetically-active radiation (PAR) with normalised fitted values of observed chlorophyll concentrations at Windsor in the first boosted regression tress (BRT) model

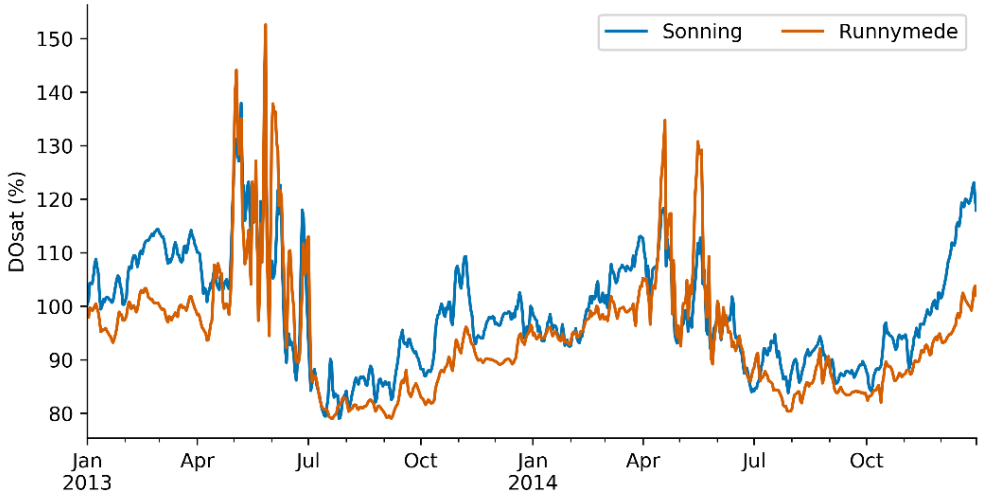

Figure C.5: Modelled (hourly QUESTOR) time-series of percentage dissolved oxygen saturation (DO_{sat}) at Sonning and Runnymede during 2013-2014

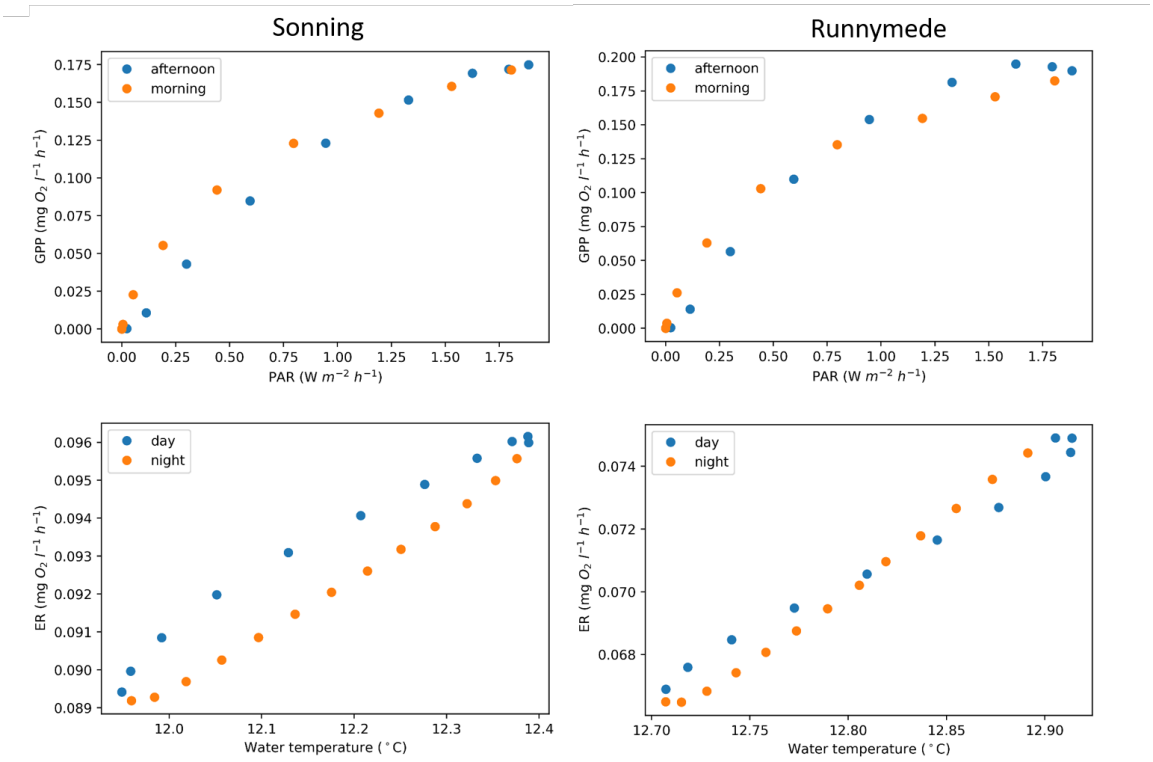

Figure C.6: Diurnal variation (annually averaged) of gross primary production (GPP) in response to photosynthetically-active radiation (PAR), and diurnal variation (annually averaged) of ecosystem respiration (ER) in response to modelled (hourly QUESTOR) water temperature at Sonning and Runnymede

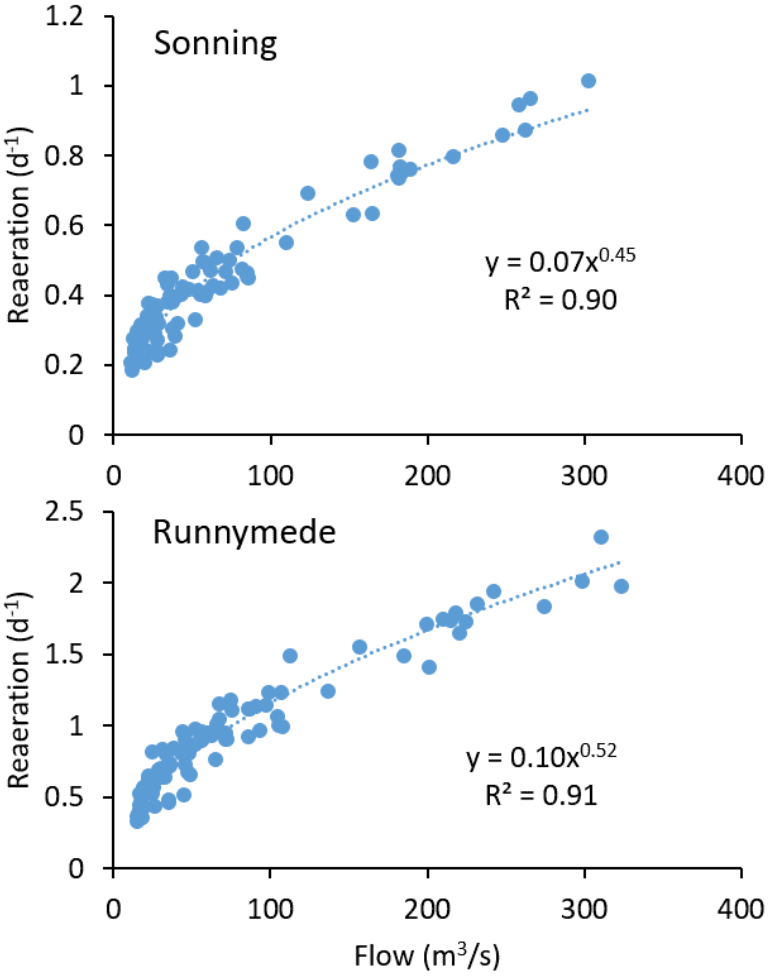

Figure C.7: Power regression between modelled (hourly QUESTOR) reaeration and observed flows at Sonning and Runnymede during 2013-2014

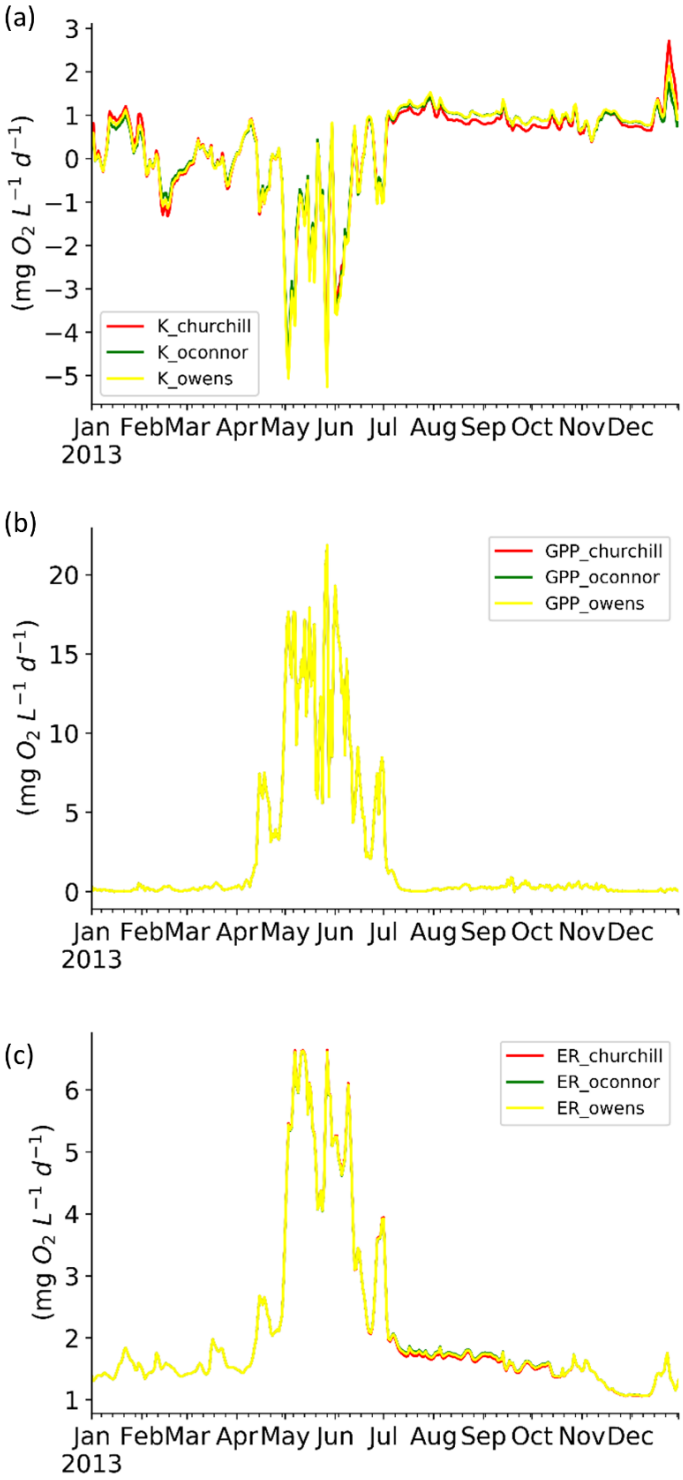

Figure C.8: Comparison of hourly QUESTOR model performance using different empirical equations (by Churchill et al. (1962), O'Connor and Dobbins (1958) and Owens (1964)) to estimate reaeration at the air-water surface. (a), (b) and (c) represents daily fluxes of reaeration (K), gross primary production (GPP) and ecosystem respiration (ER), respectively at Windsor during 2013

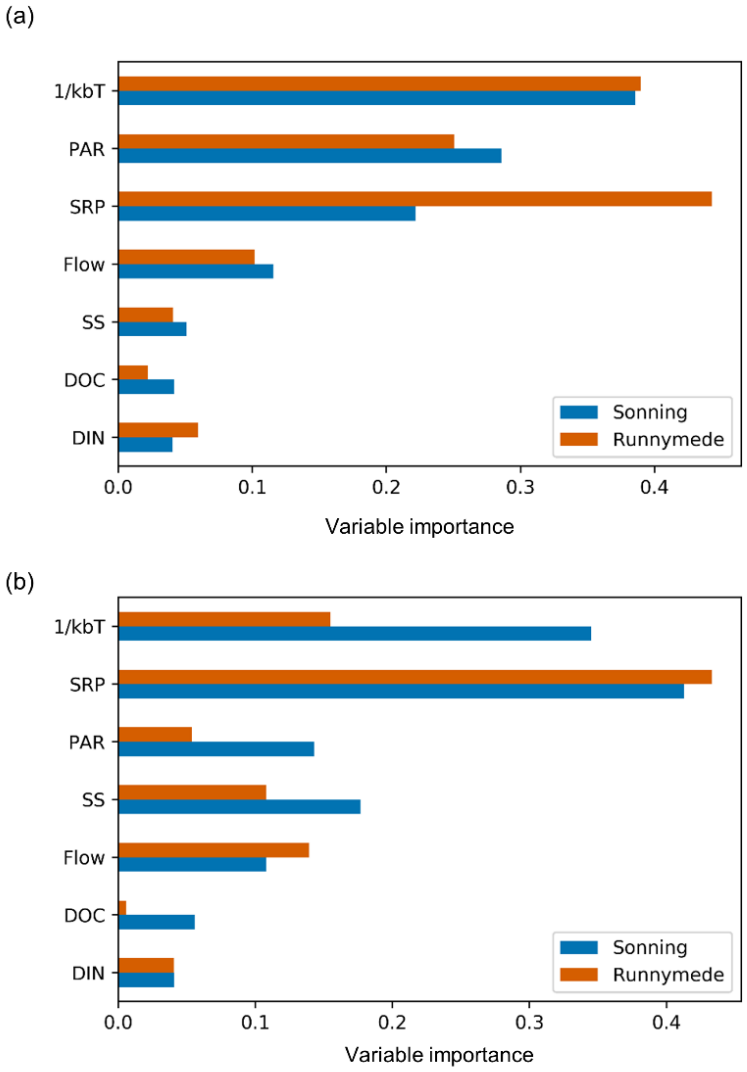

Figure C.9: Variable importance of water temperature ($1/k_bT$), inorganic phosphorus (SRP), photosynthetically-active radiation (PAR), suspended sediment (SS), flow volume, dissolved organic carbon (DOC) and dissolved inorganic nitrogen (DIN) in random forest models of gross primary production (GPP) (a) and ecosystem respiration (ER) (b)

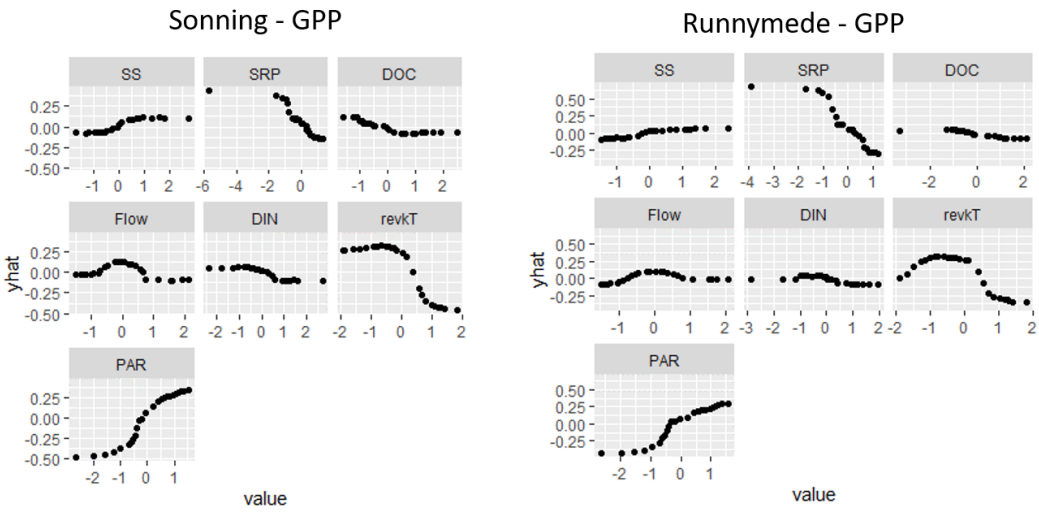

Figure C.10: Partial dependence plots for environmental controls in random forest models of gross primary production (GPP) prediction at Sonning and Runnymede sites

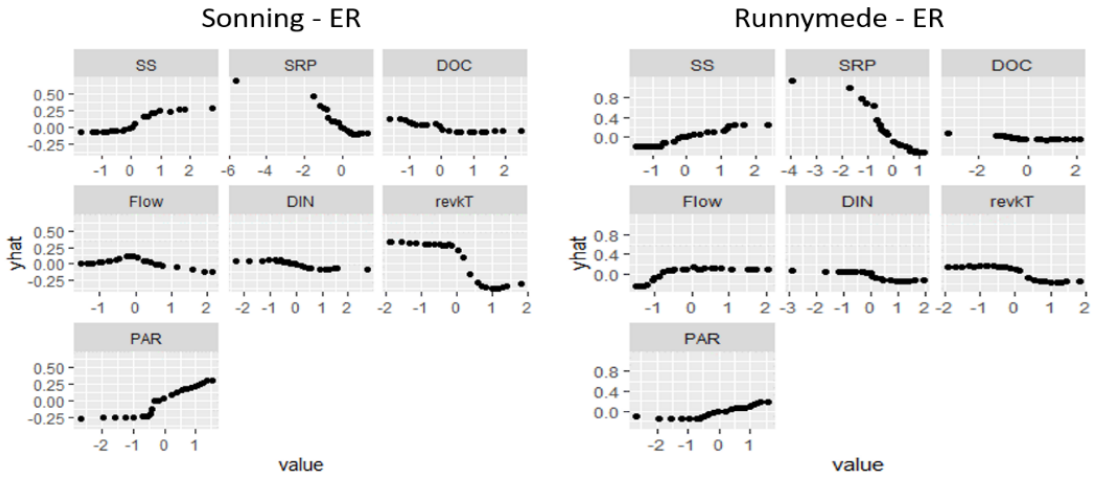

Figure C.11: Partial dependence plots for environmental controls in random forest models of ecosystem respiration (ER) prediction at Sonning and Runnymede sites

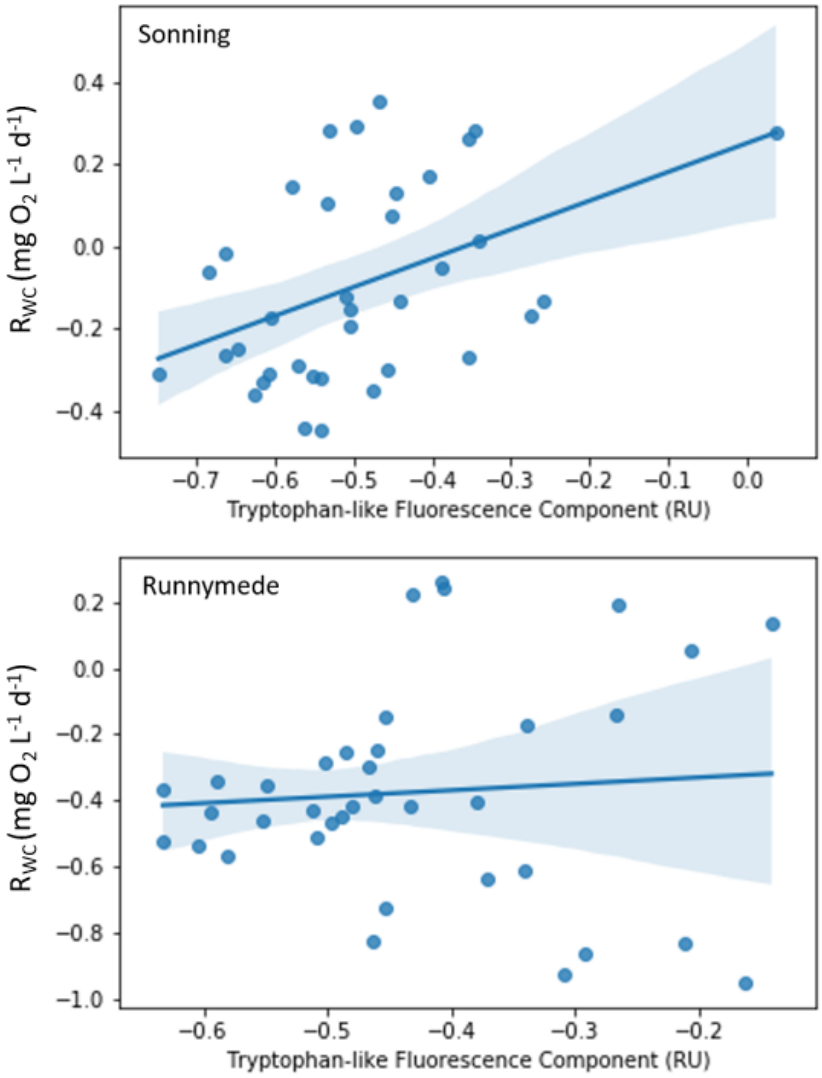

Figure C.12: Relationship between modelled (hourly QUESTOR) water column respiration (R_{WC}) and tryptophan-like fluorescence component at Sonning and Runnymede on a log/log scale

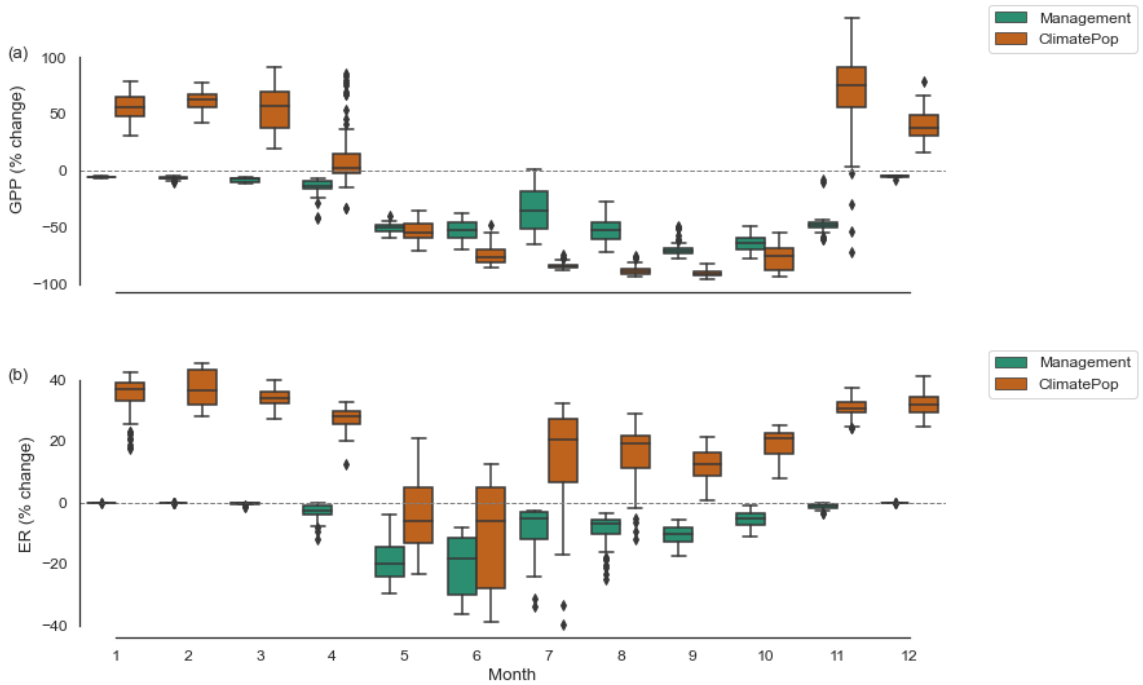

Figure C.13: Monthly percentage change in daily (a) gross primary production (GPP) and (b) ecosystem respiration (ER) in response to Management and ClimatePop scenarios

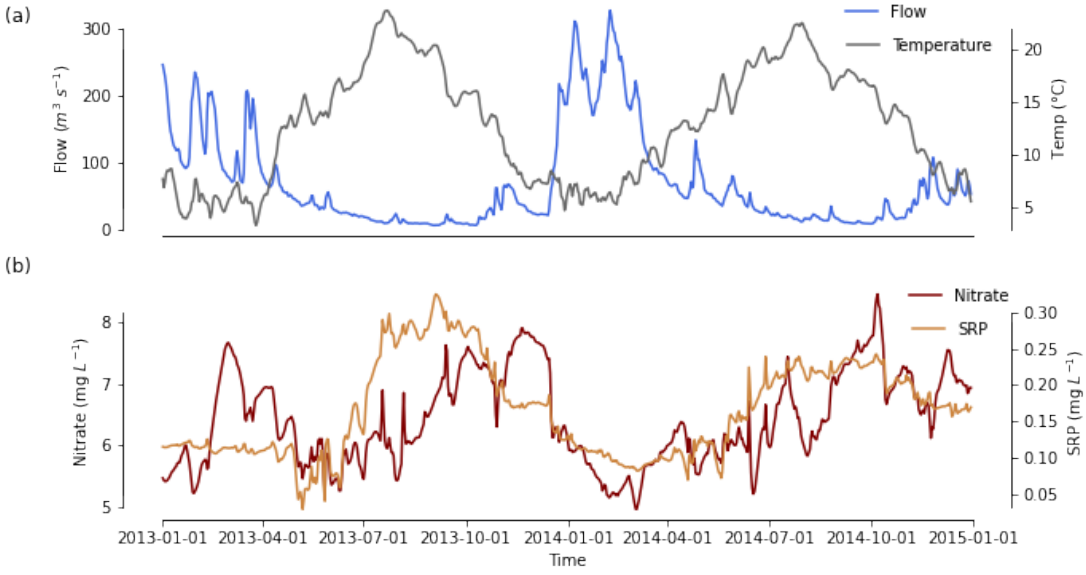

Figure C.14: Time-series of (a) flow, water temperature, and (b) nutrient concentrations at Runnymede in the Baseline scenario

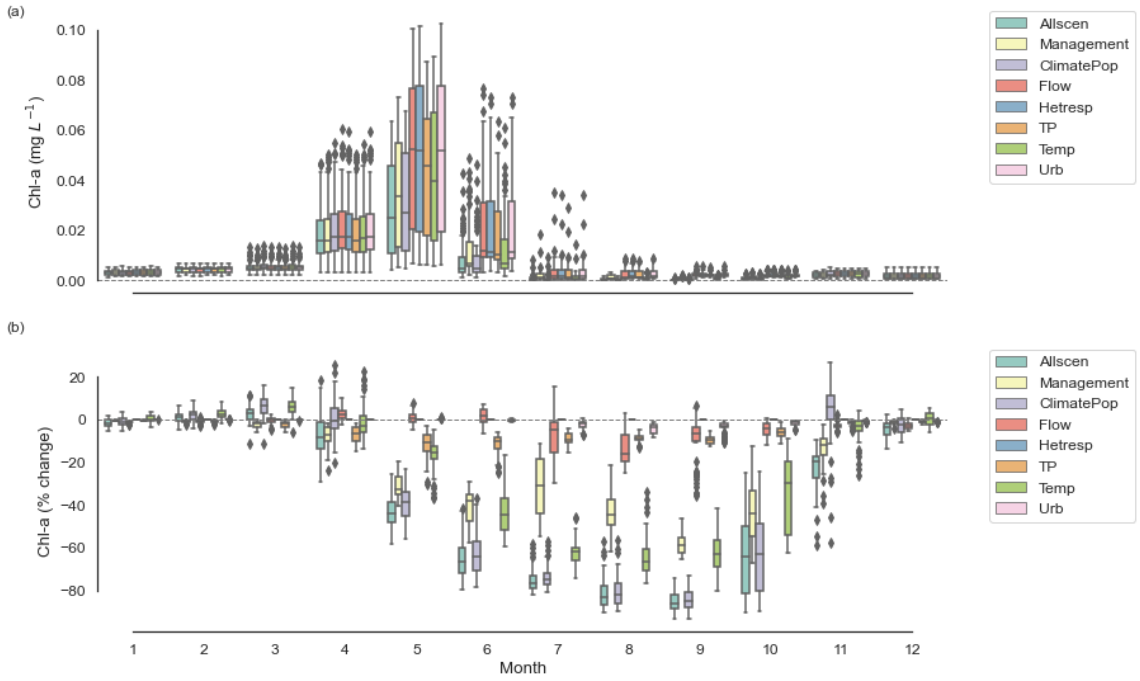

Figure C.15: Month wise variation in chlorophyll-a (Chl-a) concentrations (a) and month wise variation in relative change (percentage change) in chlorophyll-a (Chl-a) concentrations (b) in response to single and multiple stressors scenarios, depicted in the legend

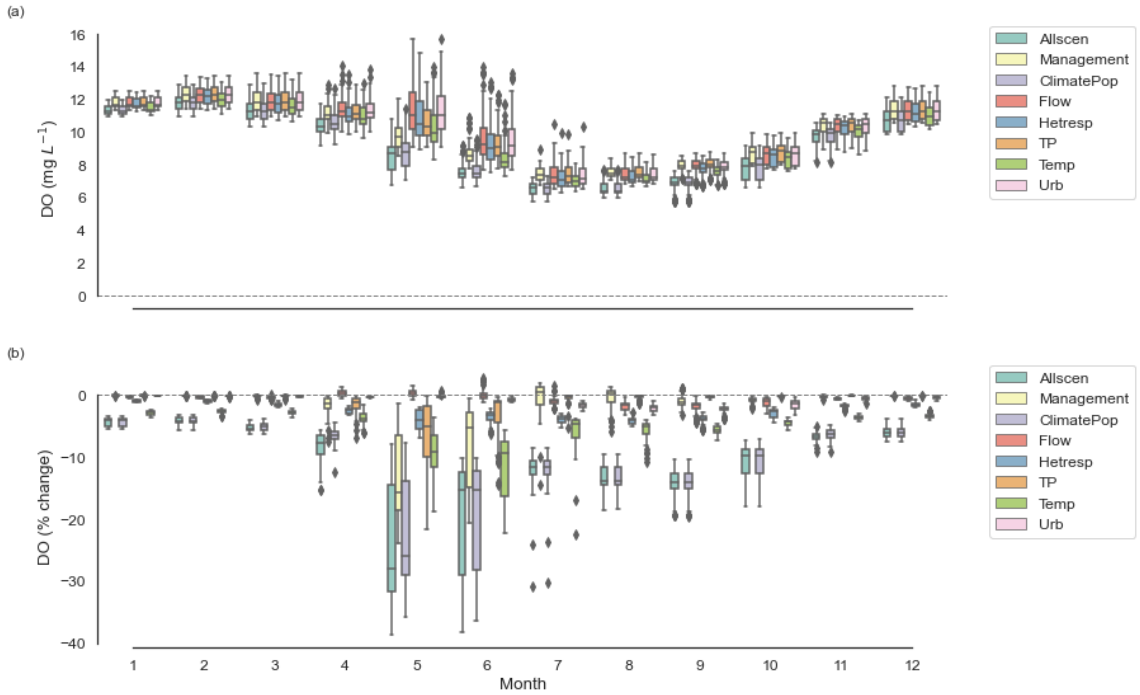

Figure C.16: Month wise variation in dissolved oxygen (DO) concentrations (a) and month wise variation in relative change (percentage change) in dissolved oxygen (DO) concentrations (b) in response to single and multiple stressors scenarios, depicted in the legend

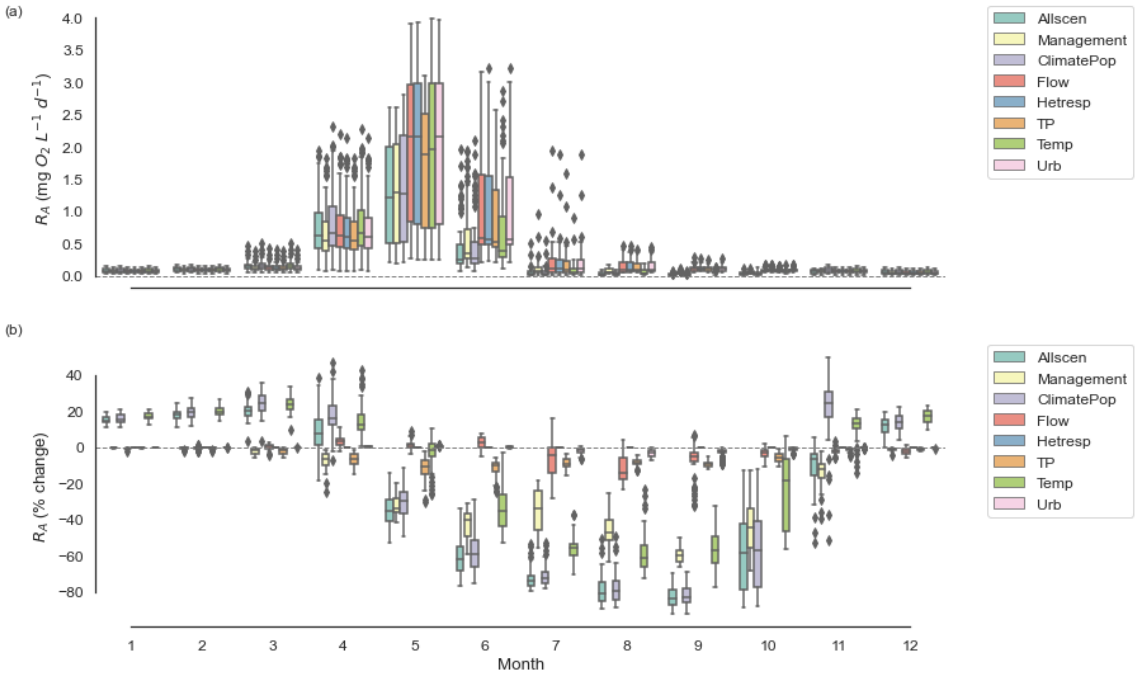

Figure C.17: Month wise variation in autotrophic respiration (R_A) (a) and month wise variation in relative change (percentage change) in autotrophic respiration (R_A) (b) in response to single and multiple stressors scenarios, depicted in the legend

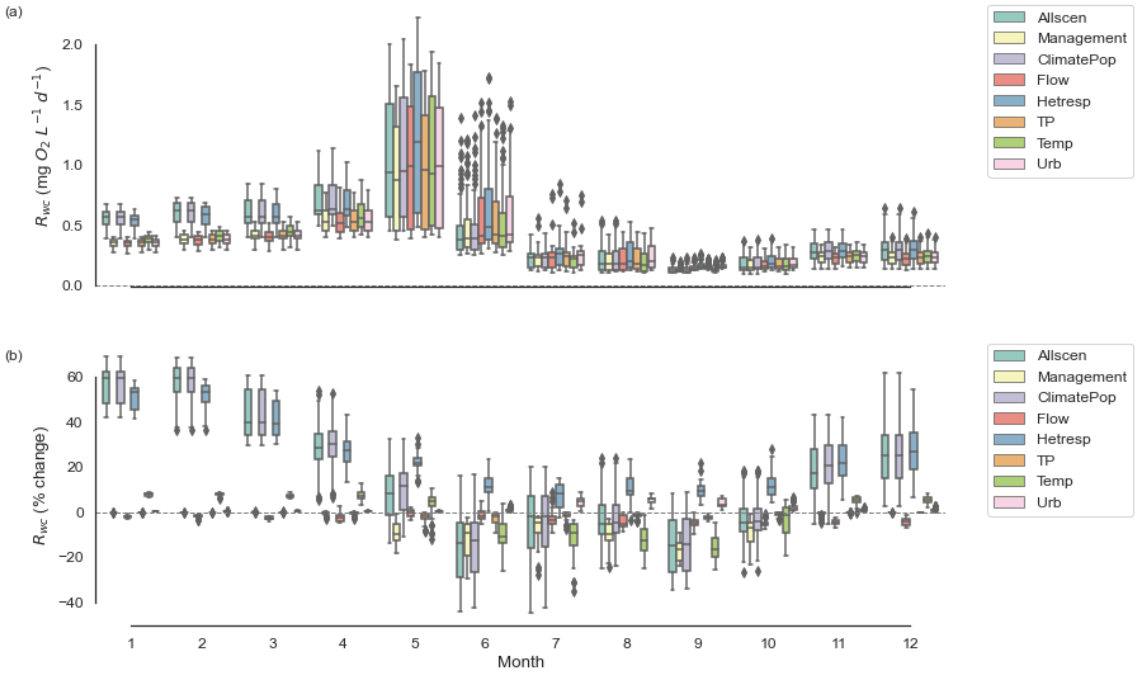

Figure C.18: Month wise variation in water column respiration (R_{wc}) (a) and month wise variation in relative change (percentage change) in water column respiration (R_{wc}) (b) in response to single and multiple stressors scenarios, depicted in the legend

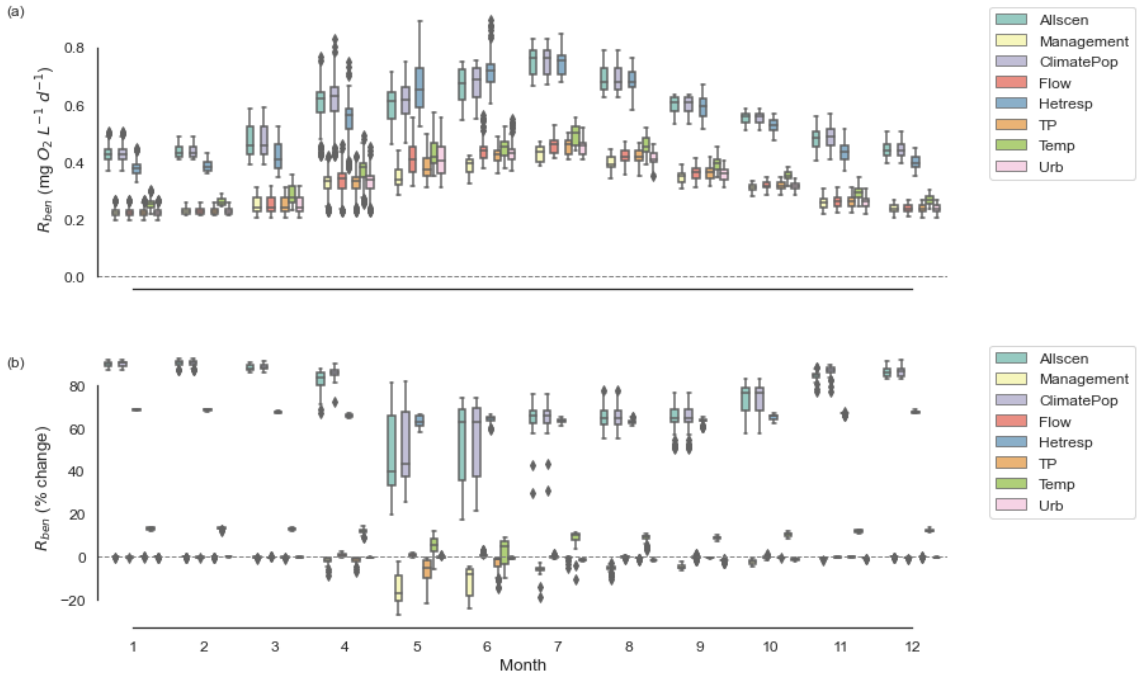

Figure C.19: Month wise variation in benthic respiration (R_{ben}) (a) and month wise variation in relative change (percentage change) in benthic respiration (R_{ben}) (b) in response to single and multiple stressors scenarios, depicted in the legend

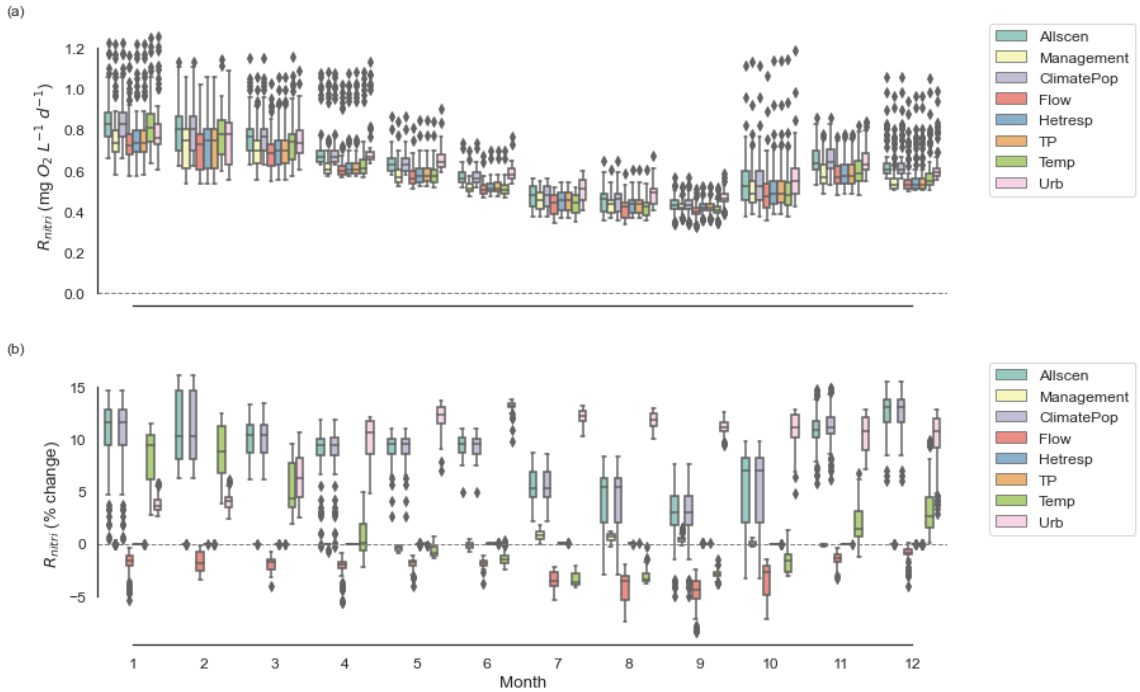

Figure C.20: Month wise variations in loss of dissolved oxygen due to nitrification (R_{nitri}) (a) and month wise variation in relative change (percentage change) in loss of dissolved oxygen due to nitrification (R_{nitri}) (b) in response to single and multiple stressors scenarios, depicted in the legend

D

MUFT MODEL: THEORY AND IMPLEMENTATION

D.1 ESTIMATION OF SOLUTE-LAG COEFFICIENT

Using average TDG travel time (Table D.1), $m = 5/3$ (Chapra, 2008) and average flood wave travel time in Eq. D.1, $\beta = 1.55$ is derived for the river section between Brokke and Hekni.

$$m = \frac{c}{u} = \frac{c}{u_s \times (1+\beta)} = \frac{\frac{10780}{190}}{\frac{10780}{807} \times (1+\beta)} \tag{D.1}$$

D.2 ESTIMATION OF FLOW ROUTING PARAMETERS

Flood wave travel time T_{flow} can be dervied from reach length and avereage celerity as shown in Eq. 5.2. Based on Eq. 5.2 and travel time relationships provided in Table 5.1,

$$T_{flow} = \frac{L}{c} = \frac{L}{m(1+\beta)u_s} \tag{D.2}$$

Solute travel time (T_s) at time t for a reach i is expresses as,

$$T_s = \frac{L_i}{u_s} = \frac{L_i}{b_i Q_t^{c_i}} \tag{D.3}$$

Substituting Eq. D.3 in Eq. D.2,

$$T_{flow} = \frac{\frac{L_1}{b_1 Q_t^{c1}} + \frac{L_1}{b_2 Q_t^{c2}} + \frac{L_3}{b_1 Q_t^{c3}}}{m(1+\beta)} \tag{D.4}$$

Values of b and c constants for each reach are provided in Table D.1.

Table D.1: Description of river reaches (L = length, W = mean width, v = velocity, τ = travel time)

Reach no	Reach name	L (m)	W (m)	b	c	Mean v (m s^{-1})	Mean τ (min)
1	Brokke - Rysstad Øy	3130	107	0.1554	0.3967	0.73	71
2	Rysstad Øy – Straume	4660	316	0.0047	0.8699	0.14	550
3	Straume - Hekni	2990	119	0.0489	0.4352	0.27	186

Table D.2: Parameter values in the inverse ADV and ADZ models optimised using the Nelder-Mead algorithm. Units are g O_2 m^{-2} d^{-1} for P_{GPPmax} and R_{ER}, and μmol quanta m^{-2} s^{-1} for k_{PAR}.

Model	Parameter	Day 1	Day 2	Day 3
ADV	P_{GPPmax}	8.64	12.96	11.52
	k_{PAR}	144	144	460
	R_{ER}	3.46	4.32	4.03
ADZ	P_{GPPmax}	13.82	14.40	12.53
	k_{PAR}	144	144	173
	R_{ER}	6.48	6.48	5.90

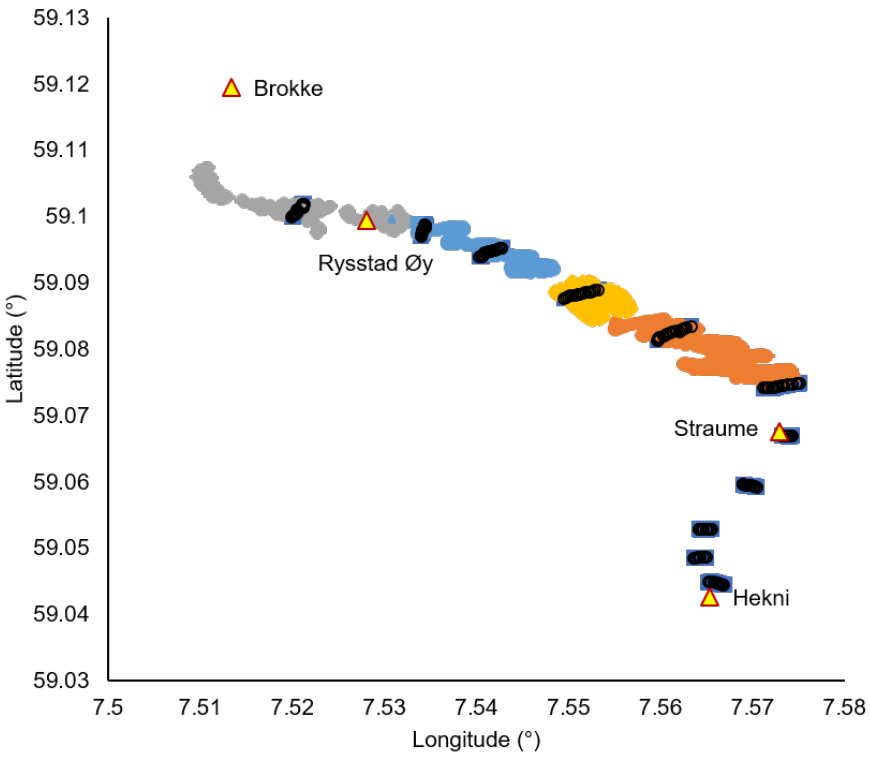

Figure D.1: Spatial distribution of depth measurements in the Otra River. Data points are represented with different colours to segregate depths taken on different days during June, 2020. The triangle markers highlight the locations of the gauging sites in the catchment (see Fig 5.2)

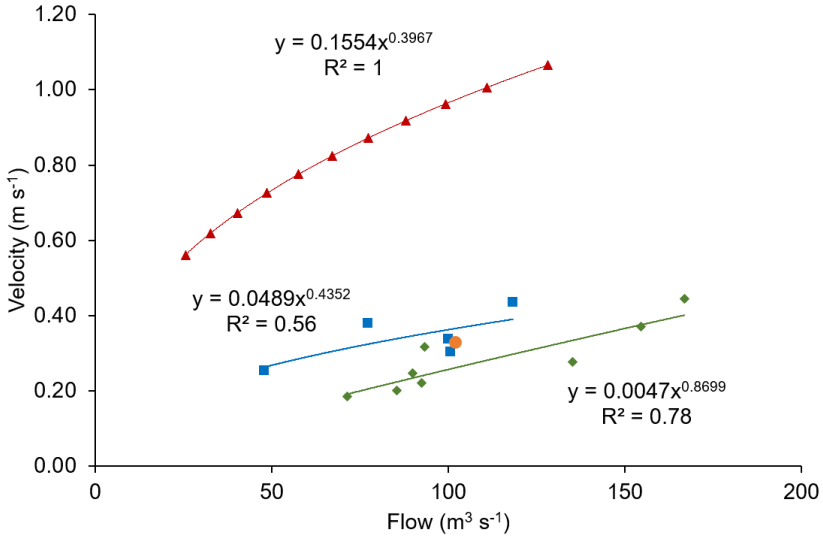

Figure D.2: Flow-velocity relationship for reach 1 (maroon, triangle markers), reach 2 (green, diamond markers) and reach 3 (blue, square markers) derived using total dissolved gas observations. Point in orange (circle marker) represents average velocity for a flow of 102 m^3 s^{-1} derived from a lime addition study between Straume and Hekni.

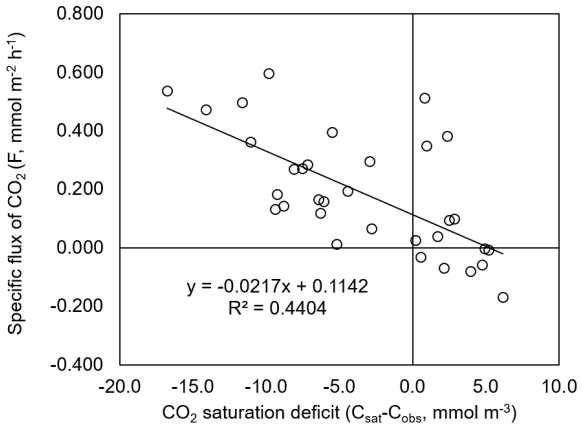

Figure D.3: Estimation of gas transfer velocity from a regression between specific flux of CO_2 derived from the floating chamber runs and CO_2 saturation deficit derived from the gas chromatograph analyses

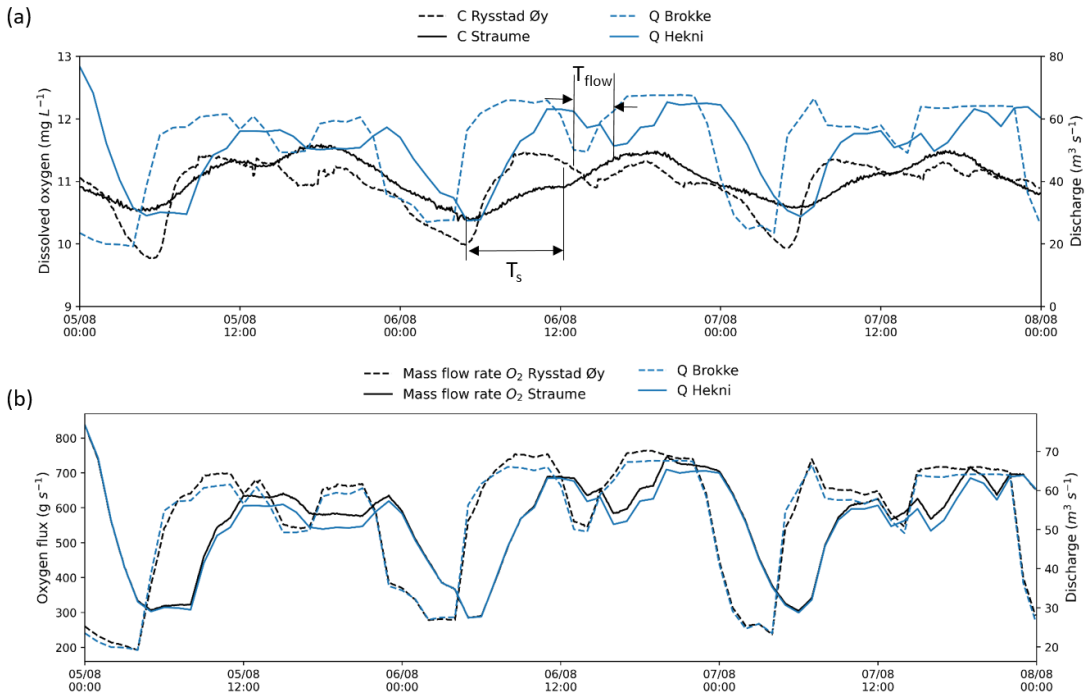

Figure D.4: Time-series of observed dissolved oxygen concentrations C and observed flow Q (a) and time-series of observed mass flow rate of oxygen and observed flow Q at sites within the study stretch (b)

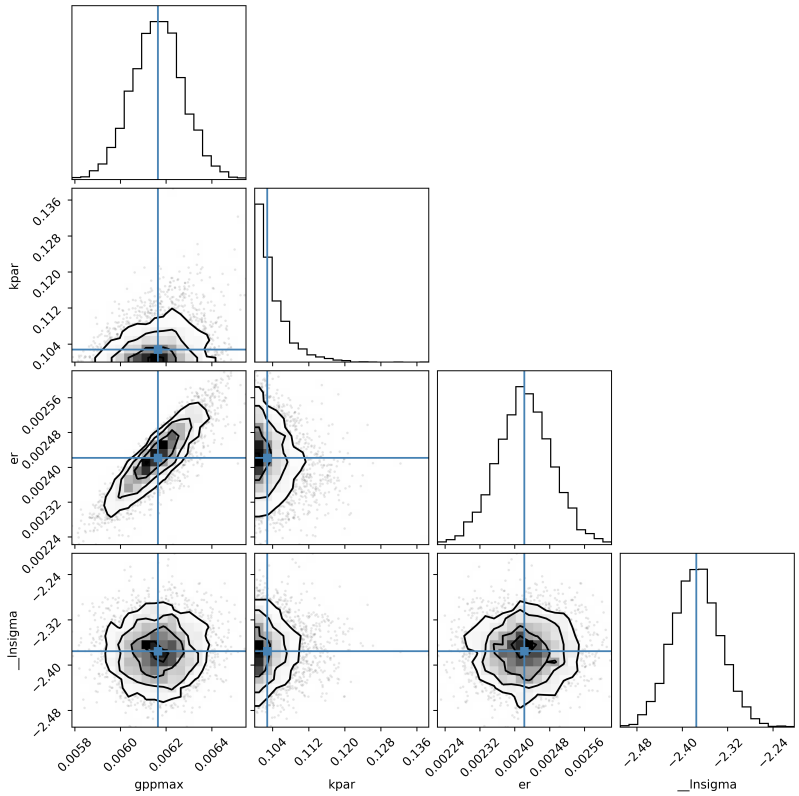

Figure D.5: Day 1. Posterior distribution of inverse ADV model parameters gppmax (P_{GPPmax}), kpar (k_{PAR}) and er (R_{ER}) using MCMC algorithm. Blue lines show the median values of posterior probability distribution of model parameters. _lnsigma parameter is used to estimate the true uncertainty in the data.

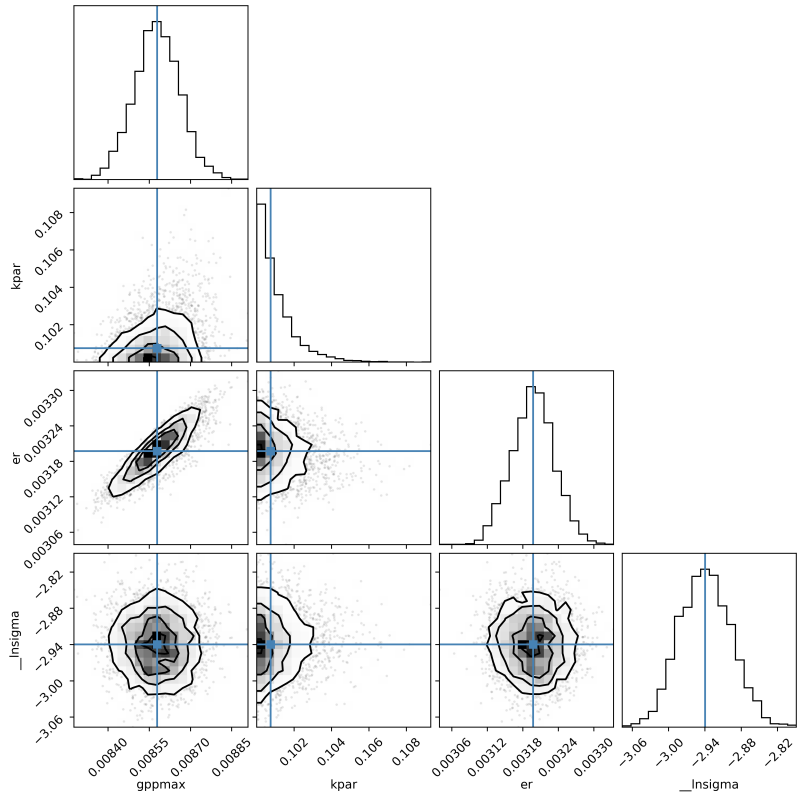

Figure D.6: Day 2. Posterior distribution of inverse ADV model parameters gppmax (P_{GPPmax}), kpar (k_{PAR}) and er (R_{ER}) using MCMC algorithm. Blue lines show the median values of posterior probability distribution of model parameters. _lnsigma parameter is used to estimate the true uncertainty in the data.

BIBLIOGRAPHY

Abbaspour, K. C., E. Rouholahnejad, S. Vaghefi, R. Srinivasan, H. Yang, and B. Kløve (2015). "A continental-scale hydrology and water quality model for Europe: Calibration and uncertainty of a high-resolution large-scale SWAT model". In: *Journal of hydrology* 524, pp. 733–752.

Abbaspour, Karim C, Jing Yang, Ivan Maximov, Rosi Siber, Konrad Bogner, Johanna Mieleitner, Juerg Zobrist, and Raghavan Srinivasan (2007). "Modelling hydrology and water quality in the pre-alpine/alpine Thur watershed using SWAT". In: *Journal of hydrology* 333.2-4, pp. 413–430.

Acreman, M. C., I. C. Overton, J. King, P. J. Wood, I. G. Cowx, M. J. Dunbar, E. Kendy, and W. J. Young (2014). "The changing role of ecohydrological science in guiding environmental flows". In: *Hydrological Sciences Journal* 59.3-4, pp. 433–450.

Acreman, Michael C and Michael J Dunbar (2004). "Defining environmental river flow requirements–a review". In: *Hydrology and Earth System Sciences* 8.5, pp. 861–876.

Acuña, V and K Tockner (2010). "The effects of alterations in temperature and flow regime on organic carbon dynamics in Mediterranean river networks". In: *Global Change Biology* 16.9, pp. 2638–2650.

Acuña, V, C Vilches, and A Giorgi (2011). "As productive and slow as a stream can be—the metabolism of a Pampean stream". In: *Journal of the North American Benthological Society* 30.1, pp. 71–83.

Acuña, Vicenç, Adonis Giorgi, Isabel Muñoz, Urs Uehlinger, and Sergi Sabater (2004). "Flow extremes and benthic organic matter shape the metabolism of a headwater Mediterranean stream". In: *Freshwater Biology* 49.7, pp. 960–971.

Acuña, Vicenç, Isabel Muñoz, Adonis Giorgi, Meritxell Omella, Francesc Sabater, and Sergi Sabater (2005). "Drought and postdrought recovery cycles in an intermittent Mediterranean stream: structural and functional aspects". In: *Journal of the North American Benthological Society* 24.4, pp. 919–933.

Akaike, Hirotugu (1973). "Information theory and an extension of the maximum likelihood principle". In: *2nd international symposium on information theory*, pp. 267–281.

Alberts, Jeremy M, Jake J Beaulieu, and Ishi Buffam (2017). "Watershed land use and seasonal variation constrain the influence of riparian canopy cover on stream ecosystem metabolism". In: *Ecosystems* 20.3, pp. 553–567.

Allan, J David (2004). "Landscapes and riverscapes: the influence of land use on stream ecosystems". In: *Annu. Rev. Ecol. Evol. Syst.* 35, pp. 257–284.

Appling, Alison P, Robert O Hall Jr, Charles B Yackulic, and Maite Arroita (2018a). "Overcoming equifinality: Leveraging long time series for stream metabolism estimation". In: *Journal of Geophysical Research: Biogeosciences* 123.2, pp. 624–645.

Appling, Alison P, Jordan S Read, Luke A Winslow, Maite Arroita, Emily S Bernhardt, Natalie A Griffiths, Robert O Hall, Judson W Harvey, James B Heffernan, Emily H

Stanley, et al. (2018b). "The metabolic regimes of 356 rivers in the United States". In: *Scientific data* 5.1, pp. 1–14.

Argerich, Alba, Roy Haggerty, Eugènia Martí, Francesc Sabater, and Jay Zarnetske (2011). "Quantification of metabolically active transient storage (MATS) in two reaches with contrasting transient storage and ecosystem respiration". In: *Journal of Geophysical Research: Biogeosciences* 116.G3.

Aristegi, Lide, Oihana Izagirre, and Arturo Elosegi (2009). "Comparison of several methods to calculate reaeration in streams, and their effects on estimation of metabolism". In: *Hydrobiologia* 635.1, pp. 113–124.

Aristi, Ibon, Maite Arroita, Aitor Larrañaga, Lydia Ponsatí, Sergi Sabater, Daniel von Schiller, Arturo Elosegi, and Vicenç Acuña (2014). "Flow regulation by dams affects ecosystem metabolism in Mediterranean rivers". In: *Freshwater biology* 59.9, pp. 1816–1829.

Arroita, Maite, Arturo Elosegi, and Robert O Hall Jr (2019). "Twenty years of daily metabolism show riverine recovery following sewage abatement". In: *Limnology and Oceanography* 64.S1, S77–S92.

Arroita, Maite, Lorea Flores, Aitor Larrañaga, Aingeru Martínez, Miren Martínez-Santos, Olatz Pereda, Estilita Ruiz-Romera, Libe Solagaistua, and Arturo Elosegi (2017). "Water abstraction impacts stream ecosystem functioning via wetted-channel contraction". In: *Freshwater Biology* 62.2, pp. 243–257.

Arthington, Angela H, Anik Bhaduri, Stuart E Bunn, Sue E Jackson, Rebecca E Tharme, Dave Tickner, Bill Young, Mike Acreman, Natalie Baker, Samantha Capon, et al. (2018). "The Brisbane declaration and global action agenda on environmental flows (2018)". In: *Frontiers in Environmental Science* 6, p. 45.

Ashraf, Faisal Bin, Ali Torabi Haghighi, Joakim Riml, Knut Alfredsen, Jarkko J Koskela, Bjørn Kløve, and Hannu Marttila (2018). "Changes in short term river flow regulation and hydropeaking in Nordic rivers". In: *Scientific reports* 8.1, pp. 1–12.

Aspray, Katie L, Joseph Holden, Mark E Ledger, Chris P Mainstone, and Lee E Brown (2017). "Organic sediment pulses impact rivers across multiple levels of ecological organization". In: *Ecohydrology* 10.6, e1855.

Bachiller-Jareno, N, MG Hutchins, MJ Bowes, MB Charlton, and HG Orr (2019). "A novel application of remote sensing for modelling impacts of tree shading on water quality". In: *Journal of environmental management* 230, pp. 33–42.

Balbi, David M (2000). "Suspended chlorophyll in the River Nene, a small nutrient-rich river in eastern England: long-term and spatial trends". In: *Science of the total environment* 251, pp. 401–421.

Barton, K (2016). *Package "MuMIn": Multi-Model Inference. R package, Version 1.15. 6.*

Bastviken, David, Ingrid Sundgren, Sivakiruthika Natchimuthu, Henrik Reyier, and Magnus Gålfalk (2015). "Cost-efficient approaches to measure carbon dioxide (CO_2) fluxes and concentrations in terrestrial and aquatic environments using mini loggers". In: *Biogeosciences* 12.12, pp. 3849–3859.

Basu, BK and FR Pick (1997). "Phytoplankton and zooplankton development in a lowland, temperate river". In: *Journal of Plankton Research* 19.2, pp. 237–253.

Batt, Ryan D, Stephen R Carpenter, Jonathan J Cole, Michael L Pace, and Robert A Johnson (2013). "Changes in ecosystem resilience detected in automated measures of ecosystem metabolism during a whole-lake manipulation". In: *Proceedings of the National Academy of Sciences* 110.43, pp. 17398–17403.

Beaulieu, Jake J, Clay P Arango, David A Balz, and William D Shuster (2013). "Continuous monitoring reveals multiple controls on ecosystem metabolism in a suburban stream". In: *Freshwater Biology* 58.5, pp. 918–937.

Beck, M and Peter C Young (1975). "A dynamic model for DO—BOD relationships in a non-tidal stream". In: *Water Research* 9.9, pp. 769–776.

Beck, MB (1976). "Dynamic modelling and control applications in water quality maintenance". In: *Water Research* 10.7, pp. 575–595.

Beer, Tom and Peter C Young (1983). "Longitudinal dispersion in natural streams". In: *Journal of environmental engineering* 109.5, pp. 1049–1067.

Bencala, Kenneth E and RA Walters (1983). "Simulation of solute transport in a mountain pool-and-riffle stream-a transient storage model". In: *Water Resources Research* 19, pp. 718–724.

Bernhardt, Emily S, Robert O Hall Jr, and Gene E Likens (2002). "Whole-system estimates of nitrification and nitrate uptake in streams of the Hubbard Brook Experimental Forest". In: *Ecosystems* 5.5, pp. 419–430.

Bernhardt, Emily S, Jim B Heffernan, Nancy B Grimm, Emily H Stanley, JW Harvey, M Arroita, Alison P Appling, MJ Cohen, William H McDowell, RO Hall Jr, et al. (2018). "The metabolic regimes of flowing waters". In: *Limnology and Oceanography* 63.S1, S99–S118.

Bernhardt, Emily S, Phil Savoy, Michael J Vlah, Alison P Appling, Lauren E Koenig, Robert O Hall Jr, Maite Arroita, Joanna R Blaszczak, Alice M Carter, Matt Cohen, et al. (2022). "Light and flow regimes regulate the metabolism of rivers". In: *Proceedings of the National Academy of Sciences* 119.8, e2121976119.

Bernot, Melody J, Daniel J Sobota, Robert O Hall Jr, Patrick J Mulholland, Walter K Dodds, Jackson R Webster, Jennifer L Tank, Linda R Ashkenas, Lee W Cooper, Clifford N Dahm, et al. (2010). "Inter-regional comparison of land-use effects on stream metabolism". In: *Freshwater Biology* 55.9, pp. 1874–1890.

Beven, Keith and Jim Freer (2001). "Equifinality, data assimilation, and uncertainty estimation in mechanistic modelling of complex environmental systems using the GLUE methodology". In: *Journal of hydrology* 249.1-4, pp. 11–29.

Billen, Gilles, Josette Garnier, and Philippe Hanset (1994). "Modelling phytoplankton development in whole drainage networks: the RIVERSTRAHLER model applied to the Seine river system". In: *Phytoplankton in Turbid Environments: Rivers and Shallow Lakes*. Springer, pp. 119–137.

Birk, Sebastian, Daniel Chapman, Laurence Carvalho, Bryan M Spears, Hans Estrup Andersen, Christine Argillier, Stefan Auer, Annette Baattrup-Pedersen, Lindsay Banin,

Meryem Beklioğlu, et al. (2020). "Impacts of multiple stressors on freshwater biota across spatial scales and ecosystems". In: *Nature Ecology & Evolution* 4.8, pp. 1060–1068.

Blaszczak, Joanna R, Joseph M Delesantro, Dean L Urban, Martin W Doyle, and Emily S Bernhardt (2019). "Scoured or suffocated: Urban stream ecosystems oscillate between hydrologic and dissolved oxygen extremes". In: *Limnology and Oceanography* 64.3, pp. 877–894.

Boorman, David B (2003a). "LOIS in-stream water quality modelling. Part 1. Catchments and methods". In: *Science of the Total Environment* 314, pp. 379–395.

– (2003b). "LOIS in-stream water quality modelling. Part 2. Results and scenarios". In: *Science of the Total Environment* 314, pp. 397–409.

Borges, Alberto V, François Darchambeau, Thibault Lambert, Cédric Morana, George H Allen, Ernest Tambwe, Alfred Toengaho Sembaito, Taylor Mambo, José Nlandu Wabakhangazi, Jean-Pierre Descy, et al. (2019). "Variations in dissolved greenhouse gases (CO_2, CH_4, N_2O) in the Congo River network overwhelmingly driven by fluvial-wetland connectivity". In: *Biogeosciences* 16.19, pp. 3801–3834.

Bormans, Myriam and Ian T Webster (1999). "Modelling the spatial and temporal variability of diatoms in the River Murray." In: *Journal of Plankton Research* 21.3.

Bott, TL, JT Brock, CS Dunn, RJ Naiman, RW Ovink, and RC Petersen (1985). "Benthic community metabolism in four temperate stream systems: an inter-biome comparison and evaluation of the river continuum concept". In: *Hydrobiologia* 123.1, pp. 3–45.

Bottacin-Busolin, Andrea, Gabriel Singer, Mattia Zaramella, Tom J Battin, and Andrea Marion (2009). "Effects of streambed morphology and biofilm growth on the transient storage of solutes". In: *Environmental science & technology* 43.19, pp. 7337–7342.

Bowes, Michael J, Linda K Armstrong, Sarah A Harman, Heather D Wickham, David JE Nicholls, Peter M Scarlett, Colin Roberts, Helen P Jarvie, Gareth H Old, Emma Gozzard, et al. (2018). "Weekly water quality monitoring data for the River Thames (UK) and its major tributaries (2009–2013): the Thames Initiative research platform". In: *Earth System Science Data* 10.3, pp. 1637–1653.

Bowes, MJ, Ea Gozzard, AC Johnson, PM Scarlett, Ca Roberts, DS Read, LK Armstrong, SA Harman, and HD Wickham (2012). "Spatial and temporal changes in chlorophyll-a concentrations in the River Thames basin, UK: are phosphorus concentrations beginning to limit phytoplankton biomass?" In: *Science of the Total Environment* 426, pp. 45–55.

Bowes, MJ, M Loewenthal, DS Read, MG Hutchins, C Prudhomme, LK Armstrong, SA Harman, HD Wickham, E Gozzard, and L Carvalho (2016). "Identifying multiple stressor controls on phytoplankton dynamics in the River Thames (UK) using high-frequency water quality data". In: *Science of the Total Environment* 569, pp. 1489–1499.

Bowie, George L, William B Mills, Donald B Porcella, Carrie L Campbell, James R Pagenkopf, Gretchen L Rupp, Kay M Johnson, PWH Chan, Steven A Gherini, CE Chamberlin, et al. (1985). "Rates, constants, and kinetics formulations in surface water quality modeling". In: *Epa* 600, pp. 3–85.

Breiman, Leo (2001). "Random forests". In: *Machine learning* 45.1, pp. 5–32.

Brown, Linfield C and Thomas O Barnwell (1987). *The enhanced stream water quality models QUAL2E and QUAL2E-UNCAS: documentation and user manual*. EPA.

Bunn, SE, EG Abal, MJ Smith, SC Choy, CS Fellows, BD Harch, MJ Kennard, and Fran Sheldon (2010). "Integration of science and monitoring of river ecosystem health to guide investments in catchment protection and rehabilitation". In: *Freshwater Biology* 55, pp. 223–240.

Bunn, Stuart E and Peter M Davies (2000). "Biological processes in running waters and their implications for the assessment of ecological integrity". In: *Assessing the ecological integrity of running waters*. Springer, pp. 61–70.

Burrell, Teresa K, Jonathan M O'Brien, S Elizabeth Graham, Kevin S Simon, Jon S Harding, and Angus R McIntosh (2014). "Riparian shading mitigates stream eutrophication in agricultural catchments". In: *Freshwater Science* 33.1, pp. 73–84.

Bussi, Gianbattista, Victoria Janes, Paul G Whitehead, Simon J Dadson, and Ian P Holman (2017). "Dynamic response of land use and river nutrient concentration to long-term climatic changes". In: *Science of the Total Environment* 590, pp. 818–831.

Caissie, Daniel (2006). "The thermal regime of rivers: a review". In: *Freshwater biology* 51.8, pp. 1389–1406.

Calizza, Edoardo, Maria Letizia Costantini, David Rossi, Pasquale Carlino, and Loreto Rossi (2012). "Effects of disturbance on an urban river food web". In: *Freshwater Biology* 57.12, pp. 2613–2628.

Canale, Raymond P and Allan H Vogel (1974). "Effects of temperature on phytoplankton growth". In: *Journal of the environmental engineering Division* 100.1, pp. 231–241.

Chapra, Steven C (2008). *Surface water-quality modeling*. Waveland press.

Chapra, Steven C and Dominic M Di Toro (1991). "Delta method for estimating primary production, respiration, and reaeration in streams". In: *Journal of environmental engineering* 117.5, pp. 640–655.

Chapra, Steven C and Robert L Runkel (1999). "Modeling impact of storage zones on stream dissolved oxygen". In: *Journal of Environmental Engineering* 125.5, pp. 415–419.

Chowanski, Kurt, Lisa Kunza, Gregory Hoffman, Laurel Genzoli, and Emily Stickney (2020). "River management alters ecosystem metabolism in a large oligotrophic river". In: *Freshwater Science* 39.3, pp. 534–548.

Churchill, MA, HL Elmore, and RA Buckingham (1962). "The prediction of stream reaeration rates". In: *Journal Sanitary Engineering Division* 88.

Cimorelli, L, L Cozzolino, A D'Aniello, F Morlando, D Pianese, and VP Singh (2016). "A new semi-Lagrangian routing procedure for constituent transport in steady and unsteady flow velocity fields". In: *Journal of Hydrology* 538, pp. 216–230.

Cook, Robert A, Ben Gawne, Rochelle Petrie, Darren S Baldwin, Gavin N Rees, Daryl L Nielsen, and Nathan SP Ning (2015). "River metabolism and carbon dynamics in response to flooding in a lowland river". In: *Marine and Freshwater Research* 66.10, pp. 919–927.

Cox, BA (2003a). "A review of currently available in-stream water-quality models and their applicability for simulating dissolved oxygen in lowland rivers". In: *Science of the total environment* 314, pp. 335–377.

– (2003b). "A review of dissolved oxygen modelling techniques for lowland rivers". In: *Science of the Total Environment* 314, pp. 303–334.

Crooks, SM and PS Naden (2007). "CLASSIC: a semi-distributed rainfall-runoff modelling system". In: *Hydrology and Earth System Sciences* 11.1, pp. 516–531.

Crossman, J, PG Whitehead, MN Futter, L Jin, Maria Shahgedanova, M Castellazzi, and AJ Wade (2013). "The interactive responses of water quality and hydrology to changes in multiple stressors, and implications for the long-term effective management of phosphorus". In: *Science of the Total Environment* 454, pp. 230–244.

Datry, Thibault (2012). "Benthic and hyporheic invertebrate assemblages along a flow intermittence gradient: effects of duration of dry events". In: *Freshwater Biology* 57.3, pp. 563–574.

Davidson, JF (1957). "The determination of diffusion coefficient for sparingly soluble gases in liquids". In: *Trans. Instn Chem. Engrs.* 35, pp. 51–60.

Davies, Peter M, Robert J Naiman, Danielle M Warfe, Neil E Pettit, Angela H Arthington, and Stuart E Bunn (2013). "Flow–ecology relationships: closing the loop on effective environmental flows". In: *Marine and Freshwater Research* 65.2, pp. 133–141.

Deflandre, A, RJ Williams, FJ Elorza, J Mira, and DB Boorman (2006). "Analysis of the QUESTOR water quality model using a Fourier amplitude sensitivity test (FAST) for two UK rivers". In: *Science of the total environment* 360.1-3, pp. 290–304.

Demars, Benoît O L, Peter Dörsch, Kirstine Thiemer, Francois Clayer, Susanne Claudia Schneider, Sebastian Franz Stranzl, Ulrich Pulg, and Gaute Velle (2021). *Hydropower: gas supersaturation and the role of aquatic plant photosynthesis for fish health*. Tech. rep. 7633-2021. Norwegian Institute for Water Research.

Demars, Benoit OL, J Russell Manson, Jon S Olafsson, Gisli M Gislason, Rakel Gudmundsdottir, GUY Woodward, Julia Reiss, Doris E Pichler, Jes J Rasmussen, and Nikolai Friberg (2011). "Temperature and the metabolic balance of streams". In: *Freshwater Biology* 56.6, pp. 1106–1121.

Demars, Benoît O L (2019). "Hydrological pulses and burning of dissolved organic carbon by stream respiration". In: *Limnology and Oceanography* 64.1, pp. 406–421.

Demars, Benoît OL, Gísli M Gíslason, Jón S Ólafsson, J Russell Manson, Nikolai Friberg, James M Hood, Joshua JD Thompson, and Thomas E Freitag (2016). "Impact of warming on CO2 emissions from streams countered by aquatic photosynthesis". In: *Nature Geoscience* 9.10, pp. 758–761.

Demars, Benoît OL, Joshua Thompson, and J Russell Manson (2015). "Stream metabolism and the open diel oxygen method: Principles, practice, and perspectives". In: *Limnology and Oceanography: Methods* 13.7, pp. 356–374.

Descy, J-P, Etienne Everbecq, Véronique Gosselain, Laurent Viroux, and JS Smitz (2003). "Modelling the impact of benthic filter-feeders on the composition and biomass of river plankton". In: *Freshwater biology* 48.3, pp. 404–417.

Dodds, Walter K (2006). "Eutrophication and trophic state in rivers and streams". In: *Limnology and oceanography* 51.1part2, pp. 671–680.

– (2007). "Trophic state, eutrophication and nutrient criteria in streams". In: *Trends in ecology & evolution* 22.12, pp. 669–676.

Dodds, Walter K and Jonathan J Cole (2007). "Expanding the concept of trophic state in aquatic ecosystems: it's not just the autotrophs". In: *Aquatic Sciences* 69.4, pp. 427–439.

Dodds, Walter K, Sophie A Higgs, Margaret J Spangler, James Guinnip, Jeffrey D Scott, Skyler C Hedden, Bryan D Frenette, Ryland Taylor, Anne E Schechner, David J Hoeinghaus, et al. (2018). "Spatial heterogeneity and controls of ecosystem metabolism in a Great Plains river network". In: *Hydrobiologia* 813.1, pp. 85–102.

Dodds, Walter K, Allison M Veach, Claire M Ruffing, Danelle M Larson, Jason L Fischer, and Katie H Costigan (2013). "Abiotic controls and temporal variability of river metabolism: multiyear analyses of Mississippi and Chattahoochee River data". In: *Freshwater Science* 32.4, pp. 1073–1087.

Domingues, Rita B, Tânia P Anselmo, Ana B Barbosa, Ulrich Sommer, and Helena M Galvão (2011). "Light as a driver of phytoplankton growth and production in the freshwater tidal zone of a turbid estuary". In: *Estuarine, Coastal and Shelf Science* 91.4, pp. 526–535.

Dortch, Quay and Terry E Whitledge (1992). "Does nitrogen or silicon limit phytoplankton production in the Mississippi River plume and nearby regions?" In: *Continental shelf research* 12.11, pp. 1293–1309.

Du, Enhao, Timothy E Link, John A Gravelle, and Jason A Hubbart (2014). "Validation and sensitivity test of the distributed hydrology soil-vegetation model (DHSVM) in a forested mountain watershed". In: *Hydrological processes* 28.26, pp. 6196–6210.

Dudgeon, David, Angela H Arthington, Mark O Gessner, Zen-Ichiro Kawabata, Duncan J Knowler, Christian Lévêque, Robert J Naiman, Anne-Hélène Prieur-Richard, Doris Soto, Melanie LJ Stiassny, et al. (2006). "Freshwater biodiversity: importance, threats, status and conservation challenges". In: *Biological reviews* 81.2, pp. 163–182.

Eatherall, A, DB Boorman, RJ Williams, and R Kowe (1998). "Modelling in-stream water quality in LOIS". In: *Science of the total environment* 210, pp. 499–517.

Elith, Jane, John R Leathwick, and Trevor Hastie (2008). "A working guide to boosted regression trees". In: *Journal of animal ecology* 77.4, pp. 802–813.

Elmore, HL t and TW Hayes (1960). "Solubility of atmospheric oxygen in water". In: *Proc. Am. Sot. Civil Engrs*. Vol. 86, pp. 41–53.

Ensign, Scott H and Martin W Doyle (2005). "In-channel transient storage and associated nutrient retention: Evidence from experimental manipulations". In: *Limnology and Oceanography* 50.6, pp. 1740–1751.

Estevez, Edurne, Tamara Rodríguez-Castillo, Mario Álvarez-Cabria, Francisco J Penas, Alexia María González-Ferreras, María Lezcano, and José Barquín (2017). "Analysis of structural and functional indicators for assessing the health state of mountain streams". In: *Ecological indicators* 72, pp. 553–564.

Everbecq, Etienne, Véronique Gosselain, Laurent Viroux, and J-P Descy (2001). "Potamon: a dynamic model for predicting phytoplankton composition and biomass in lowland rivers". In: *Water Research* 35.4, pp. 901–912.

Feio, MJ, T Alves, M Boavida, A Medeiros, and MAS Graça (2010). "Functional indicators of stream health: A river-basin approach". In: *Freshwater Biology* 55.5, pp. 1050–1065.

Feld, Christian K, Pedro Segurado, and Cayetano Gutierrez-Canovas (2016). "Analysing the impact of multiple stressors in aquatic biomonitoring data: A 'cookbook'with applications in R". In: *Science of the Total Environment* 573, pp. 1320–1339.

Fellows, Christine S, Maurice H Valett, and Clifford N Dahm (2001). "Whole-stream metabolism in two montane streams: Contribution of the hyporheic zone". In: *Limnology and Oceanography* 46.3, pp. 523–531.

Ferreira, Verónica, Arturo Elosegi, Scott D Tiegs, Daniel von Schiller, and Roger Young (2020). "Organic Matter Decomposition and Ecosystem Metabolism as Tools to Assess the Functional Integrity of Streams and Rivers–A Systematic Review". In: *Water* 12.12, p. 3523.

Fezzi, Carlo, Amii R Harwood, Andrew A Lovett, and Ian J Bateman (2017). "The environmental impact of climate change adaptation on land use and water quality". In: *Building a Climate Resilient Economy and Society*. Edward Elgar Publishing.

Fisher, Stuart G and Gene E Likens (1973). "Energy flow in Bear Brook, New Hampshire: an integrative approach to stream ecosystem metabolism". In: *Ecological monographs* 43.4, pp. 421–439.

Foreman-Mackey, Daniel, David W Hogg, Dustin Lang, and Jonathan Goodman (2013). "emcee: the MCMC hammer". In: *Publications of the Astronomical Society of the Pacific* 125.925, p. 306.

Fuß, Thomas, Barbara Behounek, Amber J Ulseth, and Gabriel A Singer (2017). "Land use controls stream ecosystem metabolism by shifting dissolved organic matter and nutrient regimes". In: *Freshwater Biology* 62.3, pp. 582–599.

Gameson, ALH (1957). "Weirs and the aeration of rivers". In: *J. Inst. Wat. Engrs* 11, pp. 477–490.

Gao, Fuchang and Lixing Han (2012). "Implementing the Nelder-Mead simplex algorithm with adaptive parameters". In: *Computational Optimization and Applications* 51.1, pp. 259–277.

Garnier, Josette, Gilles Billen, and Laurent Palfner (1999). "Understanding the oxygen budget and related ecological processes in the river Mosel: the RIVERSTRAHLER approach". In: *Man and river systems*. Springer, pp. 151–166.

Genzoli, Laurel and Robert O Hall Jr (2016). "Shifts in Klamath River metabolism following a reservoir cyanobacterial bloom". In: *Freshwater Science* 35.3, pp. 795–809.

Gillespie, Ben R, Paul Kay, and Lee E Brown (2020). "Limited impacts of experimental flow releases on water quality and macroinvertebrate community composition in an upland regulated river". In: *Ecohydrology* 13.2, e2174.

Gooseff, Michael N, Justin LaNier, Roy Haggerty, and Kenneth Kokkeler (2005). "Determining in-channel (dead zone) transient storage by comparing solute transport

in a bedrock channel–alluvial channel sequence, Oregon". In: *Water Resources Research* 41.6.

Gosselain, Véronique, Laurent Viroux, and J-P Descy (1998). "Can a community of small-bodied grazers control phytoplankton in rivers?" In: *Freshwater Biology* 39.1, pp. 9–24.

Grace, Michael R, Darren P Giling, Sally Hladyz, Valerie Caron, Ross M Thompson, and Ralph Mac Nally (2015). "Fast processing of diel oxygen curves: Estimating stream metabolism with BASE (BAyesian Single-station Estimation)". In: *Limnology and Oceanography: Methods* 13.3, pp. 103–114.

Grill, Günther, B Lehner, Michele Thieme, B Geenen, D Tickner, F Antonelli, S Babu, Pasquale Borrelli, L Cheng, H Crochetiere, et al. (2019). "Mapping the world's free-flowing rivers". In: *Nature* 569.7755, pp. 215–221.

Grizzetti, B, A Pistocchi, C Liquete, A Udias, F Bouraoui, and W Van De Bund (2017). "Human pressures and ecological status of European rivers". In: *Scientific reports* 7.1, pp. 1–11.

Grueber, Catherine E, Shinichi Nakagawa, Rebecca J Laws, and Ian G Jamieson (2011). "Multimodel inference in ecology and evolution: challenges and solutions". In: *Journal of evolutionary biology* 24.4, pp. 699–711.

Guasch, Helena, Eugènia Martí, and Sergi Sabater (1995). "Nutrient enrichment effects on biofilm metabolism in a Mediterranean stream". In: *Freshwater Biology* 33.3, pp. 373–383.

Gücker, Björn, Mario Brauns, and Martin T Pusch (2006). "Effects of wastewater treatment plant discharge on ecosystem structure and function of lowland streams". In: *Journal of the North American benthological society* 25.2, pp. 313–329.

Haggerty, R and P Reeves (2002). "STAMMT-L version 1.0 user's manual". In: *Sandia National Laboratories [ERMS# 520308]*, pp. 1–76.

Haggerty, Roy, Eugènia Martí, Alba Argerich, Daniel Von Schiller, and Nancy B Grimm (2009). "Resazurin as a "smart" tracer for quantifying metabolically active transient storage in stream ecosystems". In: *Journal of Geophysical Research: Biogeosciences* 114.G3.

Halbedel, Susanne and Olaf Büttner (2014). "MeCa, a toolbox for the calculation of metabolism in heterogeneous streams". In: *Methods in Ecology and Evolution* 5.9, pp. 971–975.

Hall, Robert Jr O and Jennifer L Tank (2003). "Ecosystem metabolism controls nitrogen uptake in streams in Grand Teton National Park, Wyoming". In: *Limnology and oceanography* 48.3, pp. 1120–1128.

Hall, Robert O, Jennifer L Tank, Michelle A Baker, Emma J Rosi-Marshall, and Erin R Hotchkiss (2016). "Metabolism, gas exchange, and carbon spiraling in rivers". In: *Ecosystems* 19.1, pp. 73–86.

Hall Jr, Robert O (2016). "Metabolism of streams and rivers: Estimation, controls, and application". In: *Stream ecosystems in a changing environment*. Elsevier, pp. 151–180.

Hall Jr, Robert O and Jake J Beaulieu (2013). "Estimating autotrophic respiration in streams using daily metabolism data". In: *Freshwater Science* 32.2, pp. 507–516.

Hall Jr, Robert O and Erin R Hotchkiss (2017). "Stream metabolism". In: *Methods in stream ecology*. Elsevier, pp. 219–233.

Hall Jr, Robert O and Jennifer L Tank (2005). "Correcting whole-stream estimates of metabolism for groundwater input". In: *Limnology and Oceanography: Methods* 3.4, pp. 222–229.

Hall Jr, Robert O and Amber J Ulseth (2020). "Gas exchange in streams and rivers". In: *Wiley Interdisciplinary Reviews: Water* 7.1, e1391.

Hanna, Dalal EL, Stephanie A Tomscha, Camille Ouellet Dallaire, and Elena M Bennett (2018). "A review of riverine ecosystem service quantification: Research gaps and recommendations". In: *Journal of Applied Ecology* 55.3, pp. 1299–1311.

Hanson, Paul C, Kathleen C Weathers, and Timothy K Kratz (2016). "Networked lake science: How the Global Lake Ecological Observatory Network (GLEON) works to understand, predict, and communicate lake ecosystem response to global change". In: *Inland Waters* 6.4, pp. 543–554.

Hardenbicker, Paulin, Susanne Rolinski, Markus Weitere, and Helmut Fischer (2014). "Contrasting long-term trends and shifts in phytoplankton dynamics in two large rivers". In: *International Review of Hydrobiology* 99.4, pp. 287–299.

Heathwaite, AL (2010). "Multiple stressors on water availability at global to catchment scales: understanding human impact on nutrient cycles to protect water quality and water availability in the long term". In: *Freshwater Biology* 55, pp. 241–257.

Heffernan, James B and Matthew J Cohen (2010). "Direct and indirect coupling of primary production and diel nitrate dynamics in a subtropical spring-fed river". In: *Limnology and oceanography* 55.2, pp. 677–688.

Hijmans, Robert J, Steven Phillips, John Leathwick, Jane Elith, and Maintainer Robert J Hijmans (2017). *Package 'dismo'*. 1, pp. 1–68.

Hill, BH, AT Herlihy, and PR Kaufmann (2002). "Benthic microbial respiration in Appalachian Mountain, Piedmont, and Coastal Plains streams of the eastern USA". In: *Freshwater Biology* 47.2, pp. 185–194.

Hill, Walter R and Sarah M Dimick (2002). "Effects of riparian leaf dynamics on periphyton photosynthesis and light utilisation efficiency". In: *Freshwater Biology* 47.7, pp. 1245–1256.

Hill, Walter R, Shari E Fanta, and Brian J Roberts (2009). "Quantifying phosphorus and light effects in stream algae". In: *Limnology and oceanography* 54.1, pp. 368–380.

Hilton, John, Matthew O'Hare, Michael J Bowes, and J Iwan Jones (2006). "How green is my river? A new paradigm of eutrophication in rivers". In: *Science of the Total Environment* 365.1-3, pp. 66–83.

Hindmarsh, Alan C (1983). "ODEPACK, a systematized collection of ODE solvers". In: *Scientific computing*, pp. 55–64.

Hoellein, Timothy J, Denise A Bruesewitz, and David C Richardson (2013). "Revisiting Odum (1956): A synthesis of aquatic ecosystem metabolism". In: *Limnology and Oceanography* 58.6, pp. 2089–2100.

Holtgrieve, Gordon W, Daniel E Schindler, Trevor A Branch, and Z Teresa A'mar (2010). "Simultaneous quantification of aquatic ecosystem metabolism and reaeration using a

Bayesian statistical model of oxygen dynamics". In: *Limnology and Oceanography* 55.3, pp. 1047–1063.

Holtgrieve, Gordon W, Daniel E Schindler, and KathiJo Jankowski (2016). "Comment on Demars et al. 2015,"Stream metabolism and the open diel oxygen method: Principles, practice, and perspectives"". In: *Limnology and Oceanography: Methods* 14.2, pp. 110–113.

Hotchkiss, ER, RO Hall Jr, RA Sponseller, D Butman, J Klaminder, H Laudon, Martin Rosvall, and J Karlsson (2015). "Sources of and processes controlling CO_2 emissions change with the size of streams and rivers". In: *Nature Geoscience* 8.9, pp. 696–699.

Hrachowitz, Markus, Ophélie Fovet, Laurent Ruiz, T Euser, S Gharari, R Nijzink, J Freer, HHG Savenije, and C Gascuel-Odoux (2014). "Process consistency in models: The importance of system signatures, expert knowledge, and process complexity". In: *Water resources research* 50.9, pp. 7445–7469.

Hudson, Naomi, Andy Baker, and Darren Reynolds (2007). "Fluorescence analysis of dissolved organic matter in natural, waste and polluted waters—a review". In: *River research and applications* 23.6, pp. 631–649.

Hudson, Naomi, Andy Baker, David Ward, Darren M Reynolds, Chris Brunsdon, Cynthia Carliell-Marquet, and Simon Browning (2008). "Can fluorescence spectrometry be used as a surrogate for the Biochemical Oxygen Demand (BOD) test in water quality assessment? An example from South West England". In: *Science of the total environment* 391.1, pp. 149–158.

Huryn, Alexander D, Jonathan P Benstead, and Stephanie M Parker (2014). "Seasonal changes in light availability modify the temperature dependence of ecosystem metabolism in an arctic stream". In: *Ecology* 95.10, pp. 2826–2839.

Hutchins, MG, C Abesser, C Prudhomme, JA Elliott, JP Bloomfield, MM Mansour, and OE Hitt (2018). "Combined impacts of future land-use and climate stressors on water resources and quality in groundwater and surface waterbodies of the upper Thames river basin, UK". In: *Science of the Total Environment* 631, pp. 962–986.

Hutchins, MG and MJ Bowes (2018). "Balancing water demand needs with protection of river water quality by minimising stream residence time: an example from the Thames, UK". In: *Water Resources Management* 32.7, pp. 2561–2568.

Hutchins, MG, G Harding, HP Jarvie, TJ Marsh, MJ Bowes, and M Loewenthal (2020). "Intense summer floods may induce prolonged increases in benthic respiration rates of more than one year leading to low river dissolved oxygen". In: *Journal of Hydrology X* 8, p. 100056.

Hutchins, MG, AC Johnson, A Deflandre-Vlandas, S Comber, P Posen, and D Boorman (2010). "Which offers more scope to suppress river phytoplankton blooms: reducing nutrient pollution or riparian shading?" In: *Science of the Total Environment* 408.21, pp. 5065–5077.

Hutchins, MG, RJ Williams, C Prudhomme, MJ Bowes, HE Brown, AJ Waylett, and M Loewenthal (2016). "Projections of future deterioration in UK river quality are hampered by climatic uncertainty under extreme conditions". In: *Hydrological Sciences Journal* 61.16, pp. 2818–2833.

Hutchins, Michael G and Olivia E Hitt (2019). "Sensitivity of river eutrophication to multiple stressors illustrated using graphical summaries of physics-based river water quality model simulations". In: *Journal of hydrology* 577, p. 123917.

Ishwaran, Hemant and UB2018 Kogalur (2017). *Random forests for survival, regression and classification (RF-SRC)*. 1.

Izagirre, Oihana, Urko Agirre, Miren Bermejo, Jesús Pozo, and Arturo Elosegi (2008). "Environmental controls of whole-stream metabolism identified from continuous monitoring of Basque streams". In: *Journal of the North American Benthological Society* 27.2, pp. 252–268.

Izagirre, Oihana, Miren Bermejo, Jesús Pozo, and Arturo Elosegi (2007). "RIVERMET©: An Excel-based tool to calculate river metabolism from diel oxygen–concentration curves". In: *Environmental Modelling & Software* 22.1, pp. 24–32.

Jackson, Michelle C, Charlie JG Loewen, Rolf D Vinebrooke, and Christian T Chimimba (2016). "Net effects of multiple stressors in freshwater ecosystems: a meta-analysis". In: *Global change biology* 22.1, pp. 180–189.

Jankowski, Kathi Jo, Francine H Mejia, Joanna R Blaszczak, and Gordon W Holtgrieve (2021). "Aquatic ecosystem metabolism as a tool in environmental management". In: *Wiley Interdisciplinary Reviews: Water* 8.4, e1521.

Jarvie, Helen P, Colin Neal, Richard J Williams, Margaret Neal, Heather D Wickham, Linda K Hill, Andrew J Wade, Alan Warwick, and John White (2002). "Phosphorus sources, speciation and dynamics in the lowland eutrophic River Kennet, UK". In: *Science of the Total Environment* 282, pp. 175–203.

Jarvie, Helen P, Andrew N Sharpley, Timothy Kresse, Phillip D Hays, Richard J Williams, Stephen M King, and Lawrence G Berry (2018). "Coupling high-frequency stream metabolism and nutrient monitoring to explore biogeochemical controls on downstream nitrate delivery". In: *Environmental science & technology* 52.23, pp. 13708–13717.

Jarvie, Helen P, Andrew N Sharpley, Paul JA Withers, J Thad Scott, Brian E Haggard, and Colin Neal (2013). "Phosphorus mitigation to control river eutrophication: murky waters, inconvenient truths, and "postnormal" science". In: *Journal of Environmental Quality* 42.2, pp. 295–304.

Jassby, Alan D and Trevor Platt (1976). "Mathematical formulation of the relationship between photosynthesis and light for phytoplankton". In: *Limnology and oceanography* 21.4, pp. 540–547.

Kaplan, Louis A and Thomas L Bott (1989). "Diel fluctuations in bacterial activity on streambed substrata during vernal algal blooms: effects of temperature, water chemistry, and habitat". In: *Limnology and Oceanography* 34.4, pp. 718–733.

Kaplan, Louis A and J Denis Newbold (1993). "Biogeochemistry of dissolved organic carbon entering streams". In: *Aquatic microbiology: An ecological approach*, pp. 139–165.

Karr, James R (1991). "Biological integrity: a long-neglected aspect of water resource management". In: *Ecological applications* 1.1, pp. 66–84.

Kaylor, Matthew J, Seth M White, W Carl Saunders, and Dana R Warren (2019). "Relating spatial patterns of stream metabolism to distributions of juveniles salmonids at the river network scale". In: *Ecosphere* 10.6, e02781.

Koenig, Lauren E, Ashley M Helton, Philip Savoy, Enrico Bertuzzo, James B Heffernan, Robert O Hall Jr, and Emily S Bernhardt (2019). "Emergent productivity regimes of river networks". In: *Limnology and Oceanography Letters* 4.5, pp. 173–181.

Köhler, Jan (1995). "Growth, production and losses of phytoplankton in the lowland River Spree: carbon balance". In: *Freshwater Biology* 34.3, pp. 501–512.

Kominoski, John S, Amy D Rosemond, Jonathan P Benstead, Vlad Gulis, and David WP Manning (2018). "Experimental nitrogen and phosphorus additions increase rates of stream ecosystem respiration and carbon loss". In: *Limnology and Oceanography* 63.1, pp. 22–36.

Koschorreck, Matthias, Yves T Prairie, Jihyeon Kim, and Rafael Marcé (2021). "CO2 is not like CH4–limits of and corrections to the headspace method to analyse pCO2 in water". In: *Biogeosciences* 18, pp. 1619–1627.

Kunz, Manuel J, Alfred Wüest, Bernhard Wehrli, Jan Landert, and David B Senn (2011). "Impact of a large tropical reservoir on riverine transport of sediment, carbon, and nutrients to downstream wetlands". In: *Water Resources Research* 47.12.

Kupilas, Benjamin, Daniel Hering, Armin W Lorenz, Christoph Knuth, and Björn Gücker (2017). "Hydromorphological restoration stimulates river ecosystem metabolism". In: *Biogeosciences* 14.7, pp. 1989–2002.

Kurz, Marie J, Jennifer D Drummond, Eugènia Martí, Jay P Zarnetske, Joseph Lee-Cullin, Megan J Klaar, Silvia Folegot, Toralf Keller, Adam S Ward, and Jan H Fleckenstein (2017). "Impacts of water level on metabolism and transient storage in vegetated lowland rivers: Insights from a mesocosm study". In: *Journal of Geophysical Research: Biogeosciences* 122.3, pp. 628–644.

Lack, TJ (1971). "Quantitative studies on the phytoplankton of the Rivers Thames and Kennet at Reading". In: *Freshwater Biology* 1.2, pp. 213–224.

Larroudé, S, Nicolas Massei, P Reyes-Marchant, C Delattre, and JF Humbert (2013). "Dramatic changes in a phytoplankton community in response to local and global pressures: a 24-year survey of the river Loire (France)". In: *Global Change Biology* 19.5, pp. 1620–1631.

Lázár, Attila N, AJ Wade, PG Whitehead, C Neal, and M Loewenthal (2012). "Reconciling observed and modelled phytoplankton dynamics in a major lowland UK river, the Thames". In: *Hydrology Research* 43.5, pp. 576–588.

Lázár, Attila N, Andrew J Wade, and Brian Moss (2016). "Modelling primary producer interaction and composition: an example of a UK lowland river". In: *Environmental Modeling & Assessment* 21.1, pp. 125–148.

Lees, Matthew J and Luis Camacho (2000). "Modelling solute transport in rivers under unsteady flow conditions—an integrated velocity conceptualisation. British Hydrological Society". In: *7th national hydrology symposium. Newcastle, Sept*, pp. 4–6.

Lees, Matthew J, Luis Camacho, and P Whitehead (1998). "Extension of the QUASAR river water quality model to incorporate dead-zone mixing". In: *Hydrology and Earth System Sciences* 2.2/3, pp. 353–365.

Lees, Matthew J, Luis A Camacho, and Steven Chapra (2000). "On the relationship of transient storage and aggregated dead zone models of longitudinal solute transport in streams". In: *Water Resources Research* 36.1, pp. 213–224.

Leggieri, Leonardo, Claudia Feijoó, Adonis Giorgi, Nicolás Ferreiro, and Vicenç Acuña (2013). "Seasonal weather effects on hydrology drive the metabolism of non-forest lowland streams". In: *Hydrobiologia* 716.1, pp. 47–58.

Lemm, Jan U, Markus Venohr, Lidija Globevnik, Kostas Stefanidis, Yiannis Panagopoulos, Jos van Gils, Leo Posthuma, Peter Kristensen, Christian K Feld, Judith Mahnkopf, et al. (2021). "Multiple stressors determine river ecological status at the European scale: Towards an integrated understanding of river status deterioration". In: *Global Change Biology* 27.9, pp. 1962–1975.

Levi, Peter S, Jennifer L Tank, Janine Rüegg, David J Janetski, Scott D Tiegs, Dominic T Chaloner, and Gary A Lamberti (2013). "Whole-stream metabolism responds to spawning Pacific salmon in their native and introduced ranges". In: *Ecosystems* 16.2, pp. 269–283.

Li, Guoyuan, C Rhett Jackson, and Kristin A Kraseski (2012). "Modeled riparian stream shading: Agreement with field measurements and sensitivity to riparian conditions". In: *Journal of hydrology* 428, pp. 142–151.

Lind, PR, BJ Robson, and BD Mitchell (2007). "Multiple lines of evidence for the beneficial effects of environmental flows in two lowland rivers in Victoria, Australia". In: *River Research and Applications* 23.9, pp. 933–946.

Lindenschmidt, Karl-Erich (2006). "The effect of complexity on parameter sensitivity and model uncertainty in river water quality modelling". In: *Ecological Modelling* 190.1-2, pp. 72–86.

Lorke, Andreas, Pascal Bodmer, Christian Noss, Zeyad Alshboul, Matthias Koschorreck, Celia Somlai-Haase, David Bastviken, Sabine Flury, Daniel Frank McGinnis, Andreas Maeck, et al. (2015). "Technical note: Drifting versus anchored flux chambers for measuring greenhouse gas emissions from running waters". In: *Biogeosciences* 12.23, pp. 7013–7024.

Mackay, EB, H Feuchtmayr, MM De Ville, SJ Thackeray, N Callaghan, M Marshall, G Rhodes, Christopher A Yates, Penny J Johnes, and SC Maberly (2020). "Dissolved organic nutrient uptake by riverine phytoplankton varies along a gradient of nutrient enrichment". In: *Science of the Total Environment* 722, p. 137837.

Malmqvist, Björn and Simon Rundle (2002). "Threats to the running water ecosystems of the world". In: *Environmental conservation* 29.2, pp. 134–153.

Manson, J Russell, Steve G Wallis, and Donna Hope (2001). "A conservative semi-Lagrangian transport model for rivers with transient storage zones". In: *Water Resources Research* 37.12, pp. 3321–3329.

Manson, JR, BOL Demars, SG Wallis, and V Mytnik (2010). "A combined computational and experimental approach to quantifying habitat complexity in Scottish upland streams". In: *Proceedings of Hydropredict*.

Marcarelli, Amy M, Robert W Van Kirk, and Colden V Baxter (2010). "Predicting effects of hydrologic alteration and climate change on ecosystem metabolism in a western US river". In: *Ecological Applications* 20.8, pp. 2081–2088.

Martin, Nancy, Preston McEachern, Tong Yu, and David Z Zhu (2013). "Model development for prediction and mitigation of dissolved oxygen sags in the Athabasca River, Canada". In: *Science of the Total Environment* 443, pp. 403–412.

Martinsen, Kenneth Thorø, Theis Kragh, and Kaj Sand-Jensen (2018). "A simple and cost-efficient automated floating chamber for continuous measurements of carbon dioxide gas flux on lakes". In: *Biogeosciences* 15.18, pp. 5565–5573.

Mejia, Francine H, Alexander K Fremier, Joseph R Benjamin, J Ryan Bellmore, Adrianne Z Grimm, Grace A Watson, and Michael Newsom (2019). "Stream metabolism increases with drainage area and peaks asynchronously across a stream network". In: *Aquatic Sciences* 81.1, pp. 1–17.

Meng, Fangang, Guocheng Huang, Xin Yang, Zengquan Li, Jian Li, Jing Cao, Zhigang Wang, and Li Sun (2013). "Identifying the sources and fate of anthropogenically impacted dissolved organic matter (DOM) in urbanized rivers". In: *Water research* 47.14, pp. 5027–5039.

Meybeck, Michel (2003). "Global analysis of river systems: from Earth system controls to Anthropocene syndromes". In: *Philosophical Transactions of the Royal Society of London. Series B: Biological Sciences* 358.1440, pp. 1935–1955.

Millennium Ecosystem Assessment (2010). *Ecosystems and Human Well-being: General synthesis*, p. 18.

Minaudo, Camille, Florence Curie, Yann Jullian, Nathalie Gassama, and Florentina Moatar (2018). "QUAL-NET, a high temporal-resolution eutrophication model for large hydrographic networks". In: *Biogeosciences* 15.7, pp. 2251–2269.

Minshall, G Wayne, Kenneth W Cummins, Robert C Petersen, Colbert E Cushing, Dale A Bruns, James R Sedell, and Robin L Vannote (1985). "Developments in stream ecosystem theory". In: *Canadian Journal of Fisheries and Aquatic Sciences* 42.5, pp. 1045–1055.

Moe, Therese Fosholt and Benoît Olivier Laurent Demars (2017). *Årsrapport krypsivovervåking 2017*. Tech. rep. 7202-2017. Norsk institutt for vannforskning.

Moriasi, Daniel N, Jeffrey G Arnold, Michael W Van Liew, Ronald L Bingner, R Daren Harmel, and Tamie L Veith (2007). "Model evaluation guidelines for systematic quantification of accuracy in watershed simulations". In: *Transactions of the ASABE* 50.3, pp. 885–900.

Mulholland, Patrick J, Erich R Marzolf, Jackson R Webster, Deborah R Hart, and Susan P Hendricks (1997). "Evidence that hyporheic zones increase heterotrophic metabolism and phosphorus uptake in forest streams". In: *Limnology and oceanography* 42.3, pp. 443–451.

Mulholland, PJ, CS Fellows, JL Tank, NB Grimm, JR Webster, SK Hamilton, Eugènia Martí, L Ashkenas, WB Bowden, WK Dodds, et al. (2001). "Inter-biome comparison of factors controlling stream metabolism". In: *Freshwater biology* 46.11, pp. 1503–1517.

Murphy, James M, DMH Sexton, Geoff J Jenkins, BB Booth, CC Brown, Robin T Clark, M Collins, GR Harris, EJ Kendon, RA Betts, et al. (2009). *UK climate projections science report: climate change projections*.

Naimi, Babak (2015). *USDM: Uncertainty analysis for species distribution models. R package version 1.1–15*.

Nebgen, Elizabeth L and Kyle S Herrman (2019). "Effects of shading on stream ecosystem metabolism and water temperature in an agriculturally influenced stream in central Wisconsin, USA". In: *Ecological Engineering* 126, pp. 16–24.

Newbold, JD, PJ Mulholland, JW Elwood, and RV O'neill (1982). "Organic carbon spiralling in stream ecosystems". In: *Oikos*, pp. 266–272.

Niyogi, Dev K, Kevin S Simon, and Colin R Townsend (2003). "Breakdown of tussock grass in streams along a gradient of agricultural development in New Zealand". In: *Freshwater biology* 48.9, pp. 1698–1708.

O'Connor, Donald J and William E Dobbins (1958). "Mechanism of reaeration in natural streams". In: *Transactions of the American Society of Civil Engineers* 123.1, pp. 641–666.

Odum, Howard T (1956). "Primary production in flowing waters". In: *Limnology and oceanography* 1.2, pp. 102–117.

Old, GH, PS Naden, M Harman, MJ Bowes, C Roberts, PM Scarlett, DJE Nicholls, LK Armstrong, HD Wickham, and DS Read (2019). "Using dissolved organic matter fluorescence to identify the provenance of nutrients in a lowland catchment; the River Thames, England". In: *Science of The Total Environment* 653, pp. 1240–1252.

Olden, Julian D and Robert J Naiman (2010). "Incorporating thermal regimes into environmental flows assessments: modifying dam operations to restore freshwater ecosystem integrity". In: *Freshwater Biology* 55.1, pp. 86–107.

ONS (2015). *What do the 2014-based National Population Projections show?* URL: https://www.ons.gov.uk/peoplepopulationandcommunity/populationandmigration/populationprojections/bulletins/nationalpopulationprojections/2015-10-29. (accessed: 16.03.2022).

Owens, MR (1964). "Some reaeration studies in streams". In: *Inter. J. Air Water Poll.* 8, pp. 469–486.

Paerl, Hans W and Jef Huisman (2009). "Climate change: a catalyst for global expansion of harmful cyanobacterial blooms". In: *Environmental microbiology reports* 1.1, pp. 27–37.

Palmer, Margaret A, ES Bernhardt, JD Allan, Phillip Spencer Lake, G Alexander, Shane Brooks, J Carr, S Clayton, CN Dahm, J Follstad Shah, et al. (2005). "Standards for ecologically successful river restoration". In: *Journal of applied ecology* 42.2, pp. 208–217.

Palmer, Margaret A and Catherine M Febria (2012). "The heartbeat of ecosystems". In: *science* 336.6087, pp. 1393–1394.

Palumbo, James E and Linfield C Brown (2014). "Assessing the performance of reaeration prediction equations". In: *Journal of Environmental Engineering* 140.3, p. 04013013.

Pardo, Isabel, Lenka Kuglerová, Liliana García, and Eugènia Martí (2022). "Nutrient availability modulates the effect of water abstraction on the metabolism of 2 lowland forested streams". In: *Freshwater Science* 41.2, pp. 000–000.

Pascoal, Cláudia, Manuela Pinho, Fernanda Cássio, and Pedro Gomes (2003). "Assessing structural and functional ecosystem condition using leaf breakdown: studies on a polluted river". In: *Freshwater Biology* 48.11, pp. 2033–2044.

Pathak, Devanshi, Michael Hutchins, Lee Brown, Matthew Loewenthal, Peter Scarlett, Linda Armstrong, David Nicholls, Michael Bowes, and François Edwards (2021). "Hourly prediction of phytoplankton biomass and its environmental controls in lowland rivers". In: *Water Resources Research* 57.3, e2020WR028773.

Pathak, Devanshi, Michael Hutchins, Lee E Brown, Matthew Loewenthal, Peter Scarlett, Linda Armstrong, David Nicholls, Mike Bowes, François Edwards, and Gareth Old (2022). "High-resolution water-quality and ecosystem-metabolism modeling in lowland rivers". In: *Limnology and Oceanography*.

Payn, Robert A, RO Hall Jr, Theodore A Kennedy, Geoffrey C Poole, and Lucy A Marshall (2017). "A coupled metabolic-hydraulic model and calibration scheme for estimating whole-river metabolism during dynamic flow conditions". In: *Limnology and Oceanography: Methods* 15.10, pp. 847–866.

Perkins, Daniel M, Gabriel Yvon-Durocher, Benoît OL Demars, Julia Reiss, Doris E Pichler, Nikolai Friberg, Mark Trimmer, and Guy Woodward (2012). "Consistent temperature dependence of respiration across ecosystems contrasting in thermal history". In: *Global Change Biology* 18.4, pp. 1300–1311.

Pinheiro, Jose, Douglas Bates, Saikat DebRoy, Deepayan Sarkar, and R Core Team (2007). *Linear and nonlinear mixed effects models*. 57, pp. 1–89.

Poff, N LeRoy, J David Allan, Mark B Bain, James R Karr, Karen L Prestegaard, Brian D Richter, Richard E Sparks, and Julie C Stromberg (1997). "The natural flow regime". In: *BioScience* 47.11, pp. 769–784.

Poff, N LeRoy and John H Matthews (2013). "Environmental flows in the Anthropocence: past progress and future prospects". In: *Current Opinion in Environmental Sustainability* 5.6, pp. 667–675.

Poff, N Leroy and Julie KH Zimmerman (2010). "Ecological responses to altered flow regimes: a literature review to inform the science and management of environmental flows". In: *Freshwater biology* 55.1, pp. 194–205.

Poole, Geoffrey C and Cara H Berman (2001). "An ecological perspective on in-stream temperature: natural heat dynamics and mechanisms of human-causedthermal degradation". In: *Environmental management* 27.6, pp. 787–802.

Prudhomme, C., S. Dadson, D. Morris, J. Williamson, G. Goodsell, S. Crooks, L. Boolee, H. Davies, G. Buys, and T. Lafon (2012). "Future flows climate data". In: DOI: 10.5285/bad1514f-119e-44a4-8e1e-442735bb9797. URL: https://doi.org/10.5285/bad1514f-119e-44a4-8e1e-442735bb9797.

Prudhomme, Christel, Tracey Haxton, S Crooks, C Jackson, Andrew Barkwith, Jennifer Williamson, J Kelvin, Jonathan Mackay, Lei Wang, A Young, et al. (2013). "Future Flows

Hydrology: an ensemble of daily river flow and monthly groundwater levels for use for climate change impact assessment across Great Britain". In: *Earth System Science Data* 5.1, pp. 101–107.

Pulg, Ulrich, Sebastian Stranzl, Knut W Vollset, Bjørn T Barlaup, Espen Olsen, Bjørnar Skår, and Gaute Velle (2016). *Gassmetning i Otra nedenfor Brokke kraftverk*. Tech. rep. 1892-8889. NORCE Norwegian Research Centre AS.

Rankinen, Katri, José Enrique Cano Bernal, Maria Holmberg, Kristiina Vuorio, and Kirsti Granlund (2019). "Identifying multiple stressors that influence eutrophication in a Finnish agricultural river". In: *Science of the Total Environment* 658, pp. 1278–1292.

Rapport, David J, Robert Costanza, and Anthony J McMichael (1998). "Assessing ecosystem health". In: *Trends in ecology & evolution* 13.10, pp. 397–402.

Raymond, Peter A, Jens Hartmann, Ronny Lauerwald, Sebastian Sobek, Cory McDonald, Mark Hoover, David Butman, Robert Striegl, Emilio Mayorga, Christoph Humborg, et al. (2013). "Global carbon dioxide emissions from inland waters". In: *Nature* 503.7476, pp. 355–359.

Raymond, Peter A and James E Saiers (2010). "Event controlled DOC export from forested watersheds". In: *Biogeochemistry* 100.1, pp. 197–209.

Raymond, Peter A, Christopher J Zappa, David Butman, Thomas L Bott, Jody Potter, Patrick Mulholland, Andrew E Laursen, William H McDowell, and Denis Newbold (2012). "Scaling the gas transfer velocity and hydraulic geometry in streams and small rivers". In: *Limnology and Oceanography: Fluids and Environments* 2.1, pp. 41–53.

Read, Daniel S, Michael J Bowes, Lindsay K Newbold, and Andrew S Whiteley (2014). "Weekly flow cytometric analysis of riverine phytoplankton to determine seasonal bloom dynamics". In: *Environmental Science: Processes & Impacts* 16.3, pp. 594–603.

Reichert, Peter, Dietrich Borchardt, Mogens Henze, Wolfgang Rauch, Peter Shanahan, László Somlyódy, and Peter Vanrolleghem (2001). "River water quality model no. 1 (RWQM1): II. Biochemical process equations". In: *Water science and Technology* 43.5, pp. 11–30.

Reichert, Peter, Urs Uehlinger, and Vicenç Acuña (2009). "Estimating stream metabolism from oxygen concentrations: effect of spatial heterogeneity". In: *Journal of Geophysical Research: Biogeosciences* 114.G3.

Reis Oliveira, Paula C dos, Harm G van der Geest, Michiel HS Kraak, and Piet FM Verdonschot (2019). "Land use affects lowland stream ecosystems through dissolved oxygen regimes". In: *Scientific reports* 9.1, pp. 1–10.

Reynaud, Arnaud and Denis Lanzanova (2017). "A global meta-analysis of the value of ecosystem services provided by lakes". In: *Ecological Economics* 137, pp. 184–194.

Reynolds, CS (2000). "Hydroecology of river plankton: the role of variability in channel flow". In: *Hydrological Processes* 14.16-17, pp. 3119–3132.

Reynolds, CS and J-P Descy (1996). "The production, biomass and structure of phytoplankton in large rivers". In: *Large Rivers*, pp. 161–187.

Reynolds, CS and MS Glaister (1993). "Spatial and temporal changes in phytoplankton abundance in the upper and middle reaches of the River Severn". In: *Large Rivers*, pp. 1–22.

Ridgeway, Greg (2007). *Generalized Boosted Models: A guide to the gbm package*. 1, p. 2007.

Roberts, Brian J and Patrick J Mulholland (2007). "In-stream biotic control on nutrient biogeochemistry in a forested stream, West Fork of Walker Branch". In: *Journal of Geophysical Research: Biogeosciences* 112.G4.

Roberts, Brian J, Patrick J Mulholland, and Walter R Hill (2007). "Multiple scales of temporal variability in ecosystem metabolism rates: results from 2 years of continuous monitoring in a forested headwater stream". In: *Ecosystems* 10.4, pp. 588–606.

Rode, Michael, Andrew J Wade, Matthew J Cohen, Robert T Hensley, Michael J Bowes, James W Kirchner, George B Arhonditsis, Phil Jordan, Brian Kronvang, Sarah J Halliday, et al. (2016). "Sensors in the stream: the high-frequency wave of the present". In: *Environ. Sci. Technol.*

Roley, Sarah S, Jennifer L Tank, Natalie A Griffiths, Robert O Hall Jr, and Robert T Davis (2014). "The influence of floodplain restoration on whole-stream metabolism in an agricultural stream: insights from a 5-year continuous data set". In: *Freshwater Science* 33.4, pp. 1043–1059.

Rørslett, Bjørn (1988). "Aquatic weed problems in a hydroelectric river: the R. Otra, Norway". In: *Regulated Rivers: Research & Management* 2.1, pp. 25–37.

Runkel, Robert L (1998). *One-dimensional transport with inflow and storage (OTIS): A solute transport model for streams and rivers*. Vol. 98. US Department of the Interior, US Geological Survey.

Runkel, Robert L and Kenneth E Bencala (1995). "Transport of reacting solutes in rivers and streams". In: *Environmental hydrology*. Springer, pp. 137–164.

Ruse, Les and Alison Love (1997). "Predicting phytoplankton composition in the River Thames, England". In: *Regulated Rivers: Research & Management: An International Journal Devoted to River Research and Management* 13.2, pp. 171–183.

Sabater, Francesc, Andrea Butturini, Eugènia MartÍ, Isabel Muñoz, Anna Romaní, Joanne Wray, and Sergi Sabater (2000). "Effects of riparian vegetation removal on nutrient retention in a Mediterranean stream". In: *Journal of the North American Benthological Society* 19.4, pp. 609–620.

Sabater, Sergi and Klement Tockner (2009). "Effects of hydrologic alterations on the ecological quality of river ecosystems". In: *Water scarcity in the Mediterranean*, pp. 15–39.

Santos Santos, Tania F and Luis A Camacho (2022). "An Integrated Water Quality Model to Support Multiscale Decisions in a Highly Altered Catchment". In: *Water* 14.3, p. 374.

Savoy, Phil and Judson W Harvey (2021). "Predicting light regime controls on primary productivity across CONUS river networks". In: *Geophysical Research Letters* 48.10, e2020GL092149.

Savoy, Philip, Emily Bernhardt, Lily Kirk, Matthew J Cohen, and James B Heffernan (2021). "A seasonally dynamic model of light at the stream surface". In: *Freshwater Science* 40.2, pp. 286–301.

Sayers, PB, M Horritt, E Penning-Rowsell, and A McKenzie (2015). "Climate Change Risk Assessment 2017: Projections of future flood risk in the UK". In: *Research undertaken by Sayers and Partners on behalf of the Committee on Climate Change. Published by Committee on Climate Change, London*.

Schinegger, Rafaela, Clemens Trautwein, Andreas Melcher, and Stefan Schmutz (2012). "Multiple human pressures and their spatial patterns in european running waters". In: *Water and Environment Journal* 26.2, pp. 261–273.

Schöl, Andreas, Volker Kirchesch, Tanja Bergfeld, Franz Schöll, Jost Borcherding, and Dieter Müller (2002). "Modelling the chlorophyll a content of the River Rhine–Interrelation between riverine algal production and population biomass of grazers, rotifers and the zebra mussel, Dreissena polymorpha". In: *International Review of Hydrobiology* 87.2-3, pp. 295–317.

Segatto, Pier Luigi, Tom J Battin, and Enrico Bertuzzo (2020). "Modeling the coupled dynamics of stream metabolism and microbial biomass". In: *Limnology and Oceanography* 65.7, pp. 1573–1593.

– (2021). "The Metabolic Regimes at the Scale of an Entire Stream Network Unveiled Through Sensor Data and Machine Learning". In: *Ecosystems*, pp. 1–18.

Sincock, Andrew Michael (2002). "Conceptual river water quality modelling under dynamic conditions". PhD thesis. Imperial College London.

Sincock, Andrew Michael and MJ Lees (2002). "Extension of the QUASAR River-Water Quality Model to Unsteady Flow Conditions". In: *Water and Environment Journal* 16.1, pp. 12–17.

Sincock, Andrew Michael, Howard S Wheater, and Paul G Whitehead (2003). "Calibration and sensitivity analysis of a river water quality model under unsteady flow conditions". In: *Journal of Hydrology* 277.3-4, pp. 214–229.

Song, Chao, Walter K Dodds, Janine Rüegg, Alba Argerich, Christina L Baker, William B Bowden, Michael M Douglas, Kaitlin J Farrell, Michael B Flinn, Erica A Garcia, et al. (2018). "Continental-scale decrease in net primary productivity in streams due to climate warming". In: *Nature Geoscience* 11.6, pp. 415–420.

Spear, Robert C and GM Hornberger (1980). "Eutrophication in peel inlet—II. Identification of critical uncertainties via generalized sensitivity analysis". In: *Water research* 14.1, pp. 43–49.

Standing Committee of Analysts (1989). *5 Day Biochemical Oxygen Demand (BOD5)*. Tech. rep.

Stanley, Emily H, Stuart G Fisher, and Jeremy B Jones Jr (2004). "Effects of water loss on primary production: a landscape-scale model". In: *Aquatic Sciences* 66.1, pp. 130–138.

Steele, John H (1962). "Environmental control of photosynthesis in the sea". In: *Limnology and oceanography* 7.2, pp. 137–150.

Streeter, HW and Earle B Phelps (1925). *A study of the pollution and natural purification of the Ohio River. III. Factors concerned in the phenomena of oxidation and reaeration*. Tech. rep. 146. United States Public Health Service.

Suarez, Vivian V Camacho, Robert J Brederveld, Marieke Fennema, Antonio Moreno-Rodenas, Jeroen Langeveld, Hans Korving, Alma NA Schellart, and James D Shucksmith (2019). "Evaluation of a coupled hydrodynamic-closed ecological cycle approach for modelling dissolved oxygen in surface waters". In: *Environmental modelling & software* 119, pp. 242–257.

Tank, Jennifer L, Emma J Rosi-Marshall, Natalie A Griffiths, Sally A Entrekin, and Mia L Stephen (2010). "A review of allochthonous organic matter dynamics and metabolism in streams". In: *Journal of the North American Benthological Society* 29.1, pp. 118–146.

Uehlinger, U, B Kawecka, and CT Robinson (2003). "Effects of experimental floods on periphyton and stream metabolism below a high dam in the Swiss Alps (River Spöl)". In: *Aquatic Sciences* 65.3, pp. 199–209.

Uehlinger, Urs (2000). "Resistance and resilience of ecosystem metabolism in a flood-prone river system". In: *Freshwater Biology* 45.3, pp. 319–332.

– (2006). "Annual cycle and inter-annual variability of gross primary production and ecosystem respiration in a floodprone river during a 15-year period". In: *Freshwater Biology* 51.5, pp. 938–950.

Uehlinger, Urs and Markus W Naegeli (1998). "Ecosystem metabolism, disturbance, and stability in a prealpine gravel bed river". In: *Journal of the North American Benthological Society* 17.2, pp. 165–178.

Ulseth, Amber J, Robert O Hall, Marta Boix Canadell, Hilary L Madinger, Amin Niayifar, and Tom J Battin (2019). "Distinct air–water gas exchange regimes in low-and high-energy streams". In: *Nature Geoscience* 12.4, pp. 259–263.

Val, Jonatan, David Chinarro, María Rosa Pino, and Enrique Navarro (2016). "Global change impacts on river ecosystems: a high-resolution watershed study of Ebro river metabolism". In: *Science of the Total Environment* 569, pp. 774–783.

Van Griensven, A and W Bauwens (2005). "Application and evaluation of ESWAT on the Dender basin and the Wister Lake basin". In: *Hydrological Processes: An International Journal* 19.3, pp. 827–838.

Vandenberghe, Veronique, A Van Griensven, and W Bauwens (2001). "Sensitivity analysis and calibration of the parameters of ESWAT: Application to the river Dender". In: *Water Science and Technology* 43.7, pp. 295–301.

Venables, WN and BD Ripley (2002). *Modern applied statistics with S*. Springer New York, NY.

Viers, Joshua H (2017). "Meeting ecosystem needs while satisfying human demands". In: *Environmental Research Letters* 12.6.

Villegas, Iraides and Griselda de Giner (1973). "Phytoplankton as a biological indicator of water quality". In: *Water Research* 7.3, pp. 479–487.

Virtanen, Pauli, Ralf Gommers, Travis E. Oliphant, Matt Haberland, Tyler Reddy, David Cournapeau, et al. (2020). "SciPy 1.0: Fundamental Algorithms for Scientific Computing in Python". In: *Nature Methods* 17, pp. 261–272. DOI: 10.1038/s41592-019-0686-2.

Von Schiller, Daniel, Vicenç Acuña, Ibon Aristi, Maite Arroita, Ana Basaguren, Alberto Bellin, Luz Boyero, Andrea Butturini, Antoni Ginebreda, Eleni Kalogianni, et al. (2017).

"River ecosystem processes: A synthesis of approaches, criteria of use and sensitivity to environmental stressors". In: *Science of the Total Environment* 596, pp. 465–480.

Von Schiller, Daniel, Thibault Datry, Roland Corti, Arnaud Foulquier, Klement Tockner, R Marcé, G García-Baquero, I Odriozola, B Obrador, A Elosegi, et al. (2019). "Sediment respiration pulses in intermittent rivers and ephemeral streams". In: *Global Biogeochemical Cycles* 33.10, pp. 1251–1263.

Vörösmarty, Charles J, Peter B McIntyre, Mark O Gessner, David Dudgeon, Alexander Prusevich, Pamela Green, Stanley Glidden, Stuart E Bunn, Caroline A Sullivan, C Reidy Liermann, et al. (2010). "Global threats to human water security and river biodiversity". In: *nature* 467.7315, pp. 555–561.

Wagner, Richard J, Robert W Boulger Jr, Carolyn J Oblinger, and Brett A Smith (2006). *Guidelines and standard procedures for continuous water-quality monitors: station operation, record computation, and data reporting*. Tech. rep.

Wallace, Todd A and Deborah Furst (2016). "Open water metabolism and dissolved organic carbon in response to environmental watering in a lowland river–floodplain complex". In: *Marine and Freshwater Research* 67.9, pp. 1346–1361.

Wallis, Stephen G and J Russell Manson (2018). "Flow dependence of the parameters of the transient storage model". In: *Free surface flows and transport processes*. Springer, pp. 477–488.

Wallis, Stephen G, PC Young, and KJ Beven (1989). "Experimental investigation of the aggregated dead zone model for longitudinal solute transport in stream channels". In: *Proceedings of the Institution of Civil Engineers* 87.1, pp. 1–22.

Wang, Junna, Zhonglong Zhang, and Billy Johnson (2019). "Low flows and downstream decline in phytoplankton contribute to impaired water quality in the lower Minnesota River". In: *Water research* 161, pp. 262–273.

Wantzen, Karl Matthias, Aziz Ballouche, Isabelle Longuet, Ibrahima Bao, Hamady Bocoum, Lassana Cissé, Malavika Chauhan, Pierre Girard, Brij Gopal, Alioune Kane, et al. (2016). "River Culture: an eco-social approach to mitigate the biological and cultural diversity crisis in riverscapes". In: *Ecohydrology & Hydrobiology* 16.1, pp. 7–18.

Watson, Fred, Rob Vertessy, Tom McMahon, Bruce Rhodes, and Ian Watson (2001). "Improved methods to assess water yield changes from paired-catchment studies: application to the Maroondah catchments". In: *Forest Ecology and Management* 143.1-3, pp. 189–204.

Waylett, AJ, MG Hutchins, AC Johnson, MJ Bowes, and M Loewenthal (2013). "Physico-chemical factors alone cannot simulate phytoplankton behaviour in a lowland river". In: *Journal of hydrology* 497, pp. 223–233.

Webster, Jackson R, Patrick J Mulholland, Jennifer L Tank, H Maurice Valett, Walter K Dodds, Bruce J Peterson, William B Bowden, Clifford N Dahm, Stuart Findlay, Stanley V Gregory, et al. (2003). "Factors affecting ammonium uptake in streams–an inter-biome perspective". In: *Freshwater Biology* 48.8, pp. 1329–1352.

Weiss, Ray F (1970). "The solubility of nitrogen, oxygen and argon in water and seawater". In: *Deep Sea Research and Oceanographic Abstracts*. Vol. 17. 4. Elsevier, pp. 721–735.

Welker, Martin and Norbert Walz (1998). "Can mussels control the plankton in rivers?—a planktological approach applying a Lagrangian sampling strategy". In: *Limnology and Oceanography* 43.5, pp. 753–762.

Whitehead, Paul G, Gianbattista Bussi, Michael J Bowes, Daniel S Read, Michael G Hutchins, J Alex Elliott, and Simon J Dadson (2015). "Dynamic modelling of multiple phytoplankton groups in rivers with an application to the Thames river system in the UK". In: *Environmental Modelling & Software* 74, pp. 75–91.

Whitehead, PG and GM Hornberger (1984). "Modelling algal behaviour in the River Thames". In: *Water research* 18.8, pp. 945–953.

Whitehead, PG, A Howard, and C Arulmani (1997a). "Modelling algal growth and transport in rivers: a comparison of time series analysis, dynamic mass balance and neural network techniques". In: *Hydrobiologia* 349.1, pp. 39–46.

Whitehead, PG, RJ Williams, and DR Lewis (1997b). "Quality simulation along river systems (QUASAR): model theory and development". In: *Science of the Total Environment* 194, pp. 447–456.

Winslow, Luke A, Jacob A Zwart, Ryan D Batt, Hilary A Dugan, R Iestyn Woolway, Jessica R Corman, Paul C Hanson, and Jordan S Read (2016). "LakeMetabolizer: an R package for estimating lake metabolism from free-water oxygen using diverse statistical models". In: *Inland Waters* 6.4, pp. 622–636.

Wright, Richard F, Raoul-Marie Couture, Anne B Christiansen, José-Luis Guerrero, Øyvind Kaste, and Bjørn T Barlaup (2017). "Effects of multiple stresses hydropower, acid deposition and climate change on water chemistry and salmon populations in the River Otra, Norway". In: *Science of The Total Environment* 574, pp. 128–138.

Yang, Hong, Tom Andersen, Peter Dörsch, Koji Tominaga, Jan-Erik Thrane, and Dag O Hessen (2015). "Greenhouse gas metabolism in Nordic boreal lakes". In: *Biogeochemistry* 126.1, pp. 211–225.

Ye, Sheng, Timothy P Covino, Murugesu Sivapalan, Nandita B Basu, Hong-Yi Li, and Shao-Wen Wang (2012). "Dissolved nutrient retention dynamics in river networks: A modeling investigation of transient flows and scale effects". In: *Water Resources Research* 48.6.

Young, RG, CD Matthaei, and CR Townsend (2006). *Functional indicators of river ecosystem health–final project report. Prepared for Ministry for the Environment*. Tech. rep. Cawthron Report.

Young, RG, CR Townsend, and C Matthaei (2004). "Functional indicators of river ecosystem health–an interim guide for use in New Zealand". In: *Cawthron Rep* 870, pp. 495–523.

Young, Roger G, Christoph D Matthaei, and Colin R Townsend (2008). "Organic matter breakdown and ecosystem metabolism: functional indicators for assessing river ecosystem health". In: *Journal of the North American Benthological Society* 27.3, pp. 605–625.

Zhang, Y, AL Collins, S McMillan, ER Dixon, E Cancer-Berroya, C Poiret, and A Stringfellow (2017). "Fingerprinting source contributions to bed sediment-associated organic matter

in the headwater subcatchments of the River Itchen SAC, Hampshire, UK". In: *River Research and Applications* 33.10, pp. 1515–1526.

Zimmerman, Julie KH, Benjamin H Letcher, Keith H Nislow, Kimberly A Lutz, and Francis J Magilligan (2010). "Determining the effects of dams on subdaily variation in river flows at a whole-basin scale". In: *River Research and Applications* 26.10, pp. 1246–1260.

Zoboli, Ottavia, Katerina Schilling, Anna-Lena Ludwig, Norbert Kreuzinger, and Matthias Zessner (2018). "Primary productivity and climate change in Austrian lowland rivers". In: *Water Science and Technology* 77.2, pp. 417–425.

Zuur, Alain F, Elena N Ieno, and Chris S Elphick (2010). "A protocol for data exploration to avoid common statistical problems". In: *Methods in ecology and evolution* 1.1, pp. 3–14.